DETRITAL ZIRCON GEOCHRONOLOGY AND SEQUENCE STRATIGRAPHY OF THE EUREKA QUARTZITE FORMATION ADJACENT TO THE TOOELE ARCH, WESTERN UTAH AND EASTERN NEVADA

A Thesis

by

MARIO ALBERTO LIRA

Submitted to the Office of Graduate and Professional Studies of
Texas A&M University
in partial fulfillment of the requirements for the degree of

MASTER OF SCIENCE

Chair of Committee,	Michael Pope
Committee Members,	Brent Miller
	Walter Ayers
Head of Department,	John Giardino

August 2015

Major Subject: Geology

ABSTRACT

The Middle-Late Ordovician Eureka Quatzite in western Utah and eastern Nevada is a unique supermature quartz arenite composed of very fine-medium grain, well-rounded, well-sorted sands that were deposited along the Early Paleozoic passive margin of western Laurentia. The Eureka Quartzite and its equivalents are the only regionally widespread siliciclastic deposits within a thick Cambrian – Devonian carbonate sequence. The Eureka Quartzite thins from Lakeside, Utah to Ruby, Nevada where the Tooele Arch sub-divides the western Utah Middle Ordovician rocks into the Ibex basin of west-central Utah and the northern Utah basin. Facies interpretations and detrital zircon data were used to establish depositional environment and provenance of the Eureka Quartzite sands adjacent to the Tooele Arch. Depositional environments in this area record an offshore-to-onshore shelf transition with five facies. Offshore facies are more commonly recognized in the Crystal Peak and Wah Wah Mountain sections, the center of the Ibex basin. Facies B-E are recognized in additional locations more proximal to the Tooele Arch or the Laurentian shoreline. Three high frequency sequences (E1, E2, E3) are recorded in the Crystal Peak section with sequence E2 only occurring in locations more proximal to the shoreline and the Tooele Arch. A majority of well exposed outcrops are dominated by intense bioturbation (Bioturbation Index 5-6).

Detrital zircon signatures in all Eureka Quartzite samples in this study show a strong dual-peaked distribution of Paleoproterozoic-Archean and Trans-Hudson Orogenic (~2.6-2.8 Ga and ~1.8-2.0 Ga, respectively) age zircons. ~1.6-1.8 Ga grains correspond to the nearby Yavapai-Mazatzal provinces. Small, but persistent peaks at ~2.0-2.1 Ga, ~2.4-2.6 Ga, ~2.9-

3.0 Ga, give insight into additional provenance areas. Most of the sediment in the Middle-Late Ordovician Eureka Quartzite was shed off the Transcontinental Arch, Wyoming Craton and multiple smaller terranes east of the Laurentian margin. Underlying Late Proterozoic and Cambrian siliciclastic units commonly contain Grenville (0.8-1.2 Ga) and granite-rhyolite province derived zircons (1.4-1.5 Ga) that are essentially absent in the Eureka Quartzite, however, indicating its sands are primarily first cycle deposits and multi-cycled detritus was not a large contributor. It is unlikely that the west-east trending Tooele Arch provided siliciclastic sediment to the Eureka Quartzite. Detrital Zircon data suggests potential for influence by the arch on sediment distribution patterns, however additional data is required. The two locations most proximal to the Tooele Arch show a consistently weak Archean ~2.6-2.8 Ga peak, suggesting limited sediment input from Archean crust, such as the Wyoming province, Medicine Hat Block, or Sask province. Dual-peak zircon signatures vary temporally at locations and may reflect changes in provenance and the potential impact of relative sea level during deposition.

DEDICATION

In memory of my Father, Alberto Luis Lira (1963-2014)

ACKNOWLEDGEMENTS

I would like to express my sincere gratitude to my committee chair, Dr. Michael Pope, for allowing me to carry forth my academic ambitions over the course of my studies, both as an undergraduate and graduate student, at Texas A&M. Seven years ago I would have never thought the kid from Small Town, Texas would get the opportunity to travel the western United States encountering some of the most fascinating geology in North America. I want to thank my committee members, Dr. Brent Miller and Dr. Walter Ayers, for their guidance and support throughout the duration of this project. Their knowledge and expertise have been of great help evaluating data and refining this paper.

The friends and faculty within the Department of Geology & Geophysics have been nothing short of amazing. Dr. Ray Guillemette and Luz Romero were key members throughout this study and I am extremely grateful for their assistance. To the many friends I made over the years, thank you all for making the semesters easier to handle and for making the late nights in Rm.308 a little more bearable. I especially want to thank you all for the comfort through the worst of times. I also want to thank Taylor Law for his help out in the field, trekking throughout Utah and Nevada.

I really want to thank my family, my father, mother, and brothers, for all their support and encouragement through it all. I especially want to thank my Wife, who has been through so much as we worked our way through school. The love, patience, and guidance through the good and bad were more than I could ask for.

Thank you to the American Chemical Society for sponsoring this research project and to the Geological Society of America-Research Grant for their contribution to my field work.

TABLE OF CONTENTS

Page

ABSTRACT ii

DEDICATION iv

ACKNOWLEDGEMENTS v

TABLE OF CONTENTS vi

LIST OF FIGURES viii

LIST OF TABLES ix

INTRODUCTION 1

- Geologic Setting 2
- Previous Provenance Work 4

METHODS 6

- Field Work and Sample Location 6
- Sample Preparation 6
- Sample Analysis 8
- Data Reduction 9
- Zircon Data Presentation 10

RESULTS 12

- Measured Sections 12
- Facies Descriptions and Interpretations 14
- Zircon Standard Results 16
- Detrital Zircon Results 18
- Detrital Zircon Variability 20

DISCUSSION 22

- Depositional Environment 22
- Sequence Stratigraphy 22
- Potential Detrital Sources 24
- Sequence Stratigraphy and Provenance Change 26

CONCLUSION 29

REFERENCES 31

APPENDIX A 39

APPENDIX B 53

APPENDIX C 56

APPENDIX D 78

APPENDIX E 87

APPENDIX F 96

APPENDIX G 110

APPENDIX H 119

LIST OF FIGURES

FIGURE Page

1. Map of Western North America and Basement Rocks 39
2. Stratigraphic Correlation Chart of Middle-Upper Ordovician Quartz Arenites of Western United States and U.S. Mid-Continent 40
3. Map of Western Utah and Eastern Nevada Study Areas (modified from Webb, 1958) 41
4. Measured Sections with Sequence Stratigraphic and Facies Interpretations 42
5. Mounted Zircons with Corresponding Backscattered Electron and Cathodoluminescence Images 43
6. Depositional Environments Profile 44
7. Pictures of Offshore Environment 45
8. Pictures of Lower Shoreface Environment 46
9. Pictures of Middle Shoreface Environment 47
10. Pictures of Upper Shoreface Environment 48
11. Pictures of Tidal-Subtidal Flat Environment 49
12. Standard Zircon Results 50
13. Detrital Zircon Results 51
14. Impact of Sequence Stratigraphy on Provenance (from Pope, 2008) 52

LIST OF TABLES

TABLE Page

1. Study Locations 53

2. Facies Descriptions and Interpretations.....54

3. Similarity and Overlap 55

INTRODUCTION

The Middle-Late Ordovician Eureka Quatzite is a unique supermature quartz arenite that was deposited along the Early Paleozoic passive margin of western Laurentia (Webb, 1956, 1958; Ketner 1968; Gehrels & Dickinson, 1995; Wallin, 1990). The Eureka Quartzite and its equivalents are the only regionally widespread (Fig. 1) mature siliciclastic deposits within the thick Cambrian – Devonian carbonate dominated successsion (Webb, 1958). The quartz arenite is well exposed in the eastern Great Basin of Nevada and Utah (Webb, 1958). Depositional environments for the Eureka Quartzite and age equivalents (Fig. 2) range from eolian to near shore and shallow-marine settings with a majority having been deposited during a prolonged Middle Ordovician sea level lowstand (Webb, 1958; Klein, 1975). Ordovician rocks, particularly quartz arenites, are either absent or relatively thin between Early and Late Ordovician strata across the broad, west-east oriented Tooele Arch (Webb, 1956, 1958; Hintze, 1959). Detrital zircon geochronology of Middle-Late Ordovician quartz arenite suggests the source for the Ordovician quartz arenites units was the Peace River Arch, Canada, and sand was transported by longshore currents along the Laurentian shoreline (Gehrels and Dickinson, 1995; Gehrels et al., 1995; Gehrels, 2000). Trends in these quartzite units include southward thinning, fining, and increased maturation along the western Laurentian margin (Ketner, 1966, 1968).

The primary objective of this study is to determine the provenance of the Eureka Quartzite strata at proximal locations along the Tooele Arch through the integration of laser ablation inductively coupled plasma mass spectrometry (LA-ICP-MS), detrital zircon geochronology and sequence stratigraphic principles.

This study focuses on fourteen detrital zircon samples from five geographic locations in western Utah and eastern Nevada (Fig. 3). Detrital zircon populations will assist in establishing if the Tooele Arch was an active structural element during Ordovician sediment deposition as well as if it supplied detritus to the Ordovician units. The sequence stratigraphy of the Eureka Quartzite records the spatial and temporal distribution of sand sources throughout the Middle-Late Ordovician (Pope, 2008).

Geologic Setting

The Late Proterozoic breakup of the supercontinent Rodinia initiated rifting of western Laurentia (Stewart, 1972; Bond and Kominz, 1984; Hoffman, 1989). The western Laurentia passive margin persisted from the latest Neoproterozoic to the Late Devonian resulting in deposition of a thick Lower Paleozoic succession (Armstrong, 1968; Druschke et al., 2009), most of which are shallow water carbonates. Paleogeographic reconstructions place the western Laurentian margin in the northern hemisphere with a general northeast-southwest trend, nearly parallel to the equator at low tropical latitudes (Witzke, 1990; Van der Voo, 1993). Most tectonic reconstructions suggest the Cordilleran passive margin did not to receive its sediment from a western source (Wallin, 1990, 1993; Gehrels et al., 2000). The Middle-Late Ordovician quartz arenite was deposited across the length of the western passive margin, except in areas where topographically high structures (e.g. Lemhi Arch, Salmon River Arch, Tooele Arch) formed relief, which restricted sediment deposition and preservation (Sloss, 1954; Webb, 1958; Hintze 1959; Armstrong, 1975; Ruppel et al., 1975). Ordovician quartz arenite thicknesses vary regionally between 100-150 meters along much of the Laurentian shore (Ketner, 1968; Druschke et al., 2009). Sedimentary structures in the Eureka Formation, as well as the presence of locally interfingering dolostone beds with the

Ordovician sands indicates most siliciclastic deposition occurred in shallow marine environments (Webb, 1958; Drueschke et al., 2009). The age of this unit is uncertain due to the lack of abundant fossils (Fig. 2). Regionally, conodont biostratigraphy and stable isotope chemostratigraphy indicate the Eureka Quartzite was deposited from middle Mohawkian to early Cincinnatian (Sweet, 2000; Saltzman et al., 2003; Saltzman and Young, 2005).

The vitreous quartz arenite was deposited unconformably on underlying carbonate units across a sharp contact (Webb, 1958; Zimmerman and Cooper, 1999). The Eureka Quartzite was previously sub-divided into three distinguishable units which outcrop regionally: 1) a locally developed basal quartz sandy dolomite and brown-reddish cross-bedded quartz sandstone, 2) vitreous white quartz arenite constitutes the bulk of the unit, and 3) an uppermost dolomitic quartz arenite (Webb, 1958). The upper unit is now interpreted to be the lowermost part of the overlying Ely Springs Dolomite (Leatham, 1985) and the Eureka Quartzite and overlying Ely Spring Dolomite contact is unconformable and the duration of this hiatus is uncertain (Zimmerman and Cooper, 1999).

The Eureka Quartzite thins from Lakeside, Utah to Ruby, Nevada, where the Tooele Arch sub-divides the western Utah Middle Ordovician rocks into the Ibex basin of west-central Utah and the northern Utah basin (Webb, 1958). The Tooele Arch is recognized as the most western continuation of the Proterozoic Uinta Mountains, and it is thought that uplift of the arch occurred from the Cambrian through the Upper Devonian (Burchfiel et al., 1992; Pooele et al., 1992). The Swan Peak Quartzite (Fig. 3), in southwest Idaho, pinches out against the northern flank of the Tooele Arch (Hintze, 1959). The Eureka Quartzite is present in areas adjacent to the Tooele Arch proposed location (Fig. 3), but it is not preserved over an extensive part of northwestern Utah and eastern Nevada (Webb, 1958; Hintze, 1959).

Isopach maps of the Eureka Quartzite and age equivalent units consistently show an absence of quartz arenite over the Tooele Arch (Webb, 1958; Ross, 1964). Previous studies (Oaks et al., 1977) suggest that early Paleozoic sedimentation in the northern portion of the western North American Great Basin was influenced by this positive feature.

Previous Provenance Work

Initial detrital zircon data from the Eureka Quartzite, and its age equivalent units, record distinct grain populations that are consistent within these quartz arenites (Gehrels et al., 1995; Gehrels and Dickinson, 1995; Gehrels, 2000). However, these samples were not incorporated in any stratigraphic context and thus do not give insight to spatial or temporal changes of grain populations throughout the Eureka Quartzite. Zircon data were acquired from four detrital zircon samples of a total of 158 grains (Gehrels et al., 1995) using isotope dilution thermal ionization mass spectrometry (ID-TIMS). This is a high spatial resolution method that delivers data with high precision and accuracy, but it requires a great deal of time and capital to achieve such high-quality data. The data have a dual peak distribution of ~1.8-2.0 Ga and ~2.5-2.8 Ga age ranges. Smaller peaks include age populations of ~2.1 Ga and ~0.8-1.2 Ga. Subsequent data analysis of ~100 grains acquired through laser ablation inductively coupled plasma mass spectrometry (LA-ICP-MS) on the same samples used for ID-TIMS analysis verified the previous results (Gehrels pers. com., 2008). The current transportation model suggests that sediment was delivered through long-shore drift currents (Fig. 1) along the western passive margin (Gehrels and Dickinson, 1995; Gehrels et al., 1995). The Peace River Arch, B.C., Canada was proposed as the sole sediment source based on southward thinning and increase in textural maturity (Ketner, 1966, 1968; Gehrels, 2000). This transportation model would limit the potential for more proximal sources from exposed

basement rock east of the passive margin. More recent detrital zircon geochronologic studies of the Middle-Late Ordovician quartz arenite are incorporated in a sequence stratigraphic framework and may provide more insight on the complex depositional patterns of this Ordovician unit (Baar, 2009; Wulf, 2011; Hutto, 2012; Workman, 2013).

METHODS

Field Work and Sample Location

Detailed stratigraphic sections of the Eureka Quartzite were measured from the Pogonip Group-basal Eureka Formation contact to the upper Eureka Formation-Ely Springs Dolomite contact (Fig. 4). Descriptions included grain size, sorting, roundness, and sedimentary structures. Samples of the Eureka Quartzite and the basal sandy Ely Springs Dolomite were collected at well exposed outcrops (Table 1). Samples were collected at the base and top of the Eureka Formation and samples of the Ely Springs Dolomite were collected within a meter of its contact with the Eureka Formation. In addition, samples were collected at the base and top of long-term sequences (E_1, E_2, and E_3) interpreted within the measured sections.

All samples were crushed to ~16-33 cm^3 in size on the outcrop to reduce the possibility of contamination with other units. Stratigraphic sections were measured at 5 locations (Fig. 3) adjacent to the Tooele Arch in western Utah and eastern Nevada. Sampling locations in Nevada were restricted to eastern outcrops due to structural and stratigraphic complexities in central and western Nevada produced by the onset of the Antler Orogeny (Miller et al., 1992; Dickinson, 2013). An effort to collect samples in northeastern Nevada, northwest of the Tooele Arch, was unsuccessful due to intense Tertiary volcanic cover disrupting preservation of the quartz arenite and government and private land access restrictions.

Sample Preparation

Sample preparation was completed in Texas A&M University Department of Geology & Geophysics facilities. Heavy minerals were extracted from their host rock using

conventional separation techniques. Each quartz arenite sample was crushed using a Bico Jaw Crusher and were pulverized using a Bico Disc Mill. The samples were then separated by their unique mineral density using a Wilfley Table with a peak angle of 30˚. Less dense minerals, primarily quartz, were dried and saved for future potential separations. Collected heavy minerals were rinsed in ethyl alcohol to reduce iron oxidation and were dried. Magnetic grains and metal shavings from the machinery were removed using a neodymium-boron hand magnet. Heavy minerals were separated using Methylene Iodide (MEI) under a vented-hood. Zircon and additional minerals that fell out of suspension in MEI were rinsed in acetone followed by rinsing in ethyl alcohol. The detritus was transferred to a petri dish with ethyl alcohol and examined under a binocular microscope. Using a dental pick, additional accessory minerals (apatite, titanite, pyrite) were separated from the detrital zircon grains.

Double-sided tape was adhered to a square glass plate. Rings, approximately 5 mm in diameter, were cut from a disposable pipette and were set on the tape. The ring's served as a means of restricting zircon dispersion throughout the tape and to organize the samples and standards. A random of zircon grains was pipetted from the ethyl alcohol petri dish and were placed in each ring. A ~2.5 cm diameter plastic ring was placed around the samples and epoxy was poured into the ring and allowed to solidify overnight. An epoxy puck generally contained from 1-3 unknown zircon samples with additional zircon standards. The puck was then lathed down to a thickness of ~5 mm, fine polished, then carbon coated and imaged on a Cameca SVX50 microprobe using Backscattered Electron Microscopy and Cathodoluminescence (Fig. 5). The imaging of the samples assisted in the identification of intracrystalline heterogeneity, such as cores, multiple zones, or inclusions and determining the most suitable location for *in situ* laser ablation analysis.

Zircon selection for puck mounting was executed with a quantitative analysis approach (Fedo et al., 2003). Grain characteristics, such as color and morphology, were not considered when transferring grains from the petri dish to the mounting square. This methodology allows for the analyzed grain populations, and their respective abundance, to be a result of random choice and limits the potential for sample biasing (Fedo et al., 2003). Previous detrital zircon studies on the Eureka Quarztite were pursued with a qualitative analysis approach where different grain populations were grouped and analyzed together based on a variety of optical characteristics of zircon grains (Gehrels et al., 1995; Gehrels, 2000).

Sample Analysis

Laser ablation inductively coupled plasma mass spectrometry (LA-ICP-MS), was used throughout this study on the polished mounted zircon grains with an Analyte 193 Ultra Short Pulse Excimer Laser Ablation System coupled with an Element XR High Resolution Single Collector ICP-MS in the Radiogenic Isotope Lab at Texas A&M University. LA-ICP-MS was a suitable method for this study for a multitude of reasons, including the ability to rapidly acquire a statistically reasonable number of analyses adequate for a provenance study (Kosler et al., 2001; Kosler et al., 2003; Vermeesch, 2004). Traditional provenance techniques, such as petrographic methods (Weltje et al., 2004), would be insufficient to apply to Eureka Quartzite samples due to its maturity (McBride, 2012). A large data set for each sample must be acquired to be sure that all potential sources are identified (Sircombe, 1999). Zircon standards used throughout the study included; Peixe (564 Ma, Gehrels, 2010), FC-1 (1099.9 Ma, Paces and Miller, 1993), R-33 (419.3 Ma, Black et al., 2004), and 91,500 (1065 Ma, Wiedenbeck et al., 1995). The Peixe standard was the primary standard, whereas FC-1,

R-33, and 91500 were analyzed as secondary standards. Additional standard material used included NIST 610 and 612, manufactured glass samples containing a suite of elements that were designed to provide a set of reference elements at a varying range of concentrations (Hinton, 1999). In this study, the glass samples were primarily used to warm up the laser and tune the mass spectrometer to maximize signal intensity and stability before the start of a sample analysis (Chang et al., 2006). Samples were analyzed in groups amongst the primary and secondary standards. A complete group consisted of the following order: 4 Peixe analysis, 2 FC-1 analysis, 6-7 unknown sample analyses, 2 R-33/91500 analysis, 6-7 unknown sample analyses. Laser parameters used throughout the analysis were; a repetition rate of 10 Hz, a spot size of 29.6 μm, and a fluence of 2.02 J/cm^2 (40% energy). All parameters were kept constant for standards and unknowns to minimize the potential for bias. Each analytical session began with the analysis of a zircon standard to stabilize fractionation. A single analysis consisted of a 35 second acquisition of a blank measurement recording the elemental composition of the carrier gas, an argon-helium mixture, followed by a 35 second sample measurement of the aerosol recording 300 elemental passes.

Data Reduction

Data acquired from laser ablation analysis were imported into an Excel program with Visual Basic macros in which the blank results were subtracted from the corresponding sample analysis (Chang et al., 2006). Data points outside of a linear regression with a 95% confidence range were removed. Fractionation factors were calculated from the standard zircon analysis performed before and after each group of unknown samples. Fractionation factors were then applied to their corresponding group of unknown samples using Peixe standard data (Chang et al., 2006). All zircon data were compiled into a final data summary

spreadsheet in which unknown samples with >10% discordance were culled and not reported in the final results. Concordant data were then plotted on binned histograms with probability-density plots and Tera-Wasserburg concordia diagrams utilizing Isoplot 4.15 (Ludwig, 2003). All data are presented at 1σ.

Zircon Data Presentation

Age populations for detrital zircons were determined for samples from the top and base of multiple sections. Additional samples were collected of the overlying sandy-dolomite where the Ely Springs Dolomite and the Eureka Quartzite had a distinct contact. Several samples were also collected where multiple sequences were interpreted within the measured section (Fig. 4). Individual analyzed zircon crystals varied in physical characteristics. Most of the analyzed zircons were colorless and ranged in from ~100 – 200 μm with no inclusions and minimal to no zoning. Zoned crystals were sampled at their cores to avoid crossing the laser spot into multiple zones. To minimize zircon analysis with high discordance or errors in U/Pb age calculations, highly zoned zircons or zircons with large inclusions were not analyzed. Calculated U-Pb ages >10% discordant were not recorded in the final results.

Traditionally, U-Pb data are plotted on Wetherill or Tera-Wasserburg concordia diagrams (Wetherill, 1956; Tera and Wasserburg, 1972). However, in large analytical studies, these plots are difficult to navigate visually (Sircombe, 1999). Alternatively, binned histograms and probability-density plots may be used to display measured age populations (Gehrels and Dickinson, 1995; Anderson, 2005; Sircombe, 1999). The binned histogram plots provide a suitable visual representation of prominent age populations acquired through random sampling (Anderson, 2005). A compiled image of all histogram plots allows for an efficient quantitative comparison of all study locations. Ultimately, histogram plots are

limited by the chosen bin size and the lack of incorporating errors associated with each age. The bin size is arbitrary and requires a median between a minimum value that will distribute data into too much detail and a maximum value that will over-smooth data and limit grain populations to only a few peaks (Sircombe, 2000).

The bin width in this data set is 50 Ma. Probability-density plots consider the individual age errors in trying to calculate the probability-density distribution. As a result, the probability-density plot is not only effected by the number of grains per age population, but is also a result of the precision of the data within a specific age range (Sircombe, 2000). In this study, binned histograms and probability-density plots are used in conjunction.

RESULTS

Measured Sections

The Eureka Quartzite was described in five locations in proximity to the, west-east trending, Tooele Arch (Fig. 3). The Davis Mountains and Pahvant Range sections are located more landward relative to the Cordilleran passive margin (Kay, 1951; Hintze, 1959; Pooele and others, 1992). The Davis Mountains section is approximately 29 km (18 miles) from Vernon, Utah. The thickness of the measured section is 74 m, but the basal contact with the Pogonip Group was not exposed. The Eureka Quartzite is naturally fractured throughout the study area and is heavily iron stained. The contact with the overlying Ely Springs Dolomite is sharp. Two samples were retrieved from the Davis Mountains location, from the base of the exposed outcrop, and the top of the outcrop just below the Ely Springs Dolomite contact (Fig. 4).

The Pahvant Range section is approximately 117 km (72 miles) southeast of the Davis Mountains section and is 45 m thick. Samples were collected at the base and top at this location. The basal contact with the underlying Pogonip Group was covered. The upper contact with the Ely Springs Formation was visibly sharp in areas where soil did not cover the outcrop. This section is heavily bioturbated in multiple areas including the base and throughout most of its middle portion.

The Crystal Peak (Wah Wah Mountains) section is located furthest south, approximately 133 km (82 miles) southwest from the Pahvant Range Section, and within the Ibex Basin, also recognized as the House Range embayment. It is the thickest section in the study at 203 meters (Webb, 1958; Hintze, 1959; Rees, 1986). The basal contact of the Eureka Quartzite with the underlying Crystal Peak Dolomite is transitional, with siliciclastic

sediments increasing through the transition between the two formations. The boundary between the Eureka Quartzite and the underlying Crystal Peak Dolomite was chosen based on a distinct change in the weathering profile and the absence of chert nodules more prominent in the dolomite. Sedimentary structures throughout the section are difficult to recognize due to the supermature nature of the rock. The upper contact with the overlying Fish Haven Dolomite is a sharp, well defined surface. Samples were collected at the base and top of the Eureka Quartzite. Additional samples within the unit were collected at the top of interpreted internal sequences (Fig. 4), and at the base of the overlying Ely Springs Dolomite Formation.

The Schell Creek Range section is about 123 km (76 miles) northwest of the Crystal Peak section and about 13 km (8 miles) of McGill, NV. The section is 33 meters thick. The basal contact with the Pogonip Group is covered. The section has a unique pockmarked texture throughout the outcrop. The upper contact with the Ely Springs Formation is a sharp, irregular unconformity across the outcrop. Samples were collected from the base and top of the Eureka Formation, as well as from the Ely Springs Dolomite just above the upper contact.

The Cherry Creek Range section is 69 km (25 miles) northwest of the Schell Creek Range section. It is 31 meters thick and has several covered intervals. The basal contact is transitional. The outcrop has a 12 meter thick interval that is extremely bioturbated and has a pockmarked texture similar to the Schell Creek Range section. The contact with the overlying Ely Springs Formation is covered by soil and scree. Quartz arenite samples at this location were collected at the base and top of the exposed outcrop.

Facies Description and Interpretations

Five facies (Fig. 6) types are recognized at different study locations in the Eureka Quartzite (Table 2). The facies vary vertically throughout each location. By identifying the variability of each facies at each location, depositional environments and the effects of relative sea level changes were interpreted.

Clastic input in Facies A was initially minimal and deposited sediment were predominantly very fine to fine grain sands with silty-finely crystalline dolomite (Miller, 1977; Howard et al., 1981). A common bedding feature is thin, 1-3 cm thick parallel laminations, which were preserved where bioturbation was less intense. Additional features include massive beds with fine to medium coarse grained sandstone that is more persistent at the base of the section. Intensely bioturbated beds are uncommon, but are preserved in several beds (Miller, 1977; Howard et al., 1981). Facies A represents an offshore environment that occurs only at the Crystal Peak section (Fig. 7).

The depositional environment of Facies B produced low-angle cross laminations with increased bioturbation. Bed thickness varies from thin to medium, 0.5 to 3 m. Quartz arenite characteristics in this facies generally are very fine to fine, well rounded, and well sorted sand. Massive beds also occur within this facies. Facies B records a lower shoreface environment (Fig. 8), identified by preservation of cross laminae that indicate a higher energy environment (Arnott, 1993).

Facies C consists of fine to medium grain sandstone in medium to thick beds. Low-angle planar cross beds are occasionally preserved in this facies (Fig. 9). This facies indicates a high energy flow and considerable sediment supply (Reinson, 1984; Runkel et al., 2007). Vertical burrows are common, whereas, horizontal burrows, such as planolites, appear in the

outcrop. A distinct pock-mark weathering texture makes its first appearance in this facies. One interpretation suggests they are the result of leaching of carbonate-cemented concretions (McBride, 2012; Hintze and Davis, 2003). However, differential weathering of these intensely bioturbated intervals may also be possible. This facies is interpreted to record a middle shoreface environment.

Facies D, an upper shoreface environment, is the most easily recognized and common facies throughout the study area (Fig. 10). Grains are fine to medium, well rounded and well sorted sand. Massive quartz arenite beds with faint remnants of low-angle cross laminae also are common. *Skolithos* trace fossils are the most common structure in this facies and likely disturbed the original depositional fabric and produced it's intensely bioturbated texture. The favorable environment for organisms with the constant deposition of sediment would account for such intense sediment disturbance (Desjardins et al., 2010). The pocket-like weathering pattern recognized in Facies C is more abundant and common in Facies D (Fig. 10.A).

Facies E is fine-medium grain, well rounded, and well sorted sands that have faintly visible parallel laminations and also are intensely bioturbated (Fig. 11). Horizontal and vertical bioturbation is extremely common. The appearance of parallel laminae and heavy bioturbated sands indicates a constantly fluctuating water depth more likely controlled by high energy oscillating tides in a tidal flat or foreshore depositional environment (Reinson, 1984; Short, 1984; Plint, 2010).

The Eureka Quartzite in western Utah and eastern Nevada was deposited in a shallow marine environment along the cost of a passive margin in a shallow marine environment (Ketner, 1968; Druschke et al., 2009). Field observations suggest various transitions between depositional environments from lower shoreface to a foreshore depositional setting.

Interpreted facies record deposition along a shoreface profile (Fig. 6). The Ibex Basin, south of the Tooele Arch (Hintze, 1959), increased the preservation potential for distal shelf deposits and a thicker stratigraphic section of the Eureka Quartzite Formation. Minute percentages of dark heavy minerals, rock fragments, and organic-and iron-oxide-stained detrital clay minerals produce the distinctly uniform vitreous white color of the Eureka Quartzite and cause its bedding structures to be less obvious (McBride, 2012).

Zircon Standard Results

Secondary standards were used throughout the study to assess reproducibility and precision of the unknown detrital zircon samples. Samples FC-1, 91,500, and R33 were treated as unknown samples and then corrected using the same fractionation factors applied to the sample unknowns. Fractionation factors for correction of mass and elemental fractionation were determined by averaging 7-8 $^{206}Pb/^{238}U$, $^{207}Pb/^{235}U$, and $^{207}Pb/^{206}Pb$ analyses of the Peixe standard before and after each group of unknown samples. These averages were then divided by the respective accepted isotope ratio value for the Peixe standard (Change et al., 2006) to determine the fractionation factor. All primary and secondary standard data (FC-1- 207 analyses; R-33: 250 analyses; 91,500: 29 analyses) were compiled onto a single chart to display graphically any trends or relationships between drift or offset in fractionation factor and the resulting age calculation (Fig. 12). The upper portion of the chart displays the fractionation factors (FF = true ratio/measured ratio) for $^{206}Pb/^{238}U$, $^{207}Pb/^{235}U$, and $^{207}Pb/^{206}Pb$ isotope ratios recorded for the Peixe standard throughout this study. The $^{207}Pb/^{206}Pb$ fractionation factor ranged from 0.90-1.10. The $^{206}Pb/^{238}U$ and $^{207}Pb/^{235}U$ ratios display both scatter and distinct session-to-session offsets with an overall low of 0.66 to a high of 2.22. Analyses recorded during the month of February, 2014, for

example, show a distinctly high fractionation. These values resulted from an external issue during the transport of the carrier gas and aerosol from the laser into the mass spectrometer (e.g., an air leak into the sample housing or carrier gas line). Nevertheless, most of the secondary standard ages recorded in this time frame (especially those of R33) fall within two standard deviations of the mean, and none show elemental anomalies within their mass spectrums.

FC-1 standards averaged a $^{207}Pb/^{235}U$ age of 1092.3 Ma with a standard deviation error of 34.3 Ma. This equated to a 3.14% standard deviation and a 0.6% error from the accepted age. The average $^{206}Pb/^{238}U$ age for FC-1was 1111.6 Ma with a standard deviation error of 50.5 Ma. Percent standard deviation was 4.5% and the average age resulting from a 1.1% difference from the accepted standard age. The average $^{207}Pb/^{235}U$ age for R33 standards was 417.6 Ma with a standard deviation of 25.2 Ma. This resulted in a 6.0% standard deviation and a 0.3% difference from the R33 accepted age. $^{206}Pb/^{238}U$ data for R33 averaged 412.8 Ma with a standard deviation of 20.8 Ma. The percent standard deviation was calculated to be 5.0% with a 1.4% age difference from the accepted age. 91500 standards measured an average age of 1063.1 Ma for $^{207}Pb/^{235}U$ with a standard deviation of 17.6 Ma resulting in a 1.65% reproducibility. The average age deviated from the accepted age of 91500 by 0.17%. The average age for $^{206}Pb/^{238}U$ was 1068.9 Ma with a standard deviation of 28.1 Ma or 2.62%. The calculated average represents a 0.36% accuracy. Therefore, reproducibility is on the order from 1.6-6.0% and accuracy ranges from 0.1-1.5% for detrital zircon samples.

Detrital Zircon Results

Analysis of the samples acquired for this study highlight age population abundance and any variance from the base to the top of the formation. Sediment sourcing from multiple basement provinces is likely evident in changes in peak height of the probability density curve, the abundance of grains confined to certain age bins, and the less persistent peaks that may occasionally be recorded (Fig. 13).

The basal Davis Mountain sample is comprised of 112 zircon grains having a dual age distribution with a dominant Archean peak of ~2.5-2.9 Ga and a smaller Paleoproterozoic peak ranging from ~1.8-2.0 Ga. The apex of the Archean grains occurs between ~2.6-2.7 Ga. In addition, very small peaks of ~0.9-1.2 Ga, ~2.4-2.5 Ga, and ~2.9-3.0 Ga occur. The upper Davis Mountains sample has a similar grain distribution within its 117 grains. The ~2.5-3.0 Ga peak has decreased in abundance, whereas the 1.8-2.0 Ga peak has almost doubled in height. In both samples, the apex of the Paleoproterozoic age peak ranges from ~1.8-1.9 Ga. Less significant peaks of ~1.0-1.2 Ga, ~1.4-1.5 Ga, ~2.0-2.1 Ga, and ~2.3-2.4 Ga also occur in this sample.

The Pahvant Range basal sample consists of 104 grains having a high abundance of ~2.5-2.9 Ga grains. A small population of ~1.8-1.9 Ga grains is the second largest with less significant peaks of ~0.9-1.1 Ga and ~3.0-3.1 Ga. The upper Pahvant Range sample, consisting of 106 grains, has a less dramatic ~2.5-2.8 Ga peak that is only slightly greater in height than the ~1.8-2.0 Ga peak. Various smaller populations appear within the data, including; ~0.5 Ga, ~0.9-1.2 Ga, ~1.6 Ga, ~2.0-2.1 Ga, ~2.8-2.9 Ga.

Five samples were collected from the Crystal Peak section, including the base, the top, a sample from the overlying Ely Springs Dolomite Formation, and two samples which

correspond with the top of two interpreted sequences (E_1, E_2) within the Eureka Quartzite. All samples have a multi-peak distribution of ~1.8-2.0 Ga and ~2.5-2.8 Ga grains. The ~1.8-2.0 Ga grains are consistently the most abundant, indicated by their highest peak. A smaller peak of ~2.0-2.2 Ga also appears in all samples with a varying abundance. Additional peaks that are less significant throughout these samples represent ~0.9-1.2 Ga, ~2.3-2.5 Ga, and ~3.0-3.3 Ga zircons populations. The sample from the Ely Springs Dolomite includes a few grains of ~0.46-0.55 Ga, ~1.25 Ga, and ~1.5-1.6 Ga zircons.

The Cherry Creek Range basal sample (102 grains) consists of a larger peak of ~1.8-2.0 Ga grains and a smaller yet significant peak of ~2.5-2.8 Ga grains with several smaller peaks that, for instance, ~1.0-1.2 Ga, ~2.0-2.1 Ga, and ~2.2-2.5 Ga probability peaks. The upper Cherry Creek sample contains 100 grains displaying a similar dual grain distribution with the ~1.8-2.0 Ga peak being significantly greater than the ~2.5-2.8 Ga peak; other peaks occur at, ~2.0-2.3 and ~2.9-3.0 Ga.

The basal sample of the Schell Creek Range is comprised of 143 grains. The data shows a distinct peak of ~1.8-2.0 Ga grains and an additional, lesser peak ranging from ~2.5-2.8 Ga. Several grains recorded ages of ~2.0-2.4 Ga and very few ~1.6-1.8 Ga grains. The upper Schell Creek sample containing 115 grain analysis records a similar bimodal signature. A sharp peak of ~1.8-2.0 Ga grains dominated the dataset with a smaller ~2.5-2.8 Ga peak, with less significant peaks at ~0.9-1.0 Ga, ~2.0-2.2 Ga, and ~2.2-2.5 Ga grains. The most upper sample from the Schell Creek locality, from the base of the Ely Springs Dolomite Formation, contains 105 grains, with a large probability peak of ~1.8-2.0 Ga grains and a much smaller ~2.5-2.8 Ga peak. ~1.75-1.8 Ga grains also were common in this sample and the ~2.0-2.2 Ga population is more prominent than in the upper Eureka Quartzite sample.

Detrital Zircon Variability

Two statistical methods were used to aid in the study of spatial differences in detrital zircon populations; overlap and similarity (Table. 3). This allows analyzing samples from the same geological unit but different geographic locations. The contrasting data sets are normalized and output values range from 0.0 to 1.0. A perfect overlap or similar proportions of overlapping ages are characterized by a 1, suggesting that all grains within the tested sample were derived from the same source as the standard sample. Any subtle differences between data sets will be reflected by a decrease in the value to a minimum of 0.0 (Gehrels, 2000). Overlap indicates which grain ages within the samples overlap with ages of the standard, whereas similarity measures whether the proportions of overlapping ages are similar by summing the square root of the product of each pair of probabilities for an age over the time period of interest (Gehrels, 2000). Overlap and similarity were calculated for the basal and top samples of each study location relative to a Eureka Quartzite data set acquired by George Gehrels (Fig. 13) consisting of 99 LA-ICP-MS zircon analyses (Gehrels pers. com., 2008).

Basal samples of all study locations resulted in overlap values from 0.706-0.893 and similarity values from 0.629-0.930. Overlap values for study locations relative to Gehrels' data (Gehrels pers. com., 2008) range from 0.706-0.821 and similarity values range from 0.687-0.891. This is indicative of similar probability age peaks throughout the study locations and Gehrels' dataset. Smaller similarity values indicate there are smaller proportions of the identified probability ages, specifically at the Davis Mountains and Pahvant Range locations, which are further inboard than other locations (Fig. 3). Overlap and similarity values for samples collected at the top of each study location ranged from 0.725-

0.852 and 0.794-0.922, respectively. Values calculated relative to Gehrels' data were consistently high for both statistical comparisons indicating a good correlation of probability age peaks between datasets. The Pahvant Range sample recorded the lowest overlap value due to a very high probability peak at the 2.5-2.8 Ga and a less pronounced 1.8-2.0 Ga peak (Fig. 4).

DISCUSSION

Depositional Environment

The Eureka Quartzite Formation along the western Laurentian margin was deposited on a siliciclastic shelf during a time of tectonic stability and decreased basinal subsidence (Bond et al., 1988; Witzke, 1990; Levy and Christie-Blick, 1991). The shallow shoreface environment preserved multiple facies that were predominantly tidally influenced and heavily altered by marine organisms within an upper shoreface/foreshore setting. A decrease in bioturbation and preservation of plane-parallel laminae and low-angle cross stratification in the most upper portion of the Eureka Quartzite may represent a prograding siliciclastic shelf due to an increase in sedimentation and decrease in accommodation space (Zimmerman and Cooper, 1999). The lack of interbedded shale throughout regional outcrops and minimal detrital clay most likely indicates winnowing of clay-silt size particles that were deposited basinward (Dott, 2003; McBride, 2012). Large volumes of sediment were likely transported off the Transcontinental Arch from their source through a series of energy regimes that enhanced maturity before coming to its final depositional environment along the Cordilleran shelf (Pettijohn, 1949; Ketner, 1966; Dott et al., 1986; Dott, 2003).

Sequence Stratigraphy

Sequence stratigraphic interpretations were formed by the current understanding of sequence stratigraphic principles (Catuneanu et al., 2009). The definition of a sequence follows that of Mitchum (1977), a relatively conformable succession of genetically related strata bounded at its top and base by unconformities or their correlative conformities. Ideally, genetic surfaces within the succession would provide insight on multi-scale sequences and system tracts, but these surfaces are indistinct. The vertical stacking patterns of the

interpreted facies served as the foundation for identifying several sequences within the succession (Fig. 4). With the proposed identified facies and their relative stacking patterns, sequence stratigraphic surfaces were inferred. In each section, an abrupt change in facies associated with a transition from shallow to deeper water environments was interpreted as a sequence boundary. The Eureka Quartzite was interpreted as a transgressive succession representing a complete 3rd-order sequence (Zimmerman et al., 1999). The contact between the Eureka Quartzite and the underlying Pogonip Group is identified as the basal sequence boundary (SB-0) at the base of the Crystal Peak Section. The Eureka Quartzite and the Ely Springs Dolomite/Fish Haven contact represents the second or third sequence boundary (SB-2)/(SB-3) within the succession depending on its location. Field studies at the Crystal Peak section recorded three (E_1, E_2, E_3) high-frequency sequences (Fig. 4). Other study locations consisted of a single sequence, as sediment deposition and preservation was likely minimal at these locations because of their proximal position along the Tooele Arch or passive margin shoreline. Facies stacking patterns at the Cyrstal Peak location are consistent with a deepening in sea level likely recording a Transgressive Systems Tract. Sea level then reaches its maximum and begins to recede signifying the start of a Highstand Systems Tract. The unconformable contact between the Ely Springs Dolomite and the Eureka Quartzite Formation indicates a significant fall and erosion. The basal Ely Springs Dolomite was produced during the initial transgression that restabilished a widespread shallow-water carbonate platform over the quartz arenite on this passive margin. Regional biostratigraphy and chemostratigraphy indicate the Eureka Quartzite represents approximately a 10 m.y. period (Sweet, 2000; Saltzman et al., 2003). Smaller scale parasequences were indiscernible in the Eureka Quartzite measured sections of this study.

Potential Detrital Sources

Probability density-histogram plots consistently show a dual-peaked age distribution throughout all sample analyses suggesting a strong sediment provenance from potential inboard sources. Less pronounced peak also shed light on potential additional source areas. Composite basement maps and tectonic models assisted in deducing potential sources (e.g. Moores, 1991; Ross and Villeneuve, 2003; Whitmeyer and Karlstrom, 2007). The youngest potential source for sediment provenance, ~0.5-0.6 Ga, was granitic rocks associated with multistage rifting in western Laurentia (Whitmeyer and Karlstrom, 2007). Material of this age is not persistent and is limited to one sample. Sampled zircons within the age spectrum of ~0.9-1.3 Ga coincide with the Grenville Orogen, a tectonic event that occurred during the final assembly stages of supercontinent Rodinia consisting of polydeformed rocks metamorphosed to medium and high grade (Hoffman, 1989; Moores, 1991). The extent of the deformation is evident off the southwest coast of Labrador to the eastern U.S., central and west Texas, and in north central Mexico in the south (Mezger et al., 1992; Whitmeyer and Karlstrom, 2007). Sampled zircons within this age range may indicate recycling of sediments that were deposited originally by large fluvial systems extending to the western most parts of the Cordillera (Rainbird et al., 1992).

Zircons ranging from ~1.40-1.45 are associated with anorgenic granites, throughout the western and central U.S. (Anderson, 1989; Van Schmus et al., 1993). Middle-Late Cambrian quartz arenites also record a small population of these grains along the western Cordillera (Stewart et al., 2001). The ~1.6-1.8 Ga population are likely sourced from the proximal Yavapai and Mazatzal provinces (Fig. 1). The Yavapai province extends from Arizona to Colorado and is formed from the accretion of juvenile arc crust and multiple

magmatic episodes occurring from ~1.72-1.8 Ga. The Mazatzal province, ~1.6-1.72 Ga, extends from southwestern U.S. and continues adjacent to the Yavapai rocks and correlates to the Labradorian Orogeny in eastern Canada (Whitmeyer and Karlstrom, 2007).

The largest population of detrital zircon in this study is ~1.8-2.0 Ga grains that likely reflect sediment provenance from the Trans-Hudson Orogen (THO) that involved the suturing of the Hearne, Wyoming, and Superior crustal rocks to the Laurentian craton (Van Schmus et al., 1987; Ross and Villenueve, 2003; Whitmeyer and Karlstrom, 2007). This orogeny also includes the collision of the Medicine Hat block along the southwestern margin of the Hearne Province, just north of the Wyoming Province.

Paleoproterozoic-Archean crust accounts for an array of peaks, including the more pronounced ~2.6-2.8 Ga peak and the less consistent peak ranging from ~2.0-2.2 Ga, ~2.2-2.5 Ga, and ~2.8-3.0 Ga. Basement rocks that are associated with these ages include provinces proximal to the Cordilleran margin, such as the Hearne, Wyoming, Sask, Slave, and Medicine Hat Block (Ross and Villeneuve, 2003; Whitmeyer and Karlstrom, 2007). 2.0-2.4 Ga rifting is thought to have occurred prior to the collision between the Wyoming and Superior provinces, resulting in the deposition of passive margin sediments such as the Snowy Pass and Huronian Supergroups (Roscoe and Card, 1993). 2.01 Ga mafic dikes adjacent to the Cheyenne Thrust Belt flanking the southern edge of the Wyoming province support the rifting model (Cox et al., 2000). Crustal material of this age in the Cheyenne belt was corroborated by additional studies utilizing Nd model ages (Ball and Farmer, 1991). The Wyoming province, thought to be a continuation of the Hearne or Superior Province, consists of basement, older than ~2.5-2.7 Ga, overlain by the ~2.1-2.4 Ga marginal rocks of the Snowy Pass Supergroup spanning to ~3.0 Ga (Foster et al., 2006). The core of the Wyoming

province consists of ~3.0-3.6 Ga gneisses, deformational belts, and supercrustal rocks ranging from ~2.55-2.9 Ga (Whitmeyer and Karlstrom, 2007). The Sask Craton, previously thought to be juvenile magmatic material, is now postulated to have been derived from the Wyoming craton (Whitmeyer and Karlostrom, 2007). The age spectra of this basement rock ranges from ~2.45-3.1 Ga (Bickford et al., 2005). The Medicine Hat Block is composed of ~2.6-2.7 Ga rocks with belts of gneiss dating to ~3.3 Ga (Mueller et al., 2003; Whitmeyer and Karlstrom, 2007).

Sequence Stratigraphy and Provenance Change

Although spatial variations in detrital zircon populations are evident at different geographic locations, there is most likely an additional factor that contributed to temporal variations. As sediment from proximal sources was shed off the Transcontinental Arch onto the Cordilleran passive margin, the Eureka Quartzite and its age equivalent units along the coast recorded long-term sea level changes. Facies shifted and potential areas for sediment sources were covered or uncovered influencing the final sediment contribution (Fig. 14).

Deposition of most of the Middle Ordovician Eureka Quartzite occurred during or immediately above the Sauk-Tippicanoe sequence boundary (Sloss, 1963), during a global sea level low (Haq and Schutter, 2008). A Lowstand Systems Tract (LST) is characterized by forced regression and sediment progradation into the basin, ultimately exposing the siliciclastic shelf and inboard provinces to erosion. Sediment deposited during this time was derived from uncovered basement rock, such as the Wyoming craton and the proximal Yavapai and Mazatzal provinces, as well as the more distal Trans-Hudson Orogeny. These provinces would provide sediment for the coastal plain, deltas, or lowstand fans. Sea level eventually began to rise during the succeeding Transgressive Systems Tract (TST), which

allowed for preservation of sands below the base level profile (Zimmerman and Cooper, 1999). This may have shifted detrital zircon signatures as the potential sources and their sediment contributions changed. More proximal basement rocks are likely to fall below sea level and subsequently be covered by additional sediment being shed off of the Transcontinental Arch (Fig. 14). There was still potential for sediment input from proximal basement rocks and reworking. During the following Highstand Systems Tract (HST) base level continued to rise, but sedimentation rates likely exceeded the rate of available accommodation space generating a normal regression of the shoreline, or progradation (Catunaenu et al., 2002). Sediment was predominantly sourced from the Trans-Hudson Orogeny and reworked sediment from the previously deposited TST package. Similar provenance patterns would be evident during the Falling Stage Systems Tract (FSST).

Detrital zircon datasets from the Eureka Quartzite in the study area demonstrate signatures that are consistent with spatial and temporal variations in provenance. The lack of consistency for any one specified probability peak from the base to the top of any particular study location indicates that there are multiple basement sources from the onset of deposition of the Eureka Quartzite to the base of the Ely Springs Dolomite (Fig. 13). Detrital zircon signatures from the Davis Mountains and Pahvant Range show distinct shifts from the base to the top of the formation. A high probability peak of ~2.6-2.8 Ga grains indicates sediment derived from proximal basement rocks during low sea level. Sea level then rises and increases the amount of ~1.8-2.0 Ga grains from the more inboard Trans-Hudson Orogeny. The base and top samples of the Cherry Creek Range, Schell Creek Range, and the Crystal Peak section have similar dual signatures. This is potential a result of their geographic location and relation to the Tooele Arch. Paleoproterozoic and Archean rocks are least

persistent at locations closest to the southern flank of the topographic feature and increase in abundance in the other three locations. Sediment recycling is thought to be minimal due to the rarity of Grenville Orogen (0.9-1.2 Ga) and anorogenic granite (1.4 Ga) age zircons. Samples throughout the Crystal Peak outcrop show limited variation in zircon abundance. The accommodation space made available by the Ibex Basin was likely filled with sediment from various sources throughout Middle-Late Ordovician time and was not sensitive to oscillating sea level. Sediment shed off from the Tooele Arch would increase the potential for recycling ultimately increasing the availability of Grenville Orogenic and anorogenic granite age detritus. The consistently high peak of ~1.8-2.0 Ga grains may also indicate the importance of longshore drift currents transporting sediment along the shoreline. Additional studies of the Middle-Late Ordovician quartz arenite consistently show a distinct ~1.8-2.0 Ga peak from British Columbia, Canada to eastern California-south Nevada (Baar, 2009; Wulf, 2011; Hutto, 2011; Workman, 2012).

CONCLUSION

The Eureka Quartzite was deposited in an offshore to onshore environment, distal shallow shelf to upper shoreface/tidal flat, along a siliclastic shelf. Sand grains are predominantly very fine to medium, well-rounded, well-sorted, and silica cemented. Five facies identified throughout the study locations and their stacking patterns reveal a maximum of three high-frequency depositional sequences (E_1, E_2, E_3) preserved during deposition of the Eureka Quartzite. Limited accommodation space proximal to the shoreline and the Tooele Arch resulted in thinner sections, whereas in the House Range embayment a thicker section was deposited.

Detrital zircon signatures in all samples show a strong distribution of Archean (~2.6-2.8 Ga) and Paleoproterozoic Trans-Hudson Orogenic (~1.8-2.0 Ga) derived sediment. A common, yet not abundant grain population, ~1.6-1.8 Ga peak, corresponds to the Yavapai-Mazatzal provinces. Limited analyzed grains apparent in less persistent peaks, ~2.0-2.1 Ga, ~2.4-2.6 Ga, ~2.9-3.0 Ga, indicate additional sediment provenance from Paleoproterozoic-Archean rocks. It appears unlikely that the Tooele Arch provided sediment to the Eureka Quartzite. However, it is unclear if the west-east trending Tooele Arch did influence sediment depositional patterns. Variations in detrital zircon signatures throughout study locations and their geographic relation to the arch may indicate some relationship, but restricted sampling to the south of the structure does not provide a definite answer. The two more proximal locations to the Tooele Arch have a consistently weak ~2.6-2.8 Ga peak, suggesting limited sediment input from Paleoproterozoic-Archean crust, such as the Wyoming province, Medicine Hat Block, or Sask province. Sediment accumulation within the Ibex basin does not show any relation to sea level fluctuations or the Tooele Arch.

Commonly occurring Grenville Orogenic and anorogenic granite derived zircons in Late Proterozoic and Cambrian units are exceedingly rare, suggesting that Eureka Quartzite sands are first cycle deposits and multi-cycled detritus was not a large contributor.

The Middle-Late Ordovician Eureka Quartzite was derived from the Transcontinental Arch from multiple terranes inboard of the western Laurentia passive margin. Shifts in provenance most likely correspond to relative changes in base level. Maximum basement exposure occurred at the apex of a long-term Lowstand Systems Tract, the transition from a carbonate bank to a siliciclastic shelf. During the subsequent TST and HST, rising sea level allowed sediment to cover the more proximal basement rocks (e.g. Wyoming Craton) and increased the probability of sediment input from provinces located further inland (e.g. THO).

REFERENCES

Anderson, J.L., 1989, Proterozoic anorogenic granites of the southwestern United States, in Jenny, J.P., and Reynolds, S.J., Geologic evolution of Arizona: Tucson, Arizona Geological Society Digest, v. 17, p. 211-238.

Armstrong, R.L., 1968, Sevier Orogenic Belt in Nevada and Utah: Geological society of America Bulletin, v. 79, p. 429-458.

Armstrong, R.L., 1975, Precambrian (1500 m.y. old) rocks of Central Idaho – The Salmon River Arch and its role in Cordilleran sedimentation and tectonics: American Journal of Science, v. 275-A, p.437-467.

Arnott, R.W.C, 1993, Quasi-planar-laminated sandstone beds of the Lower Cretaceous Bootlegger Member, north-central Montana: Evidence of combined-flow sedimentation: Journal of Sedimentary Petrology, v. 63, p. 488-494.

Baar, E.E., 2009, Determining the Regional-Scale Detrital Zircon Provenance of the Middle-Late Ordovician Kinnikinic (Eureka) Quartzite, East-Central Idaho, U.S. [Master's Thesis]: Unpublished, Pullman, Washington State University, p. 1-83.

Ball, T.T., and Farmer, G.L., 1991, Identification of 2.0 to 2.4 Ga Nd model age crustal material in the Cheyenne Belt, southeastern Wyoming: Implications for Proterozoic accretionary tectonics at the southern margin of the Wyoming Craton: Geology, v. 19, p. 360-363.

Black, L.P., et al., 2004, Improved 206Pb/238U microprobe geochronology by the monitoring of a trace-element-related matrix effect; SHRIMP, ID-TIMS, ELA-ICP-MS and oxygen isotope documentation for a series of zircon standards. Chemical Geology, v. 205, p. 115-140.

Bond, G.C., and Kominz, M.A., 1984, Construction of tectonic subsidence curves for the early Paleozoic miogeocline, southern Canadian Rocky Mountains: Implications for subsidence mechanisms, age of breakup, and crustal thinning: Geological Society of America Bulletin, v.95, p. 155-173.

Bond, G.C., Kominz, M.A., and Grotzinger, J.P., 1988, Cambro-Ordovician Eustasy: Evidence from Geophysical Modelling of Subsidence in Cordilleran and Appalachian Passive Margins, in Kleinspehn, K.L. and Paola, C., eds., New Perspectives in Basin Analysis: Frontiers in Sedimentary Geology, p. 129-160.

Burchfiel, B.C., Cowan, D.S., Davis, G.A., 1992, Tectonic overview of the Cordilleran orogen in the western United States. In: Burchfiel, B.C., Lipman, P.W., Zoback, M.L., eds., The Cordilleran Orogen: Conterminous US. Geological Society of America, Boulder, CO, p. 407–479.

Catuneanu, O., 2002, Sequence stratigraphy of clastic systems: concepts, merits, and pitfalls: Journal of African Earth Sciences, v. 35, p. 1-43.

Catuneanu, O., Abreau, V., Bhattacharya, J.P., Dalrymple, R.W., et. al., 2009, Towards the standardization of sequence stratigraphy: Earth-Science Reviews, v. 92, p. 1-33.

Chang, Z., Vervoort, J. D., McClelland, W., Knaack, C., 2006, U-Pb dating of zircon by LA-ICP-MS: Geochem, Gephysics, Geosystems, v. 7, no. 5, p.1-14.

Cox, D.M., Frost, C.D., and Chamberlain, K.R., 2000, 2.01 Ga Kennedy dike swarm, southeastern Wyoming: A record of a rifted margin along the southern Wyoming province: Rocky Mountain Geology, v. 35, p. 7-30.

Desjardins, P.R., Mangano, M.G., Buatois, L.A., and Pratt, B.R., 2010, Skolithos pipe rock and associated ichnofabrics from the southern Rocky Mountains, Canada: Colonization trends and environmental controls in an Early Cambrian sand-sheet complex: Lethaia, v. 43, p. 507-528.

Dickinson, W.R., 2013, Phanerozoic palinspastic reconstructions of Great Basin geotectonics (Nevada-Utah, USA): Geosphere, v. 9, no.5, p. 1384-1396.

Druschke, P.A. Jr., Jiang, G., Anderston, T.B., and Hanson, A.D., 2009, Stromatolites in the Late Ordovician Eureka Quartzite: implications for microbial growth and preservation in siliciclastic settings: Sedimentology, v. 56, p. 1275-1291.

Dott, R.H. Jr., 2003, The importance of eolian abrasion in supermature quartz sandstones and the paradox of weathering on vegation-free landscapes: Journal of Geology, v. 111, p.387-405.

Dott. R.H. Jr., Byers, C.W., Fielder, G.W., Stenzel, S.R., and Winfree, K.E., 1986, Eolian to marine transition in Cambro-Ordovician cratonic sheet standstones of the northern Mississippi valley, U.S.A.: Sedimentology, v. 33, p. 345-367.

Farmer, G.L., and Ball, T.T., 1997, Sources of Middle Proterozoic to Early Cambrian siliciclastic sedimentary rocks in the Great Basin: A Nd isotope study: Geological Society of America Bulletin, v. 109, no. 9, p. 1193-1205.

Fedo, C.M., Sircombe, K.N, and Rainbird, R.H., 2003, Detrital zircon analysis of the sedimentary record, in Hanchar, J.M., and Hoskin, P.W.O., eds., Zircon: Reviews in Mineralogy and Geochemistry, v. 53, p. 277-303.

Foster, D.A., Mueller, P.A., Mogk, D.W., Wooden, J.L., and Vogl, J.J., 2006, Proterozoic evolution of the western margin of the Wyoming craton: Implications for the tectonic and magmatic evolution of the northern Rocky Mountains: Canadian Journal of Earth Sciences, v. 43, p. 1601-1619.

Gehrels, G.E., 2000, Introduction to detrital zircon studies of Paleozoic and Triassic strata in western Nevada and northern California, in Soreghan, M.J., and Gehrels, G.E., eds., Paleozoic and Triassic paleogeography and tectonics of western Nevada and northern California: Geological Society of America Special Paper 347, p. 1-17.

Gehrels, G.E., 2009, Unpublished data personally transferred to Dr. Michael Pope, personal communication.

Gehrels, G.E., 2010, U-Th-Pb analytical methods for Zircon (Arizona LaserChron Center, University of Arizona): https://sites.google.com/a/laserchron.org/laserchron/home/ (accessed July, 2013).

Gehrels, G.E., and Dickinson, W.R., 1995, Detrital zircon provenance of Cambrian to Triassic miogeoclinal and eugeoclinal strata in Nevada: American Journal of Science, v. 295, p.18-48.

Gehrels, G.E., Dickinson, W.R., Ross, G.M., Stewart, J.H., and Howell, D.G., 1995, Detrital zircon reference for Cambrian to Triassic miogeoclinal strata of western North America: Geology, v. 23, p. 831-834.

Hampson, G.J. and Storms, J. E.A., 2003, Geomorphological and sequence stratigraphic variability in wave-dominated, shoreface-shelf parasequences: International Association of Sedimentologists, Sedimentology, v. 50, p. 667-701.

Haq, B.U., and Schutter, S.R., 2008, A chronology of Paleozoic sea-level changes: Science, v. 322, p. 64-68.

Hinton, R.W., NIST SRM 610, 611 and SRM 612, 613 multi-element glasses: constraints from element abundance ratios measured by microprobe techniques: The Journal of Geostandards and Geoanalysis, v. 23, no. 2, p.199.

Hintze, L.F., 1959, Ordovician regional relationships in north-central Utah and adjacent areas: Guidebook to the Geology of the Wasatch and Uinta Mountains: Transition Area; Utah Geological Association, p. 46-47.

Hintze, L.F., and Davis, F.D., 2003, Geology of Millard County, Utah: Utah Geological Survey, Bulletin 133, p. 305.

Hoffman, P.F., 1989, Precambrian geology and tectonic history of North Amierca, in Bally, A.W., and Palmer, A.R., eds., The Geology of North America – An Overview: Boulder Colorado, Geological Society of America, Geology of North America 1989, v. A, p. 447-512.

Howard, J.D. and Reineck, H., 1981, Depositional facies of high-energy beach-to-offshore sequence: comparison with low-energy sequence: American Association of Petroleum Geologists Bulletin, v. 65, no. 5, p. 807-830.

Hutto, A.P., 2012, Sequence Stratigraphy and Detrital Zircon Geochronology of Middle-Late Ordovician Mt. Wilson Quartzite, British Columbia, Canada [Master's Thesis]: Unpublished, College Station, Texas A&M University, p. 1-27.

Kay, M., 1951, North American Geosynclines: Geological Society of America Memoir, v. 48, p. 131.

Ketner, K.B., 1966, Comparison of Ordovician Eugeosynclinal and Miogeosynclinal Quartzites of the Cordilleran Geosyncline: United States Geological Survey Professional Paper 550-C, p. C54-C60.

Ketner, K.B., 1968, Origin of Ordovician quartzite in the Cordilleran miogeosyncline: United States Geological Survey Professional paper 600-B, p.B169-B177.

Klein, G., 1975, Tidalites in the Eureka Quartzite (Ordovician), eastern California and Nevada, in Ginsburg, R.N., ed., Tidal Deposits, New York, Spring-Verlag, p.145-151.

Kosler, J., Fonnenland, H., Sylvester, P., Tubrett, M., Pedersen, R-B., 2001, U-Pb dating of detrital zircons for sediment provenance studies—a comparison of laser ablation ICPMS and SIMS techniques: Chemical Geology, v. 182, p. 605-618.

Kosler, J. & Sylvester, P.J., 2003, Present trends and the future of zircon in geochronology: laser ablation ICPMS: Reviews in Mineralogy and Geochemistry, v. 53, p.243-275.

Leatham, W.B., 1985, Ages of the Fish Haven and lowermost Laketown dolomites in the Bear River Range, Utah, in Kerns, G.J., and Kerns, R.L., eds., Orogenic Patterns and Stratigraphy of North Central Utah and Southeastern Idaho, p. 29-38.

Levy, M. and Christie-Blick, N., 1991, Tectonic subsidence of the early Paleozoic passive continental margin in eastern California and southern Nevada: Geological Society of America Bulletin, v. 103, p. 1590-1606.

Ludwig, K.R., 2003, Isoplot/Ex Version 3.00: A Geochronological toolkit for Microsoft Excel. Berkeley Geochronology Center, Special Publication No. 4.a, Berkely, CA, http://www.bgc.org/isoplot_etc/isoplot.html.

McBride, E.F., 2012, Heterogenous packing and quartz cementation of the Eureka Quartzarenite (Middle Ordovician), Utah and Nevada, U.S.A.: Journal of Sedimentary Research, v. 82, p. 664-680.

Mezger, K., Essene, E.J., van der Pluijm, B.A., and Halliday, A.N., 1992, U-Pb geochronology of the Grenville Orogen of Ontario and New York: Constraints on ancient crustal tectonics: Contributions to Mineralogy and Petrology, v. 114, p. 13-26.

Miller, M.F., 1977, Middle and Upper Ordovician biogenic structures and paleoenvironments, Southern Nevada: Journal of Sedimentary Petrology, v.47, no. 3, p. 1328-1338.

Miller, E.L., Miller, M.M., Stevens, C.H., Wright, J.E., and Madrid, R., 1992, Late Paleozoic paleogeographic and tectonic evolution of the western U.S. Cordillera, in Burchfiel, B.C., Lipman, P.W., and Zoback, M.L., eds., The Cordilleran Orogen: Continuous U.S.: Boulder, Colorado, Geological Society of America, The Geology of North America, v. G-3, p. 57-106.

Mitchum Jr., R.M., 1977, Seismic stratigraphy and global changes of sea level, part 11: glossary of terms used in seismic stratigraphy. In: Payton, C.E., ed., Seismic Stratigraphy – Applications to Hydrocarbon Exploration. Memoir, v. 26: American Association of Petroleum Geologists, p. 205-212.

Moores, E.M., 1991, Southwest U.S.-East Antarctic (SWEAT) connection: A hypothesis: Geology, v. 19, p. 425-428.

Mueller, P.A., Heatherington, A.L., Kelly, D.M., Wooden, J.L., and Mogk, D.W., 2002, Paleoproterozoic crust within the Great Falls tectonic zone: Implications for the assembly of southern Laurentia: Geology, v. 30, p. 127-130.

Oaks, R.Q., James, W.C., Francis, G.G., and Schulingkamp, W.J., 1977, Middle Ordovician stratigraphy and tectonics, northern Utah, southern and central Idaho: Geological Society America, Abstracts with programs, Ann. Mtg. Rocky Mtn. Section, p. 635.

Paces, J.B., and Miller, J.D.J., 1993, Precise U-Pb ages of Duluth Complex and related mafic intrusions, northeastern Minnesota: Geochronological insights to physical, petrogenetic, paleomagnetic, and tectonomagmatic processes associated with the 1.1 Ga Midcontinent Rift System. Journal of Geophysical Research v. 98, p.13997-14013.

Plint, A.G., 2010, Wave-and storm-dominated shoreline and shallow-marine systems, in James, N.P., and Dalrymple, R.W., eds., Facies Models 4, Geological Association of Canada, p. 167-184.

Poole, F. G., and eight others, 1992, Latest Precambrian to latest Devonian time; development of a continental margin, in Burchfiel, B. C., Lipman, P. W., and Zoback, M. L., The Cordilleran Orogen: conterminous U. S.: The Geology of North America, Volume G-3, Decade of North American Geology, Geological Society of America, Boulder, p. 9-56.

Pope, M.C., 2008, Detrital zircon geochronology of Late Ordovician sandstone in Wyoming suggest Talson-Thelon Orogen was a major source of siliciclastic sediment along the Transcontinental Arch: Geological Society of America Abstracts with Programs, v. 40, p.77.

Rees, M. N., 1986, A fault-controlled trough through a carbonate platform: The Middle Cambrian House Range Embayment: Geological Society of America Bulletin, v. 97, p. 1054-1069.

Reinson, G.E., 1984, Barrier-island and associated strand plain systems, in Walker, R.G., eds., Facies Models, 2nd ed.: Geoscience Canada Reprint Ser. 1, p. 119-140.

Roscoe, S.M., and Card, K.D., 1993, The reappearance of the Huronian in Wyoming: Rifting and drifting of ancient continents: Canadian Journal of Earth Sciences, v. 30, p. 2475-2480.

Ross, G.M., and Villeneuve, M.E., 2003, Provenance of the Mesoproterozoic (1.45 Ga) Belt basin (western North America): Another piece in the pre-Rodinia paleogeographic puzzle: Geological Society of America Bulletin, v. 115, p. 1191-1217.

Runkel, A.C., Miller, J.F., McKay, R.M., Palmer, A.R., and Taylor, J.F., 2007, High-resolution sequence stratigraphy of lower Paleozoic sheet sandstones in central North America: The role of special conditions of cratonic interiors in development of stratal architecture: Geological Society of America Bulletin, v. 119, p. 860-881.

Ruppel, E.T., Ross, R.J., and Schleicher, D., 1975, Precambrian Z and Lower Ordovician rocks in east-central Idaho: United States Geological Survey Professional paper 889, p. 25-34.

Saltzman, M.R. and Young, S., 2005, Long-lived glaciation in the Late Ordovician? Isotopic and sequence-stratigraphic evidence from western Laurentia: Geology, v. 33, no. 2, p. 109-112.

Saltzman, M.R., Young, S., Bergstrom, S.M., Holmden, C., and Patterson, W.P., 2003, Age and significance of the sequence boundary at the base of the Eureka Quartzite in central Nevada: Geological Society of America Abstracts with Programs, v.35, p. 473.

Scotese, C.R., Boucot, A.J., and McKerrow, W.S., 1999, Gondwanan paleogeography and paleoclimatology: Journal of African Earth Sciences, v. 28, no.1, p.99-114.

Short, A.D., 1984, Beach and nearshore facies: southeast Australia: Marine Geology, v. 60, p. 261-282.

Sloss, L.L., 1954, Lemhi Arch, a mid-Paleozoic positive element in south-central Idaho: Geological Society of America Bulletin, v. 65, no. 4, p. 385-368.

Sloss, L.L., 1963, Sequences in the Cratonic Interior of North America: Geological Society of America Bulletin, v. 74, p. 93-114.

Stewart, J.H., 1972, Initial deposits of the Cordilleran geosyncline: Evidence of late Precambrian (<850 m.y.) continental separation: Geological Society of America Bulletin, v. 83, p. 1345-1360.

Stewart, J.H., Gehrels, G.E., Barth, A.P., Link, P.K., Christie-Blick, N., and Wrucke, C.T., 2001, Detrital zircon provenance of Mesoproterozoic to Cambrian arenites in the western United States and northwestern Mexico: Geological Society of America Bulletin, v. 113, p. 1343-1356.

Sweet, W.C., 2000, Conodonts and biostratigraphy of Upper Ordovician strata along a shelf to basin transect in Central Nevada: Journal of Paleontology, v. 74, p.1148-1160.

Van der Voo, R., 1993, Paleomagnetism of the Atlantic, Tethys, and Iapetus oceans: University Press, Cambridge, United Kingdom, p. 411.

Van Schmus, W.R., Bickford, M.E., Lewry, J.F., and Macdonald, R., 1987, U-Pb geochronology in the Trans-Hudson orogeny, northern Saskatchewan, Canada: Canadian Journal of Earth Sciences, v. 24, p. 407-424.

Van Schmus, W.R., Bickford, M.E., Anderson, J.L., Bender, E.E., Anderson, R.R., Bauer, P.W., Robertson, J.M., Bowring, S.A., Condie, K.C., Denis, R.E., Gilbert, M.C., Grambling, J.A., Mawer, C.K., Shearer, C.K., Hinze, W.J., Karlstrom, K.E., Kisvarsanyi, E.B., Lidiak, E.G., Reed, J.C. Jr., Sims, P.K., Tweto, O., Silver, L.T., Treves, S.B., Williams, M.L., and Wooden, J.L., 1993, Transcontinental Proterozoic provinces, in Reed, J.C., et al., eds., Precambrian: Conterminous U.S.: Boulder, Colorado, Geological Society of America, Geology of North America, v. C-2, p. 171-334.

Wallin, E.T., 1990, Provenance of selected lower Paleozoic siliciclastic rocks in the Roberts Mountains allochthon, Nevada: Geological Society of America Special Paper 225, p. 17-32.

Wallin, E.T., 1993, Sonoma revisited: Evidence of a western Canadian provenance of the eastern Klamath & northern Sierra Nevada terranes: Geological Society of America Abstracts with Programs, v.25, no. 6, p. A-173.

Webb, G.W., 1956, Middle Ordovician detailed stratigraphic sections for western Utah and eastern Nevada: Utah Geological and Mineralogical Survey Bulletin, v. 57, p.1-77.

Webb, G.W., 1958, Middle Ordovician stratigraphy in eastern Nevada and western Utah: American Association of Petroleum Geologists Bulletin, v. 42, no. 10, p. 2335-2377.

Weltje, G.J., and von Eynatten, H., 2004, Quantitative provenance analysis of sediments: review and outlook: Sedimentary Geology, v. 171, p. 1-11.

Wiedenbeck, M., et al., 1995, Three natural zircon standards for U-Th-Pb, Lu-Hf, trace element, and REE analyses. Geostandards Newsletter, v. 19, no.1, 1-23.

Witzke, B.J., 1990, Paleoclimatic constraints for Paleozoic Paleolatitudes of Laurentia and Euramerica, in McKerrow, W.S., and Scotese, C.R., eds., Paleozoic paleogeography and biogeography; Geological Society [London] Memoir 12, p. 57-53.

Workman, B. D., 2013, Sequence Stratigraphy and Detrital Zircon Provenance of the Eureka Quartzite in south-central Nevada and eastern California [Master's Thesis]: Unpublished, College Station, Texas A&M University, p. 1-51.

Wright, W.F., 1965, Petroleum geology of the Simpson Group, west Texas and southeast New Mexico: Tulsa Geological Society Digest, v. 33, p. 62-73.

Wulf, T. D., 2011, Sequence Stratigraphy and Detrital Zircon Geochronology of the Swan Peak Quartzite, Southeastern Idaho [Master's Thesis]: Unpublished, College Station, Texas A&M University, p. 1-42.

Zimmerman, M., and Cooper, J. D., 1999, Sequence stratigraphy of the Middle Ordovician Eureka Quartzite, southeastern California and southern Nevada: Acta Universitatis Carolinae, Geologica, v. 34, no. 1, p.147-150.

APPENDIX A

FIGURES

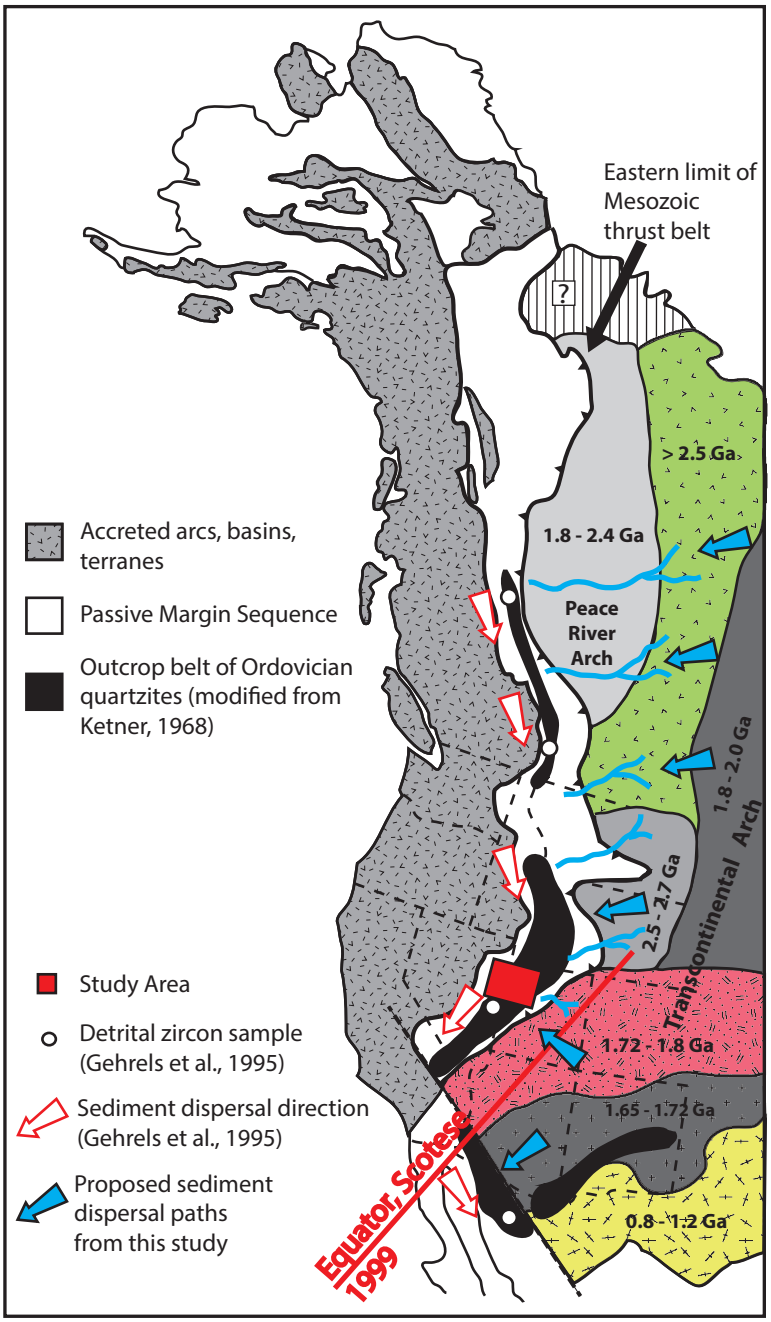

Figure 1: Map of Western North America and Basement Rocks. Basement units from; Hoffman (1989), Ross and Villeneuve (2003) and Van Schmus et al. (1993) and Ordovician quartz arenite distribution from Ketner (1968). Sediment provenance is suggested to be proximal due to inboard transport mechanisms (blue arrows). Previous detrital zircon studies suggested the Peace River Arch dominated sediment contribution due to longshore currents along western Laurentia (Gehrels et al., 1995).

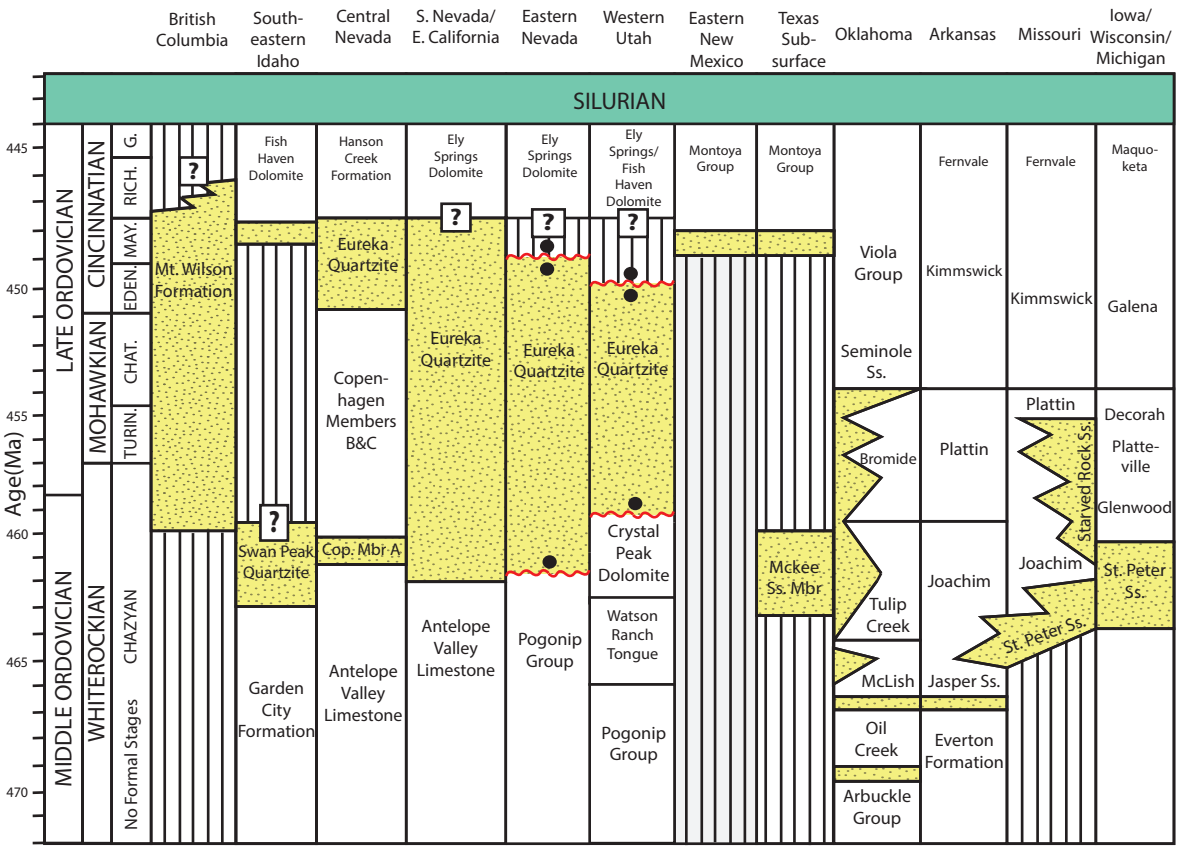

Figure 2: Stratigraphic Correlation Chart of Middle-Upper Ordovician Quartz Arenites of Western United States and U.S. Mid-Continent. Duration of units modified from Norford (1969), James and Oaks (1997), Churkin (1962), Hobbs et al. (1968), Biek (1999), Poole et al. (1995), Suhm (1997), Saltzman and Young (2005), Harris et al. (1979), and Webb (1958). Black circles denote sample locations at their respective outcrop.

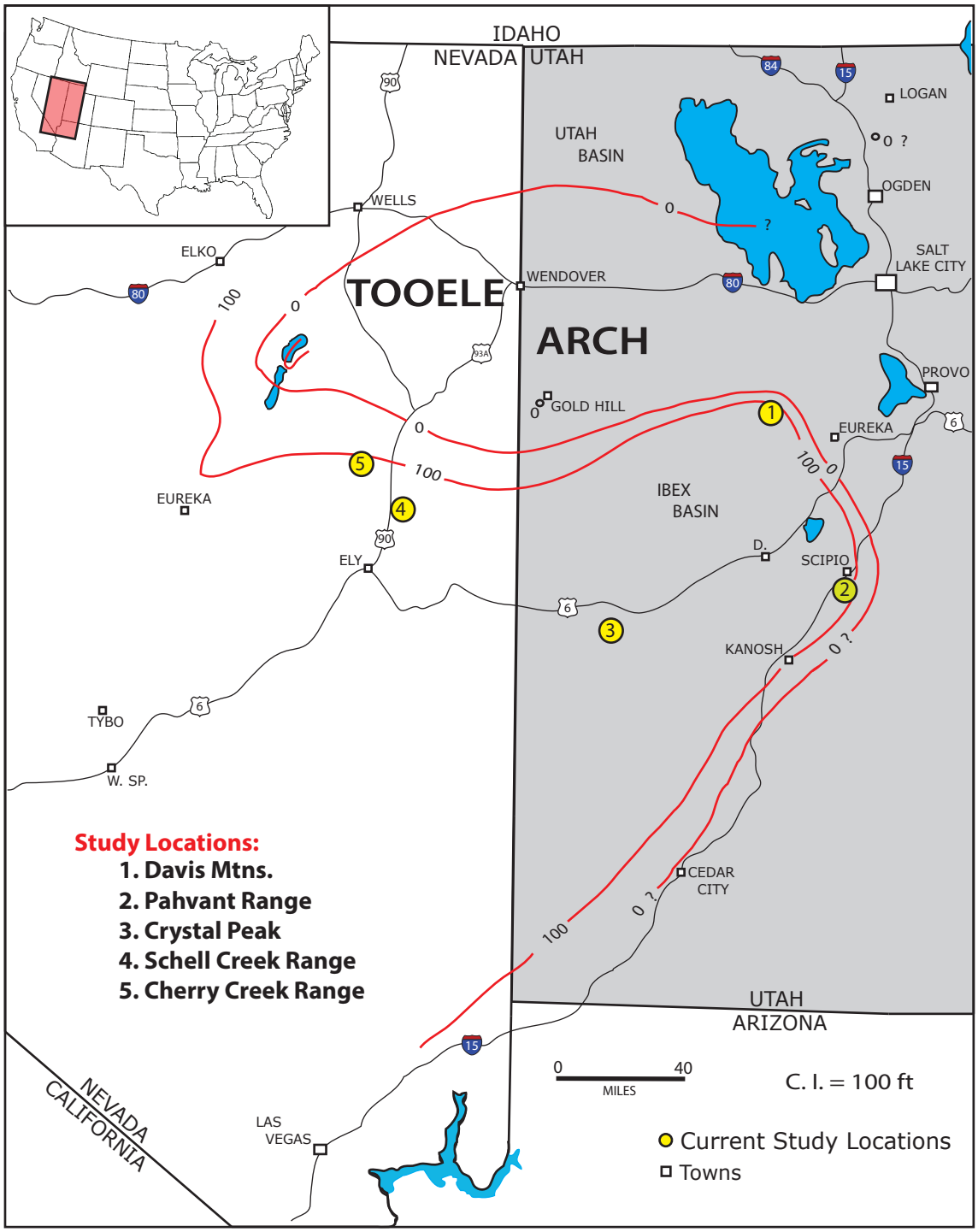

Figure 3: Map of Western Utah and Eastern Nevada Study Areas (modified from Webb, 1958). Study locations are proximaly adjacent to the Tooele Arch. 1.) Davis Mountains, 2.) Pahvant Range, 3.) Wah Wah Mountains (Crystal Peak), 4.) Schell Creek Range, 5.) Cherry Creek Range. Eureka Quartzite isopach contours show the thinning and absence of the Eureka Quartzite throughout the region emphasising the west-east trending Tooele Arch.

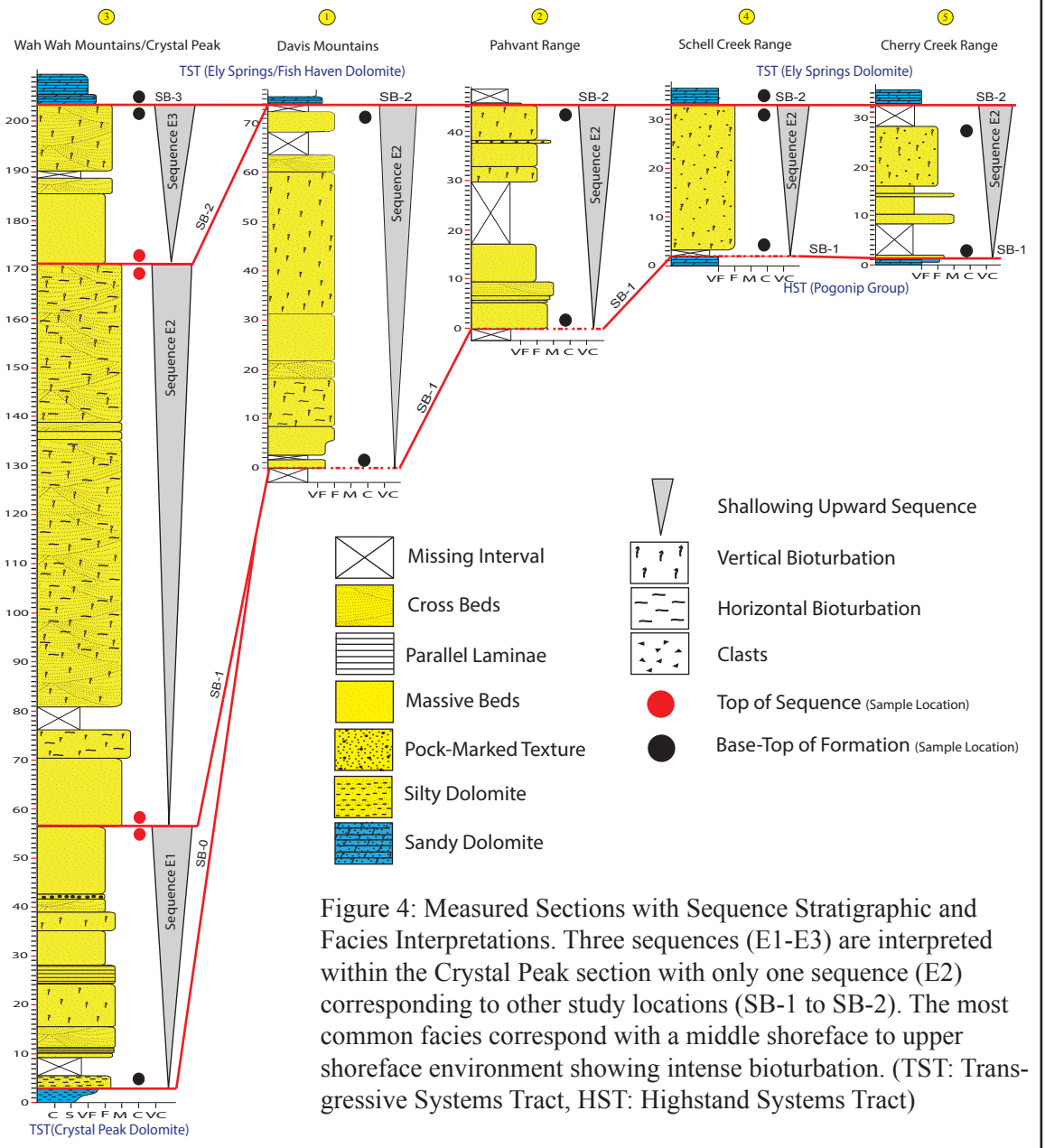

Figure 4: Measured Sections with Sequence Stratigraphic and Facies Interpretations. Three sequences (E1-E3) are interpreted within the Crystal Peak section with only one sequence (E2) corresponding to other study locations (SB-1 to SB-2). The most common facies correspond with a middle shoreface to upper shoreface environment showing intense bioturbation. (TST: Transgressive Systems Tract, HST: Highstand Systems Tract)

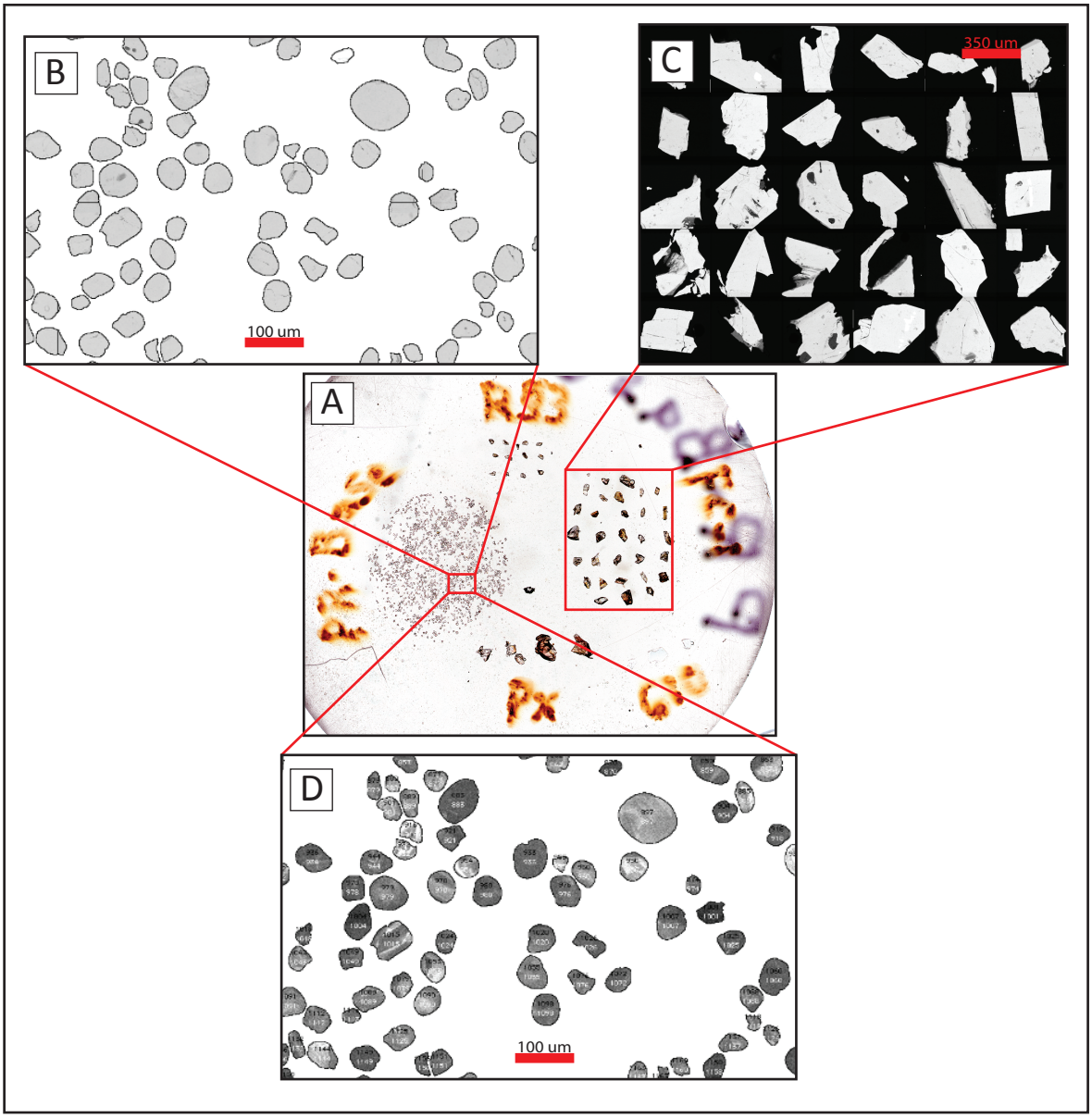

Figure 5: Mounted Zircons with Corresponding Backscattered Electron and Cathodoluminescence Images. Images are from the Pahvant Range basal sample. (A) Each epoxy puck with the mounted sample and standards was imaged using a Cameca SVX50 microprobe. (B) BSE images assist in differentiating zircon from other minerals and help identify inclusions within the grains. (C & D) CL images assist with the identification of intracrystalline heterogeneity such as zoning and inclusions within the unknown samples and standards.

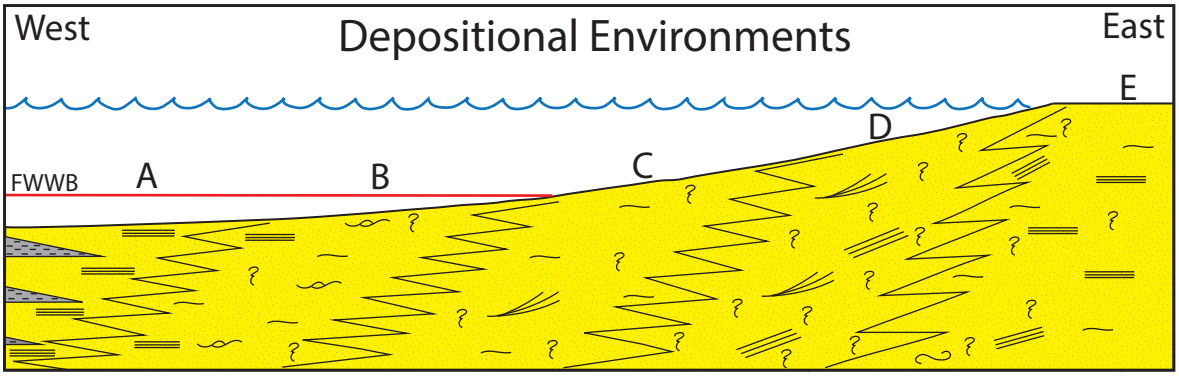

Figure 6: Depositional Environments Profile. Common facies and depositional environments found across the siliciclastic shelf. (A) offshore facies, (B) lower shoreface, (C) middle shoreface, (D) upper shoreface, and (E) subtidal and tidal flats.

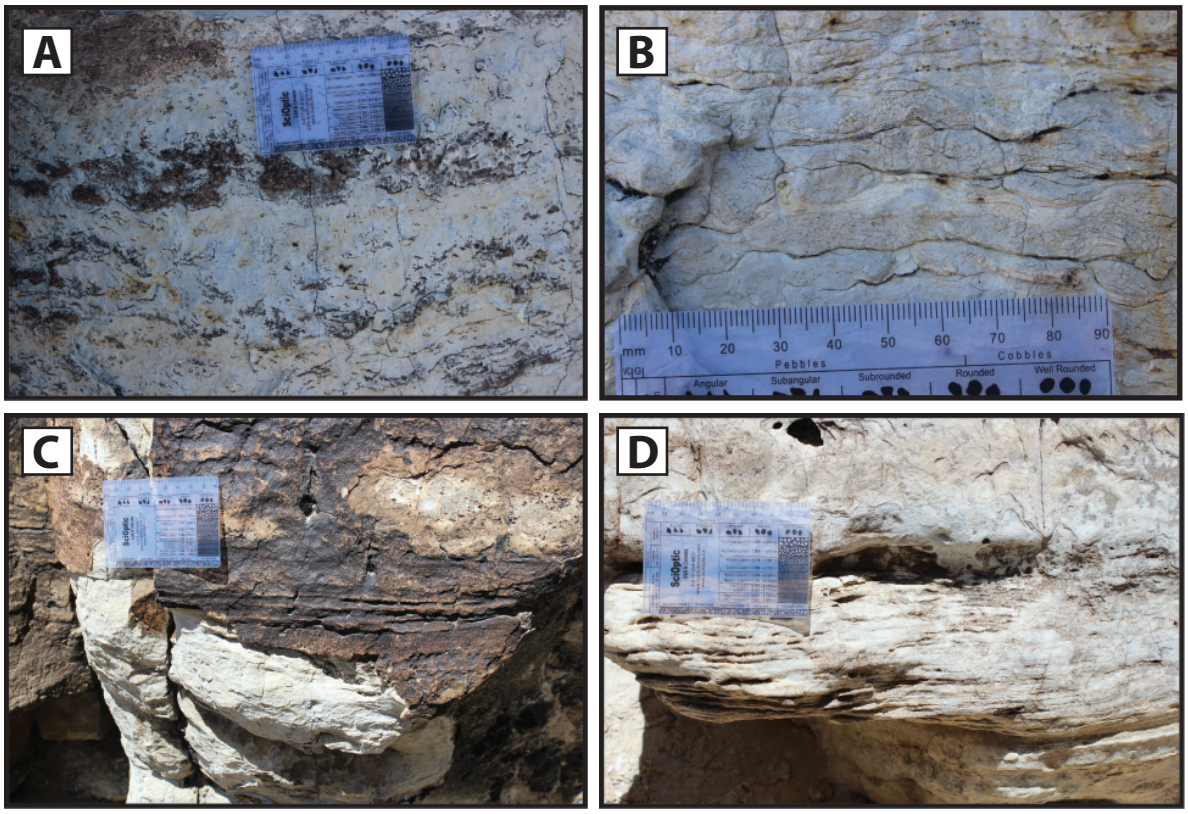

Figure 7: Pictures of Offshore Environment. (A) beds with oscillating detrital and very fine dolomitic abundance, (B) soft sediment deformation due to intense bioturbation, (C) planar laminations in dolomitic sands with high terrigenous input, and (D) horizontal planar laminations in silt-rich sediment. Grain size card is 9 cm in length. All images are from the Crystal Peak location.

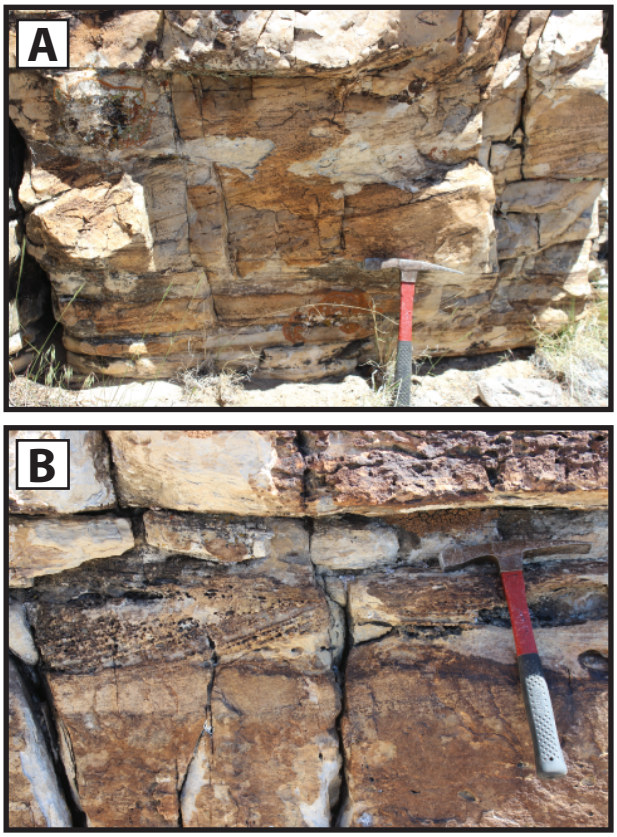

Figure 8: Pictures of Lower Shoreface Environment. (A) and (B) low-angle planar cross laminations in thin-medium sandstone beds. Images are from the Crystal Peak location.

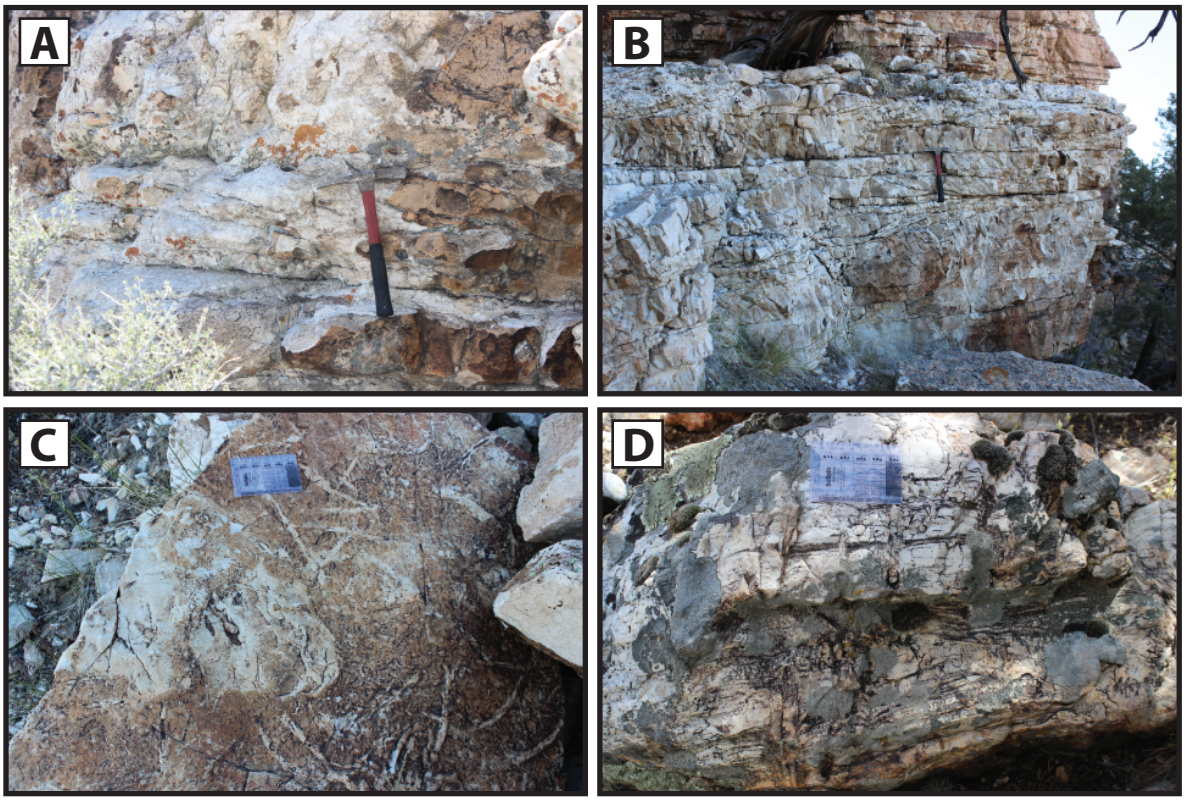

Figure 9: Pictures of Middle Shoreface Environment. (A) & (B) unidirectional low angle cross bedding at Crystal Peak location (C) bedding plane with high abudance of *Planolites* at Crystal Peak location, (D) low angle cross lamination at Pahvant Range location. Images are from multiple study locations.

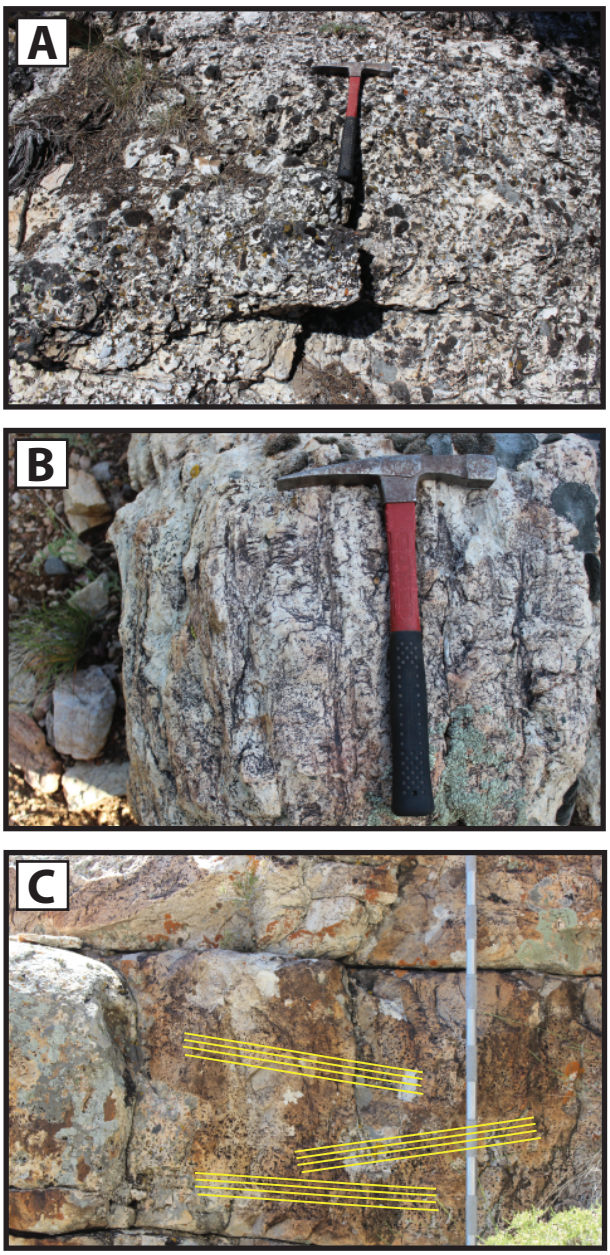

Figure 10: Pictures of Upper Shoreface Environment. (A) extensive bioturbation causing pockmark weathering at Cherry Creek Range location (B) vertical burrows, *Skolithos*, at Pahvant Range location (C) remants of low-angle cross bedding in medium bedded quartz arenite at Crystal Peak location. Images from multiple study locations.

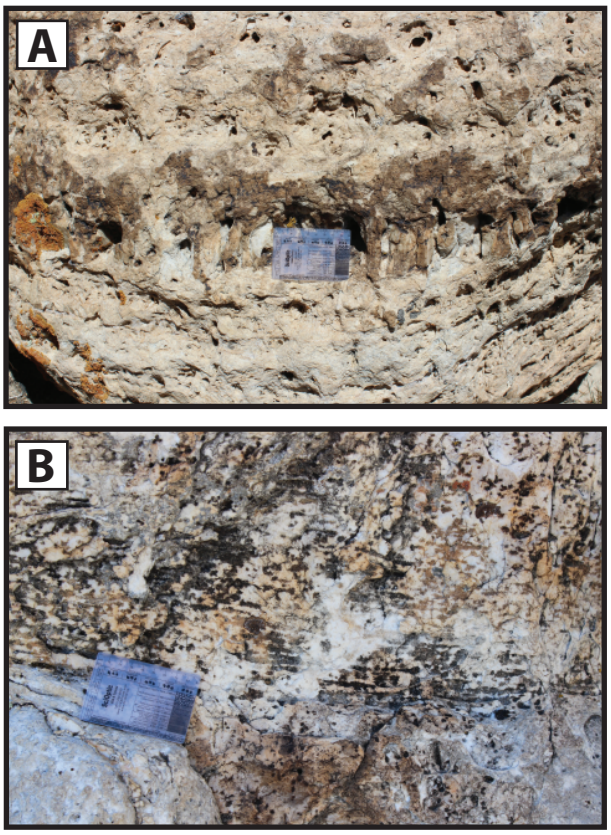

Figure 11: Pictures of Tidal-Subtidal Flat Environment. (A) & (B) intense bioturbation, *Skolithos*, in remnant parallel laminae. Grain size card is 9 cm in length. Images are from the Crystal Peak location.

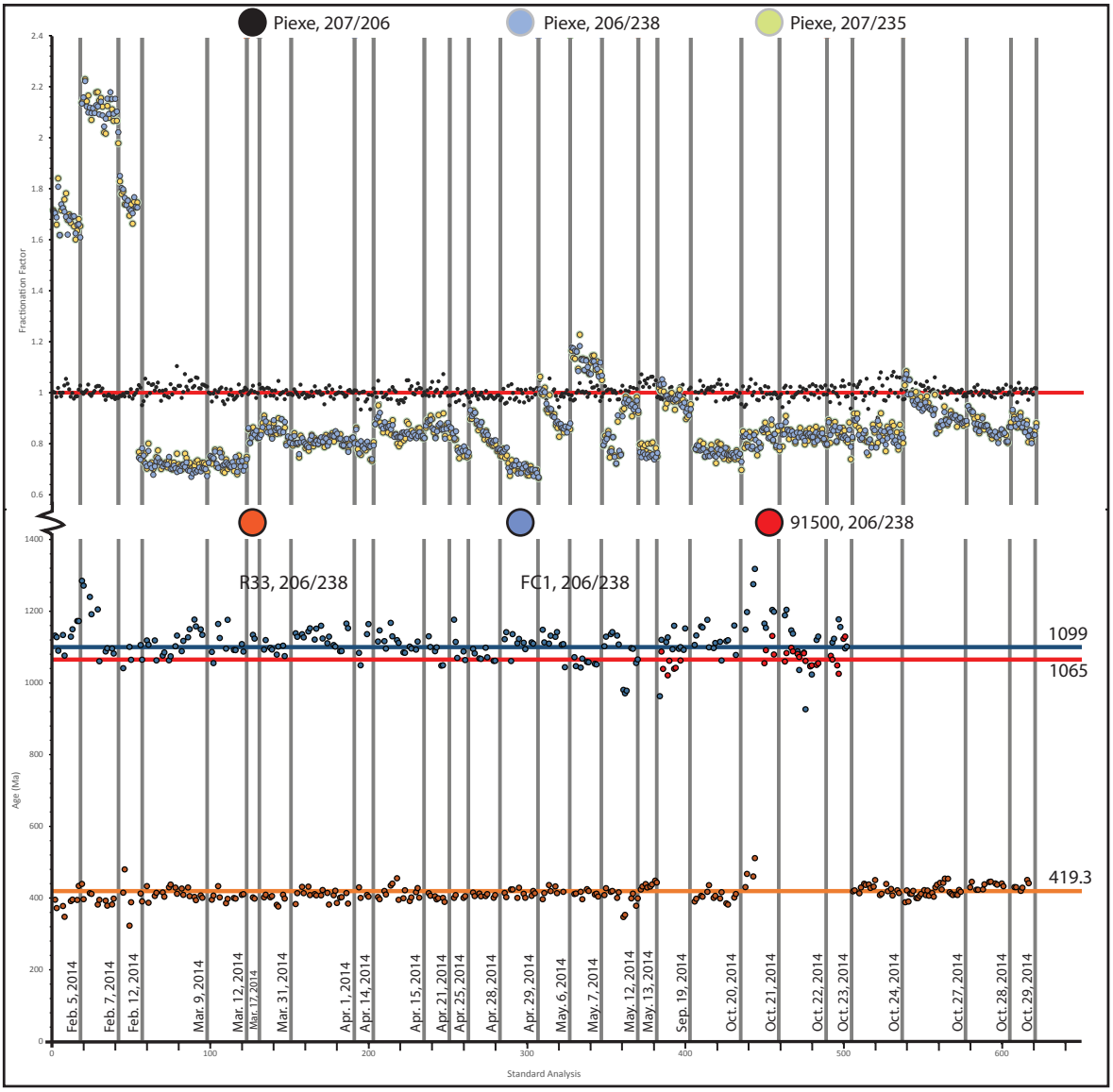

Figure 12: Standard Zircon Results. Zircon standard data analyzed throughout the course of the study. Upper half of figure displays fractionation factors for all Peixe analyses for all major isotope ratios. Lower half displays the calculated 206Pb/238U ages for the secondary standards after being corrected for elemental and mass fractionation.

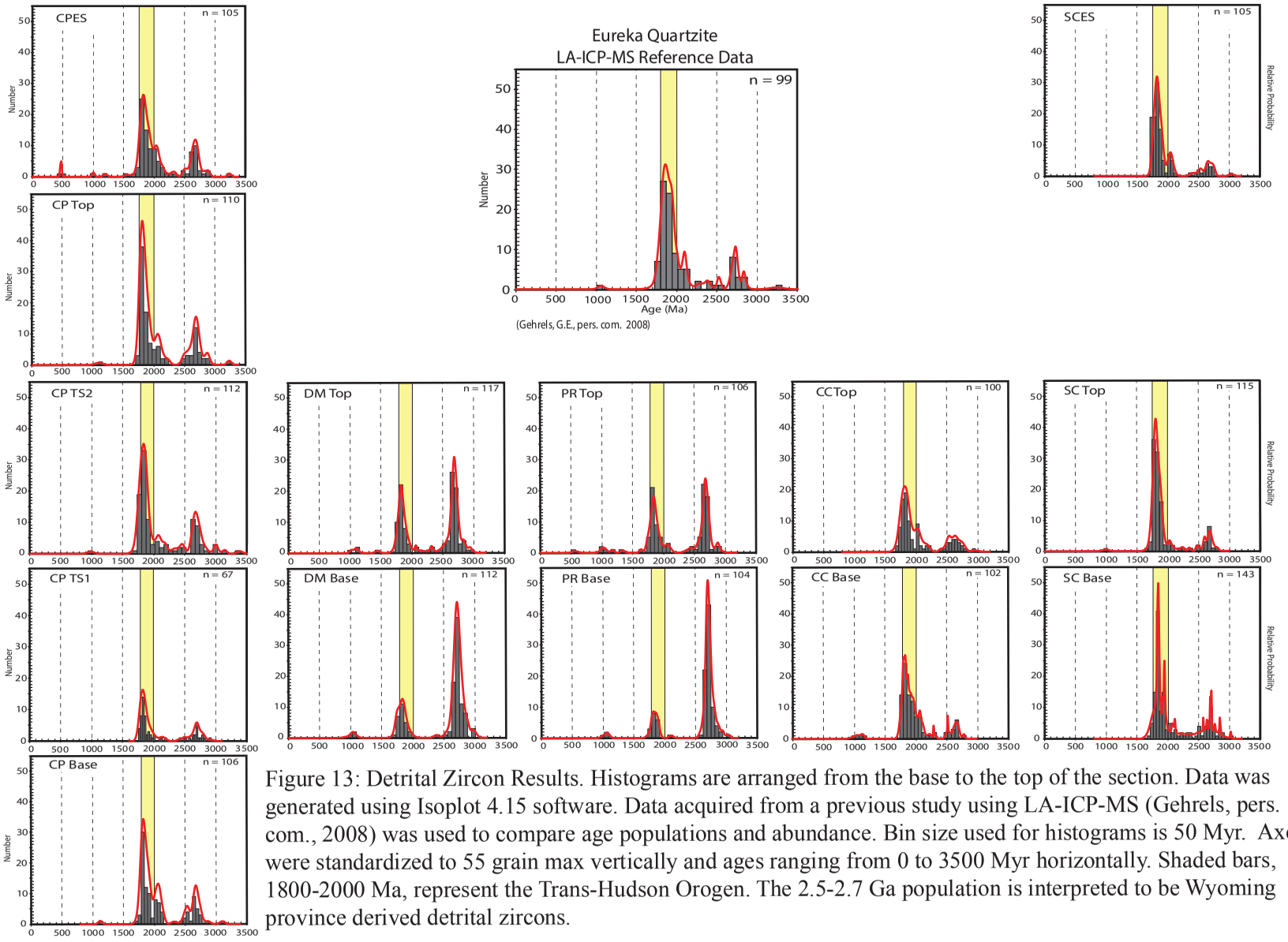

Figure 13: Detrital Zircon Results. Histograms are arranged from the base to the top of the section. Data was generated using Isoplot 4.15 software. Data acquired from a previous study using LA-ICP-MS (Gehrels, pers. com., 2008) was used to compare age populations and abundance. Bin size used for histograms is 50 Myr. Axes were standardized to 55 grain max vertically and ages ranging from 0 to 3500 Myr horizontally. Shaded bars, 1800-2000 Ma, represent the Trans-Hudson Orogen. The 2.5-2.7 Ga population is interpreted to be Wyoming province derived detrital zircons.

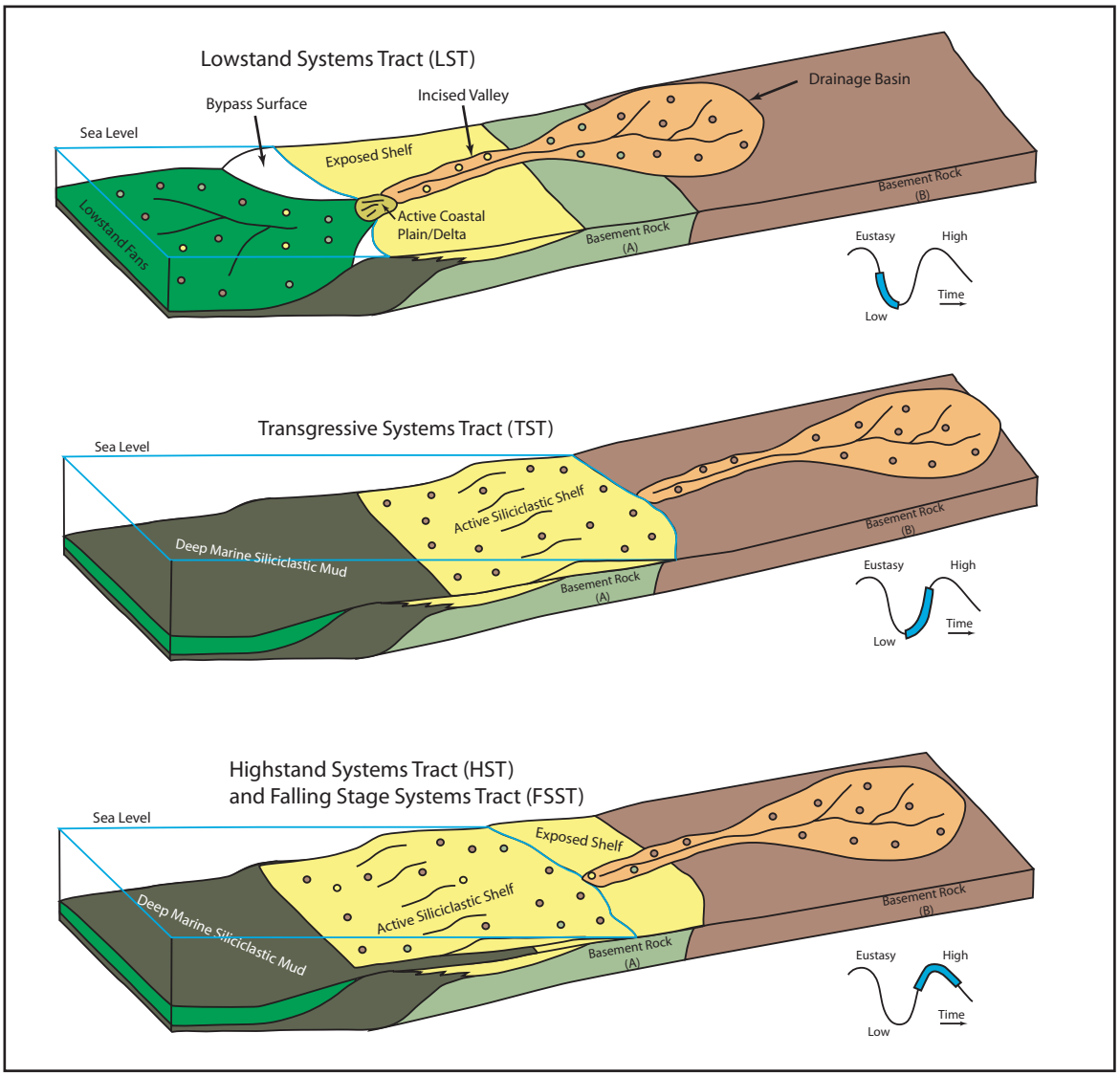

Figure 14: Impact of Sequence Stratigraphy on Provenance (from Pope, 2008). A model characterizing how the correlation between stratigraphic packages and detrital zircon populations may change with long-term changes in relative sea level (Pope, 2008). The colored dots represent different sediment sources: Siliciclastic Shelf-yellow, Basement Rock (A)-pink, Basement Rock (B)-red. During the LST, when sea level is lowest, subaerial erosion of the exposed siliciclastic shelf and further inboard basement rock will supply a large portion of sediment for coastal plains, deltas, and lowstand fans. With an increase in relative sea level during the TST the more proximal sources to the shoreline, siliciclastic shelf and Basement Rock (A), will be buried by sediment derived from sources further inboard, Basement Rock (B). As relative sea level begins to fall during the HST or FSST sediment deposition will prograde and siliciclastic detritus is derived from more proximal sources.

APPENDIX B

TABLES

Table 1: Study Locations

Location	Latitude	Longitude	UTM Zone	Easting	Northing
Crystal Peak (Wah Wah Mountains), Utah	38° 48' 10.4" N	113° 35' 48.8" W	12S	274491	4298107
Davis Mountains, Utah	40° 7' 3.5" N	112° 43' 13.7" W	12T	353389	4442233
Pahvant Range, Utah	39° 10' 22.9" N	112° 8' 27.6" W	12S	401437	4336598
Schell Creek Range, Nevada	39° 29' 15.06" N	114° 42' 58.38" W	11S	696402	4373368
Cherry Creek Range, Nevada	39° 45' 12.2" N	115° 1' 38.6" W	11S	668991	4402250

Table 2: Facies Descriptions and Interpretations

Facies	Description	Interpretation
A	Very fine to fine grain sands, silt-finely crystalline dolomite, weak to moderately lithified, thin parallel laminations, medium to massive beds, soft sediment deformation caused by limited bioturbation or dewatering.	Offshore environment transition during a transgressive systems tract from a carbonate dominated environment to a siliciclastic shelf, sands deposited as storm layer deposits (Miller, 1977; Howard et al., 1981; Zimmerman and Cooper, 1999).
B	Very fine to fine grain quartz arenite, well sorted grains, well rounded, well lithified, medium to thick beds, low angle cross laminations.	Preservation of sedimentary structures indicates a higher energy environment, limited organism activity, most likely above storm weather wave base in a lower shoreface environment (Arnott, 1993).
C	fine to medium grain quartz arenite, well sorted, well rounded, low angle cross beds, medium to thick beds (1-3 meters), vertical burrows (skolithos), horizontal burrows (planolites) begin to appear, beginning of pockmark weathering pattern.	Minimal preservation of primary sedimentary structures with increased bioturbation and constant sediment supply in a middle shoreface environment (Reinson, 1984; Runkel et al., 2007).
D	fine to medium grain quartz arenite, well sorted, well rounded, massive bedding, remnants of low-angle cross laminae are very common, intensely bioturbated, Skolithos is abundant, pockmarked texture dominates outcrop surface.	An increase in sediment supply and tidal energy increases organism activity and completely reworks sediment in a middle-upper shoreface environment (Desjardins et al., 2010).
E	Fine to medium grain quartz arenite, well sorted, well rounded, medium bed sets, parallel laminations, heavy bioturbation, pock-mark pattern.	Planar laminae indicate upper flow regime conditions in a foreshore/tidal flat environment (Plint, 2010; Short, 1984).

Table 3: Similarity and Overlap

TOP						
			OVERLAP			
Gehrels Data	Gehrels Data					
Davis Mountains	0.791	Davis Mountains				
Pahvant Range	0.725	0.826	Pahvant Range			
Crystal Peak	0.842	0.852	0.773	Crystal Peak		
Schell Creek Range	0.775	0.820	0.741	0.803	Schell Creek Range	
Cherry Creek Range	0.781	0.829	0.742	0.778	0.787	Cherry Creek Range
			SIMILARITY			
Gehrels Data	Gehrels Data					
Davis Mountains	0.794	Davis Mountains				
Pahvant Range	0.810	0.922	Pahvant Range			
Crystal Peak	0.888	0.873	0.873	Crystal Peak		
Schell Creek Range	0.826	0.811	0.801	0.898	Schell Creek Range	
Cherry Creek Range	0.861	0.820	0.825	0.913	0.897	Cherry Creek Range
BASE						
			OVERLAP			
Gehrels Data	Gehrels Data					
Davis Mountains	0.724	Davis Mountains				
Pahvant Range	0.706	0.845	Pahvant Range			
Crystal Peak	0.821	0.832	0.819	Crystal Peak		
Schell Creek Range	0.795	0.798	0.782	0.893	Schell Creek Range	
Cherry Creek Range	0.738	0.766	0.773	0.767	0.744	Cherry Creek Range
			SIMILARITY			
Gehrels Data	Gehrels Data					
Davis Mountains	0.687	Davis Mountains				
Pahvant Range	0.689	0.930	Pahvant Range			
Crystal Peak	0.891	0.779	0.776	Crystal Peak		
Schell Creek Range	0.884	0.735	0.718	0.896	Schell Creek Range	
Cherry Creek Range	0.883	0.629	0.630	0.879	0.859	Cherry Creek Range

APPENDIX C

CRYSTAL PEAK

DATA TABLES

Sample CPB (Crystal Peak-Base)								
Sample Name	238U / 206Pb	1 σ (%)	207Pb / 206Pb	1 σ (%)	206Pb / 238 U (Ma)	1 σ abs err	207 Pb / 206 Pb (Ma)	1 σ abs err
< 10 % Discordant								
CP_120	2.934	2.42%	0.12598	2.68%	1890.5	39.5	2042.6	46.7
CP_119	3.130	1.91%	0.11059	2.49%	1787.1	29.7	1809.1	44.6
CP_117	3.216	1.92%	0.11103	2.48%	1745.5	29.3	1816.4	44.3
CP_116	3.284	2.16%	0.11225	2.51%	1713.8	32.4	1836.1	44.8
CP_115	2.105	2.25%	0.16550	2.47%	2505.6	46.5	2512.7	41.0
CP_114	3.120	2.05%	0.11296	2.50%	1792.2	32.0	1847.6	44.6
CP_113	2.792	1.88%	0.12167	2.45%	1973.3	31.8	1980.9	43.1
CP_112	1.938	1.98%	0.18309	2.44%	2682.0	43.2	2681.1	39.8
CP_111	1.965	2.03%	0.18704	2.48%	2652.3	43.9	2716.3	40.4
CP_110	2.915	1.87%	0.11521	2.48%	1901.1	30.8	1883.1	44.0
CP_109	2.954	1.87%	0.11443	2.46%	1879.8	30.4	1871.0	43.8
CP_107	3.096	2.56%	0.11426	2.79%	1804.2	40.1	1868.3	49.5
CP_106	1.886	2.59%	0.18121	2.77%	2742.8	57.5	2664.0	45.1
CP_105	3.048	2.64%	0.10966	2.78%	1829.3	41.9	1793.8	49.8
CP_104	2.972	2.54%	0.11403	2.78%	1869.5	41.0	1864.6	49.4
CP_103	1.946	2.54%	0.19263	2.76%	2672.7	55.3	2764.8	44.6
CP_102	3.172	2.52%	0.11228	2.76%	1766.3	38.9	1836.6	49.2
CP_101	1.941	2.56%	0.17980	2.76%	2679.2	56.0	2651.0	45.0
CP_100	1.988	2.58%	0.18353	2.78%	2627.1	55.4	2685.0	45.3
CP_99	3.213	2.60%	0.11175	2.76%	1747.0	39.6	1828.1	49.3
CP_98	1.908	2.77%	0.18191	2.82%	2716.1	61.0	2670.3	45.9
CP_97	3.193	2.76%	0.11261	2.86%	1756.5	42.3	1842.0	50.9
CP_95	2.485	9.50%	0.12796	2.36%	2180.0	173.4	2070.2	41.0
CP_94	2.763	9.59%	0.11372	2.55%	1991.0	162.3	1859.6	45.4
CP_93	2.894	9.52%	0.10993	2.39%	1913.4	155.8	1798.3	42.9

CP_90	3.395	9.54%	0.11195	2.67%	1664.3	138.4	1831.4	47.7
CP_88	3.338	9.56%	0.11390	2.50%	1689.1	140.5	1862.5	44.5
CP_87	2.934	9.53%	0.12500	2.39%	1890.7	154.3	2028.7	41.8
CP_84	1.891	7.02%	0.19021	1.78%	2736.9	154.7	2743.9	29.0
CP_83	3.089	6.96%	0.11542	1.76%	1807.8	108.7	1886.5	31.3
CP_80	3.161	7.05%	0.11683	2.11%	1772.0	108.4	1908.3	37.4
CP_79	3.183	7.01%	0.11723	2.03%	1761.0	107.1	1914.5	36.1
CP_78	3.268	6.99%	0.11504	1.86%	1720.8	104.8	1880.5	33.2
CP_77	2.863	6.99%	0.12855	1.78%	1931.4	115.7	2078.2	31.0
CP_76	3.175	7.00%	0.11041	1.92%	1764.9	107.2	1806.1	34.5
CP_75	2.877	6.99%	0.13202	1.76%	1923.1	115.1	2125.1	30.5
CP_74	2.654	6.98%	0.12882	1.91%	2061.2	121.9	2081.9	33.2
CP_73	3.033	6.98%	0.11068	1.82%	1836.8	110.6	1810.6	32.7
CP_72	2.093	4.65%	0.18617	1.79%	2517.4	96.1	2708.6	29.2
CP_71	2.964	4.62%	0.11005	1.76%	1874.0	74.7	1800.3	31.6
CP_70	2.901	4.63%	0.11835	1.75%	1909.3	76.0	1931.5	31.1
CP_69	3.065	4.57%	0.11119	1.77%	1820.2	72.1	1819.0	31.8
CP_67	3.113	4.61%	0.11148	1.76%	1795.6	71.9	1823.7	31.5
CP_66	2.023	4.58%	0.17948	1.69%	2589.6	97.0	2648.1	27.7
CP_65	2.073	4.59%	0.16848	1.69%	2537.9	95.5	2542.6	28.1
CP_64	2.652	4.59%	0.12903	1.74%	2062.4	80.5	2084.7	30.4
CP_63	1.906	4.59%	0.18345	1.72%	2719.0	101.0	2684.3	28.2
CP_62	2.982	4.58%	0.11338	1.69%	1864.3	73.8	1854.3	30.2
CP_61	3.035	4.66%	0.11696	2.34%	1835.9	74.0	1910.3	41.4
CP_60	3.250	2.97%	0.11112	1.98%	1729.3	44.9	1817.8	35.6
CP_59	3.128	2.99%	0.11223	2.11%	1788.2	46.5	1835.9	37.7
CP_58	3.097	3.00%	0.11214	2.03%	1804.0	47.0	1834.4	36.3
CP_57	2.787	3.09%	0.13088	2.31%	1976.4	52.4	2109.9	40.0
CP_56	3.246	2.99%	0.11164	2.01%	1731.1	45.2	1826.4	36.0
CP_55	3.092	2.96%	0.10968	2.06%	1806.2	46.5	1794.1	37.0
CP_54	2.792	3.02%	0.12597	2.08%	1973.5	51.1	2042.5	36.2
CP_53	2.719	3.05%	0.12703	2.06%	2019.1	52.6	2057.3	35.9
CP_52	3.014	3.08%	0.11673	2.37%	1847.3	49.3	1906.7	42.0
CP_51	3.134	3.01%	0.11137	2.07%	1785.1	46.7	1821.8	37.0
CP_50	2.882	2.99%	0.12147	2.10%	1920.1	49.4	1978.0	36.9
CP_49	3.003	2.93%	0.11612	1.98%	1853.2	47.0	1897.3	35.1
CP_48	3.138	3.09%	0.10618	3.03%	1783.1	47.9	1734.8	54.6
CP_47	2.534	2.85%	0.14762	2.63%	2144.3	51.9	2318.5	44.5
CP_46	2.698	2.78%	0.13033	2.61%	2032.2	48.3	2102.4	45.2

CP_45	1.844	2.73%	0.20544	2.60%	2792.7	61.5	2869.9	41.7
CP_44	2.102	2.77%	0.16073	2.59%	2508.8	57.3	2463.3	43.2
CP_43	2.672	2.78%	0.12496	2.63%	2049.1	48.6	2028.2	45.9
CP_42	3.193	2.90%	0.11119	2.65%	1756.2	44.5	1818.9	47.3
CP_41	3.007	2.74%	0.10822	2.60%	1850.8	44.0	1769.6	46.8
CP_40	3.092	2.84%	0.11072	2.64%	1806.4	44.5	1811.3	47.2
CP_39	1.481	2.76%	0.23735	2.61%	3326.3	71.4	3102.3	41.0
CP_38	2.229	2.82%	0.16655	2.62%	2389.5	56.0	2523.3	43.3
CP_37	2.888	2.90%	0.11611	2.68%	1916.9	48.0	1897.2	47.4
CP_36	2.584	2.56%	0.12809	2.08%	2108.9	46.0	2071.9	36.2
CP_35	2.727	2.58%	0.12397	2.07%	2013.8	44.5	2014.1	36.3
CP_34	3.128	2.55%	0.11031	2.28%	1788.3	39.8	1804.5	40.9
CP_33	1.802	2.49%	0.18998	2.08%	2845.9	57.1	2742.0	33.8
CP_32	1.925	2.44%	0.18167	2.07%	2697.1	53.5	2668.2	33.9
CP_31	2.081	2.41%	0.16418	2.06%	2529.9	50.3	2499.2	34.2
CP_29	2.994	2.49%	0.11202	2.19%	1857.8	40.1	1832.5	39.1
CP_27	1.909	2.43%	0.17805	2.06%	2714.9	53.7	2634.8	33.8
CP_26	1.958	2.34%	0.17453	2.02%	2660.0	50.7	2601.6	33.3
CP_25	2.905	2.51%	0.10699	2.09%	1907.2	41.3	1748.8	37.7
CP_24	3.085	3.76%	0.11052	1.76%	1809.8	59.0	1807.9	31.7
CP_23	3.037	3.67%	0.11102	1.69%	1834.8	58.3	1816.1	30.4
CP_22	2.826	3.64%	0.12542	1.64%	1953.0	61.0	2034.7	28.7
CP_21	2.966	3.61%	0.10803	1.64%	1873.0	58.5	1766.4	29.7
CP_20	2.944	3.68%	0.11716	1.69%	1885.0	59.9	1913.3	30.1
CP_19	2.796	3.70%	0.11878	1.70%	1971.1	62.6	1937.9	30.1
CP_18	2.684	3.72%	0.12827	1.65%	2041.2	64.8	2074.4	28.8
CP_16	5.242	3.64%	0.07700	1.66%	1125.6	37.5	1121.2	32.8
CP_15	2.554	3.61%	0.13389	1.72%	2129.6	65.1	2149.6	29.7
CP_14	2.053	3.62%	0.18187	1.63%	2557.8	76.0	2670.0	26.8
CP_13	2.711	3.57%	0.12357	1.61%	2024.3	61.7	2008.3	28.2
CP_12	2.286	3.47%	0.16807	2.23%	2339.2	67.7	2538.5	37.0
CP_11	3.198	3.60%	0.11018	2.39%	1753.8	55.0	1802.4	42.8
CP_10	2.159	3.50%	0.16795	2.22%	2453.4	70.9	2537.3	36.7
CP_9	2.905	3.49%	0.11632	2.20%	1907.0	57.4	1900.5	39.0
CP_8	3.018	3.58%	0.11300	2.26%	1845.0	57.3	1848.2	40.4
CP_7	3.050	3.42%	0.11136	2.20%	1828.0	54.3	1821.7	39.4
CP_6	2.734	3.45%	0.12477	2.20%	2009.2	59.2	2025.5	38.5
CP_5	2.064	3.45%	0.18060	2.18%	2547.2	72.2	2658.4	35.8
CP_4	2.010	3.45%	0.18166	2.20%	2602.7	73.5	2668.1	36.0

CP_3	3.183	3.46%	0.11062	2.22%	1761.4	53.2	1809.6	39.8
CP_2	3.249	3.47%	0.11010	2.23%	1729.8	52.5	1801.1	40.0
CP_1	3.160	3.45%	0.10953	2.19%	1772.2	53.2	1791.6	39.4
> 10% Discordant								
CP_118	3.558	1.95%	0.17665	2.51%	1596.6	27.6	2621.7	41.1
CP_108	4.085	2.77%	0.17062	2.84%	1411.5	35.0	2563.7	46.8
CP_96	4.644	10.04%	0.17741	2.42%	1257.1	113.6	2628.9	39.6
CP_92	3.395	9.59%	0.11343	2.71%	1664.2	139.2	1855.0	48.2
CP_91	3.449	9.58%	0.11372	2.67%	1641.1	137.3	1859.7	47.4
CP_89	3.453	9.58%	0.11446	2.81%	1639.8	137.3	1871.4	49.8
CP_86	13.651	11.34%	0.18373	2.42%	455.7	49.7	2686.9	39.5
CP_85	3.580	9.53%	0.11076	2.48%	1587.9	132.8	1811.9	44.4
CP_82	3.614	7.01%	0.11904	1.74%	1574.7	97.1	1941.9	30.8
CP_81	3.202	6.98%	0.12104	1.74%	1751.9	106.2	1971.7	30.6
CP_68	5.134	4.65%	0.11082	1.68%	1147.1	48.7	1813.0	30.2
CP_30	3.529	2.42%	0.12814	2.05%	1608.1	34.4	2072.6	35.7
CP_28	2.892	2.48%	0.10601	2.09%	1914.4	41.0	1731.8	37.8
CP_17	2.577	3.73%	0.18211	1.67%	2114.1	66.9	2672.2	27.3

Sample TS1 (Crystal Peak-Top Sequence 1)								
Sample Name	238U / 206Pb	1 σ (%)	207Pb / 206Pb	1 σ (%)	206Pb / 238 U (Ma)	1 σ abs err	207 Pb / 206 Pb (Ma)	1 σ abs err
< 10 % Discordant								
TS1_120	3.168	3.98%	0.10842	1.76%	1768.4	61.2	1773.1	31.8
TS1_119	1.892	3.82%	0.18489	1.59%	2735.4	84.6	2697.2	26.0
TS1_115	3.196	3.83%	0.10895	1.64%	1755.0	58.6	1781.9	29.5
TS1_114	2.983	3.80%	0.11078	1.54%	1863.7	61.3	1812.3	27.7
TS1_113	1.891	3.81%	0.18339	1.58%	2736.9	84.5	2683.7	25.8
TS1_112	2.848	2.88%	0.10865	1.80%	1939.8	48.1	1776.9	32.4
TS1_111	3.089	3.01%	0.10975	1.91%	1807.7	47.2	1795.3	34.4
TS1_109	3.049	2.90%	0.11242	1.80%	1828.4	46.1	1839.0	32.2
TS1_108	2.160	2.94%	0.16300	1.81%	2452.9	59.7	2487.0	30.1
TS1_107	3.058	2.96%	0.11267	1.83%	1824.0	46.9	1843.0	32.8
TS1_106	1.988	2.91%	0.17142	1.89%	2626.8	62.5	2571.5	31.3
TS1_105	2.922	2.88%	0.10820	1.83%	1897.6	47.1	1769.3	33.0
TS1_104	2.953	2.90%	0.11336	1.89%	1879.9	47.1	1854.0	33.8
TS1_102	2.618	2.95%	0.13298	1.97%	2085.5	52.4	2137.7	34.1
TS1_101	1.831	2.83%	0.18003	1.77%	2809.5	64.0	2653.1	29.1
TS1_100	3.024	3.01%	0.11067	1.84%	1841.9	48.1	1810.4	33.1
TS1_99	2.897	2.87%	0.10996	1.82%	1911.3	47.2	1798.8	32.7
TS1_60	1.769	1.77%	0.18593	3.00%	2888.5	41.0	2706.5	48.6
TS1_59	2.836	1.70%	0.11264	2.97%	1946.9	28.4	1842.4	52.9
TS1_58	3.220	4.20%	0.11241	3.01%	1743.6	63.8	1838.7	53.5
TS1_57	2.796	1.78%	0.11099	2.98%	1971.0	30.1	1815.7	53.1
TS1_55	2.953	2.60%	0.10928	2.91%	1880.3	42.3	1787.4	52.1
TS1_54	2.491	2.57%	0.12396	2.95%	2175.6	47.3	2014.0	51.5
TS1_52	2.752	2.75%	0.11123	2.95%	1998.3	47.1	1819.6	52.6
TS1_51	2.945	2.82%	0.11062	3.03%	1884.4	46.0	1809.5	54.1
TS1_49	3.035	2.89%	0.11151	2.91%	1836.0	46.0	1824.1	52.0
TS1_48	2.662	2.50%	0.11458	2.90%	2055.7	43.8	1873.3	51.4
TS1_47	2.909	2.49%	0.11092	2.93%	1904.6	41.0	1814.5	52.2
TS1_46	1.719	2.57%	0.21112	2.90%	2955.6	60.7	2914.2	46.1
TS1_45	1.931	2.99%	0.19333	2.98%	2689.8	65.5	2770.7	48.1
TS1_44	2.735	2.52%	0.11418	2.92%	2008.8	43.3	1867.1	51.7
TS1_43	1.803	2.58%	0.18237	2.91%	2844.8	59.1	2674.5	47.3
TS1_42	3.020	2.77%	0.12241	3.03%	1843.7	44.2	1991.7	52.9

TS1_40	2.025	2.18%	0.16630	2.41%	2587.0	46.2	2520.7	40.0
TS1_39	2.992	2.02%	0.10768	2.33%	1858.6	32.6	1760.5	42.0
TS1_38	2.646	2.47%	0.12981	2.43%	2066.5	43.5	2095.4	42.1
TS1_37	2.296	2.55%	0.15590	2.32%	2330.4	49.8	2411.7	38.9
TS1_36	1.801	2.19%	0.18497	2.32%	2847.5	50.2	2698.0	37.9
TS1_35	3.156	2.24%	0.11035	2.36%	1774.4	34.7	1805.2	42.3
TS1_34	2.885	2.05%	0.11100	2.34%	1918.7	34.0	1815.8	42.0
TS1_31	2.936	2.28%	0.10887	2.35%	1889.7	37.2	1780.6	42.2
TS1_30	2.764	3.00%	0.13654	2.41%	1990.7	51.2	2183.7	41.4
TS1_29	2.901	2.25%	0.11634	2.41%	1909.2	37.1	1900.8	42.6
TS1_28	3.067	2.07%	0.10985	2.40%	1819.0	32.7	1797.0	43.1
TS1_27	2.904	1.52%	0.11334	2.22%	1907.6	25.0	1853.6	39.6
TS1_26	1.809	1.54%	0.18612	2.24%	2837.1	35.3	2708.2	36.5
TS1_25	2.909	2.06%	0.11078	2.31%	1905.0	34.0	1812.3	41.4
TS1_24	2.804	1.47%	0.11807	2.24%	1966.0	24.8	1927.1	39.6
TS1_23	1.635	1.48%	0.19633	2.21%	3076.4	36.1	2795.9	35.6
TS1_22	2.896	1.78%	0.11178	2.29%	1911.9	29.4	1828.5	40.9
TS1_21	2.029	2.11%	0.17786	2.30%	2582.8	44.8	2633.0	37.8
TS1_20	2.882	1.77%	0.11159	2.25%	1920.4	29.3	1825.5	40.3
TS1_19	2.981	1.65%	0.11206	2.27%	1864.8	26.7	1833.1	40.5
TS1_18	2.828	1.48%	0.11279	2.25%	1951.6	24.9	1844.9	40.1
TS1_14	2.088	3.32%	0.18735	2.38%	2522.4	69.0	2719.1	38.8
TS1_13	1.829	3.38%	0.19724	2.41%	2811.1	76.7	2803.5	38.9
TS1_12	1.886	3.30%	0.18509	2.38%	2741.8	73.2	2699.0	38.7
TS1_11	3.180	3.70%	0.11349	2.58%	1762.5	56.9	1856.1	45.9
TS1_10	3.215	3.55%	0.11864	2.64%	1746.0	54.1	1935.9	46.6
TS1_9	2.962	3.61%	0.12166	2.68%	1875.1	58.5	1980.6	47.0
TS1_8	2.913	3.39%	0.12002	2.54%	1902.7	55.7	1956.5	44.6
TS1_7	2.690	3.35%	0.11563	2.38%	2037.3	58.2	1889.7	42.3
TS1_6	3.181	3.85%	0.11259	2.63%	1762.2	59.1	1841.7	46.9
TS1_5	2.794	3.40%	0.11245	2.40%	1972.1	57.5	1839.4	42.8
TS1_4	2.995	3.85%	0.11794	2.64%	1857.2	61.9	1925.3	46.6
TS1_3	1.892	3.45%	0.17794	2.45%	2735.9	76.5	2633.7	40.1
TS1_2	1.724	3.36%	0.19266	2.38%	2949.2	79.1	2765.0	38.5
> 10% Discordant								
TS1_118	2.728	3.92%	0.11017	1.63%	2013.2	67.5	1802.2	29.3
TS1_117	2.755	3.85%	0.10961	1.55%	1996.2	65.8	1792.9	28.0
TS1_116	1.702	3.90%	0.17487	1.55%	2979.3	92.4	2604.8	25.6
TS1_110	2.636	2.87%	0.11293	1.78%	2073.2	50.7	1847.2	31.8

TS1_103	2.814	2.92%	0.10593	1.80%	1960.3	49.2	1730.5	32.7
TS1_56	2.737	2.01%	0.14196	2.99%	2007.7	34.5	2251.2	50.7
TS1_53	6.776	2.59%	0.10327	2.93%	887.4	21.4	1683.7	53.2
TS1_50	2.370	2.57%	0.12508	2.89%	2269.2	48.9	2029.9	50.2
TS1_41	2.849	2.37%	0.16866	2.38%	1939.6	39.6	2544.4	39.3
TS1_33	2.392	2.26%	0.23081	2.41%	2251.9	42.8	3057.6	38.0
TS1_17	5.170	1.48%	0.20988	2.23%	1139.9	15.5	2904.6	35.7
TS1_16	4.058	2.36%	0.12932	2.34%	1420.0	30.0	2088.7	40.5
TS1_15	3.199	2.13%	0.13208	2.72%	1753.6	32.6	2125.8	46.8
TS1_1	3.320	3.38%	0.11674	2.45%	1697.2	50.2	1906.9	43.4

Sample TS2 (Crystal Peak-Top Sequence 2)								
Sample Name	238U / 206Pb	1 σ (%)	207Pb / 206Pb	1 σ (%)	206Pb / 238 U (Ma)	1 σ abs err	207 Pb / 206 Pb (Ma)	1 σ abs err
< 10 % Discordant								
TS2_120	2.864	2.62%	0.11301	3.67%	1930.4	43.5	1848.3	65.0
TS2_119	1.920	2.52%	0.18099	3.66%	2702.6	55.4	2662.0	59.4
TS2_118	3.131	2.48%	0.11197	3.67%	1786.7	38.6	1831.6	65.1
TS2_117	2.327	2.36%	0.14337	3.66%	2304.6	45.5	2268.3	61.8
TS2_116	3.090	2.49%	0.11137	3.67%	1807.3	39.1	1821.9	65.1
TS2_115	1.946	2.69%	0.18223	3.68%	2673.7	58.7	2673.3	59.6
TS2_114	1.975	2.59%	0.17928	3.67%	2641.1	56.0	2646.2	59.7
TS2_113	2.935	2.54%	0.10989	3.80%	1890.2	41.5	1797.5	67.6
TS2_112	2.989	2.79%	0.11539	3.73%	1860.4	44.9	1886.0	65.7
TS2_111	2.817	2.49%	0.11541	3.69%	1958.4	41.8	1886.3	65.0
TS2_110	2.882	2.40%	0.10945	3.69%	1920.4	39.7	1790.4	65.8
TS2_109	2.917	2.52%	0.11173	3.79%	1900.3	41.4	1827.7	67.2
TS2_108	2.952	2.61%	0.11091	3.66%	1880.9	42.4	1814.5	65.0
TS2_106	2.776	2.50%	0.11029	3.66%	1983.1	42.5	1804.3	65.1
TS2_105	1.895	2.84%	0.18017	3.06%	2731.5	63.0	2654.4	49.9
TS2_104	1.847	2.63%	0.18535	3.03%	2789.0	59.3	2701.4	49.2
TS2_103	2.571	2.77%	0.13587	3.06%	2117.7	49.9	2175.2	52.4
TS2_102	2.831	2.52%	0.10879	3.03%	1950.1	42.3	1779.2	54.2
TS2_101	2.976	2.60%	0.10906	3.02%	1867.2	42.0	1783.8	54.1
TS2_100	3.182	2.78%	0.11221	3.16%	1761.5	42.6	1835.5	56.2
TS2_99	1.668	2.80%	0.22488	3.07%	3028.4	67.4	3016.0	48.4
TS2_98	3.004	2.75%	0.10422	3.06%	1852.3	44.1	1700.6	55.3
TS2_97	2.975	2.76%	0.11185	3.05%	1868.1	44.5	1829.7	54.3
TS2_96	3.038	2.73%	0.10792	3.09%	1834.5	43.4	1764.6	55.5
TS2_95	2.571	2.80%	0.12405	3.04%	2118.3	50.3	2015.2	53.0
TS2_94	2.965	2.69%	0.10820	3.07%	1873.7	43.6	1769.4	55.0
TS2_93	2.078	2.83%	0.15870	3.07%	2532.2	58.9	2441.9	51.0
TS2_92	2.747	2.71%	0.12036	3.19%	2001.3	46.4	1961.5	55.9
TS2_91	5.693	2.94%	0.07177	2.72%	1043.2	28.3	979.4	54.4
TS2_90	3.097	2.94%	0.11188	2.73%	1803.7	46.0	1830.2	48.7
TS2_89	1.887	2.89%	0.17990	2.63%	2740.7	64.2	2651.9	43.0
TS2_88	1.891	2.93%	0.18207	2.62%	2736.8	64.9	2671.8	42.7

TS2_87	3.080	2.81%	0.10968	2.67%	1812.3	44.3	1794.1	47.8
TS2_86	2.941	2.70%	0.11144	2.69%	1886.8	44.0	1823.0	48.1
TS2_85	2.819	2.74%	0.11900	2.66%	1957.5	46.0	1941.2	46.8
TS2_84	3.177	2.97%	0.11368	2.74%	1764.0	45.7	1859.0	48.6
TS2_83	2.981	2.68%	0.11288	2.68%	1864.8	43.2	1846.3	47.6
TS2_82	1.978	2.87%	0.19078	2.69%	2637.2	61.8	2748.9	43.5
TS2_81	1.970	2.80%	0.18738	2.69%	2645.9	60.6	2719.3	43.7
TS2_80	2.862	2.79%	0.11310	2.66%	1932.0	46.4	1849.8	47.3
TS2_79	1.870	2.87%	0.21937	2.67%	2761.6	64.2	2976.1	42.4
TS2_78	1.883	2.64%	0.18693	2.63%	2746.3	58.8	2715.3	42.8
TS2_77	3.265	1.92%	0.10601	1.99%	1722.2	28.9	1731.9	36.1
TS2_76	1.847	1.83%	0.19068	1.99%	2789.1	41.3	2748.0	32.4
TS2_75	2.637	2.27%	0.11739	2.12%	2072.6	40.1	1916.8	37.6
TS2_74	2.868	1.92%	0.11481	2.02%	1928.5	31.9	1876.9	35.9
TS2_72	1.912	1.97%	0.17648	2.02%	2711.6	43.4	2620.1	33.3
TS2_70	2.961	2.56%	0.11454	2.00%	1875.5	41.5	1872.6	35.6
TS2_69	2.919	2.40%	0.10810	2.03%	1899.1	39.4	1767.7	36.6
TS2_68	2.130	2.68%	0.14819	2.16%	2481.4	55.0	2325.1	36.6
TS2_66	2.089	2.84%	0.18072	2.17%	2521.4	59.0	2659.5	35.5
TS2_65	2.512	2.70%	0.13553	2.09%	2160.2	49.3	2170.8	36.0
TS2_64	3.144	2.66%	0.11126	2.11%	1780.2	41.2	1820.2	37.9
TS2_63	1.687	2.65%	0.24254	2.05%	3000.1	63.3	3136.7	32.3
TS2_62	3.089	2.73%	0.10932	2.06%	1808.1	42.8	1788.1	37.0
TS2_61	3.013	2.71%	0.10799	2.02%	1847.5	43.4	1765.7	36.5
TS2_60	1.869	2.53%	0.17802	2.01%	2763.3	56.6	2634.5	33.0
TS2_58	1.809	2.66%	0.19776	2.13%	2836.6	60.7	2807.8	34.4
TS2_57	1.978	2.65%	0.17367	2.09%	2637.6	57.2	2593.3	34.4
TS2_56	2.655	2.49%	0.12838	2.36%	2060.4	43.8	2075.9	41.0
TS2_55	3.030	2.08%	0.11092	2.32%	1838.5	33.2	1814.6	41.5
TS2_54	2.752	2.12%	0.13025	2.31%	1998.1	36.4	2101.4	40.0
TS2_53	2.651	2.50%	0.12284	2.34%	2063.6	43.9	1997.9	41.0
TS2_52	2.898	2.20%	0.10841	2.27%	1911.1	36.3	1772.9	40.9
TS2_51	1.792	2.29%	0.17760	2.32%	2858.6	52.7	2630.6	38.1
TS2_50	2.100	2.18%	0.15420	2.38%	2510.6	45.2	2393.0	39.9
TS2_49	3.009	2.34%	0.11046	2.40%	1849.6	37.5	1807.0	43.0
TS2_48	2.870	2.44%	0.11000	2.33%	1927.3	40.5	1799.4	41.8
TS2_47	2.984	2.52%	0.11241	2.44%	1863.0	40.6	1838.7	43.6
TS2_46	1.919	2.67%	0.20270	2.61%	2704.3	58.7	2848.0	41.8
TS2_45	2.627	2.21%	0.12582	2.31%	2079.4	39.1	2040.4	40.3

TS2_44	3.162	2.94%	0.11206	2.43%	1771.3	45.3	1833.1	43.4
TS2_43	2.844	2.73%	0.11260	2.33%	1942.4	45.6	1841.8	41.6
TS2_42	3.075	2.51%	0.10905	2.28%	1814.9	39.6	1783.6	41.0
TS2_41	3.008	2.45%	0.11022	2.40%	1850.2	39.4	1803.1	43.0
TS2_40	2.852	2.29%	0.11051	2.23%	1937.4	38.2	1807.8	40.0
TS2_39	2.879	2.61%	0.11195	2.23%	1921.9	43.3	1831.3	39.8
TS2_38	1.756	2.35%	0.18844	2.21%	2905.0	54.8	2728.6	36.0
TS2_37	3.154	2.72%	0.11273	2.26%	1775.4	42.0	1843.8	40.3
TS2_36	1.788	2.05%	0.18150	2.23%	2863.1	47.2	2666.6	36.4
TS2_35	2.376	1.97%	0.13560	2.20%	2264.2	37.4	2171.7	37.8
TS2_34	2.999	2.13%	0.11368	2.36%	1855.1	34.3	1859.0	42.0
TS2_33	2.186	2.03%	0.16157	2.16%	2428.4	41.0	2472.2	35.9
TS2_32	2.831	2.16%	0.11299	1.67%	1949.9	36.3	1848.1	29.8
TS2_31	3.058	2.23%	0.11441	1.64%	1823.9	35.3	1870.6	29.3
TS2_30	1.663	2.25%	0.22175	1.66%	3035.2	54.3	2993.4	26.4
TS2_29	3.172	2.03%	0.11128	1.69%	1766.7	31.3	1820.5	30.4
TS2_28	3.078	2.53%	0.10815	1.96%	1813.3	39.8	1768.4	35.4
TS2_27	3.163	2.58%	0.11477	1.98%	1770.8	39.9	1876.2	35.2
TS2_26	1.957	2.90%	0.18075	2.13%	2661.3	63.0	2659.7	34.9
TS2_25	2.972	2.66%	0.11604	1.90%	1869.7	43.0	1896.1	33.9
TS2_24	1.907	2.19%	0.18488	1.93%	2718.0	48.4	2697.1	31.5
TS2_23	2.949	2.38%	0.11156	1.97%	1882.6	38.7	1824.9	35.3
TS2_22	2.203	2.41%	0.18101	1.91%	2412.8	48.3	2662.1	31.2
TS2_21	2.576	1.93%	0.12733	1.91%	2114.5	34.7	2061.5	33.3
TS2_19	2.929	2.16%	0.10658	1.87%	1893.6	35.4	1741.8	33.9
TS2_18	2.790	2.11%	0.11361	1.84%	1974.9	35.9	1858.0	32.9
TS2_17	1.939	2.45%	0.15937	1.88%	2680.6	53.5	2448.9	31.5
TS2_16	2.506	1.93%	0.12856	1.89%	2164.4	35.4	2078.4	32.8
TS2_15	2.710	1.92%	0.11528	1.87%	2024.4	33.3	1884.3	33.3
TS2_14	2.859	2.39%	0.11506	3.04%	1933.8	39.7	1880.8	53.7
TS2_13	1.456	2.20%	0.28307	3.03%	3369.7	57.6	3379.9	46.5
TS2_12	2.894	2.29%	0.11247	3.06%	1913.4	37.8	1839.7	54.3
TS2_11	3.290	3.36%	0.10976	3.20%	1710.7	50.3	1795.5	57.2
TS2_10	1.889	2.37%	0.18841	3.10%	2738.6	52.6	2728.4	50.2
TS2_9	2.955	2.22%	0.11691	3.05%	1879.0	36.1	1909.5	53.8
TS2_8	2.653	2.54%	0.13062	3.07%	2062.1	44.7	2106.3	53.0
TS2_6	3.003	2.19%	0.10863	3.04%	1853.1	35.1	1776.6	54.4
TS2_5	3.187	2.17%	0.10582	3.04%	1759.3	33.4	1728.6	54.8
TS2_4	3.130	2.34%	0.11017	3.09%	1787.3	36.5	1802.2	55.2

TS2_3	2.997	2.42%	0.11068	3.07%	1856.4	38.9	1810.7	54.7
TS2_1	2.797	2.36%	0.11401	3.07%	1970.2	39.9	1864.3	54.5
> 10% Discordant								
TS2_107	2.785	2.45%	0.10978	3.72%	1977.6	41.6	1795.8	66.2
TS2_73	2.018	2.68%	0.11829	2.09%	2594.1	57.1	1930.6	36.9
TS2_71	2.697	2.11%	0.11236	2.00%	2033.1	36.7	1837.9	35.8
TS2_67	1.761	2.39%	0.37968	2.42%	2898.9	55.6	3830.5	36.1
TS2_59	2.818	2.65%	0.17338	3.55%	1957.5	44.6	2590.5	58.1
TS2_7	1.680	2.30%	0.18669	3.03%	3011.3	55.2	2713.2	49.1
TS2_2	2.924	2.31%	0.13494	3.15%	1896.1	37.9	2163.3	53.9

Sample CPT (Crystal Peak-Top)								
Sample Name	238U / 206Pb	1 σ (%)	207Pb / 206Pb	1 σ (%)	206Pb / 238 U (Ma)	1 σ abs err	207 Pb / 206 Pb (Ma)	1 σ abs err
< 10 % Discordant								
CP_120	1.878	1.54%	0.18890	2.08%	2751.4	34.4	2732.6	33.9
CP_119	2.325	1.67%	0.16305	2.13%	2306.5	32.3	2487.6	35.4
CP_118	3.128	1.67%	0.10970	2.08%	1788.0	26.0	1794.5	37.4
CP_117	2.903	1.66%	0.11758	2.15%	1908.4	27.4	1919.8	38.1
CP_116	1.942	1.66%	0.17112	2.08%	2677.2	36.3	2568.7	34.3
CP_115	2.903	1.74%	0.11879	2.14%	1908.4	28.6	1938.1	37.8
CP_113	3.152	1.50%	0.11460	2.07%	1776.1	23.2	1873.6	36.9
CP_112	1.771	2.07%	0.20922	2.21%	2885.5	47.9	2899.5	35.4
CP_111	3.129	2.12%	0.10962	2.25%	1787.6	33.1	1793.0	40.4
CP_110	2.702	2.19%	0.12740	2.35%	2029.7	38.1	2062.3	40.9
CP_109	1.960	2.11%	0.18401	2.21%	2657.8	45.9	2689.3	36.1
CP_108	3.335	2.11%	0.11334	2.22%	1690.6	31.3	1853.6	39.6
CP_107	2.833	2.10%	0.11503	2.21%	1948.6	35.1	1880.4	39.3
CP_106	3.109	2.13%	0.11117	2.26%	1797.6	33.3	1818.6	40.5
CP_105	2.962	2.08%	0.11655	2.27%	1875.4	33.8	1903.9	40.2
CP_104	2.867	2.27%	0.12128	2.43%	1928.9	37.7	1975.1	42.6
CP_103	3.075	2.03%	0.10793	2.20%	1815.1	32.0	1764.7	39.7
CP_102	2.622	2.04%	0.12865	2.22%	2082.4	36.3	2079.7	38.6
CP_101	2.659	2.04%	0.12967	2.29%	2058.1	35.8	2093.4	39.7
CP_100	3.027	2.09%	0.11095	2.30%	1839.9	33.4	1815.1	41.1
CP_99	3.056	2.27%	0.11128	2.45%	1824.7	35.9	1820.4	43.8
CP_97	1.795	2.91%	0.18543	2.77%	2854.3	66.8	2702.0	44.9
CP_96	2.040	2.88%	0.16945	2.80%	2571.4	60.8	2552.2	46.1
CP_95	3.066	2.90%	0.10929	2.86%	1819.5	45.8	1787.6	51.2
CP_94	3.106	3.14%	0.11089	2.98%	1799.2	49.1	1814.1	53.1
CP_93	3.032	2.98%	0.11262	2.81%	1837.3	47.5	1842.1	50.0
CP_92	2.064	3.02%	0.18180	2.83%	2546.7	63.3	2669.3	46.1
CP_91	2.858	2.86%	0.11432	2.77%	1934.1	47.6	1869.2	49.2
CP_90	2.910	2.89%	0.11939	2.81%	1904.1	47.5	1947.1	49.4
CP_89	2.631	2.90%	0.12521	2.83%	2077.0	51.3	2031.8	49.3
CP_88	2.976	2.92%	0.11146	2.82%	1867.4	47.1	1823.3	50.2
CP_87	3.012	2.94%	0.11324	2.80%	1848.3	47.0	1852.1	49.8

CP_86	2.983	2.92%	0.11114	2.79%	1863.5	47.1	1818.2	49.8
CP_85	1.902	2.93%	0.17585	2.77%	2723.9	64.8	2614.1	45.4
CP_84	1.924	3.82%	0.19984	3.23%	2697.8	83.8	2824.9	51.8
CP_83	3.065	3.73%	0.10779	3.16%	1820.1	58.8	1762.4	56.7
CP_82	2.914	3.72%	0.11305	3.17%	1902.0	60.9	1849.0	56.2
CP_81	3.012	3.73%	0.11696	3.19%	1848.3	59.6	1910.3	56.3
CP_80	2.900	3.70%	0.11455	3.21%	1910.1	60.9	1872.9	56.8
CP_79	1.976	3.76%	0.18755	3.17%	2639.6	80.9	2720.8	51.3
CP_78	3.143	3.78%	0.11039	3.21%	1780.9	58.5	1805.8	57.2
CP_77	1.912	3.77%	0.18654	3.20%	2711.6	83.0	2711.9	51.9
CP_75	5.475	3.76%	0.07586	3.26%	1081.4	37.3	1091.4	64.0
CP_73	2.964	3.71%	0.10817	3.20%	1873.9	60.1	1768.9	57.4
CP_72	2.647	4.39%	0.13621	3.28%	2065.8	77.1	2179.6	56.1
CP_71	2.981	3.73%	0.11258	3.20%	1864.9	60.2	1841.4	56.9
CP_70	3.366	1.49%	0.10739	1.92%	1676.6	21.9	1755.6	34.7
CP_69	3.214	1.67%	0.10815	2.03%	1746.3	25.5	1768.5	36.5
CP_68	2.064	1.59%	0.18380	2.00%	2547.1	33.3	2687.4	32.6
CP_66	2.107	1.45%	0.18196	1.90%	2504.1	30.1	2670.8	31.1
CP_64	2.142	1.46%	0.17595	1.97%	2469.8	29.8	2615.0	32.4
CP_63	1.831	1.41%	0.20595	1.88%	2809.3	32.0	2873.9	30.3
CP_61	3.247	1.39%	0.11001	1.87%	1730.6	21.1	1799.5	33.6
CP_60	3.106	1.52%	0.10957	2.07%	1799.1	23.9	1792.3	37.3
CP_59	3.188	1.37%	0.10858	1.88%	1758.8	21.1	1775.7	33.8
CP_58	3.174	1.40%	0.10898	1.90%	1765.8	21.6	1782.5	34.3
CP_57	3.310	1.45%	0.11095	1.99%	1702.0	21.7	1815.0	35.7
CP_56	3.198	1.60%	0.10991	2.37%	1754.1	24.6	1797.9	42.5
CP_55	2.720	1.34%	0.12709	2.19%	2018.6	23.2	2058.2	38.1
CP_54	3.214	1.40%	0.11097	2.18%	1746.3	21.3	1815.4	39.0
CP_53	2.735	1.43%	0.12810	2.31%	2008.9	24.7	2072.0	40.2
CP_52	3.172	1.33%	0.11059	2.19%	1766.7	20.6	1809.1	39.3
CP_51	2.463	1.39%	0.14036	2.15%	2196.6	25.8	2231.6	36.7
CP_50	2.688	1.42%	0.13346	2.28%	2038.6	24.8	2144.0	39.3
CP_48	2.043	1.38%	0.18008	2.23%	2568.8	29.2	2653.6	36.5
CP_47	3.135	1.34%	0.11033	2.16%	1784.8	20.9	1804.9	38.7
CP_46	3.116	1.35%	0.11150	2.16%	1794.0	21.1	1824.0	38.7
CP_45	3.247	1.35%	0.11156	2.15%	1730.9	20.5	1825.0	38.5
CP_44	3.152	1.40%	0.11037	2.19%	1776.2	21.7	1805.5	39.2
CP_43	3.005	1.35%	0.11654	2.20%	1852.0	21.7	1903.8	39.0
CP_42	3.065	1.92%	0.11575	2.38%	1820.3	30.3	1891.6	42.1

CP_41	3.248	1.88%	0.10939	2.27%	1730.4	28.5	1789.3	40.8
CP_40	3.168	1.87%	0.11106	2.30%	1768.2	28.9	1816.8	41.2
CP_39	3.082	1.88%	0.11257	2.30%	1811.5	29.6	1841.2	41.1
CP_38	3.214	1.91%	0.11334	2.40%	1746.2	29.1	1853.6	42.7
CP_37	3.199	2.13%	0.11244	2.75%	1753.3	32.6	1839.2	48.9
CP_36	3.015	1.90%	0.11175	2.30%	1846.5	30.4	1828.1	41.2
CP_35	1.565	1.87%	0.25819	2.23%	3184.2	46.9	3235.7	34.8
CP_34	1.990	1.90%	0.18774	2.28%	2624.9	40.9	2722.4	37.1
CP_33	3.290	1.91%	0.11001	2.37%	1710.8	28.7	1799.6	42.5
CP_32	3.031	1.89%	0.11755	2.32%	1837.9	30.1	1919.3	41.0
CP_31	1.996	1.86%	0.18549	2.24%	2618.3	39.8	2702.6	36.6
CP_30	1.910	2.05%	0.19165	2.44%	2714.4	45.3	2756.4	39.5
CP_29	3.142	1.89%	0.11119	2.32%	1781.1	29.3	1819.0	41.5
CP_28	2.795	1.77%	0.12484	2.68%	1971.8	30.0	2026.5	46.8
CP_27	2.715	1.85%	0.12540	2.89%	2021.5	31.9	2034.5	50.3
CP_26	1.998	1.86%	0.18351	2.80%	2615.4	39.8	2684.8	45.5
CP_25	1.954	1.76%	0.18563	2.69%	2664.1	38.4	2703.8	43.7
CP_24	3.016	1.90%	0.11686	2.94%	1846.1	30.4	1908.8	51.8
CP_23	2.686	1.78%	0.12455	2.75%	2039.9	31.1	2022.4	48.0
CP_22	2.979	1.78%	0.11185	2.74%	1865.9	28.7	1829.7	48.8
CP_21	3.139	1.73%	0.10847	2.68%	1782.6	26.9	1774.0	48.1
CP_20	3.368	1.75%	0.10891	2.68%	1676.2	25.8	1781.3	48.0
CP_19	1.909	1.80%	0.17869	2.73%	2715.6	39.8	2640.8	44.6
CP_18	2.195	1.78%	0.16686	2.68%	2419.6	35.9	2526.3	44.3
CP_17	3.004	1.76%	0.11244	2.68%	1852.6	28.3	1839.2	47.7
CP_16	2.004	1.77%	0.18512	2.67%	2609.1	37.9	2699.3	43.4
CP_15	3.052	1.78%	0.11016	2.70%	1826.9	28.2	1802.0	48.3
CP_14	1.950	3.89%	0.20286	2.99%	2668.3	84.4	2849.4	47.9
CP_12	3.224	3.86%	0.11253	3.09%	1741.7	58.6	1840.7	55.0
CP_11	2.015	3.84%	0.18359	2.98%	2597.6	81.6	2685.6	48.4
CP_10	3.227	3.84%	0.11019	3.02%	1740.0	58.3	1802.5	53.9
CP_9	3.275	3.93%	0.11219	3.22%	1717.8	59.0	1835.3	57.2
CP_8	3.174	3.86%	0.11179	3.04%	1765.4	59.3	1828.7	54.1
CP_6	3.201	3.89%	0.11030	3.17%	1752.4	59.4	1804.4	56.6
CP_5	2.931	3.91%	0.11086	3.10%	1892.5	63.9	1813.6	55.4
CP_4	2.703	3.85%	0.12802	3.01%	2029.4	66.7	2071.0	52.1
CP_3	2.098	3.87%	0.16405	3.01%	2512.7	80.0	2497.9	49.8
CP_2	2.947	3.99%	0.11832	3.26%	1883.6	64.8	1931.0	57.3
CP_1	2.738	3.88%	0.13091	3.03%	2007.0	66.6	2110.3	52.2

> 10% Discordant								
CP_114	2.335	1.51%	0.28909	2.15%	2298.0	29.1	3412.7	33.0
CP_98	2.756	3.02%	0.27487	2.76%	1995.7	51.7	3334.0	42.6
CP_76	5.212	3.73%	0.16634	3.15%	1131.5	38.6	2521.1	52.0
CP_74	3.013	3.85%	0.16605	3.66%	1847.7	61.6	2518.2	60.3
CP_67	3.451	1.41%	0.28204	2.54%	1640.5	20.5	3374.3	39.1
CP_65	3.200	1.68%	0.12619	2.59%	1753.1	25.8	2045.5	45.0
CP_62	10.042	2.48%	0.15169	1.97%	612.0	14.5	2365.1	33.3
CP_49	3.206	1.38%	0.14157	2.49%	1750.0	21.1	2246.5	42.4
CP_13	9.224	3.83%	0.10266	2.98%	663.5	24.1	1672.8	54.0
CP_7	2.555	4.69%	0.10981	3.46%	2129.1	84.5	1796.3	61.7

Sample FH (Crystal Peak-Fish Haven Dolomite Base)								
Sample Name	238U / 206Pb	1 σ (%)	207Pb / 206Pb	1 σ (%)	206Pb / 238 U (Ma)	1 σ abs err	207 Pb / 206 Pb (Ma)	1 σ abs err
< 10 % Discordant								
FH_120	2.666	2.05%	0.11522	2.73%	2053.1	36.0	1883.3	48.3
FH_119	2.681	2.14%	0.11603	2.79%	2043.6	37.4	1896.0	49.3
FH_116	1.675	1.95%	0.19043	2.70%	3017.6	46.9	2745.9	43.7
FH_114	2.503	2.43%	0.12651	2.83%	2166.9	44.5	2050.0	49.1
FH_112	2.783	3.96%	0.11176	3.10%	1979.2	67.2	1828.2	55.2
FH_111	2.975	3.98%	0.11235	3.04%	1868.1	64.2	1837.7	54.1
FH_110	1.883	4.04%	0.18026	3.03%	2745.9	89.6	2655.3	49.4
FH_109	1.895	4.13%	0.18264	3.09%	2731.7	91.4	2677.0	50.2
FH_108	3.282	4.00%	0.10407	3.09%	1714.5	59.9	1698.0	55.9
FH_107	1.952	4.06%	0.18161	3.03%	2666.0	88.1	2667.6	49.4
FH_106	2.968	4.03%	0.11305	3.08%	1872.0	65.1	1849.1	54.6
FH_103	2.708	4.01%	0.11598	3.02%	2026.1	69.4	1895.1	53.4
FH_102	1.998	4.05%	0.17435	3.04%	2615.9	86.4	2599.8	49.7
FH_101	2.524	4.03%	0.12417	3.04%	2151.8	73.3	2016.9	53.0
FH_100	2.416	4.04%	0.12595	3.05%	2232.9	75.8	2042.2	53.0
FH_99	1.750	3.98%	0.18735	3.02%	2913.3	92.7	2719.0	48.9
FH_98	13.513	2.15%	0.05543	2.00%	460.2	9.5	429.8	43.9
FH_97	3.053	2.08%	0.11234	1.79%	1826.5	33.0	1837.5	32.0
FH_96	2.938	1.95%	0.11576	1.82%	1888.7	31.9	1891.8	32.4
FH_95	1.621	1.88%	0.20687	2.02%	3097.9	46.0	2881.2	32.4
FH_94	2.886	1.94%	0.12796	1.81%	1917.9	32.1	2070.2	31.6
FH_93	1.890	2.00%	0.18383	1.78%	2737.7	44.4	2687.7	29.1
FH_92	3.040	1.97%	0.11200	1.76%	1833.1	31.4	1832.1	31.5
FH_91	5.361	2.14%	0.08007	1.88%	1102.6	21.7	1198.8	36.6
FH_90	3.145	2.28%	0.11799	1.83%	1779.8	35.4	1926.0	32.4
FH_89	2.537	2.08%	0.14600	1.78%	2142.2	37.9	2299.6	30.3
FH_88	2.075	2.22%	0.18349	1.76%	2535.2	46.3	2684.7	28.9
FH_87	2.532	1.96%	0.12574	1.83%	2145.8	35.8	2039.2	31.9
FH_86	2.788	1.88%	0.11768	1.84%	1975.7	32.0	1921.3	32.6
FH_85	1.950	2.10%	0.18575	1.75%	2668.2	45.7	2704.9	28.7

FH_84	3.187	2.14%	0.11662	2.05%	1759.2	32.9	1905.0	36.3
FH_83	2.000	2.73%	0.18965	2.34%	2614.1	58.3	2739.1	38.0
FH_82	3.157	2.17%	0.11112	2.01%	1774.0	33.5	1817.7	36.1
FH_81	3.369	1.97%	0.11387	2.06%	1675.7	29.0	1862.1	36.8
FH_80	2.122	2.13%	0.18721	2.02%	2488.6	43.9	2717.8	32.9
FH_79	2.956	1.88%	0.11606	2.03%	1878.4	30.6	1896.4	36.0
FH_78	2.956	1.97%	0.11629	2.00%	1878.5	32.0	1899.9	35.6
FH_77	1.603	1.72%	0.25879	2.01%	3124.6	42.4	3239.3	31.3
FH_75	2.864	1.98%	0.11281	2.00%	1930.3	32.9	1845.1	35.7
FH_73	1.966	1.96%	0.18686	2.02%	2651.4	42.5	2714.8	32.9
FH_71	2.162	1.99%	0.16350	2.02%	2451.1	40.5	2492.2	33.6
FH_70	2.824	2.01%	0.11081	3.19%	1953.9	33.8	1812.8	56.8
FH_69	3.334	2.18%	0.10791	3.21%	1690.9	32.4	1764.4	57.6
FH_68	3.127	2.05%	0.11679	3.30%	1788.9	32.0	1907.6	58.0
FH_67	2.982	1.91%	0.10857	3.19%	1864.3	30.8	1775.5	57.2
FH_66	3.114	1.79%	0.10957	3.21%	1795.1	28.0	1792.3	57.4
FH_65	2.949	1.78%	0.11317	3.25%	1882.3	29.0	1850.9	57.7
FH_62	2.881	2.16%	0.12564	3.22%	1920.6	35.8	2037.9	55.8
FH_61	2.959	2.43%	0.12513	3.40%	1876.8	39.4	2030.6	59.0
FH_59	2.881	1.99%	0.11942	3.22%	1920.6	33.0	1947.6	56.5
FH_58	2.090	1.78%	0.16762	3.18%	2520.6	37.0	2534.0	52.4
FH_57	1.955	1.93%	0.18527	3.21%	2663.3	41.9	2700.6	52.1
FH_56	3.241	2.83%	0.10953	2.88%	1733.5	42.9	1791.6	51.5
FH_55	2.291	2.00%	0.13137	2.62%	2334.7	39.1	2116.3	45.1
FH_54	2.750	2.07%	0.12456	2.68%	1999.5	35.4	2022.5	46.7
FH_53	2.804	1.90%	0.11177	2.77%	1966.3	32.1	1828.4	49.3
FH_52	3.417	2.05%	0.10937	2.68%	1654.9	29.8	1789.0	48.0
FH_51	2.055	2.00%	0.17880	2.63%	2555.9	42.1	2641.8	43.0
FH_50	3.037	1.89%	0.11308	2.71%	1834.8	30.1	1849.4	48.2
FH_49	1.961	1.91%	0.17863	2.67%	2656.8	41.5	2640.2	43.6
FH_48	3.214	1.75%	0.10873	2.67%	1746.3	26.8	1778.3	48.0
FH_47	2.900	1.67%	0.11783	2.64%	1909.7	27.6	1923.5	46.6
FH_46	2.685	1.86%	0.12224	2.65%	2040.8	32.4	1989.1	46.5
FH_45	3.462	1.88%	0.09633	2.70%	1635.6	27.1	1554.3	49.8
FH_44	2.866	1.87%	0.11733	2.82%	1929.5	31.1	1915.9	49.8
FH_43	2.222	1.95%	0.17496	2.63%	2395.3	38.8	2605.6	43.2
FH_42	2.765	1.53%	0.12392	2.10%	1990.4	26.2	2013.5	36.7
FH_41	2.150	1.53%	0.18120	2.04%	2462.0	31.2	2663.9	33.4
FH_40	2.754	1.60%	0.12467	2.10%	1996.8	27.4	2024.1	36.7

FH_39	2.946	1.51%	0.11123	2.06%	1884.0	24.6	1819.7	37.0
FH_38	3.169	1.62%	0.11131	2.06%	1768.0	25.0	1820.9	37.0
FH_36	3.162	1.64%	0.10775	2.05%	1771.6	25.3	1761.6	37.1
FH_35	3.181	1.66%	0.10884	2.05%	1762.0	25.6	1780.1	37.0
FH_34	12.996	1.81%	0.05774	2.17%	477.9	8.3	520.0	46.9
FH_33	3.011	1.59%	0.12152	2.20%	1848.7	25.5	1978.7	38.7
FH_32	3.001	1.65%	0.10923	2.05%	1854.0	26.5	1786.6	37.0
FH_31	3.011	1.63%	0.10942	2.09%	1848.4	26.1	1789.8	37.5
FH_30	2.624	1.49%	0.13305	2.13%	2081.5	26.5	2138.6	36.8
FH_29	3.079	1.68%	0.11187	2.12%	1813.3	26.6	1830.0	37.9
FH_28	1.934	2.05%	0.19987	1.78%	2686.7	45.0	2825.1	28.8
FH_27	2.511	2.03%	0.13345	1.77%	2160.8	37.2	2143.8	30.6
FH_26	3.112	2.04%	0.11134	1.87%	1796.5	31.9	1821.5	33.5
FH_25	2.407	1.91%	0.15014	1.74%	2240.1	36.0	2347.6	29.5
FH_23	2.970	1.92%	0.11402	1.75%	1871.0	31.2	1864.5	31.3
FH_22	2.006	1.86%	0.17867	1.73%	2607.8	39.7	2640.6	28.5
CP_21	3.253	1.85%	0.10880	1.80%	1727.8	28.0	1779.5	32.5
CP_20	3.145	1.76%	0.10902	1.78%	1780.0	27.3	1783.0	32.0
CP_19	2.624	1.83%	0.12779	1.74%	2081.5	32.4	2067.8	30.4
CP_18	3.137	1.85%	0.11918	1.70%	1783.9	28.7	1943.9	30.2
CP_17	2.976	2.04%	0.11156	1.76%	1867.6	33.0	1824.9	31.6
CP_16	3.038	1.94%	0.11210	1.79%	1834.1	30.8	1833.8	32.2
CP_15	3.028	1.92%	0.11339	1.82%	1839.3	30.6	1854.5	32.5
FH_14	3.141	2.70%	0.10837	2.23%	1781.9	42.0	1772.3	40.2
FH_13	3.156	2.69%	0.11107	2.23%	1774.6	41.6	1817.0	40.0
FH_12	3.529	2.75%	0.10795	2.14%	1608.1	39.0	1765.0	38.6
FH_11	5.949	2.66%	0.07114	2.22%	1001.7	24.6	961.5	44.6
FH_10	1.875	2.65%	0.17853	2.18%	2755.8	59.1	2639.3	35.8
FH_9	1.842	2.75%	0.20897	2.19%	2795.7	62.2	2897.6	35.1
FH_7	1.850	2.76%	0.17940	2.21%	2785.4	62.1	2647.3	36.2
FH_6	2.717	2.78%	0.12615	2.20%	2020.2	48.0	2044.9	38.4
FH_5	3.228	2.88%	0.11739	2.29%	1739.6	43.8	1916.8	40.5
FH_4	3.235	2.74%	0.10987	2.23%	1736.5	41.6	1797.2	40.0
FH_3	2.467	2.66%	0.13964	2.18%	2193.8	49.3	2222.7	37.3
FH_2	3.220	2.62%	0.11175	2.22%	1743.3	39.9	1828.1	39.7
FH_1	1.919	2.74%	0.16578	2.18%	2704.0	60.2	2515.5	36.2
> 10% Discordant								
FH_118	2.669	2.09%	0.10935	2.76%	2051.5	36.6	1788.7	49.4
FH_117	2.603	1.95%	0.11488	2.72%	2096.1	34.9	1877.9	48.2

FH_115	2.732	2.19%	0.11032	3.02%	2010.5	37.8	1804.7	53.8
FH_113	2.626	2.02%	0.11092	2.73%	2079.8	35.8	1814.6	48.8
FH_105	4.597	4.00%	0.07764	3.05%	1268.9	45.9	1137.6	59.6
FH_104	9.171	5.25%	0.19238	3.07%	667.2	33.2	2762.6	49.6
FH_76	2.181	3.10%	0.20083	2.12%	2432.6	62.4	2832.9	34.2
FH_74	2.257	2.20%	0.18193	1.98%	2364.4	43.3	2670.5	32.4
FH_72	2.533	2.09%	0.18351	2.03%	2144.7	37.9	2684.9	33.2
FH_64	3.392	2.07%	0.14738	3.19%	1665.3	30.3	2315.7	53.7
FH_63	2.860	1.93%	0.10593	3.22%	1933.2	32.1	1730.5	58.0
FH_60	3.312	2.15%	0.11813	3.19%	1700.9	32.1	1928.1	56.0
FH_55	2.291	2.00%	0.13137	2.62%	2334.7	39.1	2116.3	45.1
FH_37	3.623	1.59%	0.11191	2.04%	1571.2	22.2	1830.6	36.6

WETHERIL PLOTS

Crystal Peak-Fish Haven (FH)

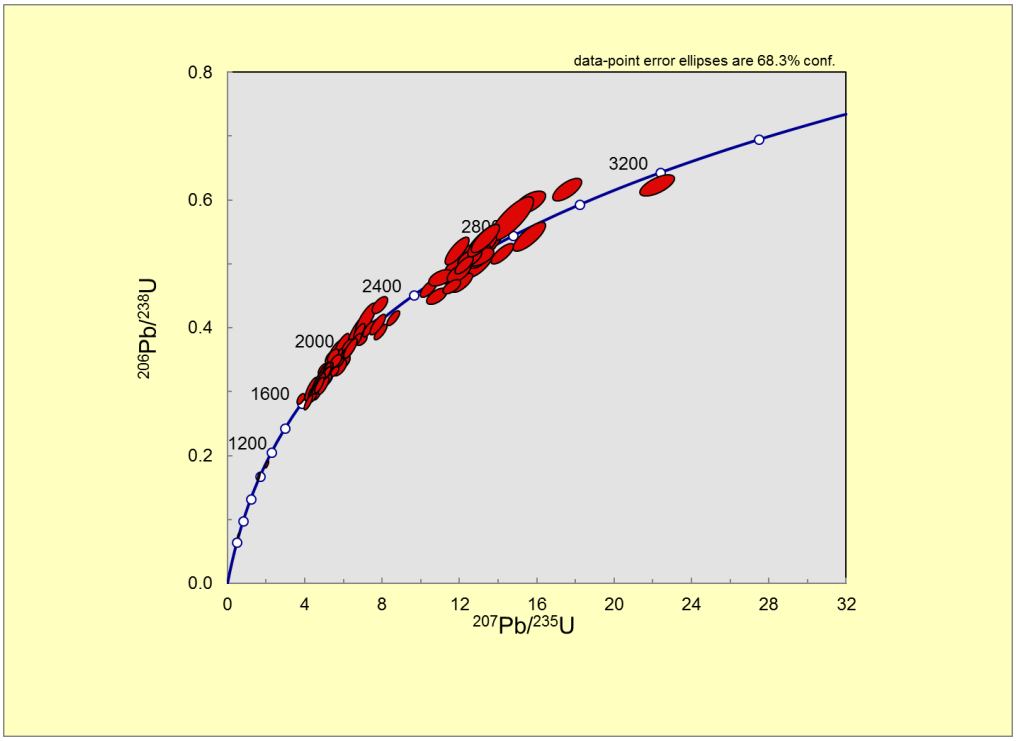

Crystal Peak-Top (CPTop)

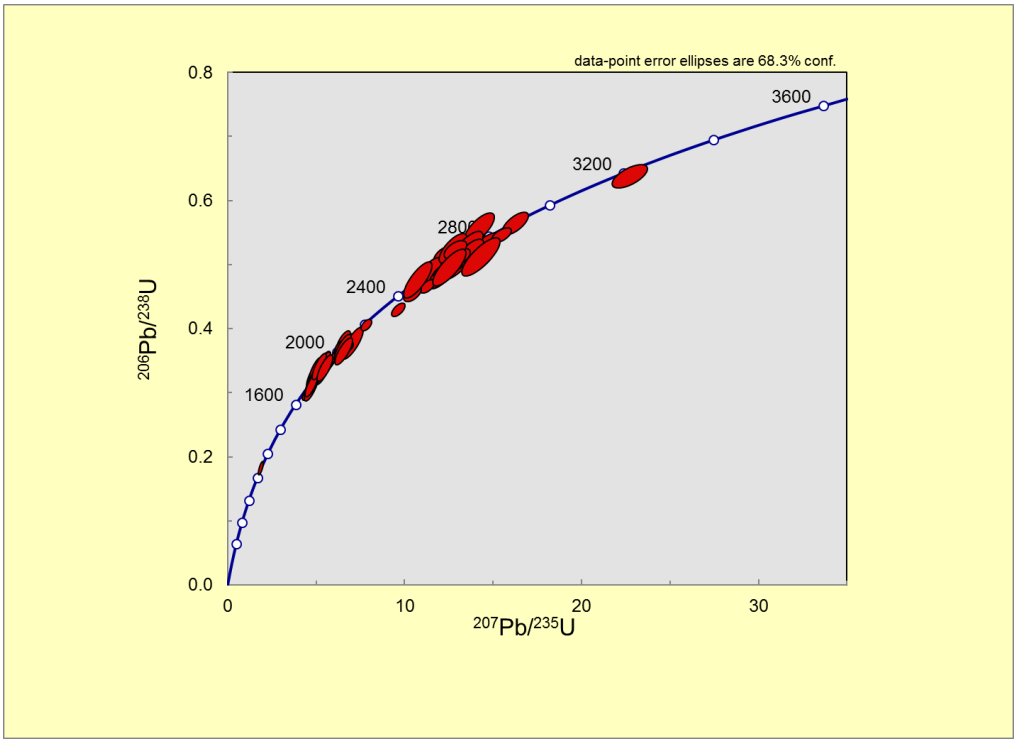

Crystal Peak-Top Sequence 2 (TS2)

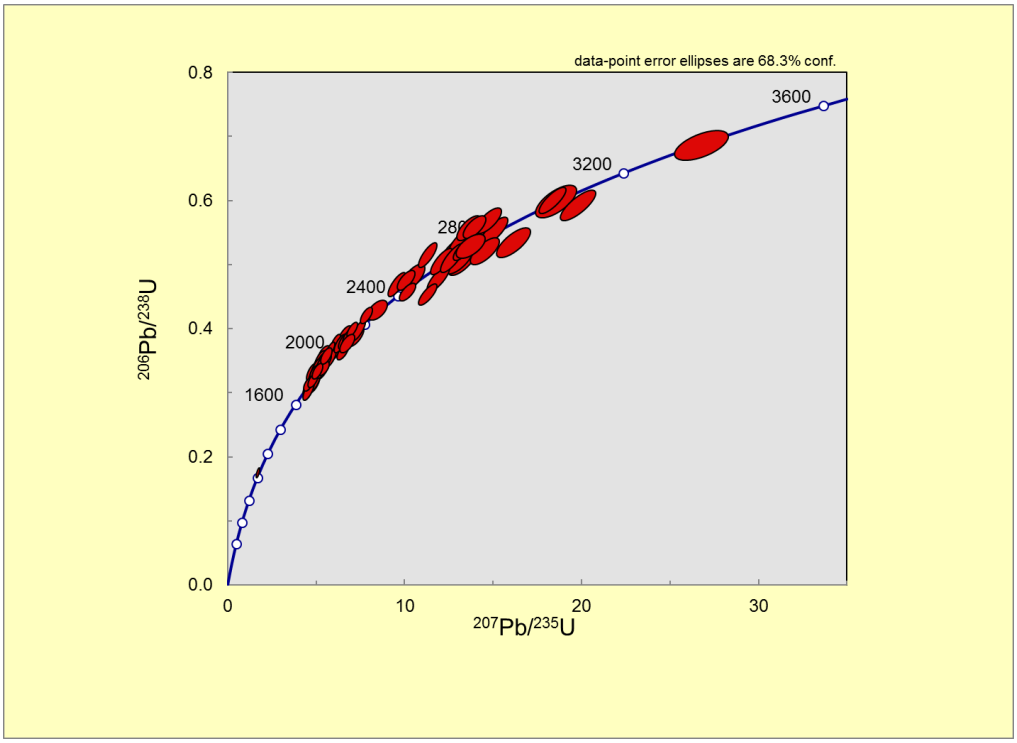

Crystal Peak-Top Sequence 1 (TS1)

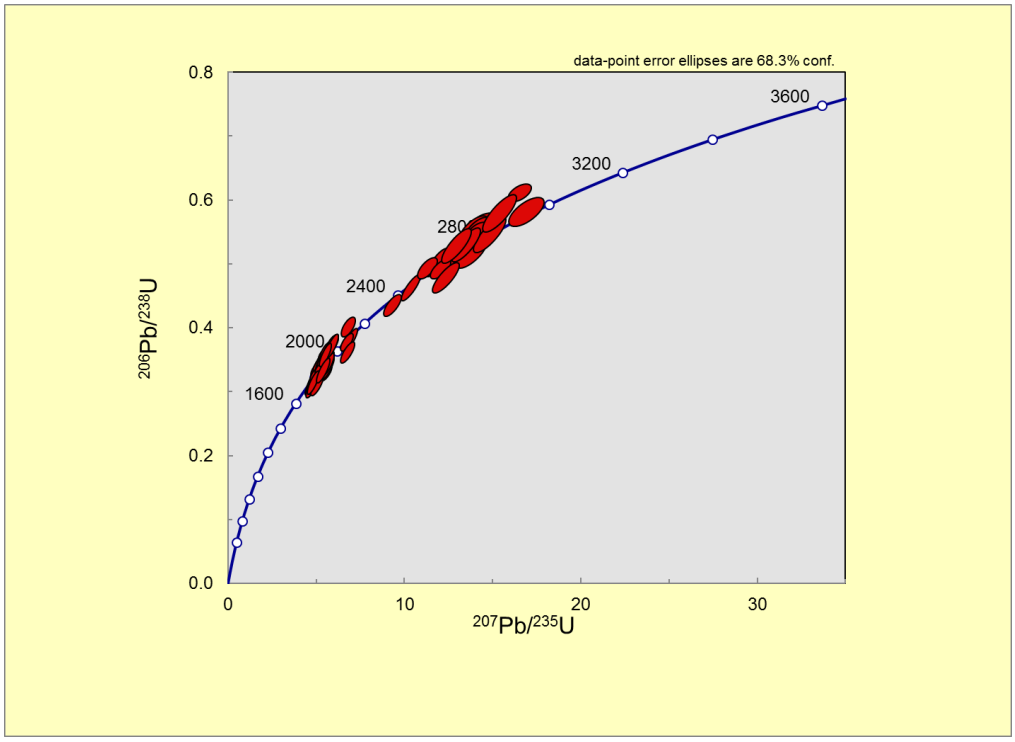

Crystal Peak-Base (CPBase)

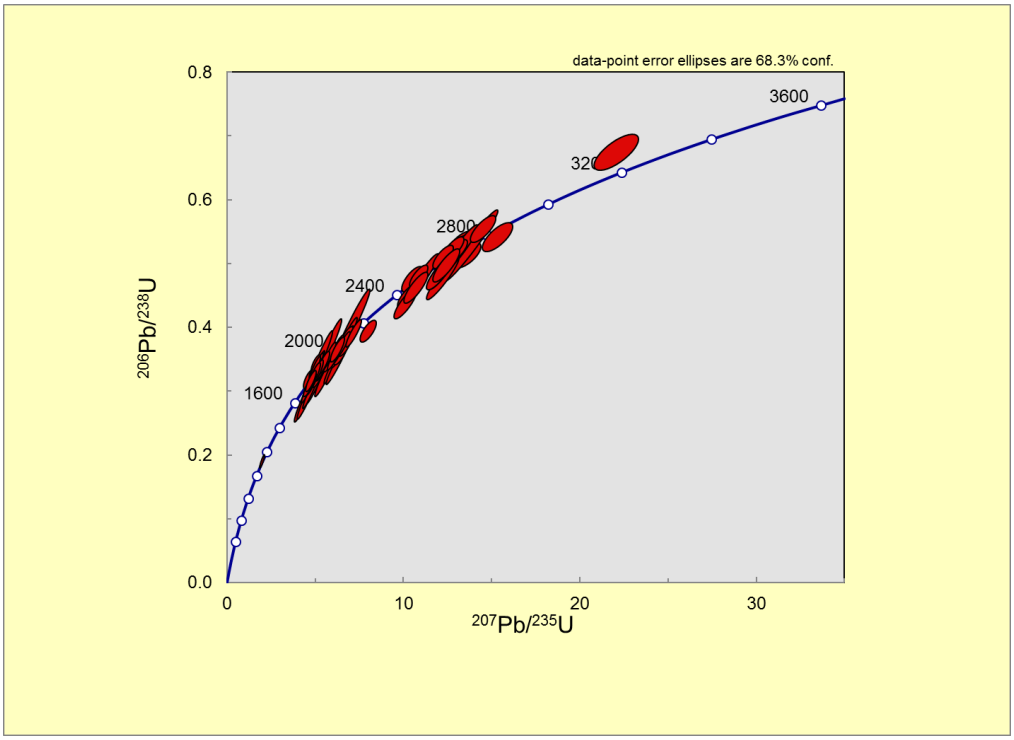

APPENDIX D

DAVIS MOUNTAINS

DATA TABLES

Sample DMB (Davis Mountains-Base)								
Sample Name	238U / 206Pb	1 σ (%)	207Pb / 206Pb	1 σ (%)	206Pb / 238 U (Ma)	1 σ abs err	207 Pb / 206 Pb (Ma)	1 σ abs err
< 10 % Discordant								
DM_120	3.401	2.21%	0.10628	1.64%	1661.7	32.3	1736.5	29.8
DM_119	1.794	1.20%	0.19907	1.65%	2855.8	27.6	2818.6	26.7
DM_118	1.924	1.22%	0.18685	1.67%	2698.1	26.9	2714.7	27.2
DM_117	1.952	1.25%	0.18637	1.64%	2667.0	27.2	2710.4	26.7
DM_116	1.798	1.19%	0.20655	1.67%	2851.1	27.4	2878.6	26.8
DM_115	3.211	1.20%	0.10690	1.65%	1747.6	18.3	1747.1	30.0
DM_114	3.018	1.35%	0.11371	1.94%	1845.1	21.7	1859.5	34.7
DM_113	2.045	1.40%	0.18204	1.71%	2566.3	29.6	2671.6	28.0
DM_112	1.935	1.32%	0.19337	1.74%	2685.2	28.9	2771.0	28.3
DM_111	5.594	1.13%	0.07345	1.76%	1060.3	11.1	1026.5	35.2
DM_110	1.826	1.23%	0.19895	1.70%	2815.0	28.0	2817.6	27.5
DM_109	1.983	1.26%	0.18550	1.68%	2631.7	27.2	2702.6	27.5
DM_108	1.913	1.23%	0.18076	2.27%	2711.2	27.2	2659.8	37.1
DM_106	1.909	1.19%	0.17843	2.22%	2715.7	26.4	2638.4	36.4
DM_105	1.822	1.35%	0.19417	2.27%	2820.8	30.8	2777.8	36.7
DM_104	1.992	1.33%	0.18120	2.25%	2623.0	28.7	2663.9	36.8
DM_103	1.894	1.28%	0.17854	2.25%	2733.5	28.4	2639.4	36.9
DM_102	1.797	1.30%	0.20507	2.26%	2852.6	29.8	2867.0	36.2
DM_101	3.014	1.22%	0.10760	2.26%	1847.0	19.6	1759.1	40.7
DM_100	3.226	1.23%	0.10472	2.31%	1740.8	18.7	1709.4	41.8
DM_99	5.450	1.28%	0.07480	2.35%	1086.0	12.8	1063.1	46.6
DM_98	1.826	1.27%	0.19660	2.22%	2814.9	28.9	2798.2	35.8
DM_97	1.950	1.20%	0.17784	2.23%	2668.4	26.1	2632.8	36.7
DM_96	2.102	1.36%	0.17989	2.24%	2508.6	28.2	2651.9	36.7
DM_95	1.941	1.25%	0.18137	2.25%	2678.3	27.4	2665.4	36.8
DM_94	1.938	1.37%	0.18268	3.66%	2681.6	30.0	2677.3	59.2

DM_93	2.079	1.45%	0.18164	3.67%	2532.0	30.2	2667.9	59.5
DM_91	1.971	1.51%	0.18018	3.65%	2645.8	32.7	2654.5	59.3
DM_90	3.173	1.39%	0.11010	3.66%	1766.1	21.5	1801.1	65.1
DM_89	1.835	1.41%	0.20022	3.65%	2804.7	32.1	2828.0	58.3
DM_88	2.862	1.33%	0.11393	3.64%	1931.9	22.2	1863.0	64.3
DM_87	2.085	1.69%	0.17673	3.67%	2525.7	35.2	2622.4	59.8
DM_86	3.073	1.39%	0.10889	3.68%	1816.0	22.0	1781.0	65.6
DM_85	2.762	1.42%	0.12039	3.69%	1991.8	24.2	1961.9	64.5
DM_84	1.993	1.26%	0.18114	3.63%	2621.0	27.0	2663.3	59.0
DM_83	1.955	1.38%	0.18269	3.65%	2662.6	30.1	2677.5	59.2
DM_82	3.141	1.82%	0.11075	3.80%	1781.8	28.2	1811.7	67.4
DM_81	5.877	1.33%	0.07135	3.67%	1013.0	12.5	967.3	73.2
DM_80	1.947	1.52%	0.18830	2.06%	2671.8	33.2	2727.4	33.6
DM_78	1.943	1.21%	0.18780	1.98%	2676.9	26.5	2723.0	32.3
DM_77	1.846	1.74%	0.18945	2.09%	2790.6	39.3	2737.4	34.0
DM_76	1.648	1.32%	0.20444	2.09%	3057.0	32.0	2861.9	33.6
DM_75	3.047	1.30%	0.10947	1.98%	1829.4	20.7	1790.6	35.7
DM_74	1.886	1.32%	0.18758	2.02%	2743.0	29.4	2721.0	32.9
DM_73	1.998	1.42%	0.19326	2.04%	2615.9	30.4	2770.1	33.1
DM_72	1.874	1.40%	0.18786	2.01%	2756.5	31.4	2723.5	32.8
DM_71	1.965	1.24%	0.18630	1.97%	2652.1	26.9	2709.7	32.1
DM_70	1.889	1.33%	0.19406	2.01%	2738.9	29.5	2776.9	32.6
DM_69	1.755	1.22%	0.21803	1.95%	2907.0	28.5	2966.2	31.1
DM_68	2.095	2.43%	0.18638	2.49%	2516.0	50.3	2710.5	40.6
DM_67	2.219	2.30%	0.15262	2.44%	2397.9	45.9	2375.5	41.0
DM_65	1.965	2.34%	0.19176	2.46%	2652.1	50.6	2757.3	39.9
DM_64	2.030	2.36%	0.18609	2.46%	2582.4	50.1	2707.9	40.0
DM_63	1.906	2.33%	0.18848	2.43%	2719.4	51.5	2729.0	39.4
DM_61	1.945	2.33%	0.18790	2.47%	2674.0	50.9	2723.9	40.1
DM_60	1.903	2.33%	0.18415	2.44%	2723.0	51.6	2690.6	39.7
DM_59	1.875	2.45%	0.18969	2.51%	2755.7	54.7	2739.5	40.7
DM_58	1.843	2.47%	0.18808	2.60%	2794.2	55.8	2725.4	42.2
DM_57	1.822	2.44%	0.20543	2.49%	2820.2	55.6	2869.8	39.9
DM_56	2.949	1.54%	0.11244	1.82%	1882.5	25.0	1839.3	32.5
DM_55	1.969	1.51%	0.18509	1.78%	2647.8	32.7	2699.0	29.1
DM_54	3.296	1.39%	0.10712	1.81%	1708.4	20.8	1750.9	32.8
DM_53	3.164	1.43%	0.11168	1.83%	1770.6	22.1	1826.9	32.8
DM_52	1.876	1.35%	0.19152	1.76%	2754.2	30.2	2755.3	28.6
DM_51	1.946	1.31%	0.17925	1.77%	2673.1	28.7	2645.9	29.1

DM_50	1.916	1.35%	0.18409	1.77%	2707.0	29.7	2690.1	28.9
DM_49	1.954	1.28%	0.18529	1.78%	2663.7	27.9	2700.8	29.1
DM_48	3.174	1.31%	0.10648	1.76%	1765.7	20.1	1740.0	32.0
DM_47	1.863	1.47%	0.18414	1.78%	2769.7	32.9	2690.5	29.1
DM_46	2.856	1.45%	0.11105	1.84%	1935.2	24.2	1816.7	33.0
DM_45	-24.919	25.11%	0.19686	1.84%	-264.0	-68.0	2800.3	29.9
DM_43	3.095	1.62%	0.11207	2.03%	1805.1	25.4	1833.2	36.3
DM_42	1.891	2.43%	0.18292	2.61%	2736.4	53.8	2679.5	42.5
DM_40	1.815	2.42%	0.19141	2.62%	2829.5	55.2	2754.3	42.4
DM_39	1.925	2.45%	0.18669	2.61%	2697.2	53.7	2713.2	42.4
DM_38	1.712	2.44%	0.22271	2.60%	2965.4	57.8	3000.4	41.2
DM_37	2.012	2.61%	0.18581	2.67%	2600.7	55.7	2705.4	43.3
DM_36	1.885	2.53%	0.18995	2.63%	2743.4	56.4	2741.7	42.6
DM_35	1.918	2.39%	0.19128	2.62%	2705.5	52.5	2753.2	42.4
DM_34	1.881	2.40%	0.19024	2.61%	2748.1	53.5	2744.2	42.3
DM_33	1.921	2.39%	0.18558	2.59%	2701.8	52.5	2703.3	42.0
DM_32	3.026	2.41%	0.11079	2.60%	1840.8	38.5	1812.3	46.5
DM_31	1.953	2.44%	0.18795	2.60%	2665.2	53.1	2724.3	42.3
DM_30	1.940	2.40%	0.17908	2.57%	2679.6	52.3	2644.4	42.1
DM_29	1.912	2.38%	0.18520	2.58%	2712.4	52.5	2700.0	42.0
DM_28	2.992	2.57%	0.11416	2.76%	1858.9	41.3	1866.7	49.0
DM_27	1.987	2.37%	0.18780	2.69%	2627.5	51.0	2723.0	43.7
DM_26	3.133	2.42%	0.11311	2.71%	1785.7	37.6	1849.9	48.3
DM_25	1.854	2.60%	0.21699	2.95%	2781.4	58.4	2958.5	46.8
DM_24	1.949	2.56%	0.19044	2.84%	2669.9	55.8	2746.0	45.9
DM_23	1.968	2.60%	0.18706	2.77%	2648.5	56.3	2716.4	45.0
DM_22	3.028	2.47%	0.11406	2.80%	1839.4	39.4	1865.1	49.6
DM_21	1.882	2.46%	0.18318	2.74%	2746.9	54.7	2681.8	44.6
DM_20	2.164	2.40%	0.16696	2.68%	2449.0	48.7	2527.4	44.3
DM_19	1.908	2.40%	0.18607	2.69%	2716.9	53.1	2707.7	43.7
DM_18	1.857	2.36%	0.19406	2.71%	2777.1	52.9	2776.9	43.8
DM_17	1.944	2.74%	0.18874	2.89%	2675.9	59.8	2731.3	46.7
DM_16	2.017	2.38%	0.17042	2.72%	2595.6	50.6	2561.8	44.7
DM_15	1.900	2.41%	0.18807	2.71%	2725.6	53.4	2725.4	44.0
DM_14	2.013	3.20%	0.18953	2.74%	2599.6	68.0	2738.1	44.3
DM_13	3.336	3.34%	0.11100	2.75%	1690.1	49.5	1815.8	49.1
DM_12	3.195	3.28%	0.11602	2.81%	1755.2	50.2	1895.7	49.8
DM_11	1.825	2.97%	0.20096	2.66%	2816.1	67.4	2834.0	42.7
DM_9	3.246	3.27%	0.11196	3.11%	1731.1	49.4	1831.5	55.3

DM_8	2.008	3.05%	0.18867	2.66%	2605.3	65.1	2730.6	43.1
DM_7	2.040	3.05%	0.18426	2.69%	2571.7	64.5	2691.6	43.8
DM_6	1.919	2.99%	0.18747	2.70%	2703.7	65.8	2720.1	43.8
DM_5	1.977	3.09%	0.18760	2.71%	2639.1	66.5	2721.3	44.0
DM_4	3.075	3.12%	0.11213	2.70%	1815.2	49.2	1834.2	48.2
DM_3	2.980	3.15%	0.11870	2.91%	1865.4	50.8	1936.8	51.1
DM_2	1.963	3.08%	0.18339	2.77%	2654.5	66.7	2683.8	45.1
DM_1	1.924	3.00%	0.18958	2.68%	2698.4	65.8	2738.5	43.4
> 10% Discordant								
DM_107	2.500	1.77%	0.17811	2.53%	2169.4	32.6	2635.3	41.5
DM_92	2.796	1.34%	0.17011	3.64%	1971.2	22.8	2558.7	59.6
DM_79	2.379	1.43%	0.17625	2.00%	2262.0	27.1	2617.9	32.9
DM_66	2.867	2.42%	0.18495	2.45%	1928.8	40.2	2697.8	39.8
DM_62	8.961	2.41%	0.06967	2.74%	682.0	15.5	918.5	55.4
DM_41	2.347	2.78%	0.28238	3.46%	2287.7	53.3	3376.1	53.0
DM_10	5.774	3.27%	0.10819	2.70%	1029.6	31.1	1769.2	48.5

Sample DMT (Davis Mountains-Top)								
Sample Name	238U / 206Pb	1 σ (%)	207Pb / 206Pb	1 σ (%)	206Pb / 238 U (Ma)	1 σ abs err	207 Pb / 206 Pb (Ma)	1 σ abs err
< 10 % Discordant								
DM_123	3.099	2.07%	0.11053	0.96%	1802.8	32.5	1808.1	17.3
DM_122	3.090	1.97%	0.11287	0.94%	1807.4	31.0	1846.1	17.0
DM_121	2.063	2.08%	0.18276	1.11%	2547.4	43.6	2678.0	18.2
DM_119	3.033	2.13%	0.11159	1.21%	1836.9	33.9	1825.5	21.8
DM_118	2.449	1.98%	0.12703	0.94%	2207.6	37.0	2057.3	16.5
DM_117	1.952	1.93%	0.18319	0.92%	2666.9	41.9	2681.9	15.2
DM_116	3.195	2.05%	0.11136	1.15%	1755.4	31.5	1821.7	20.7
DM_115	2.021	2.31%	0.18124	1.39%	2591.5	49.2	2664.3	22.8
DM_114	1.990	1.96%	0.18190	0.92%	2624.8	42.1	2670.3	15.2
DM_112	3.246	2.15%	0.10709	1.48%	1731.1	32.6	1750.5	26.8
DM_111	2.277	2.02%	0.17102	1.34%	2346.8	39.7	2567.6	22.2
DM_110	2.085	2.10%	0.17846	1.15%	2525.5	43.7	2638.6	19.0
DM_109	3.329	2.05%	0.11123	1.16%	1693.4	30.4	1819.6	20.9
DM_108	3.079	2.18%	0.11621	1.72%	1812.9	34.4	1898.7	30.7
DM_107	2.002	1.92%	0.18655	1.16%	2611.2	41.0	2712.0	18.9
DM_106	2.033	2.26%	0.18452	1.26%	2578.8	47.8	2693.9	20.7
DM_105	2.021	1.95%	0.18557	1.19%	2591.6	41.5	2703.3	19.5
DM_104	2.003	2.18%	0.18963	1.45%	2610.2	46.5	2739.0	23.7
DM_103	2.472	1.96%	0.14674	1.22%	2189.5	36.2	2308.3	20.8
DM_102	2.019	2.58%	0.19968	1.37%	2593.1	54.8	2823.5	22.2
DM_101	2.979	1.93%	0.11452	1.17%	1866.0	31.2	1872.3	21.0
DM_100	2.149	2.22%	0.17676	1.41%	2462.8	45.4	2622.7	23.2
DM_99	1.987	2.25%	0.18438	1.31%	2627.7	48.5	2692.7	21.5
DM_98	3.269	2.77%	0.10879	1.47%	1720.4	41.7	1779.3	26.6
DM_97	5.812	2.42%	0.07588	1.43%	1023.4	22.9	1091.8	28.5
DM_96	3.192	2.65%	0.11125	1.66%	1756.8	40.6	1820.0	29.8
DM_95	2.107	2.47%	0.17965	1.30%	2503.4	51.1	2649.7	21.3
DM_94	1.930	2.68%	0.19089	1.52%	2691.8	58.7	2749.9	24.7
DM_93	2.150	2.55%	0.18303	1.31%	2462.1	51.9	2680.5	21.5
DM_91	2.060	2.87%	0.19279	1.72%	2550.8	60.1	2766.1	28.0
DM_90	1.997	2.57%	0.18381	1.36%	2617.5	55.1	2687.5	22.3
DM_89	2.867	2.43%	0.11190	1.29%	1929.1	40.4	1830.5	23.2
DM_88	1.911	2.66%	0.17912	1.47%	2713.6	58.5	2644.7	24.2
DM_87	2.003	2.57%	0.18639	1.40%	2611.0	54.9	2710.6	22.9

DM_86	6.063	2.50%	0.07297	1.42%	984.1	22.7	1013.1	28.5
DM_85	1.923	2.71%	0.21323	1.48%	2699.7	59.5	2930.3	23.7
DM_84	3.291	2.52%	0.11058	1.73%	1710.3	37.7	1808.9	31.1
DM_83	2.001	2.74%	0.18362	1.80%	2613.2	58.5	2685.9	29.5
DM_82	1.905	2.76%	0.17900	1.83%	2720.3	61.1	2643.6	30.1
DM_81	2.054	2.69%	0.18751	1.74%	2557.5	56.5	2720.5	28.5
DM_79	2.513	2.68%	0.14911	1.97%	2159.3	48.9	2335.7	33.3
DM_78	3.204	2.83%	0.11336	1.90%	1751.1	43.3	1854.0	33.9
DM_77	1.916	2.70%	0.17982	1.75%	2707.1	59.5	2651.2	28.8
DM_76	2.069	2.65%	0.18741	1.86%	2541.6	55.5	2719.5	30.3
DM_75	1.955	2.55%	0.18674	1.71%	2662.7	55.5	2713.7	27.9
DM_74	1.966	2.65%	0.18369	1.73%	2650.4	57.4	2686.5	28.4
DM_73	1.805	2.69%	0.18009	1.74%	2841.3	61.5	2653.7	28.6
DM_72	3.137	2.67%	0.11018	1.80%	1783.7	41.5	1802.4	32.4
DM_71	3.114	2.61%	0.11029	1.73%	1795.2	40.8	1804.2	31.1
DM_70	2.222	1.39%	0.16909	2.21%	2395.5	27.8	2548.6	36.5
DM_69	1.694	1.38%	0.20331	2.29%	2991.3	32.9	2853.0	36.7
DM_68	1.857	1.43%	0.18472	2.26%	2777.8	32.1	2695.7	36.8
DM_67	1.983	1.34%	0.18791	2.20%	2632.0	28.9	2723.9	35.8
DM_66	2.003	1.43%	0.18342	2.19%	2610.8	30.6	2684.1	35.7
DM_65	2.907	1.44%	0.11556	2.22%	1905.6	23.7	1888.7	39.4
DM_64	1.739	1.39%	0.21813	2.19%	2929.0	32.6	2966.9	34.8
DM_62	1.894	1.40%	0.20436	2.23%	2732.8	31.0	2861.4	35.8
DM_61	2.985	1.38%	0.11968	2.36%	1862.8	22.3	1951.4	41.5
DM_60	3.033	1.37%	0.10938	2.19%	1837.1	21.9	1789.1	39.4
DM_59	3.229	1.29%	0.11052	2.19%	1739.3	19.6	1808.0	39.3
DM_58	3.125	1.43%	0.11955	2.32%	1789.6	22.2	1949.5	40.9
DM_57	1.976	1.31%	0.18222	2.19%	2639.3	28.3	2673.2	35.8
DM_56	3.258	4.05%	0.11119	1.96%	1725.6	61.0	1819.0	35.1
DM_55	2.235	4.00%	0.16437	1.77%	2383.9	79.3	2501.1	29.4
DM_54	2.174	4.11%	0.18405	1.84%	2439.8	82.9	2689.7	30.1
DM_53	1.982	4.05%	0.20236	1.80%	2633.1	86.9	2845.3	29.0
DM_52	3.357	4.04%	0.11143	1.89%	1680.6	59.4	1822.9	33.9
DM_51	3.233	4.06%	0.10855	1.83%	1737.2	61.6	1775.2	33.1
DM_50	1.963	4.07%	0.18292	1.88%	2653.8	87.9	2679.5	30.8
DM_49	2.992	4.12%	0.11204	1.84%	1858.9	66.2	1832.8	33.0
DM_48	1.993	4.01%	0.18762	1.79%	2620.8	85.7	2721.4	29.3
DM_47	2.830	4.08%	0.11443	1.86%	1950.3	68.4	1870.9	33.2
DM_46	1.724	4.16%	0.19120	1.88%	2948.4	97.8	2752.5	30.6

DM_44	2.849	4.09%	0.11847	1.96%	1939.6	68.2	1933.2	34.7
DM_43	3.104	4.07%	0.10811	1.81%	1800.2	63.6	1767.7	32.7
DM_42	3.413	2.34%	0.10932	3.84%	1656.3	34.1	1788.2	68.3
DM_41	3.233	2.23%	0.11024	3.82%	1737.3	33.9	1803.3	68.0
DM_40	2.043	2.21%	0.17988	3.79%	2568.0	46.5	2651.8	61.6
DM_39	2.126	2.35%	0.18277	3.84%	2485.1	48.3	2678.1	62.2
DM_38	3.215	2.23%	0.11112	3.83%	1746.1	34.0	1817.8	68.0
DM_37	2.529	2.32%	0.14138	3.88%	2147.6	42.3	2244.2	65.6
DM_36	3.215	2.21%	0.11041	3.86%	1745.6	33.8	1806.2	68.6
DM_35	2.036	2.35%	0.18683	3.89%	2575.9	49.8	2714.4	62.7
DM_34	3.366	2.20%	0.10831	3.84%	1676.8	32.3	1771.2	68.4
DM_33	1.937	2.37%	0.18493	3.84%	2683.7	51.8	2697.6	62.0
DM_32	2.694	2.18%	0.13195	3.82%	2034.9	38.0	2124.1	65.4
DM_31	3.369	2.21%	0.10922	3.81%	1675.5	32.5	1786.5	67.9
DM_30	2.167	2.19%	0.17307	3.79%	2446.2	44.5	2587.5	61.9
DM_29	2.045	2.17%	0.18611	3.81%	2566.2	45.7	2708.1	61.4
DM_28	2.932	2.52%	0.12700	3.83%	1892.0	41.2	2056.8	66.1
DM_27	2.153	2.31%	0.18438	3.30%	2459.3	47.0	2692.6	53.4
DM_26	2.022	1.99%	0.18137	3.15%	2590.4	42.3	2665.5	51.3
DM_25	1.929	2.00%	0.18487	3.20%	2692.9	43.9	2697.0	51.9
DM_24	1.971	2.05%	0.17917	3.19%	2645.1	44.4	2645.2	52.1
DM_23	3.164	1.92%	0.10783	3.15%	1770.4	29.7	1763.2	56.5
DM_22	3.145	2.01%	0.10948	3.16%	1779.9	31.2	1790.8	56.4
DM_21	2.953	2.30%	0.11248	3.32%	1880.3	37.3	1839.8	58.9
DM_20	2.052	2.07%	0.18153	3.18%	2559.3	43.6	2666.9	51.7
DM_19	3.090	1.99%	0.11263	3.16%	1807.3	31.2	1842.3	56.2
DM_18	3.098	2.10%	0.11659	3.26%	1803.2	33.0	1904.5	57.4
DM_17	1.989	1.99%	0.17711	3.14%	2625.8	42.8	2626.0	51.3
DM_16	2.071	1.99%	0.17624	3.14%	2539.8	41.7	2617.8	51.2
DM_15	3.141	2.03%	0.10995	3.19%	1781.9	31.5	1798.6	56.9
DM_14	2.965	2.61%	0.11525	1.98%	1873.4	42.3	1883.7	35.2
DM_13	2.039	2.85%	0.17714	2.03%	2572.3	60.1	2626.3	33.3
DM_12	2.072	2.72%	0.18261	2.01%	2538.8	56.8	2676.7	32.9
DM_11	2.154	2.80%	0.17780	2.04%	2458.1	57.0	2632.4	33.5
DM_10	1.906	2.82%	0.18553	2.09%	2718.6	62.3	2702.9	34.2
DM_9	2.248	2.60%	0.15854	1.94%	2372.7	51.4	2440.2	32.5
DM_8	5.926	2.80%	0.07630	2.21%	1005.2	26.0	1102.9	43.6
DM_7	3.090	2.71%	0.11378	2.02%	1807.5	42.6	1860.7	36.0
DM_6	4.034	2.78%	0.09050	2.12%	1427.6	35.5	1436.1	39.9

DM_5	2.012	2.66%	0.18776	1.98%	2600.8	56.7	2722.6	32.2
DM_4	1.750	2.68%	0.19785	2.02%	2913.9	62.4	2808.5	32.6
DM_3	2.114	2.68%	0.16596	2.00%	2496.8	55.2	2517.3	33.3
DM_2	3.203	2.70%	0.11106	1.99%	1751.4	41.3	1816.9	35.6
DM_1	2.942	2.62%	0.11538	1.96%	1886.2	42.8	1885.8	34.9
> 10% Discordant								
DM_124	3.324	2.39%	0.17151	0.95%	1695.3	35.6	2572.4	15.9
DM_120	1.542	2.15%	0.19228	1.28%	3222.2	54.4	2761.8	20.8
DM_113	3.582	2.00%	0.13237	1.53%	1587.1	28.1	2129.7	26.6
DM_92	2.340	2.85%	0.18770	1.47%	2294.0	54.8	2722.1	24.0
DM_80	2.556	3.01%	0.18639	1.81%	2128.7	54.4	2710.6	29.6
DM_45	1.662	4.03%	0.18277	1.79%	3036.6	97.0	2678.2	29.4

WETHERIL PLOTS

Davis Mountains-Top (DMTop)

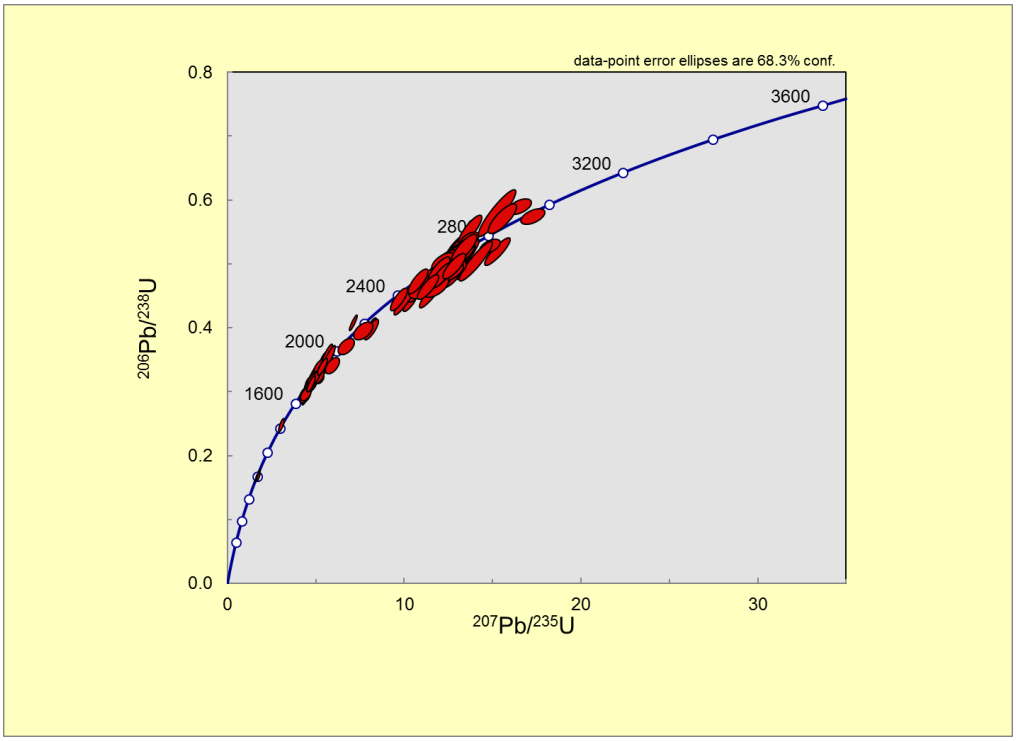

Davis Mountains-Base (DMBase)

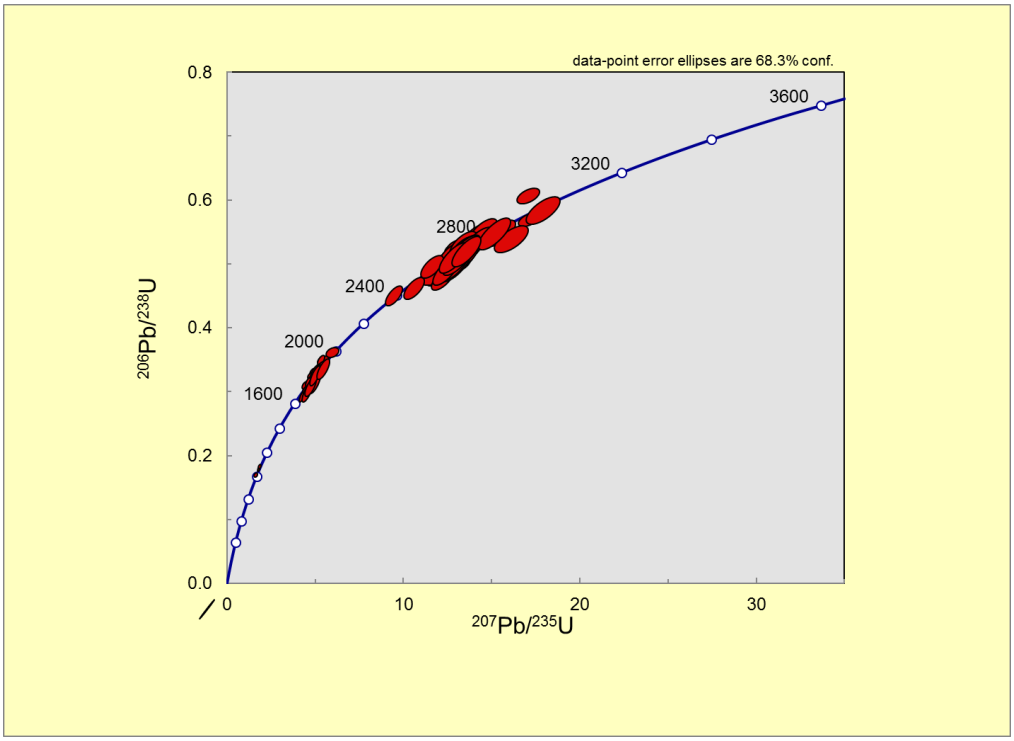

APPENDIX E

PAHVANT RANGE

DATA TABLES

Sample PRB (Pahvant Range-Base)								
Sample Name	238U / 206Pb	1 σ (%)	207Pb / 206Pb	1 σ (%)	206Pb / 238 U (Ma)	1 σ abs err	207 Pb / 206 Pb (Ma)	1 σ abs err
< 10 % Discordant								
PR_120	1.956	2.09%	0.18828	1.14%	2662.4	45.5	2727.2	18.6
PR_118	1.968	2.05%	0.18387	1.10%	2648.4	44.5	2688.1	18.0
PR_117	2.016	2.10%	0.18373	1.15%	2596.8	44.7	2686.8	19.0
PR_116	3.217	2.06%	0.11042	1.11%	1745.0	31.5	1806.4	20.0
PR_115	2.014	2.13%	0.18307	1.20%	2598.3	45.5	2680.9	19.7
PR_114	3.229	2.32%	0.11283	1.28%	1739.3	35.2	1845.5	23.0
PR_113	1.946	2.24%	0.18404	1.20%	2672.9	48.8	2689.6	19.7
PR_112	3.112	2.20%	0.11530	1.36%	1796.1	34.4	1884.6	24.2
PR_111	2.043	2.38%	0.18371	1.30%	2568.1	50.3	2686.6	21.3
PR_110	2.056	2.46%	0.18700	1.36%	2554.9	51.6	2716.0	22.3
PR_109	1.947	2.38%	0.19259	1.29%	2672.5	51.9	2764.4	21.0
PR_107	2.107	2.44%	0.18547	1.36%	2503.4	50.3	2702.4	22.4
PR_106	2.033	2.37%	0.18679	1.26%	2579.0	50.2	2714.1	20.6
PR_105	2.018	2.46%	0.18725	1.32%	2594.1	52.3	2718.1	21.6
PR_104	1.980	2.62%	0.18697	1.36%	2635.7	56.4	2715.7	22.2
PR_103	3.005	2.54%	0.11590	1.53%	1851.6	40.8	1893.9	27.3
PR_102	1.769	2.39%	0.21454	1.26%	2887.8	55.4	2940.1	20.2
PR_101	2.072	2.38%	0.18495	1.31%	2538.6	49.7	2697.8	21.4
PR_100	2.036	2.36%	0.17696	1.25%	2575.5	49.9	2624.6	20.6
PR_98	1.976	2.40%	0.18276	1.27%	2640.2	51.7	2678.1	20.8
PR_96	2.212	1.88%	0.17174	1.65%	2404.9	37.7	2574.6	27.3
PR_95	2.169	2.09%	0.18679	1.64%	2444.6	42.3	2714.1	26.8
PR_94	2.098	1.99%	0.18465	1.60%	2512.3	41.3	2695.0	26.2
PR_93	5.902	1.87%	0.07539	1.72%	1009.0	17.5	1078.8	34.2
PR_91	3.264	1.83%	0.11065	1.64%	1722.8	27.6	1810.1	29.6
PR_88	2.032	1.79%	0.18271	1.58%	2579.8	38.0	2677.6	25.8

PR_87	2.006	2.07%	0.18587	1.62%	2607.3	44.3	2706.0	26.5
PR_86	2.159	2.00%	0.18470	1.58%	2453.6	40.7	2695.6	25.9
PR_85	1.980	1.86%	0.18257	1.64%	2635.1	40.1	2676.3	26.9
PR_84	2.038	1.88%	0.18603	1.60%	2573.8	39.7	2707.3	26.2
PR_83	2.022	2.01%	0.19226	2.53%	2589.9	42.7	2761.5	40.9
PR_82	5.740	1.97%	0.07474	2.58%	1035.3	18.8	1061.6	51.0
PR_81	3.341	1.99%	0.11433	2.52%	1688.0	29.4	1869.4	44.8
PR_80	2.030	2.00%	0.18267	2.49%	2581.8	42.4	2677.3	40.7
PR_79	3.119	1.94%	0.11433	2.50%	1792.9	30.4	1869.3	44.4
PR_78	2.022	1.95%	0.18416	2.50%	2590.5	41.4	2690.7	40.7
PR_77	2.070	2.13%	0.17720	2.51%	2541.1	44.6	2626.8	41.1
PR_76	2.044	2.00%	0.18423	2.53%	2566.9	42.3	2691.3	41.2
PR_75	2.046	2.21%	0.18763	2.50%	2564.9	46.5	2721.5	40.6
PR_74	3.100	1.97%	0.11410	2.57%	1802.2	30.9	1865.8	45.7
PR_73	2.069	1.92%	0.17901	2.51%	2541.7	40.3	2643.8	41.1
PR_72	2.077	2.18%	0.19095	2.58%	2533.8	45.5	2750.4	41.7
PR_71	1.952	1.95%	0.18297	2.51%	2666.1	42.4	2679.9	40.9
PR_70	3.187	1.95%	0.11340	2.50%	1759.2	29.9	1854.6	44.5
PR_69	3.076	1.46%	0.10898	2.29%	1814.8	23.0	1782.5	41.1
PR_68	5.937	1.42%	0.07299	2.31%	1003.5	13.2	1013.7	46.1
PR_67	1.845	1.54%	0.18469	2.25%	2791.5	34.7	2695.5	36.6
PR_66	1.689	1.57%	0.20515	2.25%	2998.0	37.6	2867.6	36.1
PR_65	1.884	1.61%	0.18523	2.31%	2745.1	35.9	2700.3	37.6
PR_64	3.171	1.44%	0.11225	2.26%	1766.9	22.2	1836.2	40.4
PR_63	1.960	1.43%	0.18600	2.27%	2657.5	31.0	2707.2	37.0
PR_62	2.010	1.54%	0.18028	2.26%	2603.1	32.9	2655.4	37.1
PR_61	1.947	1.54%	0.18562	2.27%	2671.6	33.6	2703.8	37.0
PR_60	1.974	1.60%	0.18332	2.31%	2642.0	34.6	2683.2	37.6
PR_59	3.281	1.58%	0.10639	2.26%	1715.2	23.8	1738.5	40.8
PR_58	2.074	1.54%	0.18031	2.26%	2536.7	32.2	2655.7	37.0
PR_57	1.983	1.59%	0.18519	2.29%	2632.1	34.2	2699.9	37.2
PR_56	1.934	1.48%	0.18912	2.25%	2686.5	32.4	2734.5	36.6
PR_54	2.033	1.56%	0.18713	1.39%	2579.1	33.1	2717.1	22.8
PR_53	3.040	1.39%	0.11258	1.36%	1833.5	22.1	1841.5	24.4
PR_50	2.055	1.47%	0.18346	1.38%	2556.1	31.0	2684.4	22.6
PR_49	3.064	1.45%	0.10946	1.35%	1820.7	23.0	1790.5	24.3
PR_48	2.034	1.52%	0.19034	1.38%	2577.5	32.3	2745.1	22.5
PR_47	2.051	2.43%	0.19388	1.46%	2559.9	51.2	2775.3	23.8
PR_46	1.988	1.65%	0.18542	1.38%	2626.6	35.4	2702.0	22.5

PR_45	1.901	1.49%	0.18978	1.38%	2724.4	33.0	2740.2	22.5
PR_44	2.013	1.54%	0.19716	1.41%	2600.1	32.8	2802.8	23.0
PR_42	3.350	1.47%	0.10982	1.36%	1683.8	21.8	1796.5	24.5
PR_41	2.046	1.62%	0.19827	1.42%	2564.9	34.2	2812.0	23.1
PR_40	2.004	1.79%	0.18927	1.75%	2609.5	38.2	2735.8	28.4
PR_39	2.177	1.67%	0.18144	1.61%	2436.5	33.7	2666.1	26.4
PR_38	3.174	1.67%	0.11509	1.68%	1765.6	25.7	1881.2	30.0
PR_37	1.953	1.65%	0.18905	1.65%	2665.4	35.9	2733.9	27.0
PR_36	1.972	1.67%	0.18816	1.62%	2644.3	36.2	2726.1	26.4
PR_35	2.061	1.81%	0.18382	1.60%	2550.3	38.1	2687.6	26.3
PR_34	2.017	1.71%	0.18722	1.66%	2596.0	36.5	2717.9	27.1
PR_33	2.029	1.71%	0.19680	1.67%	2583.5	36.3	2799.8	27.0
PR_32	1.847	1.65%	0.19349	1.68%	2789.3	37.3	2772.1	27.3
PR_28	1.983	1.85%	0.18522	1.66%	2631.9	39.8	2700.2	27.1
PR_27	1.916	1.65%	0.18911	1.60%	2707.2	36.4	2734.4	26.1
PR_26	1.961	2.20%	0.18489	1.76%	2656.0	47.8	2697.3	28.8
PR_25	2.001	2.93%	0.20386	1.94%	2612.5	62.7	2857.4	31.2
PR_24	2.038	2.26%	0.18543	1.85%	2573.3	47.8	2702.0	30.3
PR_23	1.858	2.23%	0.18878	1.77%	2776.2	50.1	2731.6	28.8
PR_21	1.840	2.24%	0.20524	1.83%	2798.6	50.7	2868.4	29.4
PR_20	2.013	2.20%	0.18255	1.73%	2600.1	47.0	2676.1	28.4
PR_19	1.694	2.22%	0.22611	1.82%	2990.3	52.9	3024.7	28.9
PR_18	1.974	2.22%	0.18724	1.80%	2641.5	48.0	2718.0	29.3
PR_17	2.162	2.23%	0.18329	1.77%	2450.3	45.3	2682.8	29.0
PR_15	1.844	2.34%	0.18798	1.77%	2792.9	52.8	2724.6	28.9
PR_14	2.100	2.29%	0.18863	1.82%	2510.4	47.4	2730.3	29.7
PR_13	2.872	2.21%	0.13057	2.07%	1926.1	36.6	2105.6	36.0
PR_12	1.983	2.64%	0.18498	3.80%	2631.9	56.9	2698.1	61.4
PR_10	3.135	2.53%	0.11112	3.81%	1784.5	39.3	1817.8	67.5
PR_9	2.124	2.64%	0.18190	3.80%	2486.7	54.3	2670.3	61.6
PR_8	1.898	2.53%	0.19098	3.80%	2728.2	56.0	2750.6	61.0
PR_7	2.051	2.71%	0.18983	3.81%	2560.0	56.9	2740.7	61.4
PR_6	1.915	2.49%	0.19750	3.75%	2708.1	54.8	2805.7	60.1
PR_5	1.796	2.55%	0.21204	3.76%	2853.0	58.6	2921.2	59.6
PR_4	1.880	2.51%	0.19374	3.74%	2749.1	56.0	2774.1	60.1
PR_3	2.070	2.62%	0.18362	3.77%	2540.4	54.7	2685.8	61.0
PR_2	1.944	2.56%	0.20334	3.77%	2674.8	55.9	2853.2	60.0
PR_1	1.956	2.54%	0.18249	3.76%	2662.1	55.1	2675.6	60.9
TS2_11	3.290	3.36%	0.10976	3.20%	1710.7	50.3	1795.5	57.2

TS2_10	1.889	2.37%	0.18841	3.10%	2738.6	52.6	2728.4	50.2
TS2_9	2.955	2.22%	0.11691	3.05%	1879.0	36.1	1909.5	53.8
TS2_8	2.653	2.54%	0.13062	3.07%	2062.1	44.7	2106.3	53.0
TS2_6	3.003	2.19%	0.10863	3.04%	1853.1	35.1	1776.6	54.4
TS2_5	3.187	2.17%	0.10582	3.04%	1759.3	33.4	1728.6	54.8
TS2_4	3.130	2.34%	0.11017	3.09%	1787.3	36.5	1802.2	55.2
TS2_3	2.997	2.42%	0.11068	3.07%	1856.4	38.9	1810.7	54.7
TS2_1	2.797	2.36%	0.11401	3.07%	1970.2	39.9	1864.3	54.5
> 10% Discordant								
PR_119	2.513	2.71%	0.11398	1.26%	2159.6	49.6	1863.8	22.5
PR_108	2.734	2.46%	0.14787	1.35%	2009.6	42.3	2321.4	22.9
PR_99	2.456	2.48%	0.18535	1.30%	2202.1	46.2	2701.4	21.2
PR_97	2.230	2.01%	0.18936	1.62%	2388.1	40.0	2736.6	26.3
PR_92	2.406	2.12%	0.18183	1.57%	2240.7	40.0	2669.6	25.8
PR_90	2.224	1.88%	0.18115	1.59%	2393.2	37.5	2663.4	26.1
PR_55	2.750	3.04%	0.17745	1.32%	1999.2	52.0	2629.2	21.8
PR_51	3.727	1.65%	0.19607	1.28%	1532.4	22.5	2793.8	20.9
PR_43	2.192	1.43%	0.18649	1.37%	2423.1	28.8	2711.5	22.5
PR_31	2.206	1.99%	0.18412	1.61%	2410.0	40.0	2690.3	26.3
PR_29	2.580	1.79%	0.18085	1.66%	2111.5	32.2	2660.7	27.2
PR_22	2.230	2.92%	0.19236	1.80%	2388.2	57.9	2762.4	29.2
PR_16	1.630	2.42%	0.18876	1.76%	3083.6	59.1	2731.4	28.7
PR_11	3.279	2.62%	0.17929	3.75%	1715.9	39.3	2646.3	60.9

Sample PRT (Pahvant Range-Top)								
Sample Name	238U / 206Pb	1 σ (%)	207Pb / 206Pb	1 σ (%)	206Pb / 238 U (Ma)	1 σ abs err	207 Pb / 206 Pb (Ma)	1 σ abs err
< 10 % Discordant								
PR_120	2.025	3.74%	0.18279	1.17%	2587.0	79.2	2678.4	19.2
PR_119	3.300	3.72%	0.11351	1.22%	1706.4	55.5	1856.4	21.9
PR_118	3.104	3.71%	0.11592	1.24%	1800.4	58.1	1894.3	22.1
PR_117	3.559	3.76%	0.10054	1.34%	1596.2	52.9	1634.2	24.7
PR_115	5.306	3.72%	0.07894	1.42%	1113.0	38.0	1170.5	27.8
PR_114	3.201	3.73%	0.11207	1.15%	1752.5	56.9	1833.3	20.8
PR_113	3.132	3.77%	0.11415	1.20%	1786.1	58.6	1866.5	21.5
PR_112	3.220	3.72%	0.11295	1.30%	1743.4	56.6	1847.4	23.3
PR_111	2.029	3.78%	0.18378	1.25%	2583.3	79.9	2687.2	20.5
PR_110	3.086	3.74%	0.11004	1.20%	1809.6	58.7	1800.1	21.7
PR_109	3.150	3.79%	0.11274	1.26%	1777.4	58.7	1844.0	22.6
PR_108	6.274	2.33%	0.07299	2.37%	953.3	20.6	1013.7	47.3
PR_107	3.139	2.52%	0.11294	2.40%	1782.8	39.1	1847.2	42.8
PR_105	2.582	2.31%	0.13056	2.41%	2110.5	41.5	2105.5	41.6
PR_104	1.830	2.35%	0.20290	2.32%	2810.3	53.3	2849.7	37.3
PR_103	2.734	2.38%	0.12897	2.40%	2009.2	40.9	2084.0	41.6
PR_101	1.854	2.38%	0.21257	2.37%	2781.1	53.6	2925.3	37.8
PR_100	1.925	2.32%	0.18714	2.33%	2696.8	50.9	2717.2	37.8
PR_99	2.056	2.61%	0.18460	2.39%	2555.1	54.8	2694.6	39.0
PR_98	3.081	2.46%	0.11453	2.35%	1812.2	38.8	1872.5	41.8
PR_97	2.928	2.31%	0.11635	2.34%	1894.1	37.8	1900.9	41.4
PR_96	3.137	2.32%	0.11134	2.34%	1783.7	36.1	1821.4	41.8
PR_95	3.110	2.36%	0.11880	2.43%	1797.4	36.9	1938.3	42.8
PR_94	2.264	2.27%	0.15992	2.27%	2358.4	44.8	2454.8	37.8
PR_92	10.088	2.25%	0.05905	2.38%	609.3	13.0	568.8	51.0
PR_90	1.978	2.28%	0.18105	2.26%	2637.5	49.3	2662.5	37.0
PR_89	2.059	2.76%	0.18312	2.47%	2551.8	57.9	2681.3	40.3
PR_88	3.170	2.26%	0.11251	2.29%	1767.5	34.8	1840.3	41.0
PR_87	1.984	2.22%	0.19794	2.28%	2631.6	47.9	2809.3	36.7
PR_86	3.187	2.24%	0.11142	2.27%	1759.3	34.4	1822.6	40.6
PR_85	2.028	2.40%	0.18139	2.28%	2583.9	50.9	2665.6	37.2
PR_84	2.008	2.79%	0.18423	1.47%	2605.2	59.4	2691.3	24.1
PR_83	2.945	2.78%	0.11543	1.51%	1884.3	45.2	1886.6	26.9
PR_82	1.984	2.82%	0.18487	1.49%	2630.9	60.5	2697.1	24.3

PR_81	1.810	2.80%	0.20669	1.42%	2835.6	63.9	2879.7	22.9
PR_80	1.868	2.84%	0.20735	1.47%	2764.3	63.6	2885.0	23.7
PR_76	2.016	2.79%	0.18101	1.49%	2596.6	59.3	2662.1	24.5
PR_75	2.057	2.84%	0.17935	1.54%	2553.7	59.7	2646.9	25.3
PR_74	3.254	2.91%	0.11170	1.62%	1727.4	44.0	1827.2	29.0
PR_73	3.319	2.76%	0.10685	1.46%	1697.5	41.1	1746.3	26.5
PR_72	3.146	2.11%	0.10965	1.89%	1779.1	32.8	1793.6	34.0
PR_71	2.006	2.10%	0.18217	1.85%	2606.9	44.8	2672.8	30.2
PR_70	6.251	2.14%	0.07265	1.99%	956.6	19.0	1004.2	39.9
PR_69	3.179	2.49%	0.11834	2.56%	1763.3	38.2	1931.4	45.1
PR_68	3.349	2.14%	0.10800	1.87%	1684.2	31.6	1765.9	33.7
PR_67	3.117	2.21%	0.11822	2.12%	1793.5	34.5	1929.5	37.4
PR_65	3.183	2.13%	0.11030	1.86%	1761.4	32.7	1804.4	33.5
PR_64	3.232	2.21%	0.10702	1.91%	1737.8	33.6	1749.3	34.5
PR_63	3.158	2.16%	0.11179	1.88%	1773.5	33.4	1828.7	33.7
PR_62	2.025	2.11%	0.18298	1.86%	2587.7	44.9	2680.1	30.5
PR_61	3.382	2.11%	0.10618	1.87%	1669.7	30.9	1734.8	33.9
PR_60	3.240	2.31%	0.11246	2.16%	1734.0	35.0	1839.6	38.6
PR_59	3.250	2.25%	0.11209	2.20%	1729.1	34.1	1833.5	39.3
PR_58	3.234	2.36%	0.10885	2.16%	1736.6	35.9	1780.3	38.8
PR_57	2.018	2.24%	0.18100	2.09%	2594.3	47.7	2662.1	34.2
PR_56	1.992	2.21%	0.18663	2.09%	2622.2	47.4	2712.7	34.1
PR_55	2.025	2.22%	0.18229	2.10%	2586.9	47.2	2673.8	34.3
PR_54	2.096	2.55%	0.18523	2.21%	2514.4	52.8	2700.2	36.1
PR_53	2.132	2.21%	0.17247	2.07%	2479.8	45.2	2581.8	34.2
PR_52	2.679	2.42%	0.12537	2.11%	2044.7	42.3	2034.0	36.9
PR_51	2.046	2.25%	0.18057	2.20%	2565.2	47.4	2658.1	36.0
PR_50	2.874	2.36%	0.12759	2.27%	1924.5	39.1	2065.0	39.5
PR_49	2.146	2.27%	0.18832	2.11%	2466.4	46.4	2727.5	34.4
PR_48	2.069	1.94%	0.17216	2.13%	2542.2	40.7	2578.7	35.1
PR_47	1.921	2.02%	0.18723	2.18%	2702.0	44.4	2718.0	35.4
PR_46	3.275	2.09%	0.11206	2.24%	1717.7	31.4	1833.0	40.0
PR_45	3.122	2.03%	0.11765	2.38%	1791.1	31.7	1920.8	42.0
PR_43	2.110	1.97%	0.17063	2.13%	2500.4	40.8	2563.9	35.2
PR_42	3.086	2.25%	0.11112	2.36%	1809.6	35.4	1817.8	42.2
PR_41	3.112	1.94%	0.11120	2.16%	1796.2	30.4	1819.1	38.7
PR_40	1.994	2.30%	0.18479	2.20%	2620.5	49.4	2696.4	35.9
PR_39	1.985	2.08%	0.17425	2.24%	2630.0	44.7	2598.9	36.9
PR_38	1.937	2.05%	0.18608	2.20%	2683.8	44.9	2707.8	35.8

PR_37	2.270	1.97%	0.15884	2.13%	2353.3	38.7	2443.3	35.6
PR_36	2.042	1.56%	0.17575	2.53%	2569.2	32.9	2613.1	41.5
PR_35	3.136	1.50%	0.11225	2.57%	1784.3	23.4	1836.2	45.8
PR_34	1.997	1.52%	0.18076	2.55%	2616.9	32.6	2659.9	41.6
PR_33	2.151	1.62%	0.16711	2.52%	2461.2	33.1	2528.9	41.7
PR_32	1.899	1.65%	0.19106	2.56%	2726.7	36.5	2751.3	41.4
PR_31	2.067	1.55%	0.18022	2.53%	2543.6	32.4	2654.9	41.3
PR_30	2.292	1.61%	0.15242	2.54%	2333.7	31.4	2373.2	42.7
PR_29	2.809	1.60%	0.12480	2.66%	1963.1	27.0	2026.0	46.4
PR_28	3.001	1.55%	0.11311	2.59%	1853.8	24.9	1850.0	46.1
PR_27	1.957	1.55%	0.18491	2.53%	2661.0	33.6	2697.4	41.1
PR_26	2.093	1.76%	0.18849	2.55%	2517.6	36.6	2729.1	41.3
PR_25	2.032	1.65%	0.18361	2.55%	2579.7	35.0	2685.8	41.5
PR_24	3.131	2.71%	0.11499	2.68%	1786.8	42.1	1879.8	47.6
PR_23	1.978	2.60%	0.17948	2.56%	2638.2	56.0	2648.1	41.9
PR_22	3.079	2.70%	0.11440	2.75%	1813.1	42.5	1870.4	48.7
PR_21	1.821	2.66%	0.18763	2.58%	2821.5	60.6	2721.5	41.9
PR_20	2.898	2.73%	0.11432	2.85%	1910.8	44.9	1869.2	50.6
PR_19	2.011	2.58%	0.18203	2.55%	2601.9	54.9	2671.4	41.6
PR_18	2.014	2.61%	0.18339	2.57%	2599.1	55.6	2683.8	41.8
PR_15	1.919	2.55%	0.17850	2.55%	2703.7	56.0	2639.0	41.7
PR_14	3.243	2.69%	0.10956	2.61%	1732.7	40.7	1792.1	46.9
PR_13	2.088	2.64%	0.18351	2.58%	2522.1	54.9	2684.9	42.0
PR_12	2.052	2.54%	0.18099	1.73%	2559.2	53.4	2662.0	28.3
PR_11	2.073	2.56%	0.18915	1.75%	2537.9	53.4	2734.8	28.5
PR_10	2.002	2.53%	0.18936	1.78%	2611.8	54.2	2736.6	29.0
PR_9	2.091	2.55%	0.18783	1.74%	2520.1	52.9	2723.3	28.4
PR_7	2.085	2.48%	0.18846	1.73%	2525.1	51.7	2728.7	28.2
PR_6	3.081	2.64%	0.11892	1.79%	1811.8	41.6	1940.0	31.7
PR_5	2.036	2.51%	0.18036	1.70%	2575.2	53.0	2656.2	28.0
PR_4	3.265	2.60%	0.11339	1.85%	1722.1	39.2	1854.4	33.0
PR_3	4.633	2.44%	0.08600	1.81%	1259.8	27.9	1338.1	34.6
PR_1	5.444	2.47%	0.07446	1.78%	1087.1	24.7	1054.0	35.4
> 10% Discordant								
PR_116	3.509	3.86%	0.11545	1.39%	1616.4	54.9	1887.0	24.9
PR_106	3.314	2.36%	0.11599	2.40%	1700.1	35.2	1895.2	42.6
PR_93	4.944	2.44%	0.08536	2.48%	1187.4	26.4	1323.8	47.4
PR_91	2.257	2.34%	0.18420	2.26%	2364.0	46.2	2691.0	36.9
PR_79	5.092	5.21%	0.19500	1.52%	1155.9	54.9	2784.8	24.6

PR_77	3.554	2.78%	0.11621	1.43%	1598.2	39.3	1898.8	25.4
PR_66	2.131	2.15%	0.21278	1.84%	2480.7	44.1	2926.9	29.5
PR_44	3.450	2.34%	0.11418	2.86%	1640.9	33.8	1867.0	50.7
PR_17	4.171	2.67%	0.11668	2.58%	1385.3	33.2	1905.9	45.6
PR_16	4.844	2.85%	0.12674	2.58%	1209.9	31.4	2053.3	44.9
PR_8	3.410	2.64%	0.18588	1.75%	1657.7	38.4	2706.0	28.6
PR_2	2.351	2.57%	0.18707	1.76%	2284.6	49.2	2716.5	28.7

WETHERIL PLOTS

Pahvant Range-Top (PRTop)

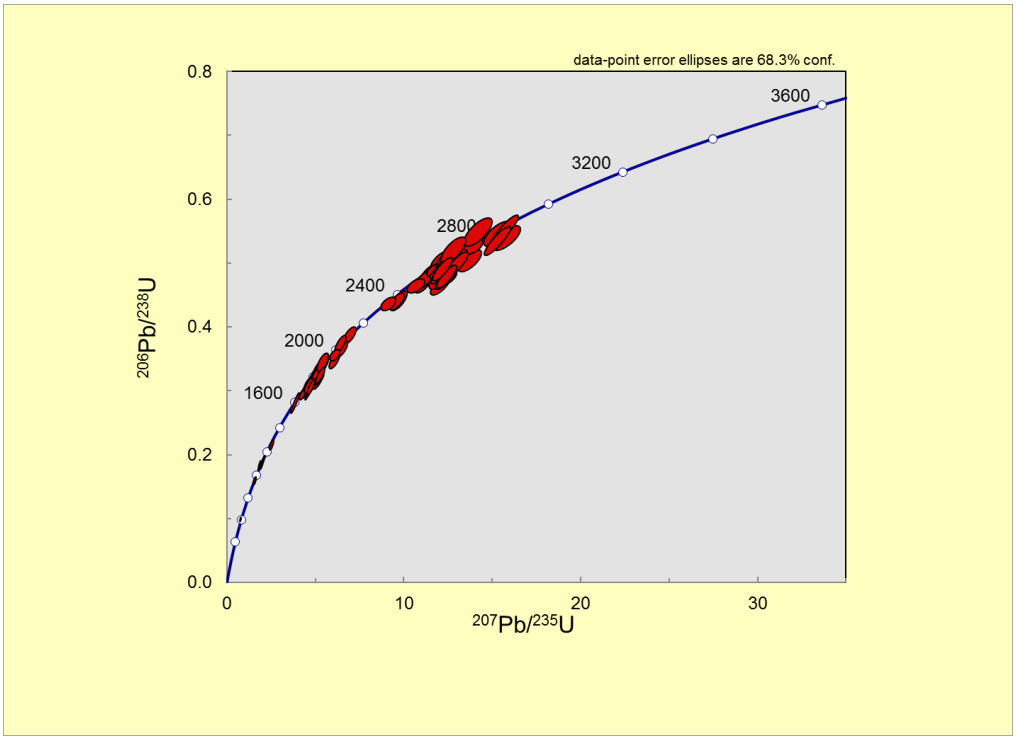

Pahvant Range-Base (PRBase)

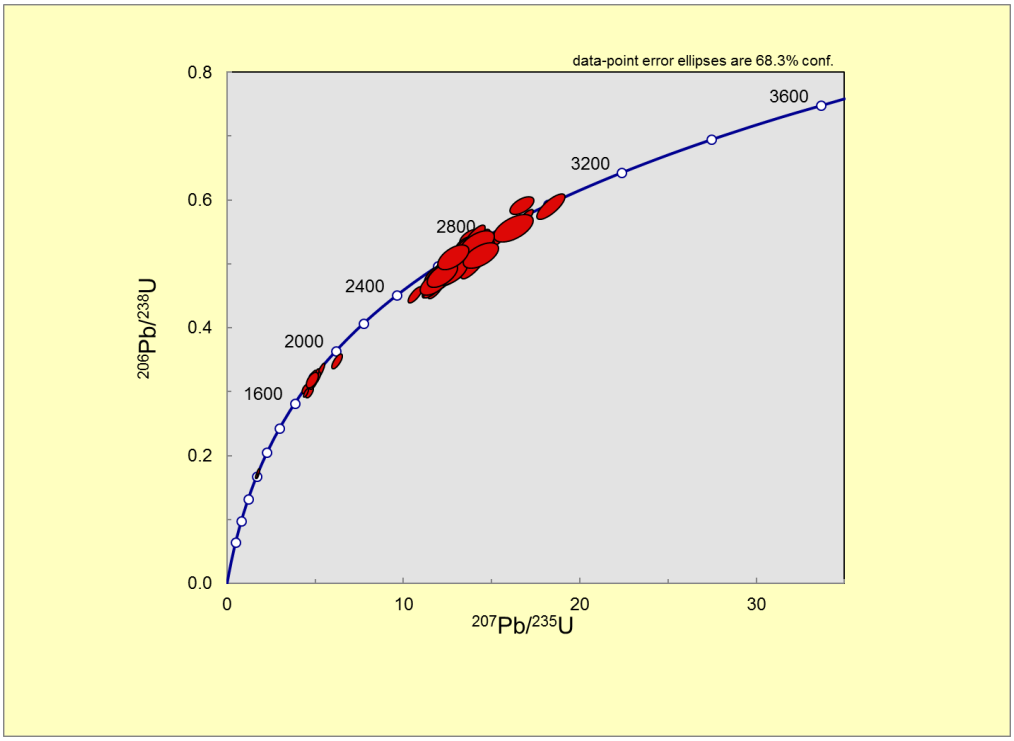

APPENDIX F

SCHELL CREEK RANGE

DATA TABLES

Sample SCB (Schell Creek Range-Base)								
Sample Name	238U / 206Pb	1 σ (%)	207Pb / 206Pb	1 σ (%)	206Pb / 238 U (Ma)	1 σ abs err	207 Pb / 206 Pb (Ma)	1 σ abs err
< 10 % Discordant								
SCB_122	1.871	2.40%	0.17956	4.32%	2760.5	53.6	2648.8	69.9
SCB_121	2.659	2.83%	0.12535	4.43%	2057.9	49.7	2033.7	76.4
SCB_120	2.939	2.27%	0.10836	4.29%	1888.1	37.0	1772.0	76.3
SCB_117	2.375	2.55%	0.13626	4.35%	2265.4	48.5	2180.2	73.9
SCB_116	1.895	2.70%	0.19016	4.42%	2732.0	59.9	2743.5	70.9
SCB_114	2.535	2.59%	0.12567	4.37%	2143.5	47.0	2038.2	75.4
SCB_112	1.626	2.77%	0.20743	4.39%	3090.5	67.7	2885.5	69.6
SCB_111	2.014	2.65%	0.16251	4.32%	2599.2	56.4	2481.9	71.1
SCB_107	2.958	3.87%	0.11047	4.60%	1877.1	62.8	1807.1	81.3
SCB_106	2.861	2.89%	0.11251	4.42%	1932.2	48.0	1840.3	78.0
SCB_103	1.844	2.69%	0.17620	4.35%	2793.0	60.7	2617.5	70.5
SCB_102	3.027	2.90%	0.11062	4.37%	1839.9	46.2	1809.6	77.3
SCB_101	3.479	2.81%	0.10619	4.33%	1628.5	40.2	1735.0	77.3
SCB_100	2.985	2.79%	0.11127	4.36%	1862.6	45.0	1820.2	77.1
SCB_98	3.031	2.81%	0.10730	4.37%	1838.1	44.7	1754.1	77.9
SCB_97	2.462	3.43%	0.14534	4.47%	2197.7	63.5	2291.8	75.0
SCB_96	1.939	2.90%	0.17953	4.37%	2681.4	63.4	2648.5	70.8
SCB_95	2.002	2.77%	0.16308	4.31%	2611.9	59.1	2487.9	70.9
SCB_93	2.842	2.74%	0.11389	4.33%	1943.6	45.8	1862.3	76.3
SCB_92	2.668	2.84%	0.12260	4.38%	2051.9	49.7	1994.5	75.8
SCB_91	1.873	2.98%	0.17769	4.38%	2757.5	66.5	2631.5	70.9
SCB_88	2.714	3.35%	0.13068	4.48%	2021.8	57.9	2107.1	76.5
SCB_87	1.929	3.05%	0.18277	4.35%	2692.8	66.7	2678.2	70.2
SCB_86	2.063	2.94%	0.15936	4.33%	2547.4	61.5	2448.9	71.4
SCB_85	2.314	3.01%	0.13827	4.33%	2315.8	58.4	2205.6	73.2
SCB_84	2.896	2.75%	0.10744	4.34%	1912.1	45.3	1756.4	77.4

SCB_83	2.974	2.93%	0.10999	4.37%	1868.6	47.4	1799.2	77.4
SCB_82	2.894	3.45%	0.10880	4.48%	1913.4	56.9	1779.4	79.5
SCB_81	2.313	2.79%	0.14306	4.37%	2316.3	54.0	2264.5	73.6
SCB_80	2.901	3.76%	0.11083	5.59%	1909.4	61.9	1813.0	98.1
SCB_79	2.780	3.98%	0.12105	5.58%	1981.0	67.6	1971.7	96.2
SCB_78	1.822	3.70%	0.18194	5.53%	2820.9	83.9	2670.6	88.7
SCB_76	2.903	3.72%	0.11795	5.55%	1907.9	61.1	1925.4	96.3
SCB_75	1.886	3.83%	0.18720	5.55%	2742.5	84.9	2717.7	88.6
SCB_74	2.578	3.70%	0.12573	5.55%	2112.8	66.3	2039.1	95.0
SCB_73	2.606	3.86%	0.12590	5.52%	2093.9	68.6	2041.5	94.5
SCB_72	3.187	3.64%	0.11120	5.55%	1759.4	55.8	1819.2	97.4
SCB_71	3.300	4.04%	0.11425	5.58%	1706.5	60.3	1868.1	97.4
SCB_69	3.122	3.68%	0.11021	5.53%	1791.2	57.3	1802.8	97.3
SCB_67	2.027	3.66%	0.17369	5.56%	2585.6	77.5	2593.5	89.8
SCB_66	1.677	4.74%	0.20797	4.94%	3015.1	113.2	2889.8	78.0
SCB_65	2.179	4.78%	0.14520	4.96%	2434.7	96.1	2290.1	82.9
SCB_64	2.280	4.76%	0.17405	4.91%	2343.9	92.9	2597.0	79.5
SCB_63	2.981	5.03%	0.11440	4.99%	1865.0	81.0	1870.4	87.3
SCB_61	3.152	4.67%	0.11156	4.91%	1776.2	72.2	1824.9	86.5
SCB_60	2.900	4.62%	0.11316	4.91%	1909.9	76.0	1850.8	86.1
SCB_59	2.975	4.62%	0.11314	4.93%	1868.0	74.5	1850.4	86.5
SCB_58	1.793	4.69%	0.20406	4.90%	2856.7	107.4	2858.9	77.5
SCB_55	2.814	4.66%	0.11084	4.97%	1960.0	78.3	1813.3	87.7
SCB_53	3.176	4.71%	0.10880	4.90%	1764.3	72.3	1779.5	86.8
SCB_52	2.483	3.21%	0.12389	3.91%	2181.7	59.1	2012.9	67.7
SCB_50	3.061	3.54%	0.11264	4.00%	1822.3	56.0	1842.5	70.7
SCB_49	2.870	3.19%	0.11632	3.92%	1927.3	52.9	1900.5	68.9
SCB_48	3.184	3.37%	0.11029	4.00%	1760.9	51.7	1804.2	71.0
SCB_44	2.903	3.36%	0.10872	3.95%	1908.0	55.2	1778.2	70.4
SCB_42	2.905	3.15%	0.10974	3.91%	1907.0	51.8	1795.1	69.5
SCB_40	1.957	3.32%	0.16588	3.91%	2661.1	71.9	2516.5	64.2
SCB_36	2.948	3.72%	0.10955	2.96%	1883.0	60.4	1791.9	52.9
SCB_35	2.988	3.76%	0.10731	2.90%	1861.1	60.4	1754.2	52.2
SCB_34	2.992	3.82%	0.10894	2.92%	1858.7	61.4	1781.8	52.3
SCB_33	2.637	3.94%	0.13775	3.12%	2072.7	69.4	2199.1	53.2
SCB_32	2.998	3.99%	0.11357	2.89%	1855.8	64.0	1857.4	51.3
SCB_30	1.879	3.89%	0.18614	2.92%	2750.9	86.6	2708.3	47.4
SCB_28	3.085	3.77%	0.11195	2.90%	1809.9	59.2	1831.3	51.6
SCB_26	2.860	3.89%	0.11346	2.92%	1932.7	64.6	1855.6	51.9

SC_22	1.848	2.10%	0.19141	2.89%	2787.7	47.2	2754.3	46.6
SC_21	2.823	1.81%	0.10476	3.02%	1954.6	30.4	1710.2	54.6
SC_20	2.977	1.81%	0.10943	2.92%	1866.8	29.3	1789.9	52.3
SC_19	2.588	2.26%	0.14944	2.96%	2105.8	40.4	2339.6	49.8
SC_18	2.999	2.80%	0.10829	3.07%	1854.8	44.9	1770.9	55.0
SC_17	2.217	1.97%	0.15294	2.89%	2400.0	39.3	2379.1	48.4
SC_15	2.869	1.50%	0.11066	2.83%	1927.9	25.0	1810.3	50.6
SC_14	1.763	1.77%	0.17919	2.95%	2895.8	41.1	2645.4	48.1
SC_13	3.093	1.60%	0.10840	2.89%	1805.7	25.1	1772.8	51.9
SC_12	3.082	1.84%	0.10672	2.04%	1811.7	29.0	1744.1	36.9
SC_10	2.135	1.84%	0.16316	2.19%	2476.7	37.8	2488.7	36.5
SC_8	2.890	2.12%	0.11252	2.39%	1915.6	35.0	1840.5	42.6
SC_7	2.791	1.78%	0.11911	2.06%	1974.0	30.2	1942.9	36.3
SC_5	1.649	1.55%	0.19740	1.98%	3055.9	37.5	2804.8	32.0
SC_4	1.943	1.95%	0.17345	2.17%	2676.2	42.5	2591.2	35.7
> 10% Discordant								
SCB_119	3.650	2.83%	0.14860	4.41%	1560.8	39.1	2329.9	73.7
SCB_118	3.321	2.52%	0.12089	4.43%	1697.0	37.5	1969.4	76.9
SCB_115	2.747	2.96%	0.10925	4.39%	2001.3	50.7	1787.0	77.9
SCB_113	2.852	2.66%	0.10730	4.31%	1937.6	44.3	1754.0	76.9
SCB_110	2.033	2.20%	0.13889	4.36%	2578.5	46.7	2213.5	73.7
SCB_109	9.925	7.33%	0.17277	4.42%	618.9	43.1	2584.7	72.0
SCB_108	2.709	3.17%	0.10472	4.40%	2025.0	54.8	1709.4	78.8
SCB_105	12.157	6.53%	0.19102	4.37%	509.6	31.9	2751.0	70.1
SCB_104	2.657	2.78%	0.11324	4.35%	2059.5	48.9	1852.0	76.6
SCB_99	6.277	3.47%	0.10717	4.43%	952.9	30.7	1751.8	79.0
SCB_94	4.209	2.73%	0.13442	4.31%	1374.0	33.7	2156.4	73.3
SCB_90	3.331	3.26%	0.12973	4.42%	1692.2	48.3	2094.3	75.7
SCB_89	5.712	2.79%	0.16415	4.32%	1040.0	26.8	2498.9	71.0
SCB_77	5.124	4.33%	0.11531	5.61%	1149.3	45.4	1884.8	97.6
SCB_70	5.546	3.92%	0.10048	5.57%	1068.7	38.5	1633.0	100.0
SCB_68	2.669	3.55%	0.11055	5.53%	2051.6	62.1	1808.4	97.2
SCB_62	3.932	4.63%	0.33113	4.91%	1460.9	60.3	3622.3	73.3
SCB_57	2.859	4.87%	0.14375	5.07%	1933.8	80.9	2272.9	84.8
SCB_56	7.529	5.58%	0.11405	4.92%	804.0	42.0	1865.0	86.3
SCB_54	2.707	4.75%	0.10731	4.96%	2026.9	82.1	1754.3	88.0
SCB_51	1.741	3.40%	0.17852	4.00%	2925.4	79.4	2639.2	64.9
SCB_47	6.196	3.99%	0.13502	4.22%	964.6	35.6	2164.3	71.8
SCB_46	2.782	3.27%	0.10839	3.91%	1979.4	55.5	1772.5	69.8

SCB_45	1.618	3.45%	0.19064	3.94%	3102.2	84.3	2747.7	63.3
SCB_43	3.804	3.31%	0.10439	3.89%	1504.7	44.2	1703.5	69.9
SCB_41	2.682	3.71%	0.10979	4.00%	2043.1	64.6	1795.9	71.1
SCB_39	1.827	3.42%	0.16697	3.92%	2814.6	77.6	2527.5	64.3
SCB_38	1.718	4.11%	0.18191	3.04%	2957.7	96.7	2670.4	49.4
SCB_37	7.363	4.38%	0.13041	3.01%	820.9	33.7	2103.5	52.0
SCB_31	5.763	4.21%	0.12538	2.91%	1031.4	40.0	2034.2	50.6
SCB_29	1.985	3.93%	0.13844	2.98%	2629.8	84.3	2207.8	50.8
SCB_27	4.231	3.84%	0.11395	2.93%	1367.7	47.1	1863.3	52.1
SCB_25	3.109	5.89%	0.12327	2.90%	1797.6	91.7	2004.1	50.6
SC_24	3.585	3.17%	0.12855	2.87%	1586.0	44.4	2078.3	49.7
SC_23	10.250	3.26%	0.09425	3.08%	600.1	18.6	1513.1	57.0
SC_21	2.823	1.81%	0.10476	3.02%	1954.6	30.4	1710.2	54.6
SC_16	2.685	1.48%	0.11097	2.82%	2041.0	25.9	1815.3	50.4
SC_11	6.743	2.16%	0.13106	2.17%	891.5	18.0	2112.2	37.6
SC_9	8.801	2.40%	0.12364	2.35%	693.8	15.8	2009.4	41.0
SC_6	2.915	1.59%	0.10548	1.97%	1901.4	26.1	1722.6	35.8
SC_3	9.725	3.43%	0.09411	2.19%	630.9	20.6	1510.4	40.9
SC_2	6.743	1.81%	0.12490	2.04%	891.5	15.1	2027.4	35.6
SC_1	7.309	1.32%	0.13365	1.96%	826.7	10.3	2146.5	33.8

Sample SCT (Schell Creek Range-Top)								
Sample Name	238U / 206Pb	1 σ (%)	207Pb / 206Pb	1 σ (%)	206Pb / 238 U (Ma)	1 σ abs err	207 Pb / 206 Pb (Ma)	1 σ abs err
< 10 % Discordant								
SCT_120	2.021	1.83%	0.18326	1.48%	2591.8	39.0	2682.6	24.3
SCT_118	2.316	1.67%	0.14079	1.44%	2313.4	32.3	2237.0	24.7
SCT_117	3.024	1.69%	0.10911	1.46%	1841.7	27.0	1784.7	26.4
SCT_116	1.851	1.74%	0.18887	1.48%	2784.3	39.3	2732.4	24.1
SCT_115	2.499	1.64%	0.14952	1.48%	2169.9	30.2	2340.4	25.0
SCT_114	2.881	1.72%	0.11540	1.50%	1920.5	28.5	1886.1	26.7
SCT_113	3.024	1.69%	0.11139	1.48%	1841.7	27.0	1822.1	26.5
SCT_112	2.865	1.62%	0.11455	1.54%	1929.7	26.9	1872.8	27.4
SCT_111	3.035	1.66%	0.10660	1.48%	1835.9	26.5	1742.1	26.9
SCT_110	3.157	1.81%	0.11043	1.68%	1774.0	28.1	1806.6	30.3
SCT_109	3.178	1.67%	0.11123	1.74%	1763.5	25.7	1819.7	31.3
SCT_108	2.889	1.54%	0.11369	1.52%	1916.1	25.4	1859.2	27.3
SCT_107	2.935	1.58%	0.11011	1.52%	1890.3	25.9	1801.2	27.4
SCT_106	1.970	1.63%	0.17612	1.46%	2646.6	35.2	2616.7	24.1
SCT_105	2.839	1.57%	0.11154	1.50%	1945.4	26.4	1824.7	27.0
SCT_104	2.812	1.56%	0.11485	1.54%	1961.4	26.3	1877.5	27.5
SCT_103	2.661	1.61%	0.11458	1.49%	2056.5	28.2	1873.2	26.6
SCT_102	2.947	1.64%	0.10859	1.55%	1883.4	26.8	1775.9	27.9
SCT_101	2.948	1.55%	0.10952	1.53%	1882.8	25.3	1791.5	27.5
SCT_100	2.943	1.72%	0.11073	1.54%	1885.8	28.1	1811.4	27.7
SCT_99	3.127	1.80%	0.11817	1.71%	1788.6	28.0	1928.7	30.4
SCT_98	2.610	2.21%	0.12448	1.14%	2091.1	39.4	2021.4	20.1
SCT_96	3.080	2.26%	0.11089	1.19%	1812.7	35.6	1814.0	21.5
SCT_95	2.965	2.29%	0.10985	1.13%	1873.4	37.1	1797.0	20.5
SCT_94	2.815	2.18%	0.11402	1.13%	1959.4	36.8	1864.4	20.3
SCT_93	2.063	2.21%	0.16062	1.13%	2547.7	46.4	2462.2	19.0
SCT_92	2.881	2.30%	0.11470	1.34%	1920.5	38.0	1875.2	24.0
SCT_91	2.025	2.29%	0.18068	1.20%	2587.2	48.5	2659.1	19.7
SCT_90	3.007	2.32%	0.11475	1.26%	1850.8	37.2	1875.9	22.5
SCT_89	2.839	2.19%	0.11663	1.24%	1945.5	36.7	1905.2	22.1
SCT_88	2.001	2.23%	0.17314	1.13%	2612.3	47.8	2588.2	18.8
SCT_87	1.890	2.19%	0.17322	1.11%	2737.8	48.6	2589.0	18.5
SCT_86	2.829	2.14%	0.11492	1.24%	1951.0	36.0	1878.7	22.1

SCT_85	3.225	2.22%	0.10702	1.21%	1740.9	33.7	1749.2	22.0
SCT_84	3.043	2.83%	0.11054	1.61%	1831.6	45.0	1808.4	29.0
SCT_83	1.758	2.71%	0.19589	1.55%	2902.4	63.1	2792.2	25.1
SCT_82	2.768	2.72%	0.11683	1.57%	1988.1	46.4	1908.2	28.0
SCT_81	2.927	2.75%	0.11179	1.58%	1894.8	44.9	1828.7	28.3
SCT_80	1.825	2.78%	0.18356	1.61%	2816.1	63.2	2685.3	26.3
SCT_79	3.076	2.78%	0.11056	1.55%	1814.3	43.8	1808.6	27.9
SCT_78	2.890	2.81%	0.11156	1.62%	1915.6	46.5	1824.9	29.0
SCT_77	2.868	2.78%	0.11142	1.54%	1928.5	46.2	1822.7	27.7
SCT_75	2.893	2.82%	0.10940	1.53%	1913.9	46.5	1789.4	27.6
SCT_74	2.864	2.77%	0.10877	1.53%	1930.4	46.1	1778.9	27.6
SCT_73	2.913	2.78%	0.11059	1.56%	1902.7	45.7	1809.1	28.1
SCT_72	3.056	2.78%	0.10804	1.57%	1825.1	44.1	1766.6	28.4
SCT_71	1.847	2.93%	0.18233	1.65%	2789.9	65.9	2674.2	27.1
SCT_70	3.036	3.99%	0.10749	2.54%	1835.1	63.4	1757.2	45.7
SCT_69	3.184	4.01%	0.10988	2.60%	1760.5	61.5	1797.4	46.6
SCT_68	2.962	3.99%	0.10889	2.54%	1875.4	64.5	1780.9	45.7
SCT_67	3.157	4.03%	0.11194	2.63%	1774.0	62.3	1831.1	46.9
SCT_66	1.884	4.02%	0.18512	2.59%	2745.2	89.3	2699.3	42.2
SCT_65	2.566	3.97%	0.12806	2.55%	2121.4	71.3	2071.5	44.2
SCT_64	5.870	4.00%	0.07209	2.62%	1014.1	37.5	988.4	52.4
SCT_63	3.003	3.95%	0.11014	2.54%	1852.9	63.3	1801.7	45.5
SCT_62	2.576	3.95%	0.12516	2.53%	2114.5	70.9	2031.0	44.1
SCT_61	2.743	4.00%	0.11682	2.56%	2003.6	68.5	1908.2	45.2
SCT_60	2.747	3.94%	0.11331	2.52%	2001.1	67.5	1853.2	44.8
SCT_59	2.601	4.04%	0.12630	2.63%	2097.3	71.9	2047.1	45.8
SCT_58	2.988	3.98%	0.10895	2.53%	1861.2	64.0	1782.0	45.4
SCT_57	2.840	3.96%	0.11439	2.54%	1944.5	66.2	1870.3	45.1
SCT_56	2.966	2.03%	0.11267	2.21%	1873.0	32.9	1843.0	39.6
SCT_55	3.040	1.96%	0.10998	2.10%	1833.4	31.2	1799.1	37.7
SCT_54	3.147	1.88%	0.10615	2.12%	1778.8	29.1	1734.3	38.4
SCT_53	2.386	1.81%	0.13588	2.11%	2256.3	34.4	2175.4	36.3
SCT_52	1.959	2.11%	0.18201	2.14%	2659.0	45.8	2671.3	35.1
SCT_51	1.916	2.05%	0.18317	2.08%	2707.7	45.1	2681.7	33.9
SCT_50	2.970	1.98%	0.11709	2.12%	1870.9	32.1	1912.2	37.5
SCT_49	3.051	2.21%	0.10841	2.27%	1827.6	35.1	1772.9	40.8
SCT_48	3.222	2.04%	0.11382	2.36%	1742.3	31.1	1861.2	42.0
SCT_47	2.776	2.23%	0.11199	2.18%	1983.4	38.0	1831.9	39.0
SCT_46	3.002	2.01%	0.11111	2.15%	1853.4	32.2	1817.6	38.5

SCT_45	2.642	1.94%	0.12329	2.07%	2069.1	34.2	2004.4	36.4
SCT_44	2.921	1.96%	0.10828	2.31%	1897.8	32.2	1770.6	41.5
SCT_43	2.958	2.00%	0.11288	2.11%	1877.4	32.4	1846.4	37.7
SCT_42	3.048	2.14%	0.11242	1.59%	1828.9	34.0	1838.9	28.5
SCT_41	3.058	2.39%	0.11170	1.72%	1824.0	37.9	1827.3	30.8
SCT_40	3.212	2.02%	0.10867	1.58%	1747.1	30.8	1777.2	28.6
SCT_39	3.010	1.97%	0.10744	1.56%	1849.4	31.7	1756.5	28.2
SCT_38	2.963	1.98%	0.10919	1.72%	1874.6	32.1	1785.9	31.0
SCT_37	2.753	2.08%	0.11446	1.68%	1997.3	35.6	1871.4	30.0
SCT_35	1.991	2.25%	0.17141	1.69%	2623.9	48.2	2571.5	27.9
SCT_34	3.044	2.03%	0.10629	1.54%	1831.1	32.2	1736.7	27.9
SCT_33	2.870	2.15%	0.11777	1.99%	1927.0	35.8	1922.7	35.3
SCT_32	3.027	2.72%	0.11075	1.79%	1840.0	43.4	1811.7	32.2
SCT_31	3.130	2.05%	0.10892	1.53%	1787.3	32.0	1781.4	27.6
SCT_30	3.050	2.17%	0.10903	1.64%	1827.8	34.5	1783.3	29.6
SCT_29	2.966	2.10%	0.11106	1.73%	1873.1	34.0	1816.9	31.1
SCT_28	3.044	2.48%	0.10801	1.54%	1831.0	39.4	1766.2	28.0
SCT_27	3.328	2.49%	0.10970	1.64%	1693.9	37.0	1794.5	29.6
SCT_26	3.003	2.58%	0.10939	1.63%	1852.8	41.4	1789.2	29.3
SCT_25	3.064	2.38%	0.10502	1.50%	1820.8	37.7	1714.7	27.3
SCT_24	3.264	2.48%	0.10857	1.55%	1722.7	37.4	1775.6	28.0
SCT_23	2.181	2.35%	0.16422	1.50%	2432.6	47.5	2499.6	25.0
SCT_22	3.260	2.51%	0.10970	1.57%	1724.5	37.9	1794.4	28.3
SCT_21	2.946	2.45%	0.11081	1.54%	1884.0	39.8	1812.8	27.7
SCT_20	3.030	2.41%	0.10970	1.59%	1838.5	38.4	1794.5	28.6
SCT_19	3.171	2.48%	0.10939	1.59%	1767.2	38.2	1789.3	28.6
SCT_18	3.139	2.37%	0.11178	1.56%	1782.7	36.8	1828.5	28.0
SCT_17	3.165	2.52%	0.10893	1.54%	1770.0	38.9	1781.6	27.8
SCT_16	2.957	2.65%	0.11048	1.63%	1878.1	43.0	1807.3	29.4
SCT_15	3.169	2.55%	0.11310	1.60%	1767.9	39.4	1849.9	28.7
SCT_14	3.164	5.00%	0.10733	2.63%	1770.7	77.0	1754.5	47.4
SCT_12	3.085	5.08%	0.10652	2.70%	1810.1	79.7	1740.8	48.7
SCT_11	3.157	5.00%	0.10904	2.64%	1773.7	77.0	1783.5	47.4
SCT_10	3.020	5.10%	0.11356	2.68%	1844.1	81.3	1857.2	47.6
SCT_9	3.062	5.13%	0.10845	2.69%	1822.0	80.9	1773.5	48.2
SCT_8	3.248	5.06%	0.10741	2.68%	1730.4	76.4	1756.0	48.3
SCT_7	3.069	5.03%	0.11460	2.68%	1818.4	79.1	1873.7	47.5
SCT_6	3.047	4.98%	0.10715	2.62%	1829.5	78.8	1751.5	47.3
SCT_5	3.152	4.98%	0.10839	2.64%	1776.2	76.9	1772.5	47.4

SCT_4	2.988	5.09%	0.11266	2.65%	1860.8	81.7	1842.8	47.2
> 10% Discordant								
SCT_119	2.820	1.84%	0.15306	1.53%	1956.8	31.0	2380.3	25.8
SCT_97	2.307	2.02%	0.12033	1.21%	2321.7	39.3	1961.1	21.5
SCT_76	3.160	2.88%	0.12413	1.72%	1772.2	44.4	2016.4	30.2
SCT_36	2.134	1.95%	0.13817	1.54%	2477.8	40.1	2204.4	26.5
SCT_13	9.742	4.88%	0.17987	2.59%	629.9	29.2	2651.7	42.3

Sample SCE (Schell Creek Range-Ely Springs Dolomite Base)								
Sample Name	238U / 206Pb	1 σ (%)	207Pb / 206Pb	1 σ (%)	206Pb / 238 U (Ma)	1 σ abs err	207 Pb / 206 Pb (Ma)	1 σ abs err
< 10 % Discordant								
SCE_120	2.840	0.0278	0.11234	0.0176	1944.6	46.6	1837.6	31.5
SCE_119	2.759	0.0287	0.11609	0.0181	1993.8	49.0	1896.8	32.2
SCE_118	2.798	0.0281	0.11476	0.0188	1970.0	47.5	1876.1	33.6
SCE_117	2.958	0.0301	0.11182	0.0187	1877.3	48.8	1829.3	33.6
SCE_116	2.772	0.0273	0.11416	0.0177	1985.9	46.4	1866.7	31.6
SCE_114	2.699	0.0295	0.12567	0.0182	2032.0	51.2	2038.3	31.8
SCE_113	2.651	0.0306	0.12430	0.0180	2063.4	53.9	2018.9	31.6
SCE_112	1.844	0.0291	0.18436	0.0177	2793.6	65.6	2692.5	29.0
SCE_111	2.907	0.0288	0.10805	0.0184	1906.1	47.4	1766.9	33.3
SCE_110	2.869	0.0279	0.11627	0.0181	1927.4	46.4	1899.7	32.2
SCE_109	3.112	0.0278	0.11249	0.0193	1796.2	43.5	1840.1	34.6
SCE_108	3.055	0.0282	0.11018	0.0208	1825.2	44.6	1802.4	37.4
SCE_106	2.818	0.0289	0.11273	0.0205	1957.6	48.7	1843.9	36.7
SCE_105	2.770	0.0286	0.11575	0.0202	1986.8	48.7	1891.5	35.8
SCE_104	2.557	0.0300	0.12711	0.0218	2127.7	54.1	2058.3	38.0
SCE_103	2.977	0.0280	0.11174	0.0213	1866.7	45.1	1827.9	38.1
SCE_102	2.477	0.0276	0.12300	0.0201	2186.2	50.9	2000.3	35.2
SCE_101	3.051	0.0271	0.10988	0.0207	1827.3	43.0	1797.3	37.2
SCE_100	1.914	0.0276	0.18612	0.0214	2709.1	60.7	2708.2	34.8
SCE_99	2.649	0.0276	0.12416	0.0203	2064.8	48.5	2016.8	35.5
SCE_98	2.918	0.0274	0.11072	0.0216	1899.6	44.8	1811.3	38.7
SCE_97	2.977	0.0290	0.11523	0.0206	1866.9	46.8	1883.4	36.6
SCE_96	2.928	0.0289	0.11690	0.0216	1894.1	47.2	1909.4	38.2
SCE_95	2.961	0.0295	0.10953	0.0223	1875.8	47.9	1791.7	40.1
SCE_92	1.961	0.0277	0.17330	0.0235	2656.5	60.1	2589.8	38.7
SCE_91	1.593	0.0263	0.22750	0.0235	3141.2	65.1	3034.5	37.2
SCE_90	2.710	0.0288	0.12613	0.0236	2024.5	49.9	2044.8	41.2
SCE_88	3.072	0.0278	0.10872	0.0239	1816.4	43.8	1778.1	43.0
SCE_87	3.022	0.0278	0.11074	0.0240	1842.6	44.4	1811.6	43.0
SCE_86	3.034	0.0278	0.11403	0.0237	1836.3	44.2	1864.7	42.1
SCE_85	3.016	0.0278	0.11321	0.0239	1845.9	44.4	1851.5	42.5
SCE_84	2.918	0.0277	0.11022	0.0238	1899.6	45.3	1803.0	42.7
SCE_83	2.620	0.0273	0.12703	0.0239	2083.9	48.4	2057.2	41.6

SCE_82	2.942	0.0269	0.10861	0.0234	1886.3	43.9	1776.2	42.1
SCE_81	3.014	0.0267	0.11126	0.0235	1847.2	42.7	1820.0	42.0
SCE_80	2.612	0.0256	0.12534	0.0182	2089.5	45.6	2033.6	31.8
SCE_78	2.861	0.0265	0.12175	0.0195	1932.2	44.0	1982.0	34.2
SCE_76	2.136	0.0263	0.15299	0.0189	2475.1	53.9	2379.7	31.9
SCE_75	2.920	0.0264	0.11426	0.0187	1898.4	43.2	1868.3	33.4
SCE_74	2.971	0.0268	0.11566	0.0191	1870.1	43.3	1890.1	34.0
SCE_73	2.664	0.0264	0.12755	0.0189	2054.6	46.3	2064.4	32.9
SCE_72	2.989	0.0259	0.11069	0.0188	1860.7	41.7	1810.8	33.8
SCE_71	2.825	0.0267	0.11410	0.0187	1953.8	44.8	1865.8	33.4
SCE_70	2.190	0.0273	0.15886	0.0182	2424.6	54.9	2443.5	30.5
SCE_69	1.952	0.0255	0.18621	0.0179	2666.2	55.4	2708.9	29.2
SCE_68	3.027	0.0265	0.11291	0.0186	1840.4	42.3	1846.7	33.2
SCE_67	3.062	0.0258	0.11038	0.0182	1821.6	40.8	1805.6	32.7
SCE_66	3.050	0.0255	0.10986	0.0187	1828.3	40.5	1797.0	33.6
SCE_65	2.976	0.0236	0.11320	0.0173	1867.6	38.2	1851.5	31.0
SCE_64	1.888	0.0270	0.17932	0.0198	2740.0	60.0	2646.6	32.6
SCE_63	2.937	0.0227	0.10918	0.0178	1889.3	37.0	1785.8	32.1
SCE_62	2.894	0.0231	0.11190	0.0171	1913.3	38.2	1830.6	30.6
SCE_61	2.841	0.0231	0.11712	0.0173	1944.1	38.7	1912.7	30.6
SCE_60	3.005	0.0238	0.11197	0.0184	1851.8	38.3	1831.6	33.1
SCE_59	1.760	0.0233	0.18847	0.0162	2900.2	54.1	2728.8	26.4
SCE_58	2.893	0.0262	0.13106	0.0176	1913.6	43.2	2112.2	30.6
SCE_57	1.829	0.0242	0.18927	0.0163	2811.8	54.9	2735.8	26.6
SCE_56	2.547	0.0219	0.12775	0.0165	2135.1	39.7	2067.3	28.8
SCE_55	1.732	0.0229	0.18185	0.0158	2937.4	53.9	2669.8	26.0
SCE_54	1.823	0.0216	0.17661	0.0153	2819.2	49.1	2621.3	25.3
SCE_53	2.914	0.0240	0.11329	0.0178	1901.8	39.3	1852.9	31.9
SCE_51	2.546	0.0221	0.12687	0.0166	2136.0	40.1	2055.1	29.1
SCE_50	2.012	0.0270	0.16923	0.0149	2601.2	57.5	2550.1	24.8
SCE_49	2.841	0.0317	0.10904	0.0195	1944.1	53.0	1783.4	35.1
SCE_48	2.966	0.0281	0.11018	0.0160	1873.0	45.5	1802.3	28.8
SCE_46	2.831	0.0275	0.11567	0.0156	1950.0	46.1	1890.4	27.8
SCE_45	1.875	0.0267	0.17926	0.0156	2755.5	59.5	2646.0	25.7
SCE_43	1.838	0.0263	0.17985	0.0146	2799.9	59.4	2651.5	24.0
SCE_42	1.800	0.0268	0.19251	0.0135	2847.8	61.5	2763.7	22.1
SCE_41	2.970	0.0278	0.11067	0.0127	1870.7	45.0	1810.5	23.0
SCE_40	2.802	0.0267	0.11553	0.0135	1967.2	45.1	1888.2	24.1
SCE_39	3.179	0.0274	0.11234	0.0131	1763.2	42.1	1837.6	23.5

SCE_38	3.067	0.0262	0.10800	0.0141	1819.3	41.4	1766.0	25.6
SCE_37	2.877	0.0278	0.11683	0.0133	1923.0	46.0	1908.2	23.7
SCE_35	2.936	0.0261	0.11218	0.0142	1889.8	42.6	1835.1	25.6
SCE_34	2.919	0.0270	0.11050	0.0125	1899.4	44.3	1807.7	22.5
SCE_33	2.979	0.0296	0.11805	0.0133	1865.8	47.8	1926.9	23.7
SCE_32	3.149	0.0298	0.11166	0.0133	1777.9	46.2	1826.7	23.9
SCE_31	2.918	0.0297	0.11602	0.0148	1899.8	48.6	1895.7	26.4
SCE_30	2.962	0.0294	0.11154	0.0135	1875.4	47.6	1824.6	24.3
SCE_29	2.964	0.0279	0.10861	0.0145	1874.0	45.2	1776.2	26.3
SCE_28	3.066	0.0261	0.11217	0.0185	1819.9	41.2	1834.9	33.2
SCE_27	3.247	0.0306	0.11069	0.0186	1730.7	46.3	1810.7	33.4
SCE_24	3.305	0.0287	0.11157	0.0189	1703.8	42.8	1825.2	33.9
SCE_23	3.157	0.0287	0.11070	0.0198	1773.7	44.4	1811.0	35.5
SCE_22	2.950	0.0272	0.11067	0.0198	1881.7	44.3	1810.4	35.5
SCE_21	2.977	0.0264	0.10825	0.0190	1866.8	42.7	1770.1	34.2
SCE_20	3.349	0.0376	0.10632	0.0210	1684.4	55.5	1737.3	38.0
SCE_19	2.877	0.0232	0.11131	0.0169	1922.9	38.5	1821.0	30.4
SCE_18	2.993	0.0241	0.10934	0.0176	1858.1	38.8	1788.4	31.7
SCE_17	2.169	0.0245	0.16604	0.0171	2444.4	49.6	2518.2	28.4
SCE_16	2.113	0.0233	0.16515	0.0172	2497.8	48.1	2509.1	28.7
SCE_15	2.808	0.0246	0.11451	0.0174	1963.7	41.5	1872.2	31.1
SCE_14	3.064	0.0420	0.10824	0.0161	1821.0	66.2	1770.0	29.1
SCE_13	2.876	0.0433	0.12506	0.0200	1923.4	71.5	2029.7	35.1
SCE_12	3.105	0.0420	0.10968	0.0164	1799.6	65.6	1794.1	29.5
SCE_11	2.917	0.0424	0.10703	0.0170	1899.9	69.4	1749.5	30.7
SCE_10	3.084	0.0440	0.11055	0.0178	1810.3	69.0	1808.5	32.0
SCE_9	2.895	0.0434	0.11821	0.0181	1912.9	71.4	1929.4	32.1
SCE_8	2.936	0.0419	0.11387	0.0162	1889.3	68.2	1862.0	28.9
SCE_5	3.043	0.0442	0.10765	0.0173	1831.5	70.1	1760.0	31.3
SCE_4	2.888	0.0415	0.10735	0.0163	1916.7	68.5	1754.8	29.5
SCE_3	3.096	0.0441	0.11111	0.0175	1804.6	69.0	1817.7	31.5
SCE_2	2.920	0.0433	0.11323	0.0166	1898.8	70.8	1851.9	29.8
SCE_1	3.083	0.0415	0.11105	0.0177	1811.0	65.2	1816.6	31.8
> 10% Discordant								
SCE_115	2.627	2.89%	0.15517	1.72%	2079.1	51.1	2403.7	29.0
SCE_107	4.809	6.33%	0.17833	2.03%	1217.8	69.8	2637.4	33.4
SCE_93	4.025	3.49%	0.10959	2.40%	1430.6	44.6	1792.7	43.0
SCE_89	3.521	6.41%	0.18097	2.52%	1611.6	90.8	2661.8	41.1
SCE_79	5.546	2.75%	0.11134	1.81%	1068.8	27.0	1821.4	32.4

SCE_53	2.914	2.40%	0.11329	1.78%	1901.8	39.3	1852.9	31.9
SCE_47	26.751	12.99%	0.14134	1.97%	236.6	30.1	2243.6	33.7
SCE_44	5.197	2.65%	0.07230	1.64%	1134.5	27.5	994.3	33.1
SCE_36	3.953	2.94%	0.10910	1.39%	1453.8	38.1	1784.4	25.0
SCE_26	2.647	2.67%	0.11074	1.93%	2065.8	47.0	1811.6	34.7
SCE_25	2.745	2.69%	0.11052	1.90%	2002.5	46.1	1808.0	34.1
SCE_7	1.718	4.35%	0.18197	1.80%	2957.0	102.4	2670.9	29.4
SCE_6	3.277	4.20%	0.18139	1.60%	1717.0	63.0	2665.6	26.3

WETHERIL PLOTS

Schell Creek Range-Ely Springs Dolomite (SCE)

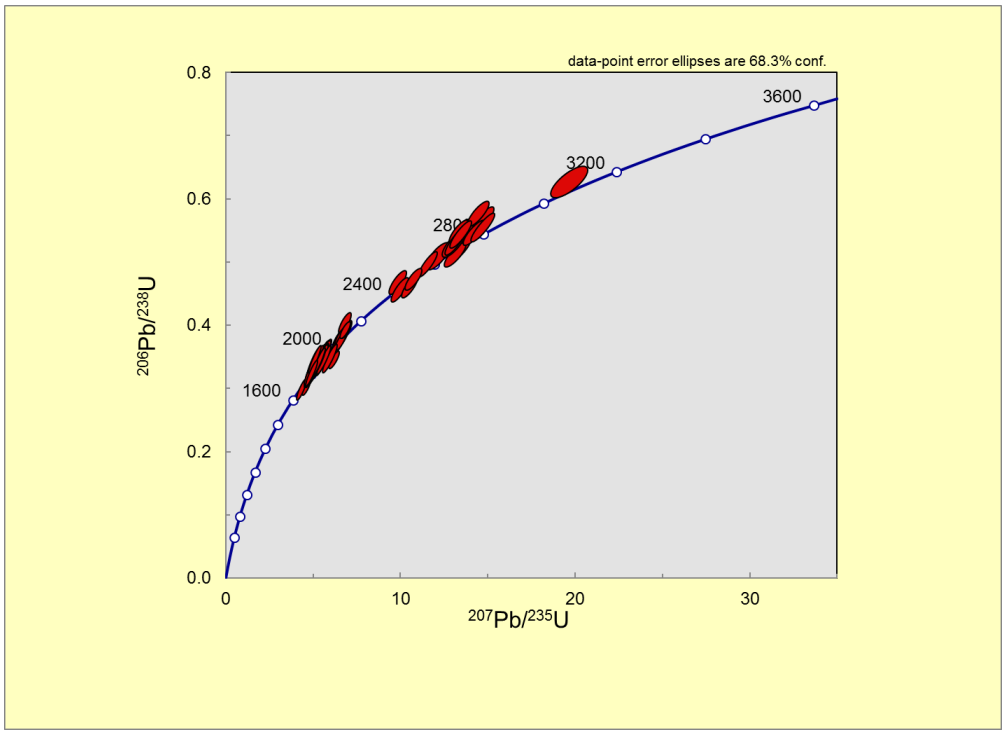

Schell Creek Range-Top (SCTop)

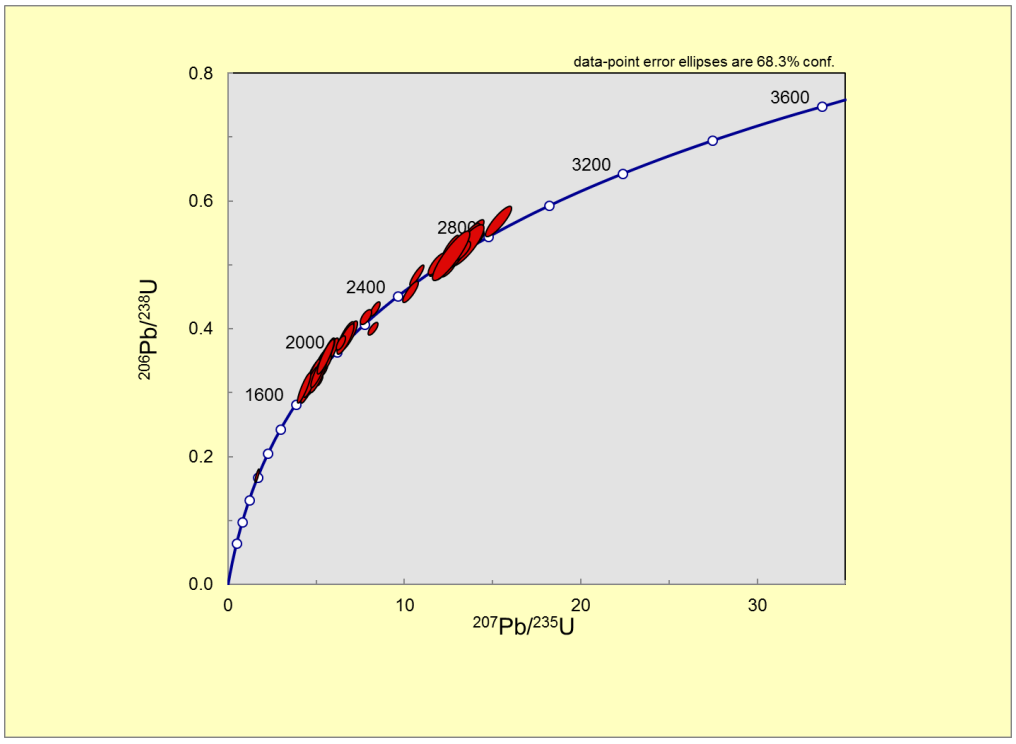

Schell Creek Range-Base (SCBase)

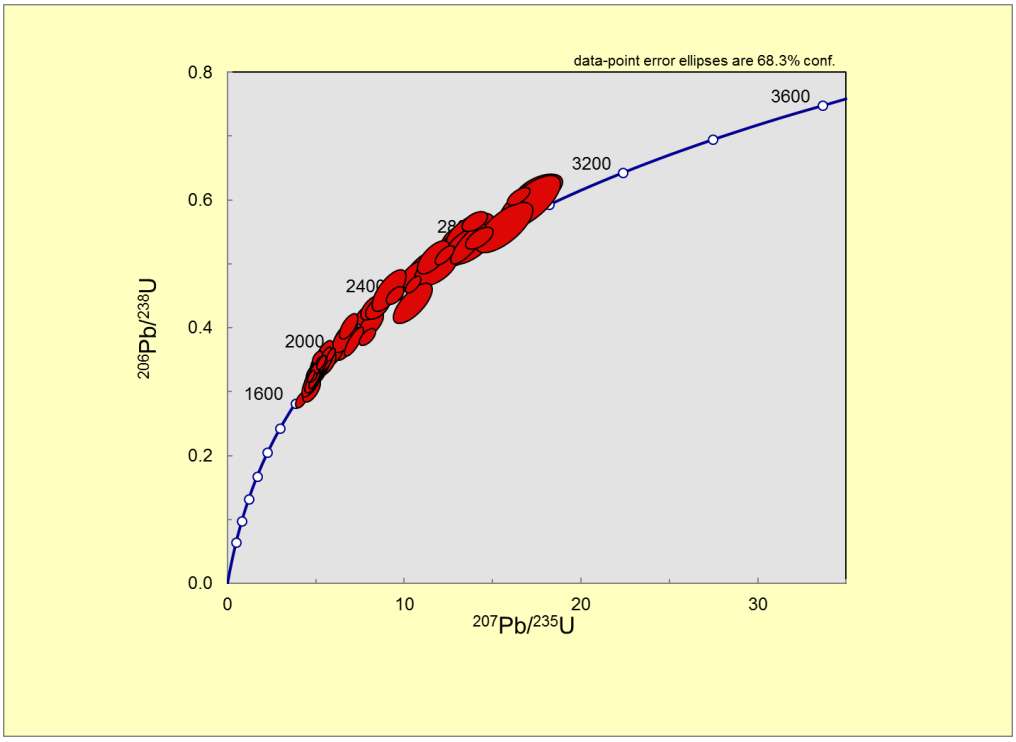

APPENDIX G

CHERRY CREEK RANGE

DATA TABLES

Sample CCB (Cherry Creek-Base)								
Sample Name	238U / 206Pb	1 σ (%)	207Pb / 206Pb	1 σ (%)	206Pb / 238 U (Ma)	1 σ abs err	207 Pb / 206 Pb (Ma)	1 σ abs err
< 10 % Discordant								
GroupACC_10	2.160	5.48%	0.16565	1.53%	2453.1	110.8	2518.3	5.5
GroupACC_9	2.566	6.14%	0.12711	1.94%	2121.6	110.1	2062.8	21.7
GroupACC_8	3.103	5.67%	0.11924	1.68%	1800.9	88.5	1949.2	13.8
GroupACC_7	2.486	5.60%	0.14464	1.56%	2179.7	102.7	2287.7	7.6
GroupACC_6	3.295	5.48%	0.10992	1.56%	1708.8	81.7	1802.5	8.1
GroupACC_5	3.408	5.54%	0.10929	1.56%	1658.5	80.5	1792.0	8.2
GroupACC_4	3.198	5.47%	0.11165	1.58%	1753.8	83.4	1830.9	9.4
GroupACC_2	3.044	5.53%	0.11058	1.61%	1831.1	87.6	1813.5	11.0
GroupACC_1	3.140	5.53%	0.11418	1.56%	1782.1	85.5	1871.4	8.2
GroupBCC_19	2.867	5.35%	0.10903	2.42%	1928.9	88.5	1783.3	43.4
GroupBCC_18	6.112	5.07%	0.07165	2.48%	976.9	45.8	976.2	49.7
GroupBCC_17	2.027	5.12%	0.17596	2.40%	2584.7	108.1	2615.2	39.5
GroupBCC_16	3.090	5.08%	0.11274	2.42%	1807.6	79.6	1844.1	43.2
GroupBCC_14	3.427	5.09%	0.10987	2.48%	1650.3	73.7	1797.2	44.5
GroupBCC_13	3.083	5.04%	0.10792	2.40%	1811.0	79.1	1764.6	43.3
GroupBCC_11	2.951	5.13%	0.12316	2.41%	1881.4	83.2	2002.5	42.2
GroupCCC_30	2.914	3.67%	0.12700	2.96%	1901.7	60.1	2056.9	51.3
GroupCCC_29	3.041	3.73%	0.11104	2.96%	1832.5	59.3	1816.5	52.7
GroupCCC_28	2.093	3.86%	0.17943	2.98%	2518.0	79.9	2647.6	48.7
GroupCCC_27	3.080	3.64%	0.10956	2.97%	1812.8	57.3	1792.0	53.1
GroupCCC_26	2.062	3.70%	0.17871	2.96%	2548.6	77.5	2640.9	48.2
GroupCCC_25	3.136	3.73%	0.11333	2.96%	1784.4	57.9	1853.5	52.6
GroupCCC_24	2.077	3.75%	0.17729	2.94%	2533.7	78.0	2627.7	48.1
GroupCCC_23	3.255	3.69%	0.11009	2.97%	1726.9	55.7	1800.8	53.0
GroupCCC_22	2.921	3.73%	0.12049	2.96%	1897.9	61.0	1963.5	51.9
GroupCCC_21	2.991	3.71%	0.12556	2.97%	1859.1	59.7	2036.7	51.6

GroupDCC_37	3.091	3.84%	0.12079	1.90%	1807.0	60.3	1967.9	33.6
GroupDCC_36	2.786	3.78%	0.12894	1.94%	1977.0	64.1	2083.5	33.7
GroupDCC_35	2.216	3.85%	0.16628	1.90%	2400.9	76.8	2520.5	31.5
GroupDCC_34	3.345	3.79%	0.11189	1.93%	1686.2	56.1	1830.3	34.6
GroupDCC_32	2.768	3.99%	0.12176	1.90%	1988.2	67.9	1982.1	33.5
GroupDCC_31	2.101	3.81%	0.18017	1.89%	2509.6	78.8	2654.5	31.1
GroupECC_11	2.964	4.37%	0.10776	1.40%	1874.3	70.7	1762.0	25.3
GroupECC_10	2.403	4.54%	0.14033	1.42%	2242.9	85.4	2231.2	24.3
GroupECC_9	2.870	4.62%	0.12946	1.49%	1927.2	76.5	2090.7	25.9
GroupECC_8	3.222	4.48%	0.10768	1.44%	1742.4	68.0	1760.5	26.0
GroupECC_7	1.927	4.34%	0.17696	1.40%	2695.0	95.0	2624.6	23.0
GroupECC_6	2.676	4.39%	0.12416	1.39%	2047.0	76.6	2016.9	24.5
GroupECC_5	3.046	4.46%	0.11473	1.42%	1830.4	70.7	1875.6	25.3
GroupECC_4	2.866	5.41%	0.12023	1.86%	1929.5	89.6	1959.6	32.8
GroupECC_3	2.501	4.52%	0.12301	1.46%	2168.2	82.7	2000.4	25.7
GroupECC_2	2.992	4.33%	0.10960	1.41%	1858.9	69.6	1792.8	25.5
GroupECC_1	2.937	4.98%	0.11060	1.48%	1889.2	81.0	1809.3	26.6
GroupFCC_24	3.247	2.79%	0.11134	1.95%	1730.9	42.2	1821.5	35.0
GroupFCC_23	3.267	2.27%	0.10706	1.80%	1721.3	34.3	1749.9	32.5
GroupFCC_22	3.026	2.29%	0.11258	1.77%	1840.5	36.6	1841.6	31.7
GroupFCC_21	2.738	2.36%	0.12480	1.80%	2006.7	40.6	2026.0	31.5
GroupFCC_20	2.853	2.48%	0.11400	1.77%	1937.0	41.4	1864.1	31.7
GroupFCC_19	3.347	3.14%	0.10867	1.81%	1685.1	46.4	1777.2	32.7
GroupFCC_18	2.487	2.33%	0.13698	1.78%	2178.7	42.9	2189.3	30.6
GroupFCC_16	3.132	2.37%	0.10790	1.78%	1786.4	36.9	1764.3	32.1
GroupFCC_15	2.116	2.18%	0.16433	1.77%	2494.7	45.0	2500.7	29.4
GroupGCC_36	2.121	4.03%	0.16751	2.03%	2490.1	82.8	2532.9	33.7
GroupGCC_35	2.589	3.54%	0.12536	2.01%	2105.4	63.2	2033.8	35.1
GroupGCC_34	3.303	3.63%	0.10936	2.03%	1705.1	54.2	1788.7	36.5
GroupGCC_32	3.055	3.92%	0.11553	2.04%	1825.5	62.0	1888.1	36.2
GroupGCC_31	2.810	3.66%	0.11947	2.00%	1962.3	61.7	1948.3	35.3
GroupGCC_30	2.926	3.50%	0.11352	2.00%	1895.4	57.3	1856.5	35.6
GroupGCC_29	2.950	3.67%	0.11010	2.02%	1881.7	59.7	1801.1	36.4
GroupGCC_28	2.984	4.16%	0.11873	2.16%	1863.3	66.9	1937.3	38.2
GroupGCC_27	3.096	3.72%	0.11422	2.05%	1804.3	58.2	1867.6	36.6
GroupGCC_26	2.865	4.04%	0.11349	2.04%	1929.9	67.0	1856.1	36.4
GroupGCC_25	2.804	3.62%	0.11667	2.00%	1965.9	61.1	1905.8	35.5
GroupHCC_48	3.083	5.10%	0.11508	1.47%	1811.1	80.0	1881.2	26.2
GroupHCC_46	2.692	5.03%	0.12959	1.52%	2036.1	87.3	2092.5	26.4

GroupHCC_45	3.306	5.06%	0.11119	1.51%	1703.4	75.3	1819.0	27.2
GroupHCC_44	3.216	5.17%	0.11260	1.59%	1745.5	78.5	1841.8	28.5
GroupHCC_43	3.087	5.03%	0.11701	1.53%	1808.8	78.8	1911.0	27.1
GroupHCC_42	3.072	5.69%	0.10968	1.54%	1816.5	89.4	1794.0	27.7
GroupHCC_40	5.969	5.18%	0.07653	1.66%	998.5	47.7	1108.9	32.8
GroupHCC_39	2.032	5.10%	0.18475	1.48%	2580.2	107.6	2695.9	24.2
GroupHCC_38	3.278	5.98%	0.11240	1.49%	1716.6	89.5	1838.5	26.7
GroupICC_60	3.051	5.44%	0.11782	0.76%	1827.8	86.0	1923.4	13.5
GroupICC_59	2.037	5.92%	0.19446	1.19%	2574.6	124.4	2780.2	19.3
GroupICC_58	3.107	5.62%	0.11283	0.79%	1798.8	87.6	1845.5	14.3
GroupICC_56	2.624	5.47%	0.12770	0.78%	2081.1	96.5	2066.5	13.7
GroupICC_55	3.198	5.55%	0.11838	1.06%	1753.9	84.7	1931.9	18.9
GroupICC_54	3.182	5.39%	0.11225	0.78%	1761.6	82.6	1836.2	14.0
GroupICC_53	2.898	5.38%	0.11472	0.69%	1911.2	88.4	1875.4	12.4
GroupICC_52	3.167	5.43%	0.11153	0.75%	1768.9	83.4	1824.5	13.6
GroupICC_51	2.861	5.39%	0.10972	0.72%	1932.5	89.4	1794.8	13.0
GroupICC_50	3.110	5.61%	0.12094	0.90%	1797.5	87.5	1970.1	16.0
Group CC_10	2.872	5.08%	0.13182	1.21%	1925.9	84.0	2122.3	21.1
Group CC_9	3.334	4.96%	0.11180	1.16%	1691.2	73.4	1828.9	20.9
GroupJCC_8	2.927	5.05%	0.11963	1.32%	1894.9	82.3	1950.7	23.4
GroupJCC_7	2.933	4.99%	0.12077	1.13%	1891.5	81.4	1967.7	20.0
GroupJCC_6	2.930	4.99%	0.12699	1.12%	1892.9	81.3	2056.8	19.6
GroupJCC_5	3.094	5.03%	0.11640	1.17%	1805.3	78.8	1901.6	20.8
GroupJCC_4	2.930	4.88%	0.11592	1.11%	1892.7	79.5	1894.2	19.8
GroupJCC_3	2.776	5.37%	0.13146	1.61%	1983.0	91.0	2117.6	28.0
GroupJCC_2	3.191	5.04%	0.11676	1.15%	1757.5	77.0	1907.2	20.5
GroupJCC_1	2.078	5.04%	0.18100	1.13%	2533.1	104.7	2662.1	18.6
GroupKCC_23	6.136	2.75%	0.07413	1.50%	973.2	24.8	1044.9	29.9
GroupK CC_22	3.315	2.93%	0.11480	1.47%	1699.6	43.6	1876.7	26.3
GroupKCC_21	3.262	2.80%	0.11165	1.41%	1724.0	42.2	1826.4	25.3
GroupKCC_20	2.090	2.77%	0.18387	1.35%	2520.9	57.5	2688.1	22.1
GroupKCC_19	3.178	2.81%	0.11702	1.45%	1763.7	43.2	1911.2	25.7
GroupKCC_18	3.274	2.75%	0.11052	1.39%	1718.3	41.4	1808.1	25.0
GroupKCC_17	5.178	2.80%	0.07781	1.45%	1138.3	29.2	1141.9	28.5
GroupKCC_16	2.393	2.70%	0.14732	1.38%	2251.0	51.2	2315.1	23.5
GroupKCC_14	3.215	3.29%	0.11107	1.50%	1745.6	50.1	1817.0	27.1
GroupKCC_13	3.038	2.61%	0.12093	1.43%	1834.2	41.5	1970.0	25.3
> 10% Discordant								
GroupKCC_15	3.307	2.67%	0.11680	1.42%	1703.2	39.9	1907.8	25.3

GroupKCC_24	3.222	2.91%	0.12433	1.54%	1742.5	44.3	2019.2	27.0
GroupJCC_11	2.926	4.95%	0.13372	1.21%	1894.9	80.7	2147.4	20.9
GroupJCC_12	3.167	5.19%	0.12337	1.42%	1769.1	79.8	2005.5	25.0
GroupICC_49	5.592	14.93%	0.11400	0.74%	1060.6	144.4	1864.1	13.3
GroupICC_57	5.504	10.57%	0.12624	1.30%	1076.3	103.9	2046.2	22.8
GroupHCC_37	4.739	5.19%	0.10990	1.47%	1234.2	58.1	1797.7	26.4
GroupHCC_41	3.313	5.18%	0.11788	1.52%	1700.3	76.9	1924.4	27.1
GroupHCC_47	3.839	5.42%	0.11125	1.48%	1492.4	71.8	1820.0	26.5
GroupGCC_33	2.992	4.01%	0.13330	2.24%	1858.6	64.4	2141.9	38.6
GroupFCC_14	32.432	11.94%	0.06011	1.84%	195.8	23.0	607.6	39.3
GroupFCC_17	7.156	5.89%	0.11014	1.79%	843.2	46.4	1801.7	32.2
GroupDCC_33	3.438	3.85%	0.11354	1.96%	1646.1	55.7	1856.9	34.9
GroupDCC_38	3.322	4.14%	0.11923	1.94%	1696.5	61.5	1944.8	34.3
GroupDCC_39	4.874	4.04%	0.22108	1.87%	1203.0	44.1	2988.6	29.8
GroupDCC_40	3.004	3.69%	0.12791	1.89%	1852.3	59.1	2069.5	32.9
GroupBCC_12	6.991	5.08%	0.11591	2.41%	861.8	40.8	1894.0	42.7
GroupBCC_15	10.725	5.10%	0.08632	2.42%	574.7	28.0	1345.3	46.0
GroupBCC_20	5.553	5.21%	0.11317	2.40%	1067.5	51.1	1850.9	42.7
GroupACC_3	3.606	5.53%	0.11255	1.54%	1577.8	76.9	1845.5	7.1
GroupFCC_13	2.736	2.08%	0.10971	1.76%	2008.5	35.8	1794.6	31.7
GroupECC_12	1.840	4.47%	0.15469	1.38%	2798.6	100.6	2398.4	23.4

Sample CCT (Cherry Creek Range-Top)								
Sample Name	238U / 206Pb	1 σ (%)	207Pb / 206Pb	1 σ (%)	206Pb / 238 U (Ma)	1 σ abs err	207 Pb / 206 Pb (Ma)	1 σ abs err
< 10 % Discordant								
CC_12	2.741	2.77%	0.12599	3.69%	2004.8	47.5	2042.8	63.8
CC_11	3.310	2.92%	0.11274	3.72%	1701.6	43.6	1844.1	65.8
CC_10	3.027	2.81%	0.11646	3.73%	1840.1	44.9	1902.6	65.5
CC_9	2.025	2.70%	0.18223	3.67%	2587.1	57.4	2673.3	59.6
CC_8	2.961	2.78%	0.11784	3.73%	1875.6	45.1	1923.7	65.4
CC_7	3.097	2.81%	0.11632	3.72%	1803.9	44.1	1900.5	65.3
CC_5	3.243	2.80%	0.11255	3.72%	1732.8	42.4	1841.1	65.8
CC_4	2.819	2.71%	0.11957	3.71%	1957.2	45.6	1949.8	64.8
CC_3	3.011	2.70%	0.11292	3.71%	1848.8	43.3	1847.0	65.6
CC_2	3.217	2.88%	0.11258	3.77%	1744.7	43.9	1841.5	66.6
CC_1	2.877	2.83%	0.11578	3.70%	1923.1	46.8	1892.0	65.1
CC_22	3.230	2.97%	0.11234	2.52%	1738.6	45.0	1837.5	45.0
CC_21	2.690	2.92%	0.12442	2.47%	2037.6	50.8	2020.5	43.1
CC_20	2.502	2.96%	0.13766	2.45%	2167.3	54.2	2198.0	42.0
CC_19	2.508	3.00%	0.13734	2.39%	2163.3	54.9	2193.9	41.0
CC_18	2.878	2.83%	0.11196	2.35%	1922.5	46.8	1831.5	41.9
CC_17	2.793	2.83%	0.12308	2.35%	1972.6	48.0	2001.3	41.1
CC_16	3.340	3.01%	0.10919	2.38%	1688.4	44.5	1786.0	42.7
CC_15	3.129	2.93%	0.10907	2.44%	1787.8	45.6	1784.0	43.8
CC_14	3.176	2.79%	0.10817	2.38%	1764.7	43.0	1768.8	42.9
CC_13	3.112	2.90%	0.11107	2.39%	1796.3	45.2	1817.1	42.8
CC_36	3.038	2.37%	0.11107	2.49%	1834.3	37.7	1816.9	44.6
CC_35	3.125	2.25%	0.10748	2.37%	1789.5	35.0	1757.1	42.8
CC_34	3.095	2.23%	0.10917	2.35%	1805.0	35.0	1785.6	42.3
CC_33	2.588	2.23%	0.12696	2.42%	2106.1	39.9	2056.3	42.0
CC_32	2.163	2.22%	0.16169	2.35%	2449.8	45.1	2473.5	39.1
CC_31	2.945	2.27%	0.11474	2.41%	1884.4	37.0	1875.7	42.7
CC_29	1.849	2.28%	0.19289	2.36%	2787.2	51.4	2766.9	38.2
CC_28	2.013	2.34%	0.17680	2.34%	2599.8	49.9	2623.0	38.5
CC_27	3.186	2.40%	0.11327	2.51%	1759.5	36.8	1852.6	44.7
CC_26	3.008	2.28%	0.11958	2.46%	1850.2	36.5	1950.0	43.4
CC_25	3.069	2.25%	0.11253	2.47%	1818.0	35.6	1840.6	44.1
CC_48	3.296	1.79%	0.11130	2.43%	1708.1	26.7	1820.7	43.5
CC_47	2.849	1.90%	0.13366	2.40%	1939.1	31.8	2146.6	41.4

CC_46	3.124	1.87%	0.11360	2.50%	1790.3	29.1	1857.8	44.5
CC_45	2.018	1.74%	0.18661	2.38%	2594.2	37.0	2712.5	38.7
CC_44	2.230	1.62%	0.16758	2.34%	2388.5	32.3	2533.6	38.8
CC_43	2.005	1.75%	0.17808	2.37%	2608.9	37.5	2635.1	38.9
CC_42	3.070	1.75%	0.11326	2.57%	1817.5	27.7	1852.3	45.7
CC_41	1.948	1.62%	0.19409	2.33%	2670.7	35.3	2777.1	37.7
CC_40	3.229	1.63%	0.11228	2.38%	1739.1	24.8	1836.6	42.5
CC_60	3.122	1.34%	0.11124	2.00%	1791.4	20.9	1819.8	35.9
CC_59	2.089	1.50%	0.18764	2.02%	2521.4	31.2	2721.6	33.0
CC_58	3.131	1.26%	0.10956	1.93%	1787.0	19.7	1792.1	34.8
CC_55	3.063	1.64%	0.12211	2.22%	1821.2	25.9	1987.3	39.1
CC_51	2.866	1.44%	0.13046	2.05%	1929.5	24.0	2104.2	35.5
CC_49	2.153	1.48%	0.16930	2.01%	2459.2	30.2	2550.7	33.3
CC_72	1.991	1.66%	0.17450	3.76%	2623.5	35.7	2601.3	61.3
CC_71	3.243	1.63%	0.10944	3.81%	1732.8	24.7	1790.1	67.8
CC_70	2.997	1.58%	0.10962	3.76%	1855.9	25.4	1793.1	66.9
CC_69	2.000	1.70%	0.17861	3.76%	2614.2	36.5	2640.0	61.2
CC_68	3.218	1.73%	0.11414	3.81%	1744.3	26.4	1866.4	67.2
CC_67	3.357	1.75%	0.10854	3.76%	1680.9	25.8	1775.0	67.1
CC_66	1.947	1.65%	0.17573	3.76%	2671.5	36.0	2613.0	61.2
CC_65	2.738	1.72%	0.12491	3.78%	2007.1	29.7	2027.5	65.4
CC_63	3.072	1.65%	0.10536	3.76%	1816.8	26.0	1720.6	67.5
CC_62	1.955	1.83%	0.17819	3.79%	2663.1	39.7	2636.1	61.6
CC_61	2.762	1.68%	0.11246	3.80%	1991.7	28.7	1839.5	67.2
CC_83	3.336	1.75%	0.10994	4.11%	1690.0	25.9	1798.4	73.0
CC_82	3.269	1.69%	0.10641	4.06%	1720.5	25.4	1738.9	72.7
CC_80	1.966	1.65%	0.18481	4.02%	2650.7	35.8	2696.5	64.9
CC_79	1.844	1.85%	0.21639	4.02%	2792.8	41.8	2954.0	63.4
CC_78	3.345	1.60%	0.10442	4.03%	1686.2	23.7	1704.0	72.4
CC_77	2.820	1.70%	0.12408	4.05%	1956.8	28.7	2015.7	70.1
CC_76	3.440	1.86%	0.10896	4.10%	1644.8	26.9	1782.2	72.9
CC_75	3.217	1.62%	0.10792	4.07%	1744.7	24.7	1764.6	72.6
CC_74	3.222	1.68%	0.10792	4.03%	1742.3	25.7	1764.6	71.9
CC_73	3.057	1.66%	0.11363	4.08%	1824.2	26.3	1858.2	71.9
CC_96	2.632	2.19%	0.13359	2.51%	2075.9	38.8	2145.7	43.2
CC_95	3.228	2.18%	0.10849	2.47%	1739.7	33.2	1774.3	44.5
CC_94	2.798	2.11%	0.12375	2.52%	1969.8	35.7	2011.0	44.0
CC_93	3.055	2.17%	0.11650	2.48%	1825.5	34.3	1903.3	43.9
CC_90	3.243	2.06%	0.10855	2.45%	1732.4	31.2	1775.3	44.0

CC_89	3.288	2.07%	0.10665	2.40%	1711.9	31.0	1742.9	43.4
CC_88	3.366	2.13%	0.11117	2.45%	1676.8	31.4	1818.6	43.8
CC_87	2.164	2.04%	0.16250	2.39%	2448.8	41.4	2481.8	39.7
CC_86	3.274	2.18%	0.10623	2.48%	1718.2	32.8	1735.6	44.7
CC_85	3.073	2.08%	0.10743	2.55%	1816.1	32.9	1756.4	45.9
CC_108	3.113	1.55%	0.10725	2.05%	1795.7	24.3	1753.2	37.0
CC_107	3.097	1.53%	0.11294	2.03%	1803.7	24.0	1847.3	36.3
CC_106	3.283	1.44%	0.10667	2.00%	1713.9	21.6	1743.3	36.3
CC_105	3.168	1.52%	0.10473	1.98%	1768.6	23.5	1709.6	35.9
CC_104	2.974	1.62%	0.12410	2.04%	1868.7	26.3	2016.0	35.7
CC_103	2.243	1.50%	0.15429	1.95%	2376.8	29.7	2394.0	32.8
CC_102	2.204	1.71%	0.17870	2.13%	2411.5	34.2	2640.8	35.0
CC_100	2.769	1.66%	0.12530	2.04%	1987.7	28.4	2033.1	35.7
CC_99	2.781	1.70%	0.12719	2.27%	1979.9	28.9	2059.5	39.6
CC_98	2.714	1.57%	0.12495	2.02%	2022.2	27.2	2028.1	35.4
CC_97	2.055	1.59%	0.17443	2.03%	2556.1	33.5	2600.7	33.4
CC_120	3.339	1.69%	0.10934	2.16%	1688.9	25.0	1788.5	38.8
CC_119	1.990	1.48%	0.16804	1.85%	2624.6	31.8	2538.2	30.7
CC_118	3.104	1.72%	0.11419	1.91%	1800.4	26.9	1867.1	34.0
CC_117	3.373	1.68%	0.10847	1.93%	1673.9	24.6	1773.9	34.8
CC_115	2.255	1.71%	0.16603	1.89%	2366.4	33.8	2518.1	31.4
CC_114	3.258	1.56%	0.11504	2.02%	1725.8	23.6	1880.4	36.0
CC_113	3.113	1.50%	0.10945	1.91%	1795.9	23.5	1790.3	34.4
CC_112	3.074	1.59%	0.11807	1.93%	1815.7	25.2	1927.3	34.2
CC_111	3.084	1.55%	0.11280	1.85%	1810.4	24.4	1845.0	33.1
CC_110	3.318	1.59%	0.11304	1.87%	1698.2	23.7	1848.8	33.4
CC_109	2.183	1.54%	0.16555	1.83%	2430.7	31.2	2513.1	30.4
> 10% Discordant								
CC_6	4.106	2.91%	0.12274	3.74%	1405.0	36.7	1996.4	64.9
CC_24	3.372	3.07%	0.11440	2.49%	1674.4	45.1	1870.5	44.2
CC_23	3.315	2.86%	0.11595	2.41%	1699.3	42.5	1894.6	42.6
CC_30	3.702	2.39%	0.11102	2.42%	1541.6	32.7	1816.2	43.3
CC_39	4.735	1.91%	0.14510	2.63%	1235.1	21.5	2289.0	44.6
CC_38	3.367	1.76%	0.11899	2.39%	1676.3	25.9	1941.1	42.1
CC_37	5.328	6.02%	0.22272	4.24%	1108.8	61.0	3000.4	66.5
CC_57	3.378	1.61%	0.12950	2.06%	1671.7	23.7	2091.2	35.8
CC_56	8.034	1.53%	0.11650	1.97%	756.3	10.9	1903.2	35.0
CC_54	6.991	1.35%	0.12567	1.96%	861.8	10.9	2038.3	34.3
CC_64	3.215	1.84%	0.15413	4.00%	1746.0	28.1	2392.3	66.5

CC_84	3.631	1.99%	0.11002	4.06%	1568.3	27.7	1799.7	72.1
CC_81	3.366	1.86%	0.14933	4.16%	1676.6	27.4	2338.3	69.5
CC_92	6.911	2.06%	0.11438	2.40%	871.2	16.7	1870.2	42.7
CC_91	9.206	4.30%	0.13988	2.56%	664.7	27.1	2225.7	43.6
CC_101	4.724	2.06%	0.12687	2.11%	1237.8	23.2	2055.0	36.7
CC_116	2.577	1.75%	0.15761	1.85%	2113.7	31.4	2430.2	31.0

WETHERIL PLOTS

Cherry Creek Range-Top (CCTop)

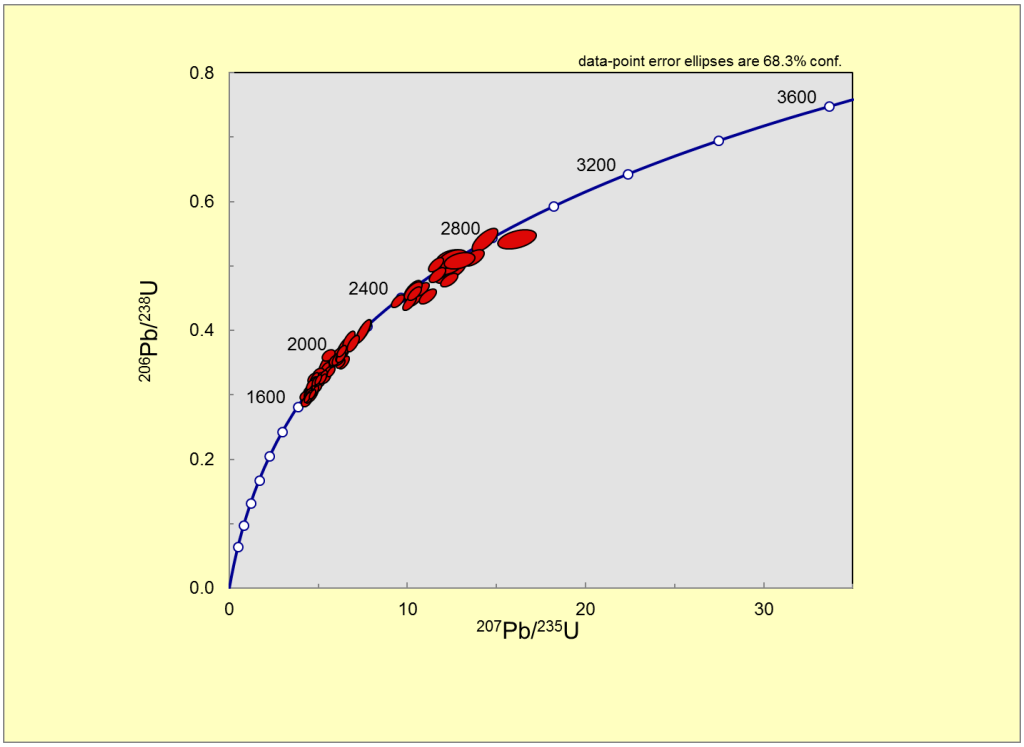

Cherry Creek Range-Base (CCBase)

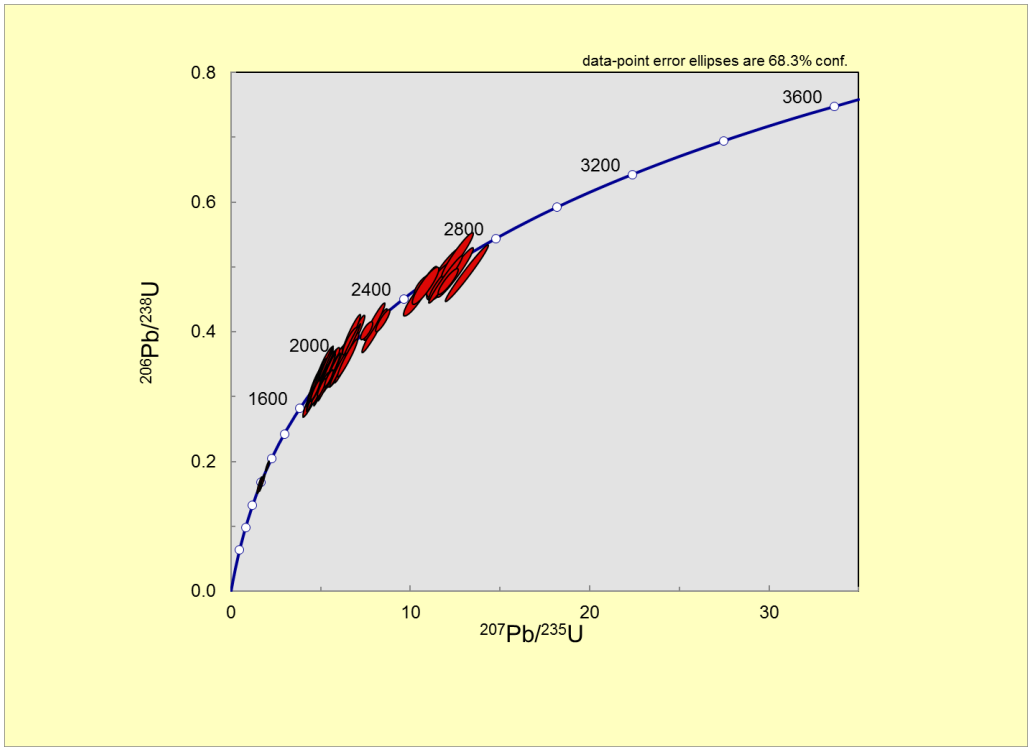

APPENDIX H

ZIRCON STANDARDS

DATA TABLES

Peixe Standard Data							
Sample Name	207/235 Intercept	1 sigma Abs Error	206/238 Intercept	1 sigma Abs Error	207/206 Average	1 sigma Abs Error	Analysis Date
Px_a	1.274115	0.02305	0.156341	0.001795	0.05911	0.000826	Feb. 5, 2014
Px_b	1.266604	0.023617	0.155844	0.001915	0.05895	0.000827	Feb. 5, 2014
Px_c	1.231947	0.020124	0.154273	0.001557	0.05792	0.000744	Feb. 5, 2014
Px_d	1.366973	0.022739	0.16526	0.001698	0.05999	0.000785	Feb. 5, 2014
Px_e	1.201453	0.026029	0.147911	0.002392	0.05891	0.000849	Feb. 5, 2014
Px_f	1.273891	0.02276	0.158993	0.0018	0.05811	0.000803	Feb. 5, 2014
Px_g	1.280604	0.048162	0.15763	0.005226	0.05892	0.001047	Feb. 5, 2014
Px_h	1.305622	0.025277	0.156333	0.00187	0.06057	0.000922	Feb. 5, 2014
Px_i	1.323119	0.042889	0.15451	0.003222	0.06211	0.001541	Feb. 5, 2014
Px_j	1.245561	0.033193	0.148105	0.002208	0.06099	0.001347	Feb. 5, 2014
Px_k	1.261863	0.022805	0.153317	0.001738	0.05969	0.00084	Feb. 5, 2014
Px_l	1.237357	0.022475	0.154771	0.001887	0.05798	0.000781	Feb. 5, 2014
Px_m	1.253742	0.022947	0.154555	0.001787	0.05883	0.000835	Feb. 5, 2014
Px_n	1.227212	0.023222	0.154741	0.001783	0.05752	0.000863	Feb. 5, 2014
Px_o	1.188757	0.02441	0.148549	0.001957	0.05804	0.000914	Feb. 5, 2014
Px_p	1.2143	0.024612	0.151646	0.001685	0.05808	0.000984	Feb. 5, 2014
Px_q	1.248505	0.030242	0.151839	0.002561	0.05964	0.001037	Feb. 5, 2014
Px_r	1.2282	0.024326	0.147124	0.001725	0.06055	0.000967	Feb. 5, 2014
Px_a	1.587724	0.022982	0.195116	0.001655	0.05902	0.000692	Feb. 7, 2014
Px_b	1.595462	0.022417	0.197308	0.001698	0.05865	0.000651	Feb. 7, 2014
Px_c	1.655358	0.022402	0.203128	0.001608	0.0591	0.000649	Feb. 7, 2014
Px_d	1.591193	0.021644	0.194021	0.001597	0.05948	0.000644	Feb. 7, 2014
Px_e	1.607965	0.02243	0.191893	0.001557	0.06077	0.00069	Feb. 7, 2014
Px_f	1.563706	0.022578	0.19366	0.001682	0.05856	0.000675	Feb. 7, 2014
Px_g	1.53722	0.023757	0.191709	0.001806	0.05816	0.000712	Feb. 7, 2014
Px_h	1.568453	0.024135	0.193456	0.001738	0.0588	0.000735	Feb. 7, 2014
Px_i	1.567315	0.024073	0.191693	0.001852	0.0593	0.000708	Feb. 7, 2014
Px_j	1.617037	0.024852	0.194538	0.001601	0.06029	0.000782	Feb. 7, 2014
Px_k	1.617966	0.025134	0.194052	0.002037	0.06047	0.000692	Feb. 7, 2014
Px_l	1.593352	0.025841	0.191189	0.002066	0.06044	0.000731	Feb. 7, 2014
Px_m	1.601041	0.026101	0.195772	0.002042	0.05931	0.000743	Feb. 7, 2014

Px_n	1.575751	0.022881	0.190868	0.001685	0.05988	0.00069	Feb. 7, 2014
Px_o	1.500445	0.016956	0.18686	0.001635	0.05824	0.000416	Feb. 7, 2014
Px_p	1.497226	0.015723	0.189702	0.001451	0.05724	0.000412	Feb. 7, 2014
Px_q	1.57785	0.017264	0.196852	0.001546	0.05813	0.000443	Feb. 7, 2014
Px_r	1.543473	0.016076	0.191352	0.001437	0.0585	0.000422	Feb. 7, 2014
Px_s	1.597252	0.016379	0.199151	0.00145	0.05817	0.00042	Feb. 7, 2014
Px_t	1.56803	0.015359	0.19675	0.001435	0.0578	0.000378	Feb. 7, 2014
Px_u	1.534095	0.015816	0.191421	0.001574	0.05812	0.000362	Feb. 7, 2014
Px_v	1.558499	0.015601	0.196807	0.001417	0.05743	0.000399	Feb. 7, 2014
Px_w	1.534456	0.015981	0.192245	0.001612	0.05789	0.000358	Feb. 7, 2014
Px_x	1.469265	0.016911	0.184815	0.00168	0.05766	0.000407	Feb. 7, 2014
Px_a	1.358161	0.01578	0.169167	0.00133	0.05823	0.000498	Feb. 12, 2014
Px_b	1.321319	0.015053	0.164842	0.001324	0.05814	0.00047	Feb. 12, 2014
Px_c	1.328805	0.016095	0.16437	0.00135	0.05863	0.000522	Feb. 12, 2014
Px_d	1.290756	0.01553	0.161291	0.001327	0.05804	0.00051	Feb. 12, 2014
Px_e	1.289675	0.015255	0.158732	0.001431	0.05893	0.000451	Feb. 12, 2014
Px_f	1.302302	0.015362	0.16033	0.001369	0.05891	0.00048	Feb. 12, 2014
Px_g	1.258334	0.017927	0.157272	0.001733	0.05803	0.000524	Feb. 12, 2014
Px_h	1.290438	0.015624	0.156728	0.001412	0.05972	0.000483	Feb. 12, 2014
Px_i	1.235016	0.016999	0.155746	0.001578	0.05751	0.000536	Feb. 12, 2014
Px_j	1.298894	0.015835	0.161509	0.001393	0.05833	0.000503	Feb. 12, 2014
Px_k	1.282392	0.01685	0.158117	0.001534	0.05882	0.000521	Feb. 12, 2014
Px_l	1.29675	0.017373	0.157847	0.001623	0.05958	0.000512	Feb. 12, 2014
Px_a	0.570007	0.018343	0.068146	0.00136	0.06067	0.001531	Mar. 9, 2014
Px_b	0.559351	0.0243	0.06751	0.001379	0.06009	0.002304	Mar. 9, 2014
Px_c	0.552678	0.022096	0.071543	0.001434	0.05603	0.001938	Mar. 9, 2014
Px_d	0.541252	0.020816	0.068925	0.001309	0.05695	0.001905	Mar. 9, 2014
Px_e	0.565732	0.025302	0.066031	0.001439	0.06214	0.002427	Mar. 9, 2014
Px_f	0.521768	0.01491	0.065099	0.001164	0.05813	0.001296	Mar. 9, 2014
Px_g	0.59484	0.022491	0.070587	0.001339	0.06112	0.001999	Mar. 9, 2014
Px_h	0.533857	0.025417	0.065861	0.001466	0.05879	0.002474	Mar. 9, 2014
Px_i	0.539402	0.014995	0.064444	0.001044	0.06071	0.001371	Mar. 9, 2014
Px_j	0.520757	0.017014	0.062061	0.001275	0.06086	0.001546	Mar. 9, 2014
Px_k	0.532748	0.012821	0.06502	0.000985	0.05943	0.001111	Mar. 9, 2014
Px_l	0.555138	0.014451	0.066878	0.001177	0.0602	0.001155	Mar. 9, 2014
Px_m	0.574613	0.01325	0.068036	0.001009	0.06125	0.001082	Mar. 9, 2014
Px_n	0.544509	0.012416	0.066545	0.000901	0.05935	0.001089	Mar. 9, 2014
Px_o	0.520816	0.012001	0.066213	0.000981	0.05705	0.001006	Mar. 9, 2014
Px_p	0.532481	0.011561	0.065045	0.000942	0.05937	0.000961	Mar. 9, 2014
Px_q	0.528603	0.011966	0.065828	0.000958	0.05824	0.00101	Mar. 9, 2014
Px_r	0.54009	0.012428	0.065753	0.000996	0.05957	0.001032	Mar. 9, 2014

Px_s	0.52539	0.011329	0.065686	0.000964	0.05801	0.000916	Mar. 9, 2014
Px_t	0.545242	0.011921	0.068427	0.00099	0.05779	0.000947	Mar. 9, 2014
Px_u	0.538366	0.012186	0.064163	0.000963	0.06085	0.001031	Mar. 9, 2014
Px_v	0.519277	0.011641	0.064372	0.000975	0.05851	0.000967	Mar. 9, 2014
Px_w	0.539094	0.012016	0.065319	0.001016	0.05986	0.000956	Mar. 9, 2014
Px_x	0.529736	0.011069	0.064306	0.000875	0.05975	0.000947	Mar. 9, 2014
Px_y	0.565186	0.01557	0.063033	0.001137	0.06503	0.001354	Mar. 9, 2014
Px_z	0.53443	0.01235	0.064085	0.001037	0.06048	0.000998	Mar. 9, 2014
Px_aa	0.529501	0.011295	0.063496	0.000963	0.06048	0.000907	Mar. 9, 2014
Px_ab	0.518936	0.011239	0.065219	0.000962	0.05771	0.000915	Mar. 9, 2014
Px_ac	0.534532	0.011361	0.065615	0.000948	0.05908	0.000921	Mar. 9, 2014
Px_ad	0.565469	0.014782	0.064883	0.001182	0.06321	0.001185	Mar. 9, 2014
Px_ae	0.552529	0.01314	0.066474	0.001098	0.06028	0.001031	Mar. 9, 2014
Px_af	0.521963	0.011518	0.063619	0.000905	0.0595	0.001003	Mar. 9, 2014
Px_ag	0.53889	0.013533	0.063433	0.001075	0.06161	0.001142	Mar. 9, 2014
Px_ah	0.521934	0.01348	0.061277	0.001016	0.06178	0.001224	Mar. 9, 2014
Px_ai	0.518378	0.012772	0.062582	0.000997	0.06008	0.001129	Mar. 9, 2014
Px_aj	0.530594	0.013575	0.063645	0.001084	0.06046	0.001155	Mar. 9, 2014
Px_ak	0.5419	0.013492	0.062971	0.001156	0.06241	0.001049	Mar. 9, 2014
Px_al	0.545893	0.01355	0.063551	0.001	0.0623	0.001196	Mar. 9, 2014
Px_am	0.534316	0.012932	0.06466	0.001077	0.05993	0.001052	Mar. 9, 2014
Px_an	0.522094	0.012495	0.063254	0.000997	0.05986	0.001078	Mar. 9, 2014
Px_ao	0.539084	0.013211	0.064315	0.00106	0.06079	0.001103	Mar. 9, 2014
Px_ap	0.538855	0.013074	0.064353	0.001032	0.06073	0.001106	Mar. 9, 2014
Px_aq	0.534041	0.016549	0.064071	0.001409	0.06045	0.00132	Mar. 9, 2014
Px_ar	0.511901	0.013204	0.061537	0.001083	0.06033	0.001137	Mar. 9, 2014
Px_a	0.539162	0.011204	0.066355	0.001116	0.05893	0.000719	Mar. 12, 2014
Px_b	0.556519	0.010284	0.06881	0.000995	0.05866	0.000675	Mar. 12, 2014
Px_c	0.535988	0.009098	0.068381	0.000845	0.05685	0.000662	Mar. 12, 2014
Px_d	0.550498	0.009185	0.067998	0.00085	0.05872	0.000649	Mar. 12, 2014
Px_e	0.577055	0.011592	0.070349	0.001058	0.05949	0.000792	Mar. 12, 2014
Px_f	0.527154	0.008886	0.065986	0.000832	0.05794	0.000648	Mar. 12, 2014
Px_g	0.5256	0.009234	0.06451	0.00089	0.05909	0.000643	Mar. 12, 2014
Px_h	0.576434	0.012352	0.069963	0.00099	0.05976	0.000962	Mar. 12, 2014
Px_i	0.566664	0.014006	0.068368	0.001189	0.06011	0.001056	Mar. 12, 2014
Px_j	0.513495	0.011265	0.065431	0.001079	0.05692	0.000823	Mar. 12, 2014
Px_k	0.510089	0.010793	0.065761	0.000892	0.05626	0.000913	Mar. 12, 2014
Px_l	0.548756	0.012128	0.066553	0.00103	0.0598	0.000944	Mar. 12, 2014
Px_m	0.520777	0.011925	0.065888	0.001033	0.05733	0.000957	Mar. 12, 2014
Px_n	0.526896	0.011298	0.065418	0.000992	0.05842	0.000886	Mar. 12, 2014
Px_o	0.533672	0.010502	0.06492	0.000886	0.05962	0.000846	Mar. 12, 2014

Px_p	0.534219	0.011139	0.066553	0.001002	0.05822	0.00084	Mar. 12, 2014
Px_q	0.514988	0.010965	0.06517	0.001008	0.05731	0.000839	Mar. 12, 2014
Px_r	0.544007	0.011002	0.068424	0.00089	0.05766	0.000893	Mar. 12, 2014
Px_s	0.50552	0.009427	0.06306	0.000813	0.05814	0.000784	Mar. 12, 2014
Px_t	0.559938	0.011438	0.066773	0.000973	0.06082	0.00087	Mar. 12, 2014
Px_u	0.53025	0.011421	0.065014	0.000997	0.05915	0.000894	Mar. 12, 2014
Px_v	0.538865	0.011916	0.067029	0.001062	0.05831	0.0009	Mar. 12, 2014
Px_w	0.519895	0.012888	0.063524	0.001066	0.05936	0.001083	Mar. 12, 2014
Px_x	0.539186	0.013812	0.065122	0.001042	0.06005	0.001201	Mar. 12, 2014
Px_y	0.556192	0.014425	0.067608	0.001079	0.05967	0.00122	Mar. 12, 2014
Px_a	0.636502	0.011898	0.078824	0.001086	0.05857	0.00074	Mar. 17, 2014
Px_b	0.597142	0.011746	0.073385	0.00107	0.05902	0.000779	Mar. 17, 2014
Px_c	0.617994	0.011416	0.075386	0.001014	0.05946	0.000752	Mar. 17, 2014
Px_d	0.641942	0.012379	0.076921	0.001075	0.06053	0.000804	Mar. 17, 2014
Px_e	0.623009	0.014012	0.076435	0.001235	0.05912	0.000925	Mar. 17, 2014
Px_f	0.619101	0.013546	0.077833	0.001214	0.05769	0.000885	Mar. 17, 2014
Px_g	0.610557	0.013139	0.075335	0.001064	0.05878	0.000954	Mar. 17, 2014
Px_h	0.63181	0.015575	0.075309	0.001249	0.06085	0.00111	Mar. 17, 2014
Px_a	0.630392	0.012918	0.076362	0.000968	0.05987	0.000964	Mar. 31, 2014
Px_b	0.654755	0.013605	0.079101	0.000954	0.06003	0.001016	Mar. 31, 2014
Px_c	0.675609	0.01424	0.082068	0.000971	0.05971	0.001042	Mar. 31, 2014
Px_d	0.649989	0.012298	0.081127	0.000899	0.05811	0.000891	Mar. 31, 2014
Px_e	0.639785	0.012093	0.077306	0.000947	0.06002	0.000864	Mar. 31, 2014
Px_f	0.653154	0.011274	0.079091	0.000857	0.05989	0.000805	Mar. 31, 2014
Px_g	0.622114	0.010821	0.07746	0.000861	0.05825	0.000779	Mar. 31, 2014
Px_h	0.613461	0.011348	0.074959	0.000904	0.05936	0.000833	Mar. 31, 2014
Px_i	0.65474	0.013642	0.08159	0.001042	0.0582	0.000958	Mar. 31, 2014
Px_j	0.638893	0.012789	0.077992	0.00106	0.05941	0.000873	Mar. 31, 2014
Px_k	0.623054	0.013049	0.078565	0.001005	0.05752	0.000954	Mar. 31, 2014
Px_l	0.668434	0.013462	0.078682	0.000943	0.06161	0.000997	Mar. 31, 2014
Px_m	0.624677	0.011435	0.077453	0.000891	0.05849	0.000833	Mar. 31, 2014
Px_n	0.664885	0.013305	0.082004	0.000963	0.0588	0.000953	Mar. 31, 2014
Px_o	0.629466	0.012243	0.077278	0.000892	0.05908	0.000925	Mar. 31, 2014
Px_p	0.640743	0.014355	0.080966	0.001127	0.0574	0.001008	Mar. 31, 2014
Px_q	0.595279	0.010242	0.072531	0.00092	0.05952	0.000692	Mar. 31, 2014
Px_r	0.61182	0.009556	0.075791	0.000873	0.05855	0.000617	Mar. 31, 2014
Px_s	0.595003	0.008918	0.073625	0.000783	0.05861	0.000619	Mar. 31, 2014
Px_t	0.609516	0.009062	0.075388	0.000814	0.05864	0.000599	Mar. 31, 2014
Px_a	0.588747	0.01698	0.073159	0.001474	0.05837	0.001204	Apr. 1, 2014
Px_b	0.624971	0.014473	0.07595	0.001146	0.05968	0.001048	Apr. 1, 2014
Px_e	0.596651	0.014953	0.07326	0.001047	0.05907	0.001216	Apr. 1, 2014

Px_f	0.592618	0.012544	0.073486	0.000986	0.05849	0.000957	Apr. 1, 2014
Px_g	0.554409	0.01062	0.069403	0.00101	0.05794	0.000722	Apr. 1, 2014
Px_h	0.6178	0.010429	0.073743	0.000846	0.06076	0.000753	Apr. 1, 2014
Px_i	0.606156	0.00926	0.075156	0.000765	0.0585	0.000666	Apr. 1, 2014
Px_j	0.598872	0.009187	0.07378	0.000763	0.05887	0.000667	Apr. 1, 2014
Px_k	0.580898	0.009901	0.073088	0.000781	0.05764	0.000765	Apr. 1, 2014
Px_l	0.584406	0.009231	0.072542	0.000772	0.05843	0.000682	Apr. 1, 2014
Px_m	0.574244	0.009014	0.071861	0.000752	0.05796	0.000678	Apr. 1, 2014
Px_n	0.599008	0.009219	0.074654	0.000757	0.05819	0.000673	Apr. 1, 2014
Px_o	0.620135	0.009171	0.075994	0.000768	0.05918	0.000639	Apr. 1, 2014
Px_p	0.586889	0.009737	0.073294	0.000772	0.05807	0.000744	Apr. 1, 2014
Px_q	0.609964	0.009423	0.073256	0.000736	0.06039	0.000709	Apr. 1, 2014
Px_r	0.605394	0.009755	0.074158	0.000831	0.05921	0.000686	Apr. 1, 2014
Px_s	0.593467	0.009025	0.073126	0.000778	0.05886	0.000639	Apr. 1, 2014
Px_t	0.606776	0.008995	0.074264	0.000731	0.05926	0.000657	Apr. 1, 2014
Px_u	0.607682	0.009458	0.07546	0.000793	0.05841	0.000671	Apr. 1, 2014
Px_v	0.596986	0.008855	0.073898	0.000697	0.05859	0.000671	Apr. 1, 2014
Px_w	0.584269	0.008751	0.075376	0.000728	0.05622	0.000644	Apr. 1, 2014
Px_x	0.619789	0.009367	0.074991	0.000686	0.05994	0.000721	Apr. 1, 2014
Px_y	0.590489	0.008722	0.072473	0.000704	0.05909	0.000657	Apr. 1, 2014
Px_z	0.616447	0.008999	0.07379	0.000692	0.06059	0.000678	Apr. 1, 2014
Px_aa	0.608455	0.008727	0.076103	0.000674	0.05799	0.000654	Apr. 1, 2014
Px_ab	0.625417	0.009084	0.076036	0.000762	0.05966	0.000627	Apr. 1, 2014
Px_ac	0.60064	0.009563	0.075813	0.00081	0.05746	0.000678	Apr. 1, 2014
Px_ad	0.626606	0.009833	0.077636	0.00078	0.05854	0.000706	Apr. 1, 2014
Px_ae	0.621653	0.009812	0.076767	0.00073	0.05873	0.00074	Apr. 1, 2014
Px_af	0.609819	0.008967	0.074931	0.000704	0.05903	0.000668	Apr. 1, 2014
Px_ag	0.622119	0.009841	0.074993	0.000863	0.06017	0.000653	Apr. 1, 2014
Px_ah	0.590917	0.009231	0.07275	0.00079	0.05891	0.000661	Apr. 1, 2014
Px_ai	0.586689	0.009928	0.072582	0.000764	0.05862	0.000777	Apr. 1, 2014
Px_aj	0.59675	0.00901	0.074659	0.000771	0.05797	0.000639	Apr. 1, 2014
Px_ak	0.601695	0.008586	0.074941	0.000693	0.05823	0.000633	Apr. 1, 2014
Px_al	0.575001	0.009696	0.070232	0.000792	0.05938	0.000744	Apr. 1, 2014
Px_am	0.596793	0.00904	0.072699	0.000798	0.05954	0.000621	Apr. 1, 2014
Px_an	0.60937	0.009757	0.07481	0.000857	0.05908	0.000661	Apr. 1, 2014
Px_ao	0.612217	0.009263	0.075388	0.000803	0.0589	0.000633	Apr. 1, 2014
Px_ap	0.601333	0.008698	0.073352	0.000776	0.05946	0.000587	Apr. 1, 2014
Px_a	0.641329	0.016422	0.078304	0.001317	0.0594	0.001147	Apr. 14, 2014
Px_b	0.578141	0.013771	0.073092	0.001146	0.05737	0.001028	Apr. 14, 2014
Px_c	0.564842	0.015934	0.069689	0.001239	0.05878	0.001288	Apr. 14, 2014
Px_d	0.561757	0.015434	0.074069	0.001273	0.05501	0.001179	Apr. 14, 2014

Px_e	0.588901	0.01894	0.072297	0.001456	0.05908	0.001481	Apr. 14, 2014
Px_f	0.582384	0.015947	0.071396	0.001253	0.05916	0.001244	Apr. 14, 2014
Px_g	0.574763	0.016738	0.073293	0.001391	0.05688	0.001256	Apr. 14, 2014
Px_h	0.584781	0.01553	0.073892	0.001351	0.0574	0.001106	Apr. 14, 2014
Px_i	0.583613	0.017067	0.07242	0.001337	0.05845	0.001326	Apr. 14, 2014
Px_j	0.548327	0.016071	0.072197	0.00134	0.05508	0.00125	Apr. 14, 2014
Px_k	0.543926	0.019943	0.067626	0.001641	0.05833	0.001603	Apr. 14, 2014
Px_l	0.598863	0.019791	0.072542	0.001423	0.05987	0.001592	Apr. 14, 2014
Px_a	0.651401	0.014016	0.080148	0.00103	0.05895	0.001017	Apr. 15, 2014
Px_b	0.656206	0.013672	0.082198	0.000998	0.0579	0.00098	Apr. 15, 2014
Px_c	0.705764	0.012053	0.082979	0.00093	0.06169	0.000795	Apr. 15, 2014
Px_d	0.656032	0.012151	0.084259	0.00104	0.05647	0.00078	Apr. 15, 2014
Px_e	0.645454	0.012463	0.079478	0.000958	0.0589	0.000888	Apr. 15, 2014
Px_f	0.627091	0.011487	0.078584	0.000896	0.05788	0.00083	Apr. 15, 2014
Px_g	0.64662	0.012324	0.080846	0.000915	0.05801	0.000889	Apr. 15, 2014
Px_h	0.638786	0.012587	0.079172	0.000892	0.05852	0.000946	Apr. 15, 2014
Px_i	0.626628	0.012709	0.079159	0.000957	0.05741	0.000935	Apr. 15, 2014
Px_j	0.652344	0.012419	0.079558	0.000871	0.05947	0.000926	Apr. 15, 2014
Px_k	0.620697	0.013036	0.078342	0.001047	0.05746	0.000931	Apr. 15, 2014
Px_l	0.662715	0.013284	0.079838	0.001018	0.0602	0.000931	Apr. 15, 2014
Px_m	0.620332	0.01213	0.075619	0.000847	0.0595	0.000954	Apr. 15, 2014
Px_n	0.622713	0.012843	0.076395	0.000948	0.05912	0.000974	Apr. 15, 2014
Px_o	0.594551	0.014421	0.075484	0.001104	0.05713	0.001106	Apr. 15, 2014
Px_p	0.586848	0.013708	0.075488	0.001044	0.05638	0.001061	Apr. 15, 2014
Px_q	0.595075	0.013575	0.075482	0.00115	0.05718	0.000971	Apr. 15, 2014
Px_r	0.608182	0.011725	0.077141	0.000913	0.05718	0.00087	Apr. 15, 2014
Px_s	0.603939	0.012551	0.077232	0.001032	0.05671	0.000903	Apr. 15, 2014
Px_t	0.609959	0.012019	0.076732	0.000927	0.05765	0.000898	Apr. 15, 2014
Px_u	0.658513	0.014352	0.07732	0.001064	0.06177	0.001044	Apr. 15, 2014
Px_v	0.651764	0.014642	0.076517	0.001101	0.06178	0.001066	Apr. 15, 2014
Px_w	0.617661	0.013798	0.075055	0.001028	0.05969	0.001053	Apr. 15, 2014
Px_x	0.632897	0.012916	0.075982	0.000884	0.06041	0.001013	Apr. 15, 2014
Px_y	0.6242	0.011949	0.077116	0.000975	0.05871	0.000844	Apr. 15, 2014
Px_z	0.614651	0.012719	0.076182	0.000931	0.05852	0.000977	Apr. 15, 2014
Px_aa	0.617359	0.011737	0.075142	0.000923	0.05959	0.000865	Apr. 15, 2014
Px_ab	0.638677	0.011967	0.075894	0.000844	0.06103	0.000921	Apr. 15, 2014
Px_ac	0.639772	0.013748	0.077346	0.001001	0.05999	0.001029	Apr. 15, 2014
Px_ad	0.626633	0.014518	0.075925	0.001016	0.05986	0.001132	Apr. 15, 2014
Px_ae	0.61028	0.013672	0.075976	0.001083	0.05826	0.001007	Apr. 15, 2014
Px_af	0.611556	0.012048	0.075141	0.00096	0.05903	0.000885	Apr. 15, 2014
Px_a	0.640491	0.018339	0.079602	0.001198	0.05836	0.001421	Apr. 21, 2014

Px_b	0.663044	0.019832	0.080886	0.001301	0.05945	0.001499	Apr. 21, 2014
Px_c	0.651995	0.01874	0.081351	0.001289	0.05813	0.001394	Apr. 21, 2014
Px_d	0.67573	0.018183	0.081717	0.001196	0.05997	0.001354	Apr. 21, 2014
Px_e	0.666776	0.020862	0.078752	0.001464	0.06141	0.001545	Apr. 21, 2014
Px_f	0.626858	0.019732	0.078164	0.001478	0.05817	0.001464	Apr. 21, 2014
Px_g	0.61309	0.018078	0.075131	0.00133	0.05918	0.001396	Apr. 21, 2014
Px_h	0.637075	0.019426	0.077543	0.001342	0.05959	0.001496	Apr. 21, 2014
Px_i	0.677744	0.018839	0.079903	0.001245	0.06152	0.001416	Apr. 21, 2014
Px_j	0.645097	0.017442	0.080466	0.001174	0.05814	0.001323	Apr. 21, 2014
Px_k	0.635668	0.018677	0.078239	0.001332	0.05893	0.001411	Apr. 21, 2014
Px_l	0.682598	0.019581	0.078335	0.00127	0.0632	0.001496	Apr. 21, 2014
Px_m	0.616867	0.018208	0.074953	0.001187	0.05969	0.001487	Apr. 21, 2014
Px_n	0.650317	0.020003	0.078533	0.00137	0.06006	0.001522	Apr. 21, 2014
Px_o	0.647274	0.020275	0.080675	0.001187	0.05819	0.001609	Apr. 21, 2014
Px_p	0.612256	0.019379	0.079317	0.001469	0.05598	0.001437	Apr. 21, 2014
Px_f	0.632498	0.012333	0.078832	0.001008	0.05819	0.000856	Apr. 25, 2014
Px_g	0.620004	0.011931	0.076954	0.000997	0.05843	0.000832	Apr. 25, 2014
Px_h	0.605191	0.01127	0.075119	0.000979	0.05843	0.000777	Apr. 25, 2014
Px_i	0.607077	0.011367	0.077598	0.001007	0.05674	0.000766	Apr. 25, 2014
Px_j	0.582805	0.010315	0.070732	0.000944	0.05976	0.000694	Apr. 25, 2014
Px_k	0.551976	0.010793	0.0701	0.000979	0.05711	0.000782	Apr. 25, 2014
Px_l	0.578859	0.010248	0.071442	0.000861	0.05877	0.000762	Apr. 25, 2014
Px_m	0.57429	0.011164	0.070642	0.000959	0.05896	0.00082	Apr. 25, 2014
Px_n	0.557633	0.010733	0.072196	0.000916	0.05602	0.000811	Apr. 25, 2014
Px_o	0.578229	0.011141	0.070691	0.000901	0.05932	0.000857	Apr. 25, 2014
Px_p	0.554951	0.010959	0.068951	0.000922	0.05837	0.000848	Apr. 25, 2014
Px_q	0.557936	0.010889	0.07006	0.000975	0.05776	0.00079	Apr. 25, 2014
Px_a	0.666143	0.010357	0.085193	0.000933	0.05671	0.000626	Apr. 28, 2014
Px_b	0.666794	0.010938	0.083032	0.000994	0.05824	0.000653	Apr. 28, 2014
Px_c	0.690623	0.010027	0.083835	0.000858	0.05975	0.000615	Apr. 28, 2014
Px_d	0.684145	0.010737	0.084317	0.001002	0.05885	0.000603	Apr. 28, 2014
Px_e	0.652182	0.010539	0.081383	0.000957	0.05812	0.000644	Apr. 28, 2014
Px_f	0.633629	0.009627	0.080105	0.000798	0.05737	0.000658	Apr. 28, 2014
Px_g	0.641606	0.010244	0.079691	0.000936	0.05839	0.000632	Apr. 28, 2014
Px_h	0.657018	0.010564	0.080887	0.000965	0.05891	0.000635	Apr. 28, 2014
Px_i	0.620213	0.009865	0.077522	0.000856	0.05802	0.000664	Apr. 28, 2014
Px_j	0.60672	0.009575	0.076439	0.000881	0.05757	0.00062	Apr. 28, 2014
Px_k	0.631964	0.010263	0.077267	0.000883	0.05932	0.000685	Apr. 28, 2014
Px_l	0.606197	0.009862	0.076299	0.000872	0.05762	0.000667	Apr. 28, 2014
Px_m	0.593978	0.009419	0.074063	0.000881	0.05817	0.00061	Apr. 28, 2014
Px_n	0.596291	0.009776	0.074257	0.000903	0.05824	0.00064	Apr. 28, 2014

Px_o	0.587852	0.009544	0.073681	0.000894	0.05786	0.000624	Apr. 28, 2014
Px_p	0.588561	0.009218	0.074284	0.000774	0.05746	0.000672	Apr. 28, 2014
Px_q	0.592265	0.010049	0.074387	0.000847	0.05775	0.000726	Apr. 28, 2014
Px_r	0.572173	0.009751	0.071243	0.00087	0.05825	0.000692	Apr. 28, 2014
Px_s	0.573905	0.009568	0.071381	0.000832	0.05831	0.000695	Apr. 28, 2014
Px_t	0.558574	0.009	0.070898	0.000859	0.05714	0.000607	Apr. 28, 2014
Px_a	0.557877	0.011601	0.070112	0.001035	0.05771	0.000845	Apr. 29, 2014
Px_b	0.580062	0.010529	0.070349	0.000824	0.0598	0.000829	Apr. 29, 2014
Px_c	0.552834	0.01033	0.071124	0.000824	0.05637	0.000827	Apr. 29, 2014
Px_d	0.560041	0.009749	0.071752	0.000831	0.05661	0.000736	Apr. 29, 2014
Px_e	0.537541	0.010786	0.064447	0.000762	0.06049	0.000981	Apr. 29, 2014
Px_f	0.501081	0.008941	0.063151	0.000805	0.05755	0.000719	Apr. 29, 2014
Px_g	0.546431	0.010249	0.0651	0.000838	0.06088	0.00083	Apr. 29, 2014
Px_h	0.532182	0.010343	0.065613	0.000841	0.05883	0.000859	Apr. 29, 2014
Px_i	0.516336	0.009758	0.065378	0.00077	0.05728	0.000846	Apr. 29, 2014
Px_j	0.534121	0.010349	0.067099	0.000856	0.05773	0.000842	Apr. 29, 2014
Px_k	0.51463	0.013147	0.062507	0.001029	0.05971	0.001167	Apr. 29, 2014
Px_l	0.515161	0.014274	0.065729	0.001289	0.05684	0.001113	Apr. 29, 2014
Px_m	0.514194	0.012125	0.062608	0.000967	0.05957	0.001061	Apr. 29, 2014
Px_n	0.521642	0.011766	0.064375	0.00084	0.05877	0.001082	Apr. 29, 2014
Px_o	0.514669	0.010981	0.065863	0.000935	0.05667	0.000902	Apr. 29, 2014
Px_p	0.534341	0.012672	0.065013	0.000985	0.05961	0.001088	Apr. 29, 2014
Px_q	0.502685	0.012338	0.062908	0.000866	0.05795	0.001178	Apr. 29, 2014
Px_r	0.502267	0.012347	0.0637	0.000919	0.05719	0.001138	Apr. 29, 2014
Px_s	0.528983	0.012808	0.064078	0.000988	0.05987	0.001118	Apr. 29, 2014
Px_t	0.509115	0.012077	0.063914	0.001	0.05777	0.00103	Apr. 29, 2014
Px_u	0.505705	0.012372	0.061536	0.000886	0.0596	0.001179	Apr. 29, 2014
Px_v	0.514087	0.013275	0.063758	0.000987	0.05848	0.001209	Apr. 29, 2014
Px_w	0.517759	0.012654	0.062607	0.000883	0.05998	0.001198	Apr. 29, 2014
Px_x	0.494318	0.011789	0.061208	0.000893	0.05857	0.001105	Apr. 29, 2014
Px_a	0.789581	0.015127	0.092658	0.001126	0.0618	0.000915	May. 6, 2014
Px_b	0.738128	0.016028	0.091646	0.001394	0.05841	0.000905	May. 6, 2014
Px_c	0.736254	0.014247	0.092254	0.00129	0.05788	0.000774	May. 6, 2014
Px_d	0.757593	0.013632	0.091636	0.001185	0.05996	0.00075	May. 6, 2014
Px_e	0.693093	0.015641	0.087526	0.001378	0.05743	0.000929	May. 6, 2014
Px_f	0.684921	0.016041	0.085469	0.001398	0.05812	0.000974	May. 6, 2014
Px_g	0.73603	0.016396	0.08582	0.001227	0.0622	0.001062	May. 6, 2014
Px_h	0.690401	0.015772	0.085617	0.001397	0.05848	0.000935	May. 6, 2014
Px_i	0.677036	0.014938	0.083029	0.001249	0.05914	0.000955	May. 6, 2014
Px_j	0.680324	0.015626	0.082674	0.00132	0.05968	0.000986	May. 6, 2014
Px_k	0.647537	0.014391	0.080768	0.001217	0.05815	0.00095	May. 6, 2014

Px_l	0.64025	0.014359	0.081144	0.001315	0.05723	0.000887	May. 6, 2014
Px_m	0.614762	0.015294	0.080208	0.001432	0.05559	0.000963	May. 6, 2014
Px_n	0.642218	0.013435	0.080234	0.001206	0.05805	0.000845	May. 6, 2014
Px_o	0.638149	0.01469	0.078892	0.001191	0.05867	0.00102	May. 6, 2014
Px_p	0.627202	0.014057	0.078538	0.00127	0.05792	0.000899	May. 6, 2014
Px_q	0.64278	0.014466	0.0793	0.001295	0.05879	0.00091	May. 6, 2014
Px_r	0.633048	0.014523	0.077184	0.001311	0.05948	0.000918	May. 6, 2014
Px_s	0.638336	0.016002	0.079144	0.001382	0.0585	0.001052	May. 6, 2014
Px_t	0.63647	0.014291	0.080482	0.001396	0.05736	0.000818	May. 6, 2014
Px_a	0.865036	0.017478	0.107612	0.001573	0.0583	0.000813	May. 7, 2014
Px_b	0.845068	0.016381	0.107338	0.001379	0.0571	0.000829	May. 7, 2014
Px_c	0.841793	0.016194	0.106455	0.001405	0.05735	0.000803	May. 7, 2014
Px_d	0.86215	0.01667	0.106192	0.001449	0.05888	0.000807	May. 7, 2014
Px_e	0.812555	0.017333	0.099202	0.001461	0.05941	0.000917	May. 7, 2014
Px_f	0.911822	0.019594	0.108202	0.001487	0.06112	0.00101	May. 7, 2014
Px_g	0.841445	0.017638	0.103371	0.001417	0.05904	0.000936	May. 7, 2014
Px_h	0.841987	0.017779	0.103154	0.001367	0.0592	0.000973	May. 7, 2014
Px_i	0.807996	0.016356	0.099579	0.001268	0.05885	0.000926	May. 7, 2014
Px_j	0.838651	0.016914	0.102905	0.001337	0.05911	0.000912	May. 7, 2014
Px_k	0.803922	0.015996	0.100635	0.001468	0.05794	0.000784	May. 7, 2014
Px_l	0.797111	0.015894	0.09847	0.001346	0.05871	0.000852	May. 7, 2014
Px_m	0.830142	0.016585	0.098143	0.001317	0.06135	0.000908	May. 7, 2014
Px_n	0.850547	0.017125	0.10272	0.001444	0.06005	0.000866	May. 7, 2014
Px_o	0.851296	0.017616	0.102672	0.001449	0.06013	0.00091	May. 7, 2014
Px_p	0.809736	0.016528	0.101062	0.001311	0.05811	0.000916	May. 7, 2014
Px_q	0.834476	0.017527	0.099967	0.001385	0.06054	0.000956	May. 7, 2014
Px_r	0.798434	0.016699	0.097216	0.001373	0.05957	0.000919	May. 7, 2014
Px_s	0.80358	0.016183	0.102273	0.001377	0.05699	0.000853	May. 7, 2014
Px_t	0.779436	0.012101	0.0976	0.001218	0.05792	0.000535	May. 7, 2014
Px_a	0.589297	0.011568	0.072749	0.001095	0.05875	0.00074	May. 12, 2014
Px_b	0.617197	0.011381	0.07412	0.001054	0.06039	0.000709	May. 12, 2014
Px_c	0.612627	0.011538	0.074861	0.001065	0.05935	0.000732	May. 12, 2014
Px_d	0.630908	0.014625	0.076699	0.001234	0.05966	0.000995	May. 12, 2014
Px_e	0.554303	0.012647	0.07026	0.001108	0.05722	0.000943	May. 12, 2014
Px_f	0.579393	0.013484	0.070441	0.001135	0.05965	0.001002	May. 12, 2014
Px_g	0.613626	0.014435	0.075523	0.001033	0.05893	0.001128	May. 12, 2014
Px_h	0.560201	0.013325	0.068425	0.001146	0.05938	0.001003	May. 12, 2014
Px_i	0.535872	0.014158	0.066101	0.001307	0.0588	0.00103	May. 12, 2014
Px_j	0.658649	0.028801	0.083308	0.001876	0.05734	0.002149	May. 12, 2014
Px_k	0.558771	0.013747	0.070624	0.00112	0.05738	0.001079	May. 12, 2014
Px_l	0.564531	0.014065	0.069149	0.001219	0.05921	0.001043	May. 12, 2014

Px_m	0.692326	0.015243	0.082971	0.001304	0.06052	0.000933	May. 12, 2014
Px_n	0.696739	0.014711	0.087906	0.001332	0.05748	0.000846	May. 12, 2014
Px_o	0.731147	0.016541	0.089243	0.001297	0.05942	0.00103	May. 12, 2014
Px_p	0.712877	0.014733	0.087894	0.00128	0.05882	0.000863	May. 12, 2014
Px_q	0.724479	0.01528	0.088691	0.00127	0.05924	0.000917	May. 12, 2014
Px_r	0.719655	0.016955	0.086693	0.001399	0.06021	0.001034	May. 12, 2014
Px_s	0.67412	0.014392	0.0873	0.001204	0.056	0.000913	May. 12, 2014
Px_t	0.707207	0.014845	0.085465	0.001177	0.06001	0.000951	May. 12, 2014
Px_u	0.688613	0.015693	0.086339	0.001244	0.05785	0.001022	May. 12, 2014
Px_v	0.730086	0.017581	0.088589	0.001456	0.05977	0.001052	May. 12, 2014
Px_w	0.683651	0.01443	0.085037	0.001191	0.05831	0.000921	May. 12, 2014
Px_a	0.592353	0.018087	0.070119	0.001337	0.06127	0.001461	May. 13, 2014
Px_b	0.595042	0.019867	0.068333	0.00147	0.06316	0.001613	May. 13, 2014
Px_c	0.581551	0.021472	0.069989	0.001535	0.06026	0.00179	May. 13, 2014
Px_d	0.589598	0.020134	0.069267	0.00157	0.06173	0.001577	May. 13, 2014
Px_e	0.572124	0.021164	0.068003	0.001618	0.06102	0.001728	May. 13, 2014
Px_f	0.594256	0.021295	0.069303	0.001551	0.06219	0.001741	May. 13, 2014
Px_g	0.567699	0.020243	0.068435	0.001679	0.06016	0.001557	May. 13, 2014
Px_h	0.594836	0.019858	0.068957	0.001437	0.06256	0.001632	May. 13, 2014
Px_i	0.598025	0.019902	0.069282	0.001412	0.0626	0.001647	May. 13, 2014
Px_j	0.565182	0.018323	0.067507	0.001434	0.06072	0.001487	May. 13, 2014
Px_k	0.581772	0.019583	0.068334	0.001558	0.06175	0.001529	May. 13, 2014
Px_l	0.557075	0.020273	0.069855	0.00194	0.05784	0.00136	May. 13, 2014
Px_a	0.75723	0.019459	0.094333	0.001887	0.05822	0.000939	Sep. 19, 2014
Px_b	0.747903	0.020966	0.09438	0.002068	0.05747	0.001005	Sep. 19, 2014
Px_c	0.766994	0.016846	0.096235	0.001614	0.0578	0.00082	Sep. 19, 2014
Px_d	0.746301	0.020286	0.094613	0.002038	0.05721	0.000948	Sep. 19, 2014
Px_e	0.697976	0.015907	0.090235	0.001494	0.0561	0.000879	Sep. 19, 2014
Px_f	0.711532	0.019211	0.090348	0.00163	0.05712	0.001147	Sep. 19, 2014
Px_g	0.724852	0.02252	0.089235	0.002043	0.05891	0.001238	Sep. 19, 2014
Px_h	0.738196	0.017108	0.089247	0.001379	0.05999	0.001036	Sep. 19, 2014
Px_i	0.742038	0.016189	0.089368	0.001203	0.06022	0.001034	Sep. 19, 2014
Px_j	0.717239	0.015811	0.089175	0.001325	0.05833	0.00095	Sep. 19, 2014
Px_k	0.693215	0.016619	0.088792	0.001382	0.05662	0.001033	Sep. 19, 2014
Px_l	0.717568	0.018345	0.089211	0.001405	0.05834	0.001175	Sep. 19, 2014
Px_m	0.73945	0.017583	0.090689	0.00133	0.05914	0.001107	Sep. 19, 2014
Px_o	0.752183	0.019091	0.090375	0.00153	0.06036	0.001141	Sep. 19, 2014
Px_n	0.712599	0.016911	0.087057	0.001307	0.05937	0.001091	Sep. 19, 2014
Px_p	0.722869	0.015446	0.086302	0.001202	0.06075	0.000984	Sep. 19, 2014
Px_q	0.704544	0.014895	0.087872	0.001211	0.05815	0.000932	Sep. 19, 2014
Px_r	0.665837	0.014126	0.084548	0.00115	0.05712	0.00093	Sep. 19, 2014

Px_s	0.670865	0.01355	0.085732	0.001107	0.05675	0.000881	Sep. 19, 2014
Px_t	0.68538	0.015097	0.083311	0.001239	0.05967	0.00097	Sep. 19, 2014
Px_u	0.708999	0.01524	0.085579	0.001109	0.06009	0.00103	Sep. 19, 2014
Px_a	0.540066	0.012466	0.065815	0.001024	0.05951	0.001014	Oct. 20, 2014
Px_b	0.570251	0.014029	0.069278	0.001044	0.0597	0.001161	Oct. 20, 2014
Px_c	0.580493	0.014019	0.071258	0.001072	0.05908	0.001116	Oct. 20, 2014
Px_d	0.575843	0.011979	0.072623	0.001009	0.05751	0.00089	Oct. 20, 2014
Px_e	0.587938	0.013399	0.072366	0.001023	0.05892	0.001053	Oct. 20, 2014
Px_f	0.601381	0.014577	0.070719	0.001099	0.06168	0.001147	Oct. 20, 2014
Px_g	0.58098	0.015061	0.070978	0.001201	0.05937	0.001166	Oct. 20, 2014
Px_h	0.59484	0.013904	0.071347	0.001169	0.06047	0.001008	Oct. 20, 2014
Px_i	0.555763	0.01383	0.068596	0.001022	0.05876	0.001171	Oct. 20, 2014
Px_j	0.574184	0.014586	0.069987	0.001063	0.0595	0.001212	Oct. 20, 2014
Px_k	0.569199	0.014665	0.068755	0.001132	0.06004	0.00119	Oct. 20, 2014
Px_l	0.564671	0.013499	0.068722	0.001102	0.05959	0.001056	Oct. 20, 2014
Px_m	0.590808	0.015995	0.071114	0.001242	0.06025	0.001246	Oct. 20, 2014
Px_n	0.568381	0.0144	0.069566	0.001096	0.05926	0.001176	Oct. 20, 2014
Px_o	0.572456	0.01452	0.068823	0.001073	0.06033	0.001207	Oct. 20, 2014
Px_p	0.537819	0.013525	0.068548	0.001072	0.0569	0.001121	Oct. 20, 2014
Px_q	0.598606	0.016963	0.071234	0.001193	0.06095	0.001393	Oct. 20, 2014
Px_r	0.59385	0.014645	0.069592	0.001146	0.06189	0.001137	Oct. 20, 2014
Px_s	0.593316	0.015881	0.070794	0.001169	0.06078	0.001281	Oct. 20, 2014
Px_t	0.56488	0.014287	0.068669	0.001191	0.05966	0.001098	Oct. 20, 2014
Px_u	0.550469	0.015243	0.069663	0.001194	0.05731	0.001246	Oct. 20, 2014
Px_x	0.546837	0.014961	0.069112	0.001162	0.05739	0.001238	Oct. 20, 2014
Px_y	0.551156	0.01286	0.069136	0.00109	0.05782	0.000995	Oct. 20, 2014
Px_z	0.555943	0.012401	0.06977	0.001046	0.05779	0.000954	Oct. 20, 2014
Px_1a	0.552804	0.012041	0.069214	0.000962	0.05793	0.000972	Oct. 20, 2014
Px_1b	0.549134	0.012281	0.068302	0.0009	0.05831	0.001054	Oct. 20, 2014
Px_1c	0.574988	0.014413	0.070171	0.001173	0.05943	0.00111	Oct. 20, 2014
Px_1d	0.549936	0.013218	0.068802	0.001035	0.05797	0.001087	Oct. 20, 2014
Px_1e	0.56401	0.012165	0.069547	0.000942	0.05882	0.000987	Oct. 20, 2014
Px_1f	0.517705	0.011519	0.066734	0.001049	0.05626	0.000886	Oct. 20, 2014
Px_a	0.630084	0.015417	0.075675	0.00132	0.06039	0.001037	Oct. 21, 2014
Px_b	0.581937	0.014289	0.075876	0.001222	0.05562	0.001031	Oct. 21, 2014
Px_c	0.592837	0.013628	0.076604	0.001221	0.05613	0.00093	Oct. 21, 2014
Px_d	0.591374	0.013343	0.072075	0.001225	0.05951	0.000883	Oct. 21, 2014
Px_e	0.628279	0.017004	0.075636	0.00139	0.06025	0.001197	Oct. 21, 2014
Px_f	0.610388	0.01499	0.07138	0.001107	0.06202	0.001181	Oct. 21, 2014
Px_g	0.579895	0.013608	0.072158	0.001171	0.05829	0.000988	Oct. 21, 2014
Px_h	0.621482	0.015503	0.076301	0.001178	0.05907	0.001157	Oct. 21, 2014

Px_i	0.626259	0.016125	0.0745	0.001165	0.06097	0.001247	Oct. 21, 2014
Px_j	0.560685	0.013801	0.07099	0.001224	0.05728	0.001007	Oct. 21, 2014
Px_k	0.580317	0.014018	0.073638	0.001096	0.05716	0.001088	Oct. 21, 2014
Px_l	0.591148	0.013439	0.071737	0.001083	0.05977	0.001016	Oct. 21, 2014
Px_a	0.634738	0.011505	0.077994	0.001077	0.05902	0.000693	Oct. 21, 2014
Px_b	0.628024	0.011514	0.078754	0.000996	0.05784	0.000768	Oct. 21, 2014
Px_c	0.655921	0.011874	0.078771	0.000985	0.06039	0.000791	Oct. 21, 2014
Px_d	0.632587	0.011869	0.078334	0.001072	0.05857	0.000752	Oct. 21, 2014
Px_e	0.623336	0.011296	0.075151	0.00098	0.06016	0.000757	Oct. 21, 2014
Px_f	0.610233	0.009171	0.075511	0.000878	0.05861	0.000558	Oct. 21, 2014
Px_g	0.649385	0.019077	0.081872	0.002026	0.05753	0.000911	Oct. 21, 2014
Px_h	0.602132	0.016001	0.07452	0.001532	0.0586	0.000987	Oct. 21, 2014
Px_i	0.622896	0.014533	0.076604	0.001363	0.05897	0.000891	Oct. 21, 2014
Px_j	0.583807	0.014301	0.072444	0.001352	0.05845	0.000927	Oct. 21, 2014
Px_k	0.631726	0.017973	0.079488	0.001909	0.05764	0.000879	Oct. 21, 2014
Px_l	0.574992	0.018576	0.072073	0.002092	0.05786	0.000821	Oct. 21, 2014
Px_a	0.643087	0.013307	0.079683	0.001084	0.05853	0.000913	Oct. 22, 2014
Px_b	0.585971	0.012584	0.076478	0.001129	0.05557	0.000867	Oct. 22, 2014
Px_c	0.633914	0.012721	0.076597	0.001094	0.06002	0.000846	Oct. 22, 2014
Px_d	0.675003	0.013764	0.080903	0.001159	0.06051	0.000878	Oct. 22, 2014
Px_e	0.635275	0.014962	0.07819	0.001362	0.05893	0.000934	Oct. 22, 2014
Px_f	0.607959	0.013315	0.077739	0.00122	0.05672	0.000867	Oct. 22, 2014
Px_g	0.6347	0.014636	0.076439	0.001344	0.06022	0.000899	Oct. 22, 2014
Px_h	0.619683	0.014075	0.077564	0.001194	0.05794	0.000968	Oct. 22, 2014
Px_i	0.608878	0.015166	0.076407	0.001253	0.0578	0.001084	Oct. 22, 2014
Px_j	0.595956	0.013749	0.073985	0.001186	0.05842	0.00097	Oct. 22, 2014
Px_k	0.624707	0.014058	0.077118	0.001337	0.05875	0.000843	Oct. 22, 2014
Px_l	0.61484	0.015952	0.075469	0.001344	0.05909	0.001115	Oct. 22, 2014
Px_m	0.640054	0.01559	0.076973	0.001259	0.06031	0.001088	Oct. 22, 2014
Px_n	0.617317	0.015951	0.075731	0.001371	0.05912	0.00109	Oct. 22, 2014
Px_o	0.621121	0.014877	0.075239	0.001199	0.05987	0.001071	Oct. 22, 2014
Px_p	0.592286	0.014141	0.074211	0.001246	0.05788	0.000983	Oct. 22, 2014
Px_q	0.632214	0.014333	0.076971	0.001149	0.05957	0.001016	Oct. 22, 2014
Px_r	0.603222	0.014171	0.07639	0.001231	0.05727	0.000979	Oct. 22, 2014
Px_s	0.638873	0.016391	0.076744	0.001394	0.06038	0.001094	Oct. 22, 2014
Px_t	0.612231	0.014363	0.075741	0.001296	0.05862	0.000941	Oct. 22, 2014
Px_u	0.634293	0.016475	0.0756	0.001424	0.06085	0.001088	Oct. 22, 2014
Px_v	0.59302	0.013461	0.073658	0.001222	0.05839	0.000905	Oct. 22, 2014
Px_x	0.643317	0.015214	0.07722	0.001255	0.06042	0.001038	Oct. 22, 2014
Px_y	0.610078	0.014665	0.074406	0.001223	0.05947	0.001043	Oct. 22, 2014
Px_z	0.609531	0.014933	0.076614	0.001418	0.0577	0.000926	Oct. 22, 2014

Px_1a	0.632184	0.014834	0.076008	0.001229	0.06032	0.001026	Oct. 22, 2014
Px_1b	0.636512	0.014886	0.07694	0.001222	0.06	0.00103	Oct. 22, 2014
Px_1c	0.603995	0.01303	0.074905	0.00106	0.05848	0.000952	Oct. 22, 2014
Px_1d	0.61049	0.014913	0.073054	0.001319	0.06061	0.000997	Oct. 22, 2014
Px_1e	0.589225	0.014841	0.073052	0.001322	0.0585	0.001025	Oct. 22, 2014
Px_a	0.662903	0.015711	0.080846	0.001264	0.05947	0.001059	Oct. 23, 2014
Px_b	0.596648	0.015224	0.076248	0.001311	0.05675	0.00107	Oct. 23, 2014
Px_c	0.654111	0.01602	0.078339	0.001284	0.06056	0.001102	Oct. 23, 2014
Px_d	0.634511	0.015554	0.077825	0.001361	0.05913	0.001016	Oct. 23, 2014
Px_e	0.657665	0.015867	0.079429	0.001306	0.06005	0.001061	Oct. 23, 2014
Px_f	0.599008	0.014639	0.074085	0.001332	0.05864	0.000971	Oct. 23, 2014
Px_g	0.623485	0.01499	0.077933	0.00138	0.05802	0.000943	Oct. 23, 2014
Px_h	0.613759	0.0162	0.07893	0.00152	0.0564	0.001018	Oct. 23, 2014
Px_i	0.62953	0.016184	0.07561	0.001278	0.06039	0.00117	Oct. 23, 2014
Px_j	0.640576	0.016663	0.075245	0.00139	0.06174	0.001131	Oct. 23, 2014
Px_k	0.632556	0.016057	0.075983	0.001416	0.06038	0.001041	Oct. 23, 2014
Px_l	0.602659	0.015424	0.075371	0.001384	0.05799	0.001034	Oct. 23, 2014
Px_m	0.597756	0.015639	0.074652	0.001328	0.05807	0.001114	Oct. 23, 2014
Px_n	0.656172	0.016493	0.078162	0.001329	0.06089	0.001127	Oct. 23, 2014
Px_o	0.548968	0.014	0.072074	0.001358	0.05524	0.00095	Oct. 23, 2014
Px_p	0.609468	0.015939	0.075559	0.001363	0.0585	0.001108	Oct. 23, 2014
Px_e	0.682289	0.024096	0.081581	0.002056	0.06066	0.001501	Oct. 24, 2014
Px_f	0.647775	0.022833	0.081492	0.002101	0.05765	0.001386	Oct. 24, 2014
Px_g	0.681977	0.02449	0.082178	0.002299	0.06019	0.001355	Oct. 24, 2014
Px_h	0.640595	0.023277	0.076327	0.002063	0.06087	0.001478	Oct. 24, 2014
Px_i	0.632578	0.024888	0.074609	0.002315	0.06149	0.001488	Oct. 24, 2014
Px_j	0.610771	0.022521	0.075124	0.001935	0.05897	0.001556	Oct. 24, 2014
Px_k	0.605781	0.021843	0.076886	0.00213	0.05714	0.001319	Oct. 24, 2014
Px_l	0.624645	0.025626	0.077915	0.002628	0.05814	0.001358	Oct. 24, 2014
Px_m	0.59969	0.021863	0.069985	0.002	0.06215	0.001407	Oct. 24, 2014
Px_n	0.561327	0.018803	0.073784	0.001952	0.05518	0.001134	Oct. 24, 2014
Px_o	0.604999	0.019831	0.07468	0.00191	0.05876	0.001204	Oct. 24, 2014
Px_p	0.592101	0.020345	0.071791	0.001867	0.05982	0.001343	Oct. 24, 2014
Px_q	0.64994	0.022641	0.078577	0.00207	0.05999	0.001367	Oct. 24, 2014
Px_r	0.626719	0.024351	0.077965	0.002291	0.0583	0.001482	Oct. 24, 2014
Px_s	0.585645	0.023464	0.071784	0.002187	0.05917	0.00154	Oct. 24, 2014
Px_t	0.596931	0.025633	0.081398	0.002746	0.05319	0.001413	Oct. 24, 2014
Px_u	0.649618	0.024582	0.075692	0.002165	0.06225	0.001542	Oct. 24, 2014
Px_v	0.683136	0.025502	0.077887	0.002291	0.06361	0.001462	Oct. 24, 2014
Px_w	0.620524	0.026106	0.07432	0.002389	0.06056	0.001644	Oct. 24, 2014
Px_x	0.611111	0.021969	0.077508	0.00208	0.05718	0.001368	Oct. 24, 2014

Px_y	0.572791	0.018243	0.072814	0.001716	0.05705	0.001222	Oct. 24, 2014
Px_z	0.644008	0.020865	0.075116	0.001749	0.06218	0.001401	Oct. 24, 2014
Px_1a	0.628132	0.02354	0.078409	0.002282	0.0581	0.001371	Oct. 24, 2014
Px_1b	0.634425	0.024858	0.077301	0.00238	0.05952	0.001442	Oct. 24, 2014
Px_1c	0.656342	0.02299	0.075767	0.002033	0.06283	0.001414	Oct. 24, 2014
Px_1d	0.646732	0.02377	0.07362	0.002043	0.06371	0.001536	Oct. 24, 2014
Px_1e	0.60286	0.019697	0.074331	0.001789	0.05882	0.001299	Oct. 24, 2014
Px_1f	0.627921	0.025655	0.072866	0.00245	0.0625	0.001451	Oct. 24, 2014
Px_1g	0.577224	0.015036	0.072251	0.001395	0.05794	0.001013	Oct. 24, 2014
Px_1h	0.649777	0.022103	0.075518	0.001706	0.0624	0.001587	Oct. 24, 2014
Px_1i	0.628043	0.022004	0.076502	0.001902	0.05954	0.00147	Oct. 24, 2014
Px_1j	0.595855	0.01723	0.075339	0.001603	0.05736	0.001123	Oct. 24, 2014
Px_a	0.764212	0.015783	0.09643	0.001414	0.05748	0.000836	Oct. 27, 2014
Px_b	0.805093	0.016632	0.098107	0.001386	0.05952	0.000897	Oct. 27, 2014
Px_c	0.781247	0.016728	0.090887	0.001493	0.06234	0.000856	Oct. 27, 2014
Px_d	0.781	0.017629	0.096046	0.001528	0.05898	0.000944	Oct. 27, 2014
Px_e	0.741078	0.017719	0.090867	0.001484	0.05915	0.001033	Oct. 27, 2014
Px_f	0.727962	0.017031	0.08847	0.001463	0.05968	0.000988	Oct. 27, 2014
Px_g	0.714199	0.017189	0.087208	0.001517	0.0594	0.000988	Oct. 27, 2014
Px_h	0.745048	0.017727	0.088339	0.001492	0.06117	0.001025	Oct. 27, 2014
Px_i	0.725387	0.017845	0.088859	0.001497	0.05921	0.001062	Oct. 27, 2014
Px_j	0.702737	0.015871	0.086132	0.001351	0.05917	0.000961	Oct. 27, 2014
Px_k	0.730578	0.01608	0.087173	0.001324	0.06078	0.000968	Oct. 27, 2014
Px_l	0.707777	0.016245	0.084919	0.001357	0.06045	0.000996	Oct. 27, 2014
Px_m	0.714722	0.016479	0.085696	0.001392	0.06049	0.000989	Oct. 27, 2014
Px_n	0.721384	0.017601	0.08792	0.001434	0.05951	0.00108	Oct. 27, 2014
Px_o	0.732557	0.017205	0.0864	0.001345	0.06149	0.001082	Oct. 27, 2014
Px_p	0.713111	0.01635	0.086136	0.001381	0.06004	0.000984	Oct. 27, 2014
Px_q	0.696856	0.017062	0.085514	0.001414	0.0591	0.001067	Oct. 27, 2014
Px_r	0.697445	0.017078	0.08521	0.00147	0.05936	0.001032	Oct. 27, 2014
Px_s	0.686353	0.017458	0.083473	0.001556	0.05964	0.001032	Oct. 27, 2014
Px_t	0.737275	0.017855	0.085623	0.001349	0.06245	0.001149	Oct. 27, 2014
Px_u	0.624551	0.013486	0.076846	0.001232	0.05894	0.000852	Oct. 27, 2014
Px_v	0.647676	0.01387	0.079242	0.001319	0.05928	0.000799	Oct. 27, 2014
Px_w	0.63306	0.013665	0.07905	0.001272	0.05808	0.000836	Oct. 27, 2014
Px_x	0.645851	0.013367	0.081185	0.001253	0.0577	0.000795	Oct. 27, 2014
Px_y	0.649582	0.013096	0.079832	0.001235	0.05901	0.000763	Oct. 27, 2014
Px_z	0.70264	0.01371	0.084468	0.001253	0.06033	0.000765	Oct. 27, 2014
Px_1a	0.665954	0.013917	0.08155	0.001264	0.05923	0.00083	Oct. 27, 2014
Px_1b	0.648457	0.012454	0.080365	0.001191	0.05852	0.000715	Oct. 27, 2014
Px_1c	0.663929	0.012432	0.08111	0.001144	0.05937	0.000731	Oct. 27, 2014

Px_1d	0.689138	0.013964	0.083531	0.001247	0.05984	0.00082	Oct. 27, 2014
Px_1e	0.680352	0.01365	0.082688	0.001194	0.05967	0.000831	Oct. 27, 2014
Px_1f	0.673645	0.012801	0.082378	0.001108	0.05931	0.000796	Oct. 27, 2014
Px_1g	0.677009	0.014729	0.083232	0.001342	0.05899	0.000862	Oct. 27, 2014
Px_1h	0.643919	0.013499	0.081543	0.001205	0.05727	0.000851	Oct. 27, 2014
Px_1i	0.6702	0.013007	0.081972	0.001172	0.0593	0.000778	Oct. 27, 2014
Px_1j	0.669424	0.013828	0.082425	0.001264	0.0589	0.000815	Oct. 27, 2014
Px_1k	0.660857	0.013348	0.080416	0.001203	0.0596	0.000809	Oct. 27, 2014
Px_1l	0.64712	0.014303	0.080827	0.001308	0.05807	0.000874	Oct. 27, 2014
Px_1m	0.655796	0.014815	0.081235	0.001409	0.05855	0.000847	Oct. 27, 2014
Px_1n	0.651152	0.014969	0.081356	0.001388	0.05805	0.000894	Oct. 27, 2014
Px_a	0.703736	0.014737	0.08661	0.001446	0.05893	0.000745	Oct. 28, 2014
Px_b	0.693855	0.014627	0.085311	0.00139	0.05899	0.000789	Oct. 28, 2014
Px_c	0.690513	0.014307	0.084681	0.00141	0.05914	0.000729	Oct. 28, 2014
Px_d	0.679378	0.014823	0.084544	0.001446	0.05828	0.00079	Oct. 28, 2014
Px_e	0.667067	0.013691	0.080433	0.001273	0.06015	0.000786	Oct. 28, 2014
Px_f	0.638673	0.01535	0.078192	0.001407	0.05924	0.000944	Oct. 28, 2014
Px_g	0.671868	0.015863	0.080236	0.001453	0.06073	0.00092	Oct. 28, 2014
Px_h	0.624832	0.015278	0.077621	0.001494	0.05838	0.00088	Oct. 28, 2014
Px_i	0.647078	0.016233	0.07988	0.001564	0.05875	0.000921	Oct. 28, 2014
Px_j	0.673024	0.013182	0.082191	0.001149	0.05939	0.000815	Oct. 28, 2014
Px_k	0.635441	0.014096	0.079454	0.001313	0.058	0.000858	Oct. 28, 2014
Px_l	0.648943	0.014624	0.079363	0.00138	0.0593	0.00085	Oct. 28, 2014
Px_m	0.647005	0.014918	0.079717	0.001416	0.05886	0.000865	Oct. 28, 2014
Px_n	0.635779	0.014968	0.077865	0.001438	0.05922	0.000865	Oct. 28, 2014
Px_o	0.62174	0.016244	0.077333	0.001551	0.05831	0.000976	Oct. 28, 2014
Px_p	0.609687	0.014586	0.076236	0.001402	0.058	0.000887	Oct. 28, 2014
Px_q	0.621848	0.014821	0.076375	0.001385	0.05905	0.000913	Oct. 28, 2014
Px_r	0.616234	0.013579	0.07745	0.001302	0.05771	0.000822	Oct. 28, 2014
Px_s	0.613556	0.015676	0.075509	0.001465	0.05893	0.00098	Oct. 28, 2014
Px_t	0.60633	0.015449	0.073387	0.001465	0.05992	0.000948	Oct. 28, 2014
PX_u	0.625158	0.014972	0.076355	0.001423	0.05938	0.000893	Oct. 28, 2014
PX_w	0.625338	0.015171	0.078371	0.001472	0.05787	0.000889	Oct. 28, 2014
PX_x	0.632658	0.015435	0.076709	0.001324	0.05982	0.001031	Oct. 28, 2014
PX_y	0.621503	0.014639	0.077033	0.001336	0.05851	0.000933	Oct. 28, 2014
Px_z	0.619277	0.015087	0.073936	0.001308	0.06075	0.001017	Oct. 28, 2014
Px_aa	0.59665	0.015401	0.074022	0.00139	0.05846	0.001035	Oct. 28, 2014
Px_ab	0.643611	0.016962	0.079138	0.001567	0.05898	0.001026	Oct. 28, 2014
Px_ac	0.656448	0.018049	0.079018	0.001653	0.06025	0.001075	Oct. 28, 2014
Px_a	0.687356	0.016426	0.085348	0.001411	0.05841	0.001008	Oct. 29, 2014
Px_b	0.672365	0.016608	0.081931	0.001419	0.05952	0.001048	Oct. 29, 2014

Px_c	0.655174	0.018472	0.079415	0.001648	0.05983	0.001142	Oct. 29, 2014
Px_d	0.641402	0.016289	0.082059	0.001494	0.05669	0.001004	Oct. 29, 2014
Px_e	0.67756	0.018274	0.08032	0.001532	0.06118	0.001167	Oct. 29, 2014
Px_f	0.683668	0.016575	0.082868	0.001448	0.05984	0.001005	Oct. 29, 2014
Px_g	0.640809	0.016491	0.079151	0.001462	0.05872	0.001052	Oct. 29, 2014
Px_h	0.657568	0.01662	0.080592	0.001465	0.05918	0.001039	Oct. 29, 2014
Px_i	0.629138	0.015743	0.0773	0.001381	0.05903	0.001034	Oct. 29, 2014
Px_j	0.660917	0.016539	0.080127	0.001475	0.05982	0.001014	Oct. 29, 2014
Px_k	0.599105	0.017355	0.075893	0.001594	0.05725	0.001142	Oct. 29, 2014
Px_l	0.63362	0.016323	0.07802	0.001414	0.0589	0.001078	Oct. 29, 2014
Px_m	0.602776	0.01726	0.073334	0.001611	0.05961	0.001095	Oct. 29, 2014
Px_n	0.617658	0.01619	0.076562	0.001459	0.05851	0.001053	Oct. 29, 2014
Px_o	0.630551	0.01719	0.07629	0.001473	0.05995	0.001153	Oct. 29, 2014
Px_p	0.654038	0.016794	0.079175	0.001423	0.05991	0.001099	Oct. 29, 2014

FC1 Standard Data							
Sample Name	207/235 Age	1 sigma Abs Error	206/238 Age	1 sigma Abs Error	207/206 Age	1 sigma Abs Error	Analysis Date
FC1_h	1105.614	43.29609	1131.73	55.97231	1054.96	30.99401	Feb. 5, 2014
FC1_i	1097.19	43.50031	1127.359	56.44727	1038.198	31.22116	Feb. 5, 2014
FC1_j	1075.554	43.03614	1089.694	54.72271	1047.378	31.21272	Feb. 5, 2014
FC1_k	1101.95	50.23368	1133.667	51.86687	1039.655	48.45006	Feb. 5, 2014
FC1_l	1041.554	48.62733	1076.084	49.7334	969.5966	48.28217	Feb. 5, 2014
FC1_m	1088.76	50.42377	1128.711	35.96842	1009.671	58.42915	Feb. 5, 2014
FC1_n	1094.621	50.46305	1149.331	36.31873	987.3518	58.51188	Feb. 5, 2014
FC1_o	1112.847	37.34489	1172.564	38.26342	997.7201	37.55099	Feb. 5, 2014
FC1_p	1119.086	38.24735	1172.33	39.9674	1016.853	37.84255	Feb. 5, 2014
FC1_a	1146.131	40.23	1284.634	49.96946	892.7587	28.38411	Feb. 7, 2014
FC1_b	1139.118	40.10554	1271.173	49.49038	895.6224	28.39837	Feb. 7, 2014
FC1_c	1130.176	37.0557	1239.754	21.63434	925.4439	35.6103	Feb. 7, 2014
FC1_d	1097.275	36.41043	1191.475	20.78477	915.0297	35.57717	Feb. 7, 2014
FC1_e	1115.465	44.55414	1205.036	36.29376	945.2831	40.08529	Feb. 7, 2014
FC1_f	1056.292	44.03949	1060.165	34.22779	1048.719	39.83612	Feb. 7, 2014
FC1_g	1075.396	41.9564	1087.447	48.25277	1051.152	29.3898	Feb. 7, 2014
FC1_h	1080.556	42.39386	1096.425	49.25986	1048.794	29.47341	Feb. 7, 2014
FC1_i	1091.95	36.31632	1095.522	52.74259	1084.968	14.39159	Feb. 7, 2014
FC1_j	1079.808	36.07249	1081.815	52.21187	1075.894	14.0616	Feb. 7, 2014
FC1_k	1067.606	37.0418	1040.958	48.13755	1122.361	23.76768	Feb. 12, 2014
FC1_m	1087.405	27.96382	1100.321	27.54957	1061.772	27.76146	Feb. 12, 2014
FC1_n	1070.733	27.56606	1064.355	25.55401	1083.894	28.65454	Feb. 12, 2014
FC1_a	1080.62	30.69949	1105.471	27.0829	1030.312	73.00107	Mar. 9, 2014
FC1_b	1059.18	30.24728	1064.651	25.86744	1047.394	72.81077	Mar. 9, 2014
FC1_c	1086.321	24.42422	1118.453	28.59168	1022.8	48.1377	Mar. 9, 2014
FC1_d	1064.806	24.06802	1106.642	28.34623	980.4156	47.51474	Mar. 9, 2014
FC1_e	1091.499	21.47442	1118.453	22.27469	1038.08	48.55608	Mar. 9, 2014
FC1_f	1053.327	20.9972	1062.496	21.40407	1034.335	47.58919	Mar. 9, 2014
FC1_g	1077.644	18.64479	1076.152	15.36135	1080.911	46.78729	Mar. 9, 2014
FC1_h	1082.108	18.94961	1084.857	16.0992	1076.821	47.05651	Mar. 9, 2014
FC1_i	1059.204	15.24846	1062.895	12.48256	1051.284	40.02595	Mar. 9, 2014
FC1_j	1058.157	15.15362	1074.113	12.42127	1025.063	40.03828	Mar. 9, 2014
FC1_k	1064.399	26.48235	1102.156	16.20068	987.3144	75.44652	Mar. 9, 2014
FC1_l	1089.324	26.65102	1131.742	16.08274	1004.994	74.97965	Mar. 9, 2014
FC1_m	1054.055	27.91499	1088.356	15.66835	983.2172	80.29524	Mar. 9, 2014
FC1_n	1077.23	28.22987	1117.067	16.01801	997.0344	80.00815	Mar. 9, 2014
FC1_o	1073.901	20.6181	1127.198	21.14668	967.1299	48.21036	Mar. 9, 2014
FC1_p	1083.177	20.77637	1149.915	21.5835	951.1806	48.64302	Mar. 9, 2014

FC1_q	1119.735	15.97851	1176.607	15.4361	1010.932	38.9368	Mar. 9, 2014
FC1_r	1092.704	15.40155	1157.441	14.19251	965.8459	39.48986	Mar. 9, 2014
FC1_s	1086.116	14.70003	1149.231	14.47754	961.687	36.1562	Mar. 9, 2014
FC1_t	1087.664	15.1231	1134.029	15.19942	996.0183	36.19294	Mar. 9, 2014
FC1_a	1079.204	20.10742	1086.115	25.01734	1065.58	35.45429	Mar. 12, 2014
FC1_b	1041.381	19.58995	1055.019	24.44446	1013.177	34.11242	Mar. 12, 2014
FC1_c	1108.319	24.59802	1164.18	27.8717	1001.24	50.94149	Mar. 12, 2014
FC1_d	1090.879	24.42415	1124.935	27.04496	1024.461	50.96395	Mar. 12, 2014
FC1_e	1087.181	19.59032	1095.305	15.7795	1071.383	49.56062	Mar. 12, 2014
FC1_f	1138.364	19.83218	1175.936	15.76153	1067.871	50.13695	Mar. 12, 2014
FC1_g	1088.117	19.14511	1091.504	19.32285	1081.497	43.70297	Mar. 12, 2014
FC1_h	1082.306	19.22465	1091.248	19.88864	1064.502	42.96714	Mar. 12, 2014
FC1_i	1091.405	19.7599	1108.033	21.84598	1058.52	41.51099	Mar. 12, 2014
FC1_j	1066.018	19.66364	1087.137	21.82087	1023.189	41.68715	Mar. 12, 2014
FC1_a	1134.431	20.94686	1134.012	22.90411	1135.131	37.70302	Mar. 17, 2014
FC1_b	1104.922	20.18421	1123.247	21.97507	1068.919	37.18052	Mar. 17, 2014
FC1_a	1079.976	21.35209	1092.524	27.35346	1054.753	29.88712	Mar. 31, 2014
FC1_b	1112.443	22.26106	1119.181	28.52384	1099.307	31.8202	Mar. 31, 2014
FC1_c	1093.366	23.24119	1097.715	22.11202	1084.684	45.73379	Mar. 31, 2014
FC1_d	1083.991	23.19967	1092.827	22.28248	1066.243	45.61507	Mar. 31, 2014
FC1_e	1073.709	23.89862	1078.842	22.46512	1063.136	47.62046	Mar. 31, 2014
FC1_f	1084.815	23.72983	1101.584	22.42107	1051.127	47.0044	Mar. 31, 2014
FC1_g	1099.4	25.91226	1103.838	37.29536	1090.311	24.40305	Mar. 31, 2014
FC1_h	1072.61	25.76697	1074.871	36.63231	1067.7	25.3285	Mar. 31, 2014
FC1_a	1110.523	32.91602	1138.117	25.44843	1058.314	73.90211	Apr. 1, 2014
FC1_b	1099.273	32.76843	1128.435	25.31187	1043.42	74.1512	Apr. 1, 2014
FC1_c	1117.09	19.28272	1135.673	22.12459	1081.469	35.34868	Apr. 1, 2014
FC1_d	1108.644	20.01165	1126.697	22.49979	1073.759	39.43037	Apr. 1, 2014
FC1_e	1127.746	16.25789	1143.327	16.55077	1098.136	32.91625	Apr. 1, 2014
FC1_f	1125.03	16.34796	1152.018	16.91786	1073.564	33.07806	Apr. 1, 2014
FC1_g	1103.738	13.54098	1120.657	14.39622	1070.625	26.82753	Apr. 1, 2014
FC1_h	1121.5	13.54153	1150.963	14.50105	1064.947	26.79681	Apr. 1, 2014
FC1_i	1132.066	20.00353	1159.103	15.2058	1080.478	45.95826	Apr. 1, 2014
FC1_j	1112.062	19.4465	1123.657	14.02084	1089.365	45.15058	Apr. 1, 2014
FC1_k	1110.181	22.95178	1110.39	19.00997	1109.582	49.77279	Apr. 1, 2014
FC1_l	1115.631	23.16207	1128.846	19.68019	1089.786	50.01512	Apr. 1, 2014
FC1_m	1110.349	16.79946	1105.35	18.04966	1094.816	32.47881	Apr. 1, 2014
FC1_n	1108.32	16.82911	1101.069	18.20645	1097.251	32.09832	Apr. 1, 2014
FC1_o	1090.228	18.42899	1088.09	23.70593	1094.519	27.34543	Apr. 1, 2014
FC1_p	1075.888	18.14653	1088.466	23.56442	1050.508	26.91498	Apr. 1, 2014
FC1_q	1130.782	17.24499	1165.301	22.99283	1064.996	27.22921	Apr. 1, 2014

FC1_r	1128.603	17.66669	1152.622	24.11234	1082.581	24.45181	Apr. 1, 2014
FC1_a	1086.592	27.22967	1083.65	29.16448	1092.514	52.71555	Apr. 14, 2014
FC1_b	1077.91	27.43916	1049.089	28.72349	1136.678	53.37388	Apr. 14, 2014
FC1_c	1124.527	24.98618	1135.915	23.44946	1102.487	54.1857	Apr. 14, 2014
FC1_d	1144.106	25.18509	1163.967	24.11954	1106.534	53.60628	Apr. 14, 2014
FC1_a	1109.011	26.49368	1115.247	24.05217	1096.899	51.26129	Apr. 15, 2014
FC1_b	1127.139	26.7302	1146.394	24.5754	1090.32	51.51537	Apr. 15, 2014
FC1_c	1104.603	16.21284	1116.243	11.80643	1081.984	35.71174	Apr. 15, 2014
FC1_d	1090.866	16.5998	1095.427	13.07033	1082.005	35.86432	Apr. 15, 2014
FC1_e	1123.954	24.69906	1167.314	24.42424	1041.638	48.85743	Apr. 15, 2014
FC1_f	1116.662	24.79439	1129.738	23.92607	1091.847	49.0803	Apr. 15, 2014
FC1_g	1113.514	17.42479	1119.26	12.76891	1102.401	39.45038	Apr. 15, 2014
FC1_h	1105.925	17.35129	1111.498	12.37229	1095.068	39.95479	Apr. 15, 2014
FC1_i	1066.361	29.02462	1084.753	12.11661	1029.01	72.24596	Apr. 15, 2014
FC1_j	1079.281	29.27943	1084.011	12.53212	1069.824	71.72591	Apr. 15, 2014
FC1_k	1079.964	18.97932	1100.961	12.22772	1038.056	44.82815	Apr. 15, 2014
FC1_l	1061.218	18.82793	1095.765	12.27191	991.0674	45.17973	Apr. 15, 2014
FC1_m	1072.089	14.79344	1092.673	11.54996	1030.571	34.14562	Apr. 15, 2014
FC1_n	1093.119	15.04059	1115.163	12.28813	1049.585	33.52432	Apr. 15, 2014
FC1_a	1100.516	23.73667	1129.737	27.37317	1043.268	40.12305	Apr. 21, 2014
FC1_b	1118.51	24.15328	1099.984	27.0498	1154.763	39.74411	Apr. 21, 2014
FC1_c	1092.63	29.40613	1088.113	22.2753	1101.889	63.38039	Apr. 21, 2014
FC1_d	1090.422	29.10425	1099.204	21.86956	1073.173	63.28296	Apr. 21, 2014
FC1_e	1047.164	33.04391	1048.126	21.71208	1044.923	75.01809	Apr. 21, 2014
FC1_f	1048.238	32.86896	1048.932	21.11179	1046.559	74.91103	Apr. 21, 2014
FC1_a	1139.497	30.15818	1176.035	43.4977	1070.158	35.16815	Apr. 25, 2014
FC1_c	1101.633	29.57446	1114.273	41.2187	1076.34	35.95675	Apr. 25, 2014
FC1_d	1072.667	29.345	1069.637	39.99541	1078.419	36.31697	Apr. 25, 2014
FC1_e	1074.228	18.45371	1087.465	15.23296	1047.446	44.46592	Apr. 25, 2014
FC1_f	1055.59	17.84217	1063.666	13.89029	1038.914	44.02971	Apr. 25, 2014
FC1_a	1078.087	21.03435	1094.555	24.52033	1045.051	33.88225	Apr. 28, 2014
FC1_b	1095.02	21.16938	1082.307	24.01315	1120.488	34.04438	Apr. 28, 2014
FC1_c	1061.081	18.42708	1068.219	23.78515	1046.649	26.23734	Apr. 28, 2014
FC1_d	1068.477	18.265	1066.961	23.32814	1071.788	26.17481	Apr. 28, 2014
FC1_e	1079.15	15.35386	1097.927	19.56909	1041.66	25.11278	Apr. 28, 2014
FC1_f	1065.696	15.21004	1071.475	19.1994	1054.123	24.47609	Apr. 28, 2014
FC1_g	1067.806	13.97688	1061.172	18.40359	1081.517	21.99694	Apr. 28, 2014
FC1_h	1071.408	14.07796	1061.649	18.75359	1091.458	20.81323	Apr. 28, 2014
FC1_a	1121.256	32.88393	1121.547	39.35474	1119.402	59.13416	Apr. 29, 2014
FC1_b	1115.722	32.88045	1141.229	40.10982	1065.062	59.81373	Apr. 29, 2014
FC1_c	1058.72	20.72415	1060.991	17.06527	1053.828	53.34546	Apr. 29, 2014

FC1_d	1117.308	21.40469	1135.888	18.11885	1081.132	53.61339	Apr. 29, 2014
FC1_e	1104.63	19.51724	1110.625	19.25327	1092.241	45.44977	Apr. 29, 2014
FC1_f	1111.03	19.47205	1122.661	19.12202	1087.732	45.65374	Apr. 29, 2014
FC1_g	1109.63	16.65591	1111.945	13.78895	1105.05	43.0374	Apr. 29, 2014
FC1_h	1078.551	16.79911	1094.05	14.32416	1047.318	44.39381	Apr. 29, 2014
FC1_i	1088.215	15.07226	1112.897	14.21899	1039.103	38.46569	Apr. 29, 2014
FC1_j	1088.978	15.03206	1109.374	14.11908	1048.372	38.24152	Apr. 29, 2014
FC1_a	1102.817	38.00614	1148.071	39.52294	1014.93	63.04695	May. 6, 2014
FC1_b	1087.405	38.21938	1112.976	39.35637	1036.869	63.46675	May. 6, 2014
FC1_c	1091.308	31.13819	1109.595	31.17202	1055.375	56.11947	May. 6, 2014
FC1_d	1109.121	31.6169	1131.399	32.31073	1066.073	55.81674	May. 6, 2014
FC1_e	1109.443	23.49581	1128.613	23.19359	1072.489	44.78052	May. 6, 2014
FC1_f	1104.976	23.23105	1141.622	22.72024	1033.96	45.41723	May. 6, 2014
FC1_g	1109.972	20.47558	1106.575	17.15851	1116.408	43.11837	May. 6, 2014
FC1_h	1094.772	20.37419	1108.068	17.45448	1068.204	43.18701	May. 6, 2014
FC1_i	1072.054	20.21596	1043.625	16.78232	1130.118	42.68633	May. 6, 2014
FC1_a	1062.818	32.42879	1071.73	34.37245	1044.502	44.96652	May. 7, 2014
FC1_b	1052.826	32.16479	1046.58	33.4116	1065.74	44.86343	May. 7, 2014
FC1_c	1038.709	28.38138	1042.674	34.60505	1031.136	33.77949	May. 7, 2014
FC1_d	1062.07	28.57694	1067.603	35.1827	1051.477	33.25845	May. 7, 2014
FC1_e	1044.516	25.09744	1058.634	22.31645	1015.178	41.38166	May. 7, 2014
FC1_f	1061.125	25.21789	1057.512	22.16149	1068.641	40.81131	May. 7, 2014
FC1_g	1043.963	31.15422	1052.971	26.35179	1025.127	52.15964	May. 7, 2014
FC1_h	1040.598	31.07674	1051.533	26.08915	1017.67	52.52333	May. 7, 2014
FC1_b	1097.928	24.40705	1102.001	29.71132	1090.58	39.94383	May. 12, 2014
FC1_c	1091.13	24.49568	1128.726	30.36981	1017.573	41.83208	May. 12, 2014
FC1_d	1107.563	34.56554	1135.772	49.95773	1053.273	38.13174	May. 12, 2014
FC1_e	1117.941	34.84621	1141.524	50.24182	1073.067	38.99293	May. 12, 2014
FC1_f	1116.43	49.98327	1131.885	76.42285	1085.356	35.59586	May. 12, 2014
FC1_g	1105.775	49.68069	1107.12	74.79866	1102.023	35.82635	May. 12, 2014
FC1_h	1012.859	61.43872	980.2897	85.67449	1084.463	48.63423	May. 12, 2014
FC1_i	1020.837	61.75538	971.0568	84.95659	1129.66	48.77166	May. 12, 2014
FC1_j	1005.668	61.0558	978.0047	85.47215	1066.939	46.64777	May. 12, 2014
FC1_k	1067.53	28.88727	1096.672	25.37709	1008.17	54.33015	May. 12, 2014
FC1_l	1064.166	28.75159	1095.079	24.91092	1001.033	54.77172	May. 12, 2014
FC1_m	1041.975	24.10241	1055.481	18.49865	1013.916	48.52121	May. 12, 2014
FC1_n	1051.774	24.06051	1065.334	18.06239	1023.884	48.57563	May. 12, 2014
FC1_a	1006.245	41.04435	962.7567	50.72216	1101.794	48.10448	Sep. 19, 2014
FC1_b	1124.383	32.9151	1120.156	36.79199	1132.151	48.61642	Sep. 19, 2014
FC1_c	1116.844	32.35122	1113.741	35.59891	1122.479	48.74154	Sep. 19, 2014
FC1_d	1121.155	24.09521	1126.809	18.89376	1110.346	45.73899	Sep. 19, 2014

FC1_e	1121.172	23.92896	1093.744	18.22642	1174.85	44.77986	Sep. 19, 2014
FC1_f	1122.758	26.63501	1159.083	24.8548	1053.136	48.16089	Sep. 19, 2014
FC1_g	1092.58	26.79093	1094.926	25.05918	1087.912	47.78362	Sep. 19, 2014
FC1_h	1091.78	31.64576	1099.652	27.73371	1076.896	59.48807	Sep. 19, 2014
FC1_i	1091.477	32.31704	1092.069	29.47286	1091.074	59.11591	Sep. 19, 2014
FC1_j	1107.783	30.65941	1151.751	22.9411	1086.401	60.16714	Sep. 19, 2014
FC1_a	1077.496	23.21938	1105.824	26.9338	1020.466	43.3942	Oct. 20, 2014
FC1_b	1096.813	23.32437	1132.113	27.38317	1027.254	42.87092	Oct. 20, 2014
FC1_c	1110.923	18.2474	1157.377	21.15659	1021.292	35.07061	Oct. 20, 2014
FC1_d	1108.915	17.70839	1154.433	19.84472	1020.899	35.61271	Oct. 20, 2014
FC1_e	1140.81	17.37629	1175.875	15.38421	1075.02	40.59441	Oct. 20, 2014
FC1_f	1085.749	17.22514	1099.206	15.42113	1059.15	40.35984	Oct. 20, 2014
FC1_g	1079.729	21.83301	1097.107	17.66868	1045.313	52.63457	Oct. 20, 2014
FC1_h	1085.567	21.43675	1111.3	16.62301	1034.78	52.51761	Oct. 20, 2014
FC1_i	1088.084	24.84238	1114.51	16.34325	1035.707	63.12786	Oct. 20, 2014
FC1_j	1048.037	24.64614	1062.051	16.90136	1019.087	62.95995	Oct. 20, 2014
FC1_k	1095.547	17.33746	1116.418	16.51038	1054.348	39.55074	Oct. 20, 2014
FC1_l	1110.048	17.35832	1119.088	16.11656	1092.419	39.73274	Oct. 20, 2014
FC1_m	1139.091	16.06252	1160.004	16.8882	1099.942	34.67093	Oct. 20, 2014
FC1_n	1078.601	16.29908	1077.83	17.17178	1080.633	35.49052	Oct. 20, 2014
FC1_a	1140.472	34.25232	1148.659	42.2375	1123.639	59.77509	Oct. 21, 2014
FC1_b	1153.716	34.42059	1197.459	43.80517	1071.131	60.12039	Oct. 21, 2014
FC1_c	1268.752	23.93143	1275.218	22.81995	1257.602	53.09753	Oct. 21, 2014
FC1_d	1273.313	23.72447	1317.635	22.86719	1199.035	53.35465	Oct. 21, 2014
FC1_a	1120.5	24.16396	1165.39	31.20268	1034.189	35.68404	Oct. 21, 2014
FC1_b	1119.144	24.1948	1153.625	30.91757	1052.521	35.96534	Oct. 21, 2014
FC1_c	1143.418	28.37059	1203.646	41.94124	1030.583	31.16868	Oct. 21, 2014
FC1_d	1148.612	28.48634	1198.357	41.82335	1055.577	31.28122	Oct. 21, 2014
FC1_a	1123.171	28.87842	1188.192	25.08456	999.9612	61.03512	Oct. 22, 2014
FC1_b	1153.556	29.49079	1203.852	25.92706	1060.702	60.59502	Oct. 22, 2014
FC1_c	1108.655	20.02202	1146.37	21.72999	1035.392	38.20299	Oct. 22, 2014
FC1_d	1106.942	20.28975	1137.183	22.33167	1047.986	37.80593	Oct. 22, 2014
FC1_e	1088.683	17.7271	1087.75	19.3715	1090.786	33.78171	Oct. 22, 2014
FC1_f	1056.139	17.48191	1036.006	18.86973	1098.23	32.91672	Oct. 22, 2014
FC1_g	1061.877	21.38748	1084.663	19.76388	1015.656	46.45306	Oct. 22, 2014
FC1_h	965.3397	21.59841	926.4817	20.46232	1055.221	44.84826	Oct. 22, 2014
FC1_i	1047.89	21.36806	1047.358	22.73515	1049.29	40.95707	Oct. 22, 2014
FC1_j	1030.856	20.98534	1023.316	22.21648	1047.18	39.75502	Oct. 22, 2014
FC1_k	1089.889	19.80167	1119.851	20.18071	1030.678	39.93612	Oct. 22, 2014
FC1_l	1106.603	18.55294	1129.295	16.97263	1062.447	39.46338	Oct. 22, 2014
FC1_a	1081.635	26.95823	1112.581	27.68978	1020.275	51.61312	Oct. 23, 2014

FC1_b	1086.26	26.36545	1122.949	26.24218	1013.874	51.85287	Oct. 23, 2014
FC1_c	1105.181	28.51385	1177.188	26.25852	965.733	60.19963	Oct. 23, 2014
FC1_d	1092.006	28.54603	1155.687	26.36403	966.8025	60.3429	Oct. 23, 2014
FC1_e	1066.104	31.04043	1095.889	22.86104	1006.859	71.83485	Oct. 23, 2014
FC1_f	1070.42	31.05303	1101.381	22.51844	1009.078	72.26678	Oct. 23, 2014

R33 Standard Data							
Sample Name	207/235 Age	1 sigma Abs Error	206/238 Age	1 sigma Abs Error	207/206 Age	1 sigma Abs Error	Analysis Date
rs33_a	399.854	22.7366	395.284	21.37005	432.216	25.6759	Feb. 5, 2014
rs33_b	388.308	23.43	371.856	21.09831	493.346	32.3672	Feb. 5, 2014
rs33_c	399.348	23.6613	377.821	20.83972	531.669	33.2998	Feb. 5, 2014
rs33_d	358.8	25.2832	347.574	18.45421	431.84	64.8983	Feb. 5, 2014
rs33_e	392.308	25.3555	391.369	19.18486	397.633	58.3495	Feb. 5, 2014
rs33_f	394.919	25.5513	395.623	19.61534	390.589	57.9361	Feb. 5, 2014
rs33_g	412.63	21.6094	394.42	15.12401	515.526	53.0772	Feb. 5, 2014
rs33_h	428.598	21.8963	433.72	16.20195	400.865	52.9776	Feb. 5, 2014
rs33_a	450.992	23.7071	439.132	19.00998	511.994	39.2615	Feb. 7, 2014
rs33_b	395.345	20.8597	396.517	17.56802	388.577	36.2047	Feb. 7, 2014
rs33_c	411.546	19.7247	413.644	8.845928	399.934	42.5449	Feb. 7, 2014
rs33_d	412.116	20.066	411.334	8.928918	416.64	43.664	Feb. 7, 2014
rs33_e	383.268	22.7333	381.681	13.75744	393.339	48.2605	Feb. 7, 2014
rs33_f	398.426	23.9179	394.755	14.68149	420.247	49.2942	Feb. 7, 2014
rs33_g	394.575	23.9048	392.524	21.18601	406.723	40.7683	Feb. 7, 2014
rs33_h	386.152	22.5917	378.582	19.12029	431.88	40.2083	Feb. 7, 2014
rs33_i	385.846	18.1576	381.963	19.87556	409.347	18.8398	Feb. 7, 2014
rs33_j	400.114	19.4497	398.282	20.99203	410.854	23.6839	Feb. 7, 2014
rs33_a	412.481	19.8419	414.832	20.13916	399.23	32.9445	Feb. 12, 2014
rs33_b	471.976	23.5593	479.771	24.58821	434.139	36.6917	Feb. 12, 2014
rs33_c	341.503	17.4033	322.962	15.23028	469.87	36.8834	Feb. 12, 2014
rs33_d	397.094	14.9763	388.222	11.00239	449.228	35.3339	Feb. 12, 2014
RS33_a	423.305	17.251	412.386	11.3151	482.641	91.0723	Mar. 9, 2014
RS33_b	384.073	15.4226	390.554	10.4744	344.615	87.3126	Mar. 9, 2014
RS33_c	418.301	14.081	433.245	12.42984	337.104	71.0395	Mar. 9, 2014
RS33_d	374.364	13.1213	386.803	11.21071	298.494	75.1497	Mar. 9, 2014
RS33_e	395.147	11.3577	405.817	8.867735	333.143	64.5285	Mar. 9, 2014
RS33_f	408.199	12.0192	414.506	9.222979	372.638	68.0429	Mar. 9, 2014
RS33_g	417.189	11.372	415.654	7.242326	425.957	68.9846	Mar. 9, 2014
RS33_h	408.046	10.1871	403.738	6.501811	432.772	59.1351	Mar. 9, 2014
RS33_i	424.883	8.59817	429.714	5.499646	398.403	50.4078	Mar. 9, 2014
RS33_j	425.613	9.18311	437.506	5.616213	361.345	58.0345	Mar. 9, 2014
RS33_k	420.68	14.1884	429.004	7.03784	374.767	85.1472	Mar. 9, 2014
RS33_l	403.935	13.6855	411.982	6.63752	357.64	85.3878	Mar. 9, 2014
RS33_m	399.543	15.3278	426.312	7.779912	246.995	101.081	Mar. 9, 2014
RS33_n	383.012	14.9377	408.759	7.404189	229.711	103.518	Mar. 9, 2014
RS33_o	414.396	11.847	429.306	8.967715	332.08	68.808	Mar. 9, 2014

RS33_p	390.407	10.9641	405.104	8.329632	304.122	65.2453	Mar. 9, 2014
RS33_q	396.535	9.20576	403.183	6.380204	357.922	59.6271	Mar. 9, 2014
RS33_r	387.608	9.05647	393.871	6.157676	350.348	60.6163	Mar. 9, 2014
RS33_s	395.727	8.67415	406.995	6.19561	330.492	56.2037	Mar. 9, 2014
RS33_t	396.524	9.13374	400.696	6.644767	372.342	58.0408	Mar. 9, 2014
RS33_a	396.881	10.0892	395.257	9.523902	406.684	42.6053	Mar. 12, 2014
RS33_b	399.196	10.4758	406.601	9.936555	356.891	47.5295	Mar. 12, 2014
RS33_c	430.535	14.1687	433.174	11.29212	417.48	72.9366	Mar. 12, 2014
RS33_d	407.334	14.047	401.646	10.72189	440.748	77.8859	Mar. 12, 2014
RS33_e	389.511	10.7064	385.396	6.683328	414.511	66.651	Mar. 12, 2014
RS33_f	401.515	10.534	397.68	6.336446	424.126	63.8555	Mar. 12, 2014
RS33_g	411.382	10.8899	399.9	8.192842	476.489	59.4308	Mar. 12, 2014
RS33_h	409.488	11.1038	398.27	8.062287	473.398	63.8412	Mar. 12, 2014
RS33_i	422.685	12.6768	408.843	9.607405	499.066	71.4895	Mar. 12, 2014
RS33_j	408.053	11.4104	410.91	9.141199	392.076	63.8499	Mar. 12, 2014
RS33_a	399.306	11.2033	401.518	9.006251	386.416	53.6884	Mar. 17, 2014
RS33_b	400.094	10.5953	398.318	8.633329	410.255	47.2777	Mar. 17, 2014
RS33_c	403.559	12.4538	401.511	11.95146	415.314	46.2121	Mar. 31, 2014
RS33_d	417.098	12.3834	409.012	11.77052	462.084	43.8918	Mar. 31, 2014
RS33_e	409.104	12.8483	402.132	9.413876	448.612	58.6906	Mar. 31, 2014
RS33_f	417.548	12.9934	405.314	9.347274	485.679	58.4176	Mar. 31, 2014
RS33_g	391.07	12.6647	380.901	8.823771	451.474	60.9355	Mar. 31, 2014
RS33_h	385.139	12.2555	376.271	8.639227	438.593	58.387	Mar. 31, 2014
RS33_i	461.804	15.0641	408.954	14.87904	733.69	35.0922	Mar. 31, 2014
RS33_j	414.321	14.5879	398.213	15.04526	504.703	43.4801	Mar. 31, 2014
RS33_a	387.723	16.219	382.997	9.484343	417.602	84.5155	Apr. 1, 2014
RS33_b	400.643	17.6701	413.658	10.93445	327.855	94.9074	Apr. 1, 2014
RS33_c	439.062	12.1474	430.992	10.57654	481.988	51.8375	Apr. 1, 2014
RS33_d	446.441	11.4761	413.371	9.173388	621.015	48.0341	Apr. 1, 2014
RS33_e	476.825	10.9274	431.845	7.597545	699.726	48.9509	Apr. 1, 2014
RS33_f	411.12	8.91305	408.223	6.766548	427.72	43.9522	Apr. 1, 2014
RS33_g	411.328	7.79986	410.655	6.216829	415.201	38.1815	Apr. 1, 2014
RS33_h	404.66	7.36007	407.32	5.912498	389.602	35.7344	Apr. 1, 2014
RS33_i	427.516	11.5665	407.284	6.601135	537.984	60.1651	Apr. 1, 2014
RS33_j	428.343	11.5403	422.225	6.559709	461.28	61.733	Apr. 1, 2014
RS33_k	426.474	12.4569	414.293	7.903499	492.64	59.2553	Apr. 1, 2014
RS33_l	395.554	11.8867	381.594	7.381554	477.771	60.9753	Apr. 1, 2014
RS33_o	424.451	9.991	407.896	7.62679	487.476	48.5641	Apr. 1, 2014
RS33_m	458.64	11.4796	420.144	8.516644	629.142	52.5133	Apr. 1, 2014
RS33_n	390.506	9.00147	386.218	7.113359	387.583	45.7716	Apr. 1, 2014
RS33_oo	406.107	10.1361	401.037	9.568421	435.064	41.4319	Apr. 1, 2014

RS33_p	405.987	10.9332	402.186	9.754724	427.685	51.8008	Apr. 1, 2014
RS33_q	422.432	9.82977	413.691	9.19829	470.319	40.8749	Apr. 1, 2014
RS33_r	392.195	9.59548	384.333	8.573863	438.711	46.1587	Apr. 1, 2014
RS33_a	565.471	21.3383	429.707	13.68428	1157.42	76.4778	Apr. 14, 2014
RS33_b	404.901	14.951	400.484	12.29878	430.197	68.9984	Apr. 14, 2014
RS33_c	423.937	13.7858	408.323	9.667361	509.637	67.2399	Apr. 14, 2014
RS33_d	414.054	13.2926	403.824	9.59905	471.349	64.3128	Apr. 14, 2014
RS33_a	422.743	14.7834	402.691	10.03157	533.732	64.0026	Apr. 15, 2014
RS33_b	405.917	14.8389	396.541	9.984379	459.72	70.3683	Apr. 15, 2014
RS33_c	428.608	10.3422	419.728	6.215891	476.889	52.5073	Apr. 15, 2014
RS33_d	416.279	10.3179	409.882	6.500429	452.143	53.0083	Apr. 15, 2014
RS33_e	451.408	14.633	434.731	10.33389	537.867	63.9502	Apr. 15, 2014
RS33_f	465.705	15.3137	440.212	10.73292	594.024	65.2287	Apr. 15, 2014
RS33_g	485.619	12.1064	455.249	6.646245	631.713	58.2159	Apr. 15, 2014
RS33_h	403.974	10.5289	394.794	7.393375	456.9	52.4681	Apr. 15, 2014
RS33_i	397.751	15.0351	399.179	5.475822	389.55	83.1917	Apr. 15, 2014
RS33_j	414.971	15.7026	421.727	5.65249	377.664	85.276	Apr. 15, 2014
RS33_k	386.93	10.7055	391.411	5.785773	360.469	62.3477	Apr. 15, 2014
RS33_l	391.677	10.0562	401.825	5.404924	332.439	56.1385	Apr. 15, 2014
RS33_m	418.691	9.68309	416.285	5.739775	432.09	54.4466	Apr. 15, 2014
RS33_n	450.324	11.3351	427.817	6.172854	567.065	62.0915	Apr. 15, 2014
RS33_o	398.358	9.16639	401.006	5.837787	383.149	51.8991	Apr. 15, 2014
RS33_a	404.476	12.9698	413.393	10.85927	353.956	58.4707	Apr. 21, 2014
RS33_b	413.082	12.3497	406.539	10.50239	449.891	47.6768	Apr. 21, 2014
RS33_c	389.402	14.5531	404.748	8.113591	299.504	78.1838	Apr. 21, 2014
RS33_d	400.666	14.9764	396.35	8.109977	425.907	76.6885	Apr. 21, 2014
RS33_e	408.104	17.0312	399.412	9.469418	457.855	90.2713	Apr. 21, 2014
RS33_f	406.726	17.6784	400.485	8.988199	442.06	88.2509	Apr. 21, 2014
RS33_g	374.018	17.0116	389.094	9.517903	281.396	93.3213	Apr. 21, 2014
RS33_a	413.095	15.7024	400.454	15.70993	483.891	52.9163	Apr. 25, 2014
RS33_b	411.798	15.7092	408.117	16.04272	432.023	53.698	Apr. 25, 2014
RS33_c	419.939	12.4756	400.48	6.736573	528.243	77.0533	Apr. 25, 2014
RS33_d	410.807	11.5939	404.943	6.86855	443.876	70.5649	Apr. 25, 2014
RS33_a	415.307	11.9673	415.305	10.14539	415.434	49.8649	Apr. 28, 2014
RS33_b	411.305	11.4781	405.52	9.933246	444.02	44.3562	Apr. 28, 2014
RS33_c	421.97	11.2541	412.352	10.1876	475.113	46.6828	Apr. 28, 2014
RS33_d	407.455	10.9635	404.636	10.07078	423.701	46.8065	Apr. 28, 2014
RS33_e	427.697	10.0127	405.518	8.124639	549.289	48.5227	Apr. 28, 2014
RS33_f	406.577	11.7607	410.899	9.214022	382.363	68.3117	Apr. 28, 2014
RS33_g	414.197	8.80994	400.785	8.102644	489.764	40.7184	Apr. 28, 2014
RS33_h	410.713	8.34336	408.064	7.720903	425.774	40.2558	Apr. 28, 2014

RS33_a	417.037	18.1817	414.22	15.92026	431.204	85.3207	Apr. 29, 2014
RS33_b	407.053	16.9136	402.222	15.14279	433.107	73.3739	Apr. 29, 2014
RS33_c	444.119	13.3278	424.099	8.279052	548.983	76.0643	Apr. 29, 2014
RS33_d	425.586	12.5862	423.816	7.853277	434.941	76.1296	Apr. 29, 2014
RS33_f	411.028	11.6865	400.449	8.354135	470.211	69.3475	Apr. 29, 2014
RS33_g	419.787	12.3591	428.749	8.954488	370.16	76.6787	Apr. 29, 2014
RS33_h	454.307	12.8252	411.794	7.337828	675.501	78.9161	Apr. 29, 2014
RS33_i	408.447	9.38767	400.538	5.745649	453.351	59.4703	Apr. 29, 2014
RS33_j	410.825	8.49205	406.048	5.816532	437.708	52.4236	Apr. 29, 2014
RS33_k	420.363	8.95719	419.572	6.183913	424.663	55.5828	Apr. 29, 2014
RS33_l	429.261	11.7011	413.292	7.213857	515.862	79.8613	Apr. 29, 2014
RS33_a	404.92	19.868	396.626	15.3145	452.874	73.2879	May. 6, 2014
RS33_b	411.584	20.2338	413.762	15.32156	399.762	79.1873	May. 6, 2014
RS33_c	426.127	17.7902	436.255	13.00018	372.121	78.9928	May. 6, 2014
RS33_d	450.533	19.7556	419.113	13.22522	614.645	83.353	May. 6, 2014
RS33_e	469.466	17.5552	432.417	11.1084	655.377	81.3609	May. 6, 2014
RS33_f	414.474	12.9295	413.464	9.442076	420.579	59.214	May. 6, 2014
RS33_g	425.333	11.9661	417.338	7.856187	468.642	57.8473	May. 6, 2014
RS33_a	400.711	17.5231	411.263	14.78943	340.237	56.8331	May. 7, 2014
RS33_b	413.488	17.9826	412.414	14.60562	419.42	57.461	May. 7, 2014
RS33_c	414.325	16.3961	417.225	15.18964	399.049	49.9644	May. 7, 2014
RS33_d	389.181	15.8142	396.462	14.8116	346.979	50.3828	May. 7, 2014
RS33_e	455.874	20.6682	424.524	16.60385	617.986	67.9451	May. 7, 2014
RS33_f	412.576	15.6515	419.72	10.88129	372.898	62.4311	May. 7, 2014
RS33_g	400.161	14.8501	409.648	10.5388	345.828	59.2661	May. 7, 2014
RS33_h	423.981	19.2391	412.167	11.83969	488.707	75.3527	May. 7, 2014
RS33_i	405.492	18.3355	404.037	12.12663	413.756	72.1942	May. 7, 2014
RS33_a	412.176	15.8591	408.12	13.06684	435.751	81.3427	May. 12, 2014
RS33_b	432.613	17.521	427.282	14.14625	461.888	89.7186	May. 12, 2014
RS33_c	428.035	20.2162	417.122	20.81006	487.978	66.3753	May. 12, 2014
RS33_d	423.172	19.0991	419.55	19.87194	443.71	63.8658	May. 12, 2014
RS33_e	427.632	27.2006	400.32	29.35799	576.413	57.6931	May. 12, 2014
RS33_f	443.838	28.0832	415.946	30.21445	589.939	64.6843	May. 12, 2014
RS33_g	346.682	30.5346	346.964	32.53273	345.342	97.1699	May. 12, 2014
RS33_h	366.449	31.1443	352.876	32.97764	453.788	77.9182	May. 12, 2014
RS33_i	392.602	14.8676	398.85	9.965186	355.644	65.4025	May. 12, 2014
RS33_j	412.463	16.995	412.285	11.22834	413.136	76.2043	May. 12, 2014
RS33_k	375.684	13.2286	378.341	8.274052	359.509	65.1911	May. 12, 2014
RS33_l	402.685	13.3274	398.926	7.950249	424.482	60.9503	May. 12, 2014
RS33_a	420.487	10.7179	423.522	7.966718	403.939	56.7166	May. 13, 2014
RS33_b	426.372	11.1588	432.049	8.22798	395.856	60.2385	May. 13, 2014

RS33_c	436.645	11.2319	439.027	8.026934	424.166	60.4269	May. 13, 2014
RS33_d	416.02	9.51075	429.471	6.018918	342.153	56.4138	May. 13, 2014
RS33_e	413.407	11.7004	432.093	5.64251	310.433	72.1764	May. 13, 2014
RS33_f	443.809	12.7201	437.999	5.764197	474.09	73.7325	May. 13, 2014
RS33_g	440.363	12.9644	448.259	6.563516	399.34	75.6791	May. 13, 2014
RS33_h	436.242	12.992	443.353	6.628947	398.921	76.5348	May. 13, 2014
RS33_a	390.233	11.7916	390.32	10.25084	389.54	52.8686	Oct. 20, 2014
RS33_b	398.819	12.7283	397.874	11.08597	404.125	58.0048	Oct. 20, 2014
RS33_c	411.129	11.4885	406.032	8.886397	440.056	63.0155	Oct. 20, 2014
RS33_d	404.424	11.4219	403.858	8.428493	407.873	67.3721	Oct. 20, 2014
RS33_e	421.865	11.8019	417.229	7.705144	447.621	70.739	Oct. 20, 2014
RS33_f	430.748	12.1629	435.93	8.00778	403.468	73.2699	Oct. 20, 2014
RS33_g	379.318	11.132	400.254	6.942274	253.989	68.886	Oct. 20, 2014
RS33_h	407.614	12.0569	405.908	7.134729	417.838	69.6039	Oct. 20, 2014
RS33_i	390.269	12.891	398.606	7.301581	341.315	75.147	Oct. 20, 2014
RS33_j	412	13.4125	416.33	7.376009	387.973	75.0246	Oct. 20, 2014
RS33_k	400.33	11.7372	385.25	8.552173	488.363	67.5057	Oct. 20, 2014
RS33_l	411.328	10.5335	381.84	7.320574	580.392	56.2197	Oct. 20, 2014
RS33_m	411.287	9.91086	401.49	7.373137	467.168	56.265	Oct. 20, 2014
RS33_n	418.694	9.78758	411.088	7.395306	461.334	53.9389	Oct. 20, 2014
RS33_a	439.102	18.2485	430.505	16.67059	482.992	72.0614	Oct. 21, 2014
RS33_b	458.734	19.7979	467.125	18.78059	415.47	80.2214	Oct. 21, 2014
RS33_c	475.255	15.3649	460.069	11.18653	549.005	78.7231	Oct. 21, 2014
RS33_d	516.081	14.6361	511.227	10.73167	537.401	68.0364	Oct. 21, 2014
RS33_a	414.597	18.0761	418.616	15.62994	392.191	72.1972	Oct. 24, 2014
RS33_b	426.7	18.6875	421.363	15.44639	455.526	76.2586	Oct. 24, 2014
RS33_c	425.923	18.5904	413.034	15.51874	496.18	71.7976	Oct. 24, 2014
RS33_d	420.983	18.0412	429.28	15.74095	375.681	71.0706	Oct. 24, 2014
RS33_e	429.983	19.1616	439.999	13.25304	375.457	89.4339	Oct. 24, 2014
RS33_f	427.511	19.5544	436.476	13.74956	378.26	91.9561	Oct. 24, 2014
RS33_g	437.744	20.1156	437.964	13.74617	435.395	93.6515	Oct. 24, 2014
RS33_h	423.836	19.5333	427.894	14.07917	400.62	89.381	Oct. 24, 2014
RS33_i	436.11	25.7466	431.827	19.46019	455.75	108.362	Oct. 24, 2014
RS33_j	443.903	26.2318	450.113	20.27979	408.775	110.653	Oct. 24, 2014
RS33_k	410.453	25.4226	408.248	14.46794	421.136	124.137	Oct. 24, 2014
RS33_l	417.104	25.9866	411.822	15.15399	444.692	123.672	Oct. 24, 2014
RS33_m	429.481	20.7908	439.339	11.58322	377.262	103.903	Oct. 24, 2014
RS33_n	436.024	21.7565	419.017	11.60148	527.179	106.559	Oct. 24, 2014
RS33_o	429.879	21.9066	425.329	12.17037	453.953	112.325	Oct. 24, 2014
RS33_p	414.909	21.1045	407.021	12.28721	458.63	107.006	Oct. 24, 2014
RS33_q	433.054	20.6547	421.538	10.53419	494.923	104.988	Oct. 24, 2014

RS33_r	422.055	20.3882	413.806	10.67572	467.523	105.72	Oct. 24, 2014
RS33_a	418.69	24.4699	388.23	22.35417	589.291	65.3582	Oct. 27, 2014
RS33_b	421.253	22.3209	421.188	20.74337	420.726	68.3944	Oct. 27, 2014
RS33_c	395.187	20.0161	390.32	18.3984	422.874	59.895	Oct. 27, 2014
RS33_d	436.934	21.7489	411.849	19.41389	570.51	58.8468	Oct. 27, 2014
RS33_e	408.078	11.0757	411.528	9.776632	388.57	40.2327	Oct. 27, 2014
RS33_f	421.939	11.9966	419.801	10.53789	433.609	43.049	Oct. 27, 2014
RS33_g	416.571	12.0196	400.15	9.893247	508.528	45.5468	Oct. 27, 2014
RS33_h	403.756	11.3323	399.79	9.950251	426.48	40.7667	Oct. 27, 2014
RS33_i	402.866	10.2546	406.222	8.215768	383.636	42.7077	Oct. 27, 2014
RS33_j	416.175	10.5452	411.594	8.212448	441.616	43.2138	Oct. 27, 2014
RS33_k	423.692	11.7501	421.893	9.0008	433.455	50.8994	Oct. 27, 2014
RS33_l	408.447	10.5744	408.252	8.232764	409.514	45.0244	Oct. 27, 2014
RS33_m	407.46	11.7821	420.82	8.093001	332.622	52.5662	Oct. 27, 2014
RS33_n	396.164	12.1376	406.264	8.384522	337.838	56.4496	Oct. 27, 2014
RS33_o	412.352	12.5538	413.978	8.399814	403.448	56.7211	Oct. 27, 2014
RS33_p	406.054	12.4022	403.771	8.479867	419.243	55.0591	Oct. 27, 2014
RS33_q	450.537	19.1903	429.77	16.94844	559.11	61.7048	Oct. 27, 2014
RS33_r	435.367	18.5759	436.819	16.93576	428.872	64.1635	Oct. 27, 2014
RS33_s	445.288	18.9231	442.081	17.37577	463.059	61.8238	Oct. 27, 2014
RS33_t	420.626	17.6496	423.873	16.25056	404.047	60.1337	Oct. 27, 2014
RS33_u	440.662	12.3806	442.296	12.07279	432.604	41.1373	Oct. 27, 2014
RS33_v	506.659	14.2506	454.152	12.66952	751.727	41.9659	Oct. 27, 2014
RS33_w	507.557	15.3252	453.585	13.28367	759.2	48.8885	Oct. 27, 2014
RS33_x	422.78	11.8998	416.171	11.21997	459.449	41.4558	Oct. 27, 2014
RS33_y	421.84	9.72386	411.717	9.306139	478.003	32.4852	Oct. 27, 2014
RS33_z	416.49	9.78763	408.464	9.133795	461.642	35.9921	Oct. 27, 2014
RS33_1a	405.414	9.28654	409.664	7.140314	381.527	43.0403	Oct. 27, 2014
RS33_1b	422.625	9.73478	408.454	6.764478	500.933	45.6485	Oct. 27, 2014
RS33_1c	433.398	10.6551	422.731	7.80864	490.659	50.2477	Oct. 27, 2014
RS33_1d	429.392	10.1549	417.129	7.189162	495.904	48.711	Oct. 27, 2014
RS33_a	426.02	16.1078	429.614	16.95477	406.459	44.5385	Oct. 28, 2014
RS33_b	439.74	16.9908	445.206	17.86676	411.06	48.6581	Oct. 28, 2014
RS33_c	416.154	10.4639	423.072	8.504372	378.345	46.7398	Oct. 28, 2014
RS33_d	419.547	11.648	422.875	9.003932	401.653	56.32	Oct. 28, 2014
RS33_e	453.712	13.1516	424.108	10.70188	607.001	58.2661	Oct. 28, 2014
RS33_f	447.836	12.8155	438.282	11.21511	497.585	56.0806	Oct. 28, 2014
RS33_g	436.052	11.5323	444.715	10.5549	390.437	50.3626	Oct. 28, 2014
RS33_h	441.653	12.4334	445.619	11.21344	420.92	54.9104	Oct. 28, 2014
RS33_i	441.035	10.4597	440.586	9.125211	443.114	42.9251	Oct. 28, 2014
RS33_j	436.913	10.378	437.137	8.89846	435.467	44.1731	Oct. 28, 2014

RS33_k	438.149	11.9236	440.677	10.7407	424.842	45.0672	Oct. 28, 2014
RS33_l	437.795	12.1976	432.648	10.60085	464.905	48.2401	Oct. 28, 2014
RS33_a	425.525	14.8751	430.298	12.32155	399.543	59.5207	Oct. 29, 2014
RS33_b	432.252	14.8649	429.912	11.91539	444.535	59.424	Oct. 29, 2014
RS33_c	427.734	13.7136	419.982	11.5886	470.574	54.2055	Oct. 29, 2014
RS33_d	423.533	13.3132	428.675	11.65968	396.502	52.2465	Oct. 29, 2014
RS33_e	441.004	12.3662	450.369	11.52675	392.773	47.383	Oct. 29, 2014
RS33_f	422.67	12.4179	441.283	11.65038	322.721	51.5737	Oct. 29, 2014

91500 Standard Data							
Sample Name	207/235 Age	1 sigma Abs Error	206/238 Age	1 sigma Abs Error	207/206 Age	1 sigma Abs Error	Analysis Date
91500_a	1055.6062	32.3067	1087.23	34.941	990.35	54.840803	Sep. 19, 2014
91500_b	1072.9412	32.7732	1038.832	34.037	1142.51	53.239603	Sep. 19, 2014
91500_c	1032.6702	24.2269	1021.077	17.452	1057.43	51.594503	Sep. 19, 2014
91500_d	1045.0801	23.7790	1061.493	16.208	1011.05	51.756772	Sep. 19, 2014
91500_e	1044.7151	26.8933	1039.068	23.319	1056.54	53.187814	Sep. 19, 2014
91500_f	1065.7409	26.4954	1041.886	21.994	1114.90	51.896091	Sep. 19, 2014
91500_g	1066.6347	31.7496	1062.384	26.169	1076.12	63.444625	Sep. 19, 2014
91500_a	1045.4291	24.1871	1054.725	29.091	1025.78	40.765478	Oct. 21, 2014
91500_b	1069.8362	24.3705	1091.012	29.584	1026.64	41.414107	Oct. 21, 2014
91500_c	1097.4051	28.6787	1130.979	40.286	1031.11	37.302763	Oct. 21, 2014
91500_d	1072.2373	28.5493	1079.013	38.909	1058.18	37.683301	Oct. 21, 2014
91500_a	1057.3979	29.2967	1059.551	25.096	1053.42	63.258911	Oct. 22, 2014
91500_b	1066.7158	28.9407	1083.183	23.654	1033.66	64.532449	Oct. 22, 2014
91500_c	1075.2856	21.6018	1097.677	23.280	1030.15	43.847635	Oct. 22, 2014
91500_d	1083.9616	20.6330	1087.808	21.047	1076.22	42.539303	Oct. 22, 2014
91500_e	1059.9804	20.775	1080.411	17.943	1018.45	48.633622	Oct. 22, 2014
91500_f	1052.8423	20.8505	1072.512	18.263	1012.57	48.6115	Oct. 22, 2014
91500_g	1045.8963	21.6394	1082.514	18.869	970.49	51.428556	Oct. 22, 2014
91500_h	1058.0525	20.8662	1061.004	16.797	1052.27	49.172247	Oct. 22, 2014
91500_i	1086.5402	22.2245	1046.142	22.840	1168.73	42.64875	Oct. 22, 2014
91500_j	1054.9372	21.5612	1048.648	22.087	1068.26	43.821033	Oct. 22, 2014
91500_k	1043.5195	18.8149	1050.185	16.092	1029.76	44.402278	Oct. 22, 2014
91500_l	1050.8992	19.1750	1054.316	16.369	1043.98	45.481603	Oct. 22, 2014
91500_a	1085.5437	27.9510	1075.496	26.580	1106.21	57.45378	Oct. 23, 2014
91500_b	1051.8919	26.9750	1064.814	25.780	1025.62	56.536605	Oct. 23, 2014
91500_d	1063.561	30.6500	1048.754	27.551	1093.73	66.230872	Oct. 23, 2014
91500_e	1041.2429	29.7956	1025.405	26.123	1074.30	65.562021	Oct. 23, 2014
91500_f	1079.8341	33.0451	1122.685	26.357	995.55	76.901231	Oct. 23, 2014
91500_g	1104.7894	32.9815	1129.001	25.101	1058.62	75.966541	Oct. 23, 2014